

Historic, Archive Document

Do not assume content reflects current scientific knowledge, policies, or practices.

aSB953
B47
1996



United States
Department of
Agriculture

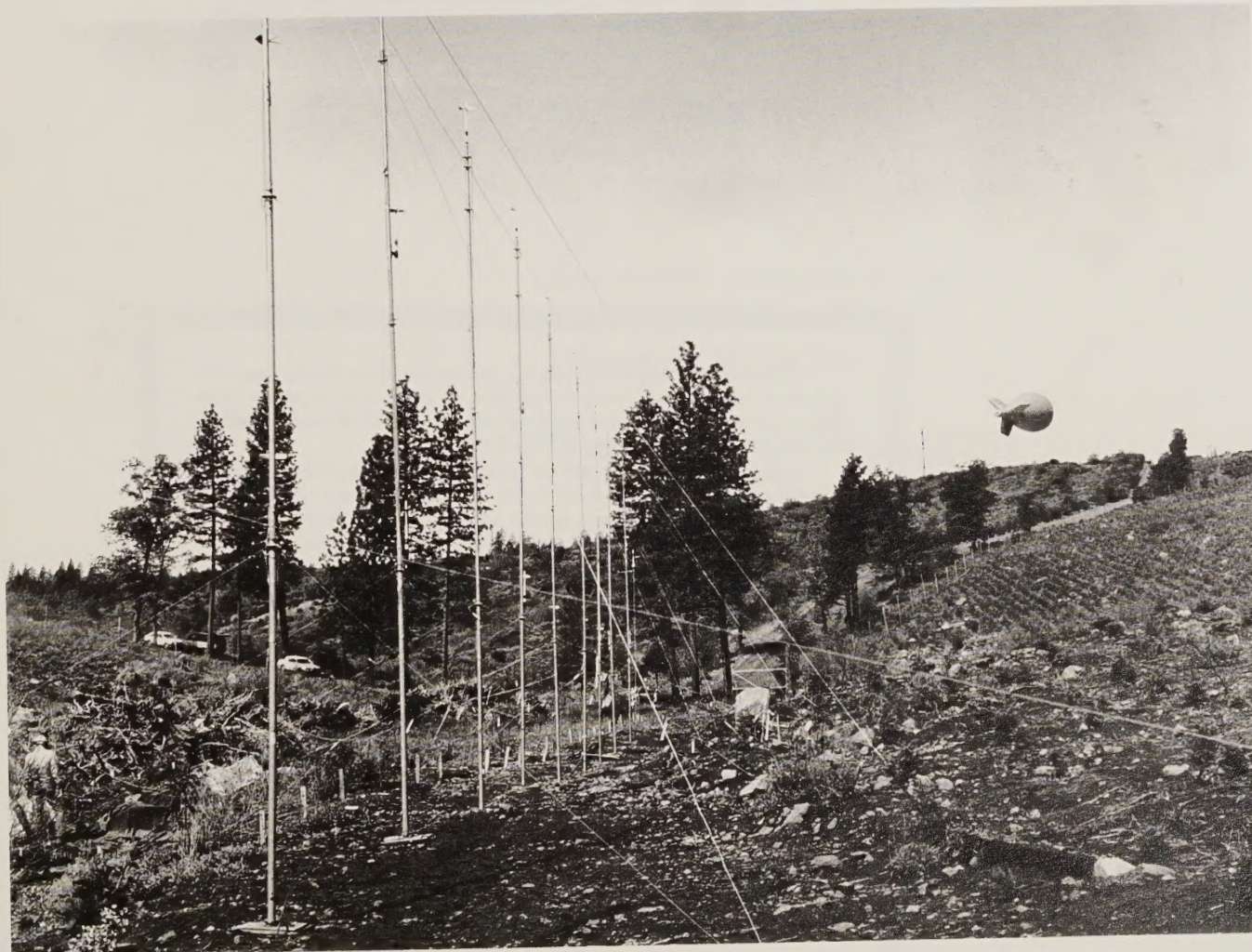


Forest Service

Forest Health
Protection

Forest Health
Technology
Enterprise Team-
Davis
2121C Second Street
Davis, CA 95616

INTERACTION OF SPRAY AIRCRAFT WAKE WITH CONVECTIVE SURFACE WINDS IN HILLY TERRAIN



FHTET 96-26
October 1996

The use of trade names and identification of firms or corporations is for the convenience of the reader; such use does not constitute an official endorsement or approval by the United States Government of any product or service to the exclusion of others that may be suitable.

This information is the sole property of the Government with unlimited rights in the usage thereof and cannot be copyrighted.

Pesticides used improperly can be injurious to human beings, animals, and plants. Follow the directions and heed all precautions on labels. Store pesticides in original containers under lock and key—out of the reach of children and animals—and away from food and feed.

Apply pesticides so that they do not endanger humans, livestock, crops, beneficial insects, fish, and wildlife. Do not apply pesticides where there is danger of drift when honey bees or other pollinating insects are visiting plants, or in ways that may contaminate water or leave illegal residues.

Avoid prolonged inhalation of pesticide sprays or dusts; wear protective clothing and equipment, if specified on the label.

If your hands become contaminated with a pesticide, do not eat or drink until you have washed. In case a pesticide is swallowed or gets in the eyes, follow the first aid treatment given on the label, and get prompt medical attention. If a pesticide is spilled on your skin or clothing, remove clothing immediately and wash skin thoroughly.

NOTE: Some States have restrictions on the use of certain pesticides. Check your State and local regulations. Also, because registrations of pesticides are under constant review by the U.S Environmental Protection Agency, consult your local forest pathologist, county agriculture agent, or State extension specialist to be sure the intended use is still registered.



Cover Photo

Vertical towers for characterization of aircraft wake during flights. Balloon is a tethered sonde for weather measurements. Program WIND, Paynes Creek, CA, 1985. Photograph by Jon Barry.

FHTET 96-26
(C.D.I. Technical Note 86-05)
October 1996

~~INTERACTION OF SPRAY~~
AIRCRAFT WAKE WITH
CONVECTIVE SURFACE WINDS
IN HILLY TERRAIN

Prepared by:

A. J. Bilanin
M. E. Teske
R. G. Geyer

Continuum Dynamics, Inc.
P.O. Box 3073
Princeton, NJ 08543

Contract No. 53-0343-1-00153

Prepared for:

USDA Forest Service
Missoula Technology
Development Center
Ft. Missoula, MT 69801
Davis, CA 95616

Robert Ekblad
Project Officer

John W. Barry
Program Manager
Program Wind



FOREWORD

Program WIND (Winds In Non-uniform Domains) was a joint meteorological research effort by the U.S. Department of Agriculture Forest Service, the U.S. Army Dugway Proving Ground and the U.S. Army Atmospheric Sciences Laboratory. Field studies were conducted in northern California during 1985 and 1987 to collect data for meteorological and spray dispersion model development and evaluation. As part of Program WIND, cooperation between the Forest Service and Dugway Proving Ground resulted in the advancement of the FSCBG (Forest Service, Cramer, Barry, and Grim) aerial spray deposition, drift and dispersion model from a research tool to an operational model. The work described in this report was sponsored by the Forest Service as part of the Program WIND cooperative effort.

Bob Ekblad, Project Officer, John Barry, Program Manager, and the authors, A.J. Bilanin, M.E. Teske and R.G. Geyer gratefully acknowledge our debt to the many who made the project possible and successful. The success of a large ongoing cooperative field study such as Program WIND depends on teamwork. Deserving special mention are: Dave Burham of the Transportation Systems Center of the Department of transportation for sharing his past experience in wake-vortex measurements and also providing the anemometers used in this project; Don Lassila for his assistance in our tower set-up and breakdown and manning the vertical camera; Jim Keetch, Bob Thomas and the rest of the Lockheed Corp. (Utah) crew for their assistance and loaning of the batteries and portable generator; the Forest Service employees who delivered our equipment to the Chico Tree Improvement Center; Jack Kennedy at the Mendocino National Forest Chico (CA) Tree Improvement Center for use of his storage space for our equipment; Jim Boyd of the Forest Service Missoula Technology Development Center for operating the cameras and helping wherever needed; and Bob Ekblad and John Barry of the Forest Service for both their on-site assistance and valuable guidance throughout the aircraft wake project.

TABLE OF CONTENTS

<u>Section</u>		<u>Page</u>
1	INTRODUCTION	1-1
1.1	Background	1-1
1.2	Program Description	1-2
1.3	Data Reduction Procedures	1-2
1.4	Conclusions and Recommendations	1-3
2	TEST EQUIPMENT AND FACILITIES	2-1
2.1	Test Aircraft	2-1
2.2	Test Site	2-1
3	TEST INSTRUMENTATION	3-1
3.1	Anemometer Towers	3-1
3.2	Anemometers	3-1
3.3	Data Acquisition System	3-2
3.4	Aircraft Altitude Measurement	3-2
3.5	Aircraft Ground Speed and Measurement	3-3
3.6	Ambient Wind and Temperature Profiles	3-3
4	TEST PROCEDURE	4-1
5	TEST MATRIX	5-1
6	UVW DATA REDUCTION	6-1
7	TOWER GRID DATA REDUCTION	7-1
7.1	Flow Field Model	7-1
7.2	Preliminary Results	7-2
8	REFERENCES	8-1

1. INTRODUCTION

1.1 Background

The first phase of program "Winds In Nonuniform Domains" (WIND) was performed jointly by the United States Department of Agriculture Forest Service and the United States Army at several sites in northern California from May through July of 1985. A specific objective of the Forest Service in this continuing program is to collect sufficient data on aircraft wake behavior over flat and moderately complex forest and rangelands to permit evaluation and improvement of selected spray dispersion models. These models include AGDISP (AGricultural DISPersal) (Ref. 1) and FSCBG (Forest Service Cramer-Barry-Grim) (Ref. 2). These initial tests provided extensive wake data over reasonably flat brushland and within two types of forest canopies. Preliminary test results and a data reduction algorithm for interpreting the data are presented in a previous report covering this test (Ref. 3).

Three significant recommendations were made as a result of these first series of tests, with regard to future tests in program WIND:

- 1) The propeller anemometers located on the instrumentation grid should be oriented vertically, since horizontally oriented anemometers are influenced by ambient (generally horizontal) crosswind effects that cannot be easily removed when analyzing the data for the location of the aircraft vortices.
- 2) The instrumentation grid itself should be extended laterally to permit wake tracking for a longer period of time, since the data reduction algorithm loses its ability to track the aircraft vortices once one of the vortices moves beyond a tower grid end.
- 3) A longer sampling time should be used to track the vortices, since, with wider spaced towers, the aircraft vortices are expected to remain within the instrumentation grid beyond the 25 to 35 seconds of data observed in the first series of tests.

These recommendations were all implemented in the second series of tests for EMCOT (Event Modeling for COmplex Terrain), preliminary results of which are presented in this report.

1.2 Program Description

The EMCOT program extended data collection to hilly terrain, in an effort to obtain meteorological and dispersion measurements which can be used to validate the EMCOT model. Complex terrain presents its own unique set of problems due to downslope and upslope drainage winds, and the complicated influence and consequence of surface layer effects.

The second series of WIND tests was performed in late April and early May of 1986, at a site in the Sierra Nevada foothills near Red Bluff, California (Section 2). A line of ten towers with three levels of anemometers was erected near the bottom of a gully in a cleared area between two ridges. Data was collected during several aircraft runs each morning. Data involved flyovers of a C-130 transport plane and a Bell 206B JetRanger perpendicular to the tower grid. Measuring equipment and data acquisition are the same as in the previous tests (Section 3). Following a standard test procedure each day (Section 4), a full test matrix of 49 tests was conducted over a twelve-day period (Section 5).

1.3 Data Reduction Procedures

Two sets of data reduction are presented in this report. Turbulence levels were recorded by sampling two UVW anemometer sets at one-second intervals during each test day, and recording the data on floppy diskettes for later analysis (Section 6). The bulk of the data from vertically oriented W anemometers were interpreted using the numerical algorithm developed in the previous work (Section 7).

1.4 Conclusions and Recommendations

The major conclusions and recommendations from this second study are as follows:

- 1) Even with the presence of downslope winds, the anemometer tower grid with vertical anemometers, spaced more widely apart, allowed for the accurate tracking of aircraft vortices for a much longer time than occurred during the first series of tests. A tower configuration of this nature should be very beneficial in future aircraft wake detection systems. In some cases, the preliminary results indicate that vortices were tracked up to 120 seconds after entering the tower grid.
- 2) A comparison of velocity traces from this test with traces from Chico and Foresthill shows that the current experiment produces noisier signals. It is assumed that the presence of downslope winds is responsible.
- 3) Surface winds above the tower grid played a significant role in altering the motion of the aircraft vortices. Although an attempt was made to account for apparent near-surface winds by positioning the aircraft flyover location, six of the 26 card deposition runs did not yield usable preliminary data. In these cases the vortices were swept away from the instrumentation grid before any sensors detected them, drainage winds severely distorted the vertical anemometer readings, or the existing data reduction algorithm was unable to locate the aircraft.
- 4) Despite the above difficulties it is clear that the bulk of the test runs contain valuable aircraft wake data that, when combined with the first series of tests and analyzed in detail with the surface deposition data, will provide a significant database for model validation.

- 5) Consequently, it is strongly recommended that additional data reduction algorithms be investigated to quantify the behavior of aircraft vortices and near-wake effects, and to catalogue the expected motion of spray deposition over the terrain examined in this study and in the previous program WIND data study. An additional series of tests, including wake data and surface deposition collection, should be undertaken in a coniferous forest to complete the experimental data package. A modification to the data reduction algorithm is expected to yield interpretable results from the test runs that could not be successfully analyzed with the existing algorithm.
- 6) This completed data package, once reduced, should provide a large series of tests from which model validation in AGDISP may take place. Models of vortex tipping, helicopters in a low forward advance, and vortex dissipation above a smooth surface and within a canopy should receive attention during a detailed data analysis program.
- 7) Addition of a canopy deposition model to AGDISP will complete all major code development.
- 8) AGDISP may then be released as a predictive tool for spray deposition studies.

2. TEST EQUIPMENT AND FACILITIES

The aircraft and test site comprise the noninstrumented components of this test program and are described in this section of the report.

2.1 Test Aircraft

Four test runs were made over the instrumentation grid by a C-130 on the first day of testing. Unfortunately, the current numerical algorithm was unable to locate vortex centroids during these runs. It is anticipated that the C-130 wake characteristics will have to be included more carefully in the vortex algorithm to permit interpretation of the C-130 runs. Consequently, the bulk of data reduction will be confined to the helicopter flyovers that comprise the rest of the test flights.

A Bell 206B JetRanger helicopter owned by Chuck Jones Flying Service was used for these test runs. The weight of the helicopter was approximately 2100 lbs when fully loaded with water, with only 80 lbs of liquid released after completing the spray runs each day. The helicopter landed in a clearing after each run to receive further instructions. The spray material consisted of water, blue food coloring for traceability, and glycerine to retard evaporation of the water droplets.

2.2 Test Site

All tests were performed on a privately owned Jones Christmas tree farm approximately 25 miles east of Red Bluff, California (Figure 2-1). This area consists of a pair of ridges, between which runs a small stream which leads outward from the forested end of the site through the test area. The ground was covered with seedlings approximately 2 ft high with a 5 ft spacing. The site was instrumented with program WIND towers for meteorological data.

The ten 30-ft wake towers were located along the stream on an access road (Figure 2-2). A spacing of 20 ft was maintained between the towers. These wake towers had an east-west orientation where the upslope and downslope winds are parallel to the tower line. The towers were numbered 1 through 10 with tower 1 located on the east (uphill) end of the gully. The grade of the terrain was approximately 6.6% from tower 1 to tower 10. A small tent was pitched 20 ft perpendicular to the center of the tower grid to house the computer, power supplies and test engineer.

On the north ridge, an orange marker was placed on the ground and lined up with an identical marker on the south ridge to guide the helicopter pilot over the appropriate tower. These markers were moved in response to the anticipated upslope or downslope winds to maximize the vortex penetration and persistence in the tower grid. A radar gun was operated from the south marker.

The three Forest Service sample card lines were located north of the stream just below the north ridge crest, along the tower line, and south of the stream just below the south ridge crest.

A tethersonde was operated by Nowcasting of Chico during spray tests. It was located approximately 150 ft downslope from tower 10 and measured wind velocity, direction and wet/dry bulb temperatures at various levels above the ground.

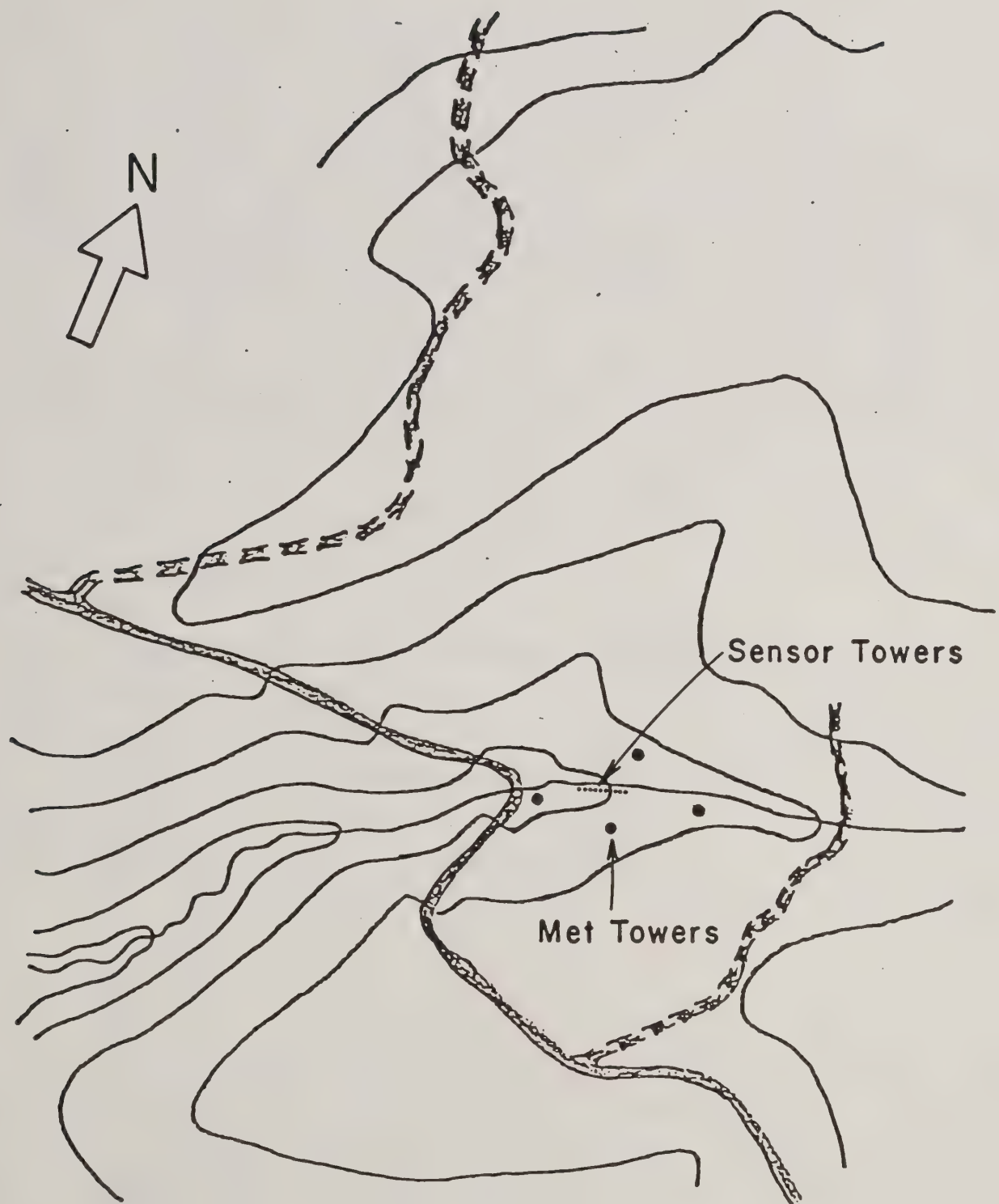


Figure 2-1. Jones area test site.

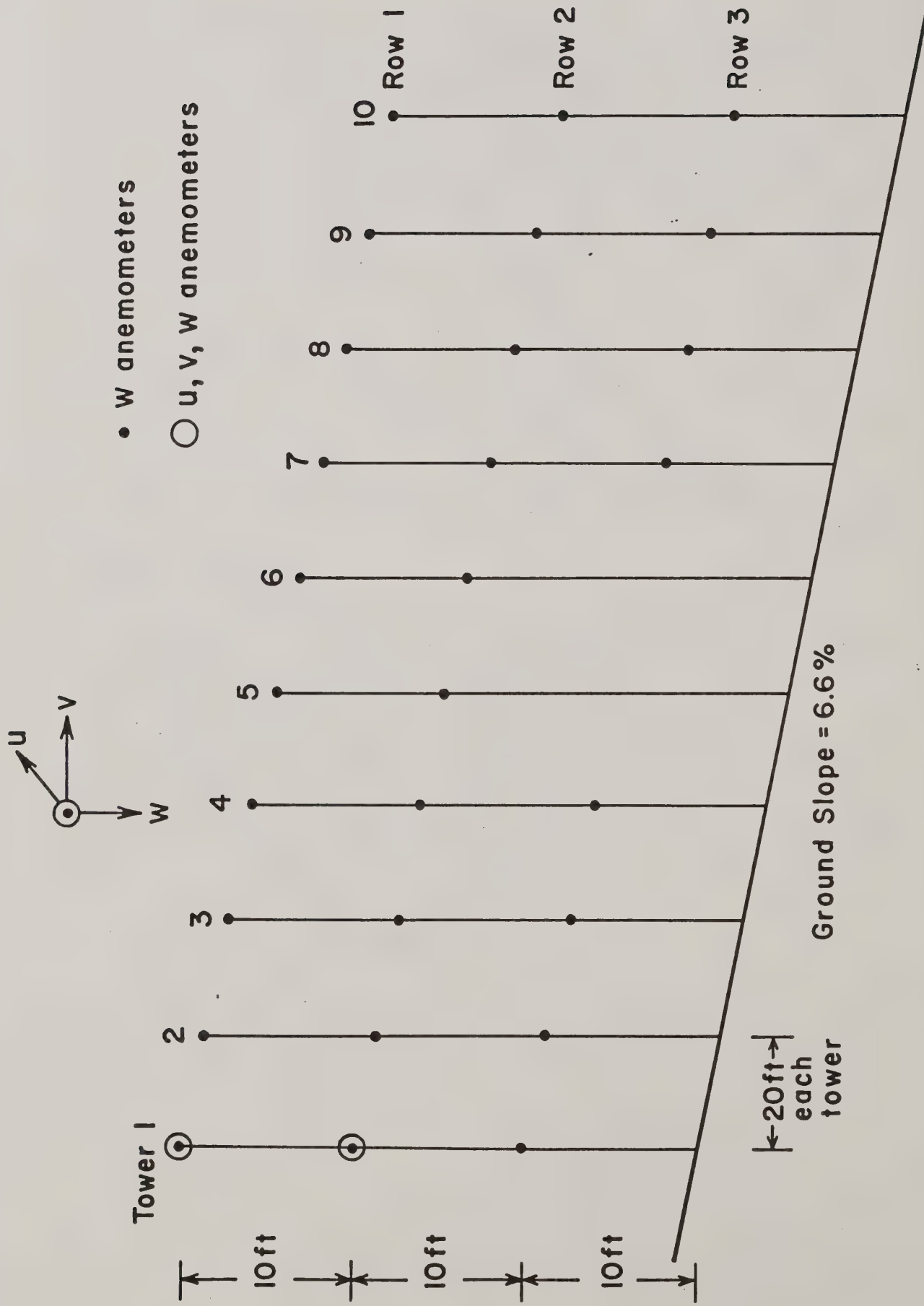


Figure 2-2. Anemometer instrumentation grid used for wake velocity measurements (not to scale).

3. TEST INSTRUMENTATION

The primary instrumentation consisted of a vertical grid of tower-mounted anemometers (shown previously in Figure 2-2), with the wake velocity signals sampled and recorded by a digital data acquisition system during the aircraft flight over the towers. UVW sampling was also done during the time between spray runs. Aircraft altitude was measured photographically. Ground speed was measured by Doppler radar and with photographs, and video recordings were taken of vortex patterns whenever possible. A more detailed description of the instrumentation system is given below.

3.1 Anemometer Towers

The towers used to mount the flow measuring instrumentation were telescoping masts which were extended to a height of 30 ft. The towers were placed in a single line along the stream at 20-ft intervals, yielding a 180-ft grid span. The anemometers were mounted vertically at the 10, 20 and 30-ft levels on each tower. In addition to the vertical sensors, two UVW sensors were mounted on tower 1 at the 20 and 30-ft levels.

3.2 Anemometers

Gill anemometers manufactured by the R.M. Young Company, on loan to the U.S. Forest Service from the Transportation Systems Center of the U.S. Department of Transportation were used for this study. Four-bladed propellers (19 cm in diameter) were coupled with the DC generators to complete the anemometer. The anemometers were mounted on the towers oriented vertically in the plane of the tower to measure the vertical velocities of the wake.

The anemometers were mounted on the masts at three heights. All masts had anemometers mounted at the three positions; however, due to the 32-channel limit on the data acquisition system, not all of the anemometers were monitored during the wake study. The anemometers were electrically connected

to the data acquisition system with filtering capacitors in accordance with the manufacturer's recommendations in order to attenuate the voltage ripples resulting from the brushes contacting different armature segments in the generator.

3.3 Data Acquisition System

The data acquisition system consisted of an IBM Portable PC with two Data Translation DT2801 auxiliary boards to sample and digitize 32 channels of analog voltage signals from the anemometers (Figure 3-1). Sampling was carried out at a rate of 100 samples/sec (each anemometer was sampled every 0.34 sec). The full scale analog voltages ± 1.25 volts were converted to the digital representations 0/4095, respectively, and stored in memory. A maximum of four minutes of data could be sampled continuously (before reaching memory limits) and stored for post test conversion to engineering units and further analysis.

During the time between spray runs, the two UVWs were sampled at one-second intervals. This data was stored on floppy diskettes to be converted later to engineering units and one-minute averages.

3.4 Aircraft Altitude Measurement

The altitude of the aircraft as it passed over the grid of anemometers was measured by photogrammetry. A vertically oriented 35 mm Nikon with electric film transport took pictures of the aircraft flyby at the rate of six frames/sec. The apparent length of the spray boom was compared with the length in calibration photographs taken at known distance from the aircraft. The lateral position of the aircraft with respect to the towers can also be obtained from these photographs.

3.5 Aircraft Ground Speed and Measurement

Aircraft ground speed was measured using a U.S. Forest Service supplied Doppler radar speed gun. The operator was positioned at the south flight path marker. As the aircraft approached, it remained sufficiently far away so that the line of sight measurement was a satisfactory approximation of true ground speed. The calibration of the unit was checked with a tuning fork with frequency simulating a flight speed of 50 mph. This particular unit worked well except for the flights under 20 mph.

3.6 Ambient Wind and Temperature Profiles

Along with the UVW data obtained from tower 1, the Forest Service placed four towers (Campbells) at various locations around the test site to measure the UVW wind components at 3 and 10-meter heights. These Campbells also recorded temperature and heat flux and stored this information onto cassette tapes. Additionally, Atmospheric Sciences Laboratory (ASL) recorded extensive meteorological altitude profile data with their met towers.

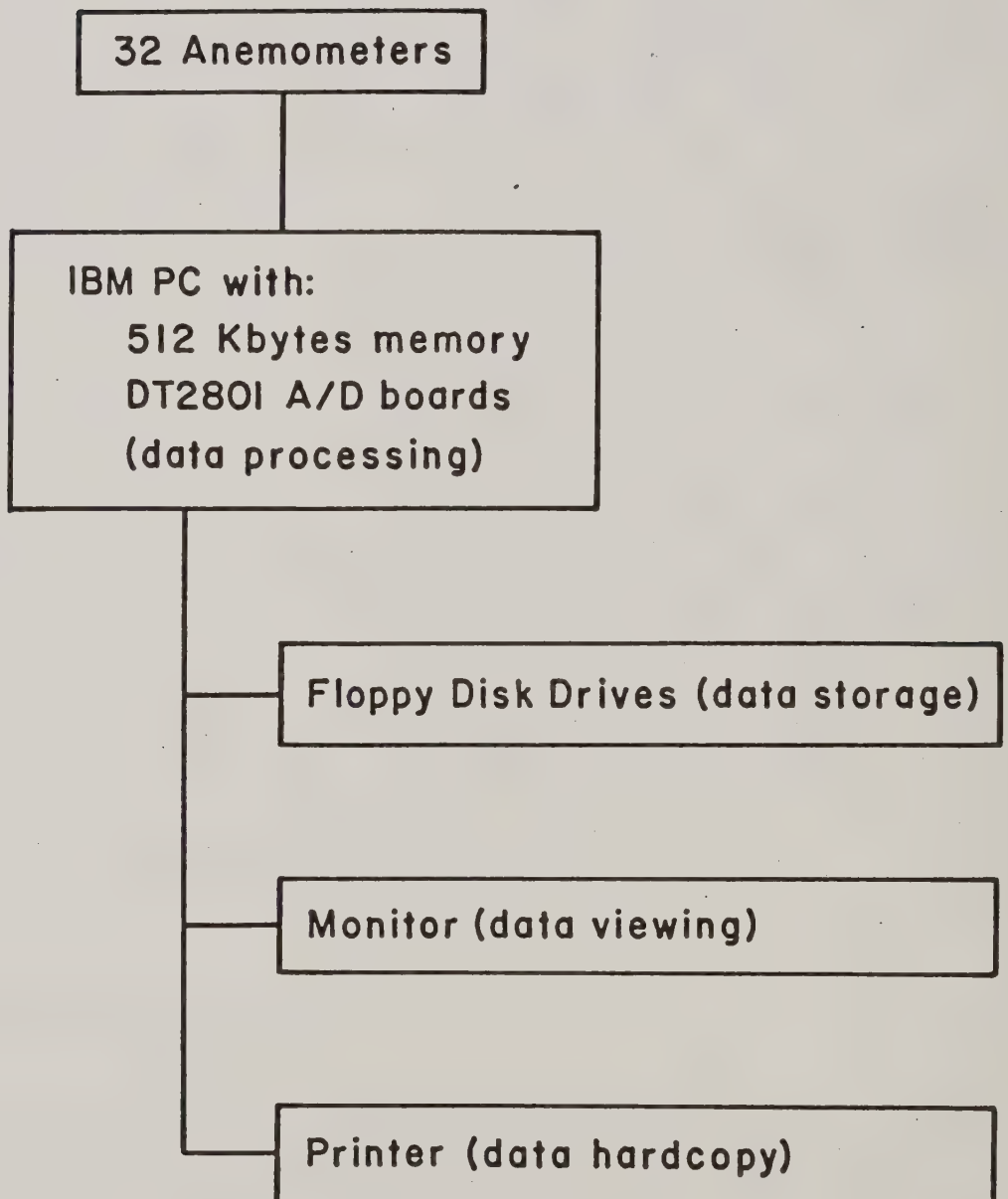


Figure 3-1. Instrumentation schematic for wake flow field tests.

4. TEST PROCEDURE

Personnel arrived on-site prior to sunrise for each day of testing. The IBM Portable PC was connected to the anemometers and battery/generator power, and the data acquisition system (DAS) was checked out. Some of the mornings were very cold and errors occurred on the DAS. These errors were eliminated by allowing the computer system to warm-up for a few minutes.

Once the system had successfully completed its checkout, the UVW sampling began at one-second intervals. During this time, Forest Service personnel placed the sampling cards out on the three card lines. The aircraft would also arrive and land in a clearing a few hundred yards north of the towers.

The test coordinator would relay the desired flight conditions to the pilot who would then fly over the desired tower based on the crosswind data and placement of the north-south orange markers. The computer operator would initiate the data acquisition sequence based on visual contact with the aircraft. The test coordinator, standing at the south marker, would record the ground speed of the helicopter using the Doppler radar gun. The vertically oriented camera under the flyover tower would take a burst of pictures to record the height and position of each flyover. The computer would then continue to sample for approximately two minutes and the data would be stored onto a floppy diskette. The helicopter would land in the clearing and await further instructions.

After the computer had finished storing the wake data, sampling of the UVW anemometers began once again. The sampling cards would be collected after they had dried, and new cards would be put in their place. This procedure took approximately 35 to 45 minutes per spray run.

Depending on crosswind conditions the helicopter would be instructed to fly once again over the desired tower, and the procedure would be repeated about four times each morning. After the spray runs had been completed, two more helicopter runs were made without spray at various speeds for additional wake study data collection.

During the entire testing period, the tethersonde recorded wind and temperature data at various heights above the ground.

In several instances the anemometer data was reviewed on-site to report any anomalous behavior occurring during testing. After returning from the test site, all of the data was backed up and reduced for analysis. The wake data was sent to Continuum Dynamics, Inc. for processing, to locate the vortices using programs resident on Continuum Dynamics, Inc.'s Microvax II computer system. Midway through testing, one set of results was sent back to the test site, and adjustments were made in the flyover speeds of the helicopter.

5. TEST MATRIX

The objective of the test program was to collect aircraft wake data (vortex trajectories) in a hilly terrain, while also through other experiments, collect surface deposition data. Most of the test runs were performed with a helicopter, flying a range of forward speeds from near hover to high forward advance. Although aircraft speed and height were also measured during the flyovers, these data were beneficial only in supporting the data reduction algorithm's choice of where the aircraft vortices first encountered the instrument grid.

The complete test matrix and pertinent comments regarding the data runs are contained in Table 5-1.

TABLE 5-1

Test Matrix

<u>Run No.</u>	<u>Card No.</u>	<u>Day</u>	<u>Time</u>	<u>Tower</u>	<u>Speed (mph)</u>	<u>Aircraft</u>
1	-	04/27	0854	Center	230	C-130
2	-	04/27	0905	Center	230	C-130
3	-	04/27	0916	Center	230	C-130
4	-	04/27	0926	Center	230	C-130
5	1	04/28	0638	4	82	Bell 206B
6	2	04/28	0802	4	72	Bell 206B
7	3	04/28	0907	7	59	Bell 206B
8	4	04/29	0630	4	62	Bell 206B
9	5	04/29	0714	4	57	Bell 206B
10	6	04/29	0806	7	54	Bell 206B
11	7	04/29	0906	7	52	Bell 206B
12	-	04/29	0953	7	40	Bell 206B
13	-	04/29	1001	7	25	Bell 206B
14	8	04/30	0608	4	56	Bell 206B
15	9	04/30	0652	4	50	Bell 206B
16	10	04/30	0732	1	46	Bell 206B
17	11	04/30	0838	7	50	Bell 206B
18	-	04/30	0925	9	38	Bell 206B
19	-	04/30	0931	9	33	Bell 206B
20	12	05/01	0635	2	62	Bell 206B
21	-	05/04	0615	4	72	Bell 206B
22	-	05/04	0620	4	65	Bell 206B
23	-	05/04	0627	4	56	Bell 206B
24	-	05/04	0635	2	52	Bell 206B
25	-	05/04	0641	2	45	Bell 206B
26	-	05/04	0648	2	38	Bell 206B
27	-	05/04	0655	2	30	Bell 206B
28	-	05/04	0702	2	33	Bell 206B
29	-	05/04	0708	2	27	Bell 206B
30	-	05/04	0715	2	Near Hover	Bell 206B
31	-	05/04	0721	2	71	Bell 206B
32	-	05/04	0727	2	55	Bell 206B
33	-	05/04	0739	Center	Near Hover	Bell 206B
34	-	05/04	0800	Center	Near Hover	Bell 206B
35	-	05/04	0803	Center	Near Hover	Bell 206B
36	16	05/04	0909	Center	56	Bell 206B
37	17	05/04	0954	9	49	Bell 206B
38	18	05/04	1040	9	52	Bell 206B

TABLE 5-1 (Cont'd)

<u>Run No.</u>	<u>Card No.</u>	<u>Day</u>	<u>Time</u>	<u>Tower</u>	<u>Speed (mph)</u>	<u>Aircraft</u>
39	19	05/07	0820	2	52	Bell 206B
40	20	05/07	0911	9	53	Bell 206B
41	21	05/07	0950	9	54	Bell 206B
42	22	05/07	1024	9	53	Bell 206B
43	-	05/08	0703	2	90	Bell 206B
44	-	05/08	0708	2	89	Bell 206B
45	23	05/08	0727	2	57	Bell 206B
46	24	05/08	0812	9	54	Bell 206B
47	25	05/08	0846	9	57	Bell 206B
48	26	05/08	0932	9	Unknown	Bell 206B
49	-	05/08	0938	9	51	Bell 206B

6. UVW DATA REDUCTION

Two UVW sensors were mounted on tower 1 at the 20 and 30-ft levels and sampled at one-second intervals when aircraft flyovers were not occurring. Table 6-1 summarizes the date and sampling times for the collected UVW data.

Figures 6-1 to 6-18 display the wind velocity time histories for each of the sensors for each of the six days. These traces are one-minute averages of the one-second data. Gaps between the traces are the times when the spray runs were performed and the UVWs were not sampled. Several of the plots show an A/D sampling error, indicated by a significant spike in the velocity signal. When this event occurs, the digital acquisition system is reset to function properly. Only sixteen such events were encountered from over 374,000 data points taken.

The displayed data confirms the presence of a strong upslope-downslope east-west drainage wind typically between 1 and 3 m/sec, with the horizontal velocity vector shifting occasionally as much as 45° to the north-south. These velocity levels are large in comparison to the vertical W velocities recorded. The success in analyzing the tower grid data (examined in the next section) again illustrates the usefulness of collecting only vertical velocity data, even in a complex terrain. Discerning the "mean" lateral velocity and removing these values from the tower data to recover the position and strength of the aircraft vortices using horizontal anemometers would be a formidable task under the flow conditions studied during these tests.

TABLE 6-1

UVW Data Summary

<u>Date</u>	<u>Times of Sampling (PDT)</u>	<u>Time Interval (sec)</u>
04/28	0555-0618 0643-0755 0807-0906 0912-0943	0.9874
04/29	0608-0624 0638-0712 0719-0801 0813-0903 0914-0950	1.0016
04/30	0544-0606 0614-0649 0658-0729 0737-0835 0845-0923	1.0014
05/04	0544-0611 0808-0904 0914-0951	1.0012
05/07	0602-0817 0827-0859 0918-0948	1.0016
05/08	0543-0659 0714-0724 0805-0810 0816-0845 0852-0922	1.0010

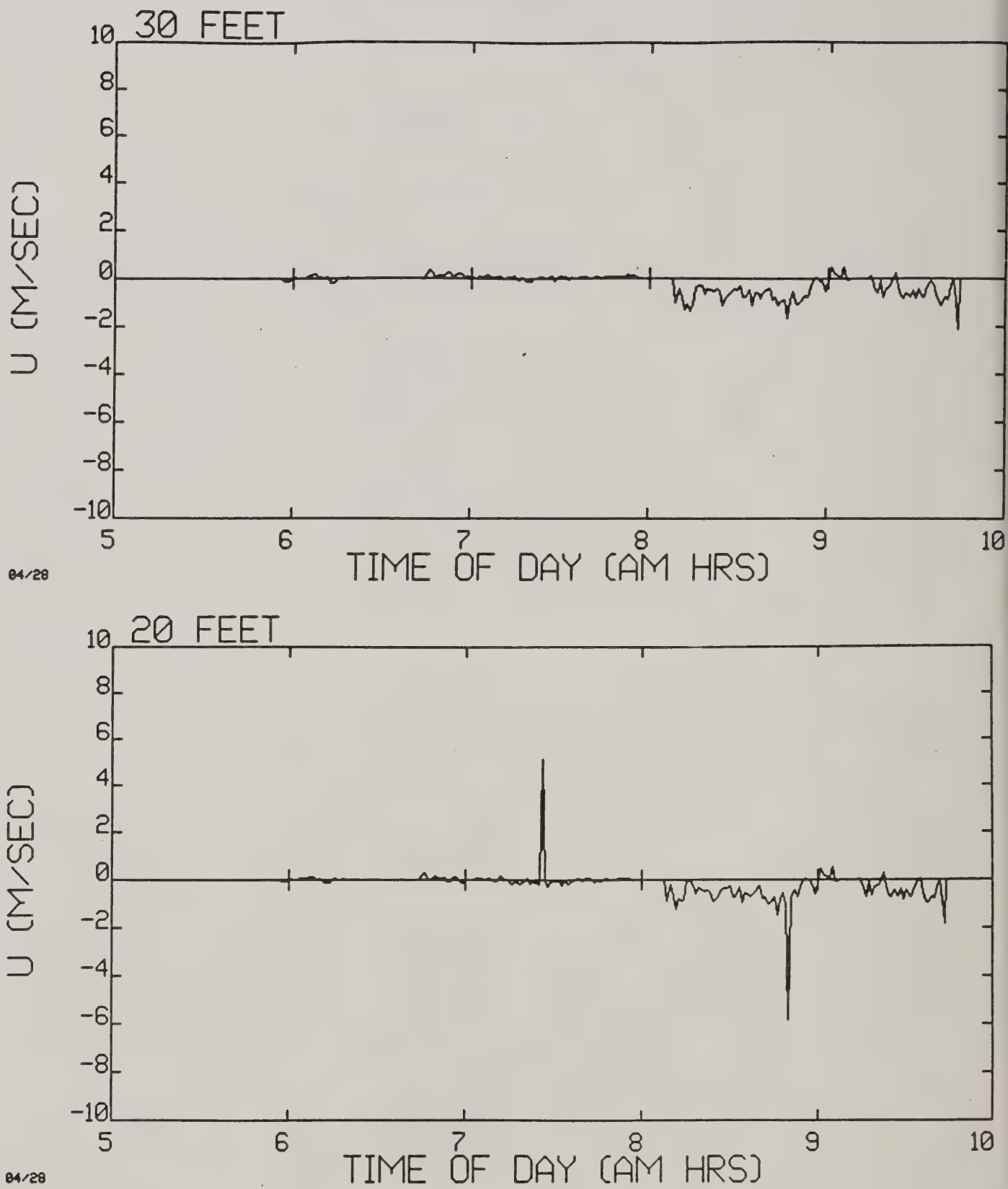


Figure 6-1. One minute averaged axial U velocity profiles at 30 and 20 ft on tower 1 during test day 04/28. Positive velocities point south; negative velocities point north. Four time intervals are included, along with two A/D data dropout points at the 20 ft anemometer.

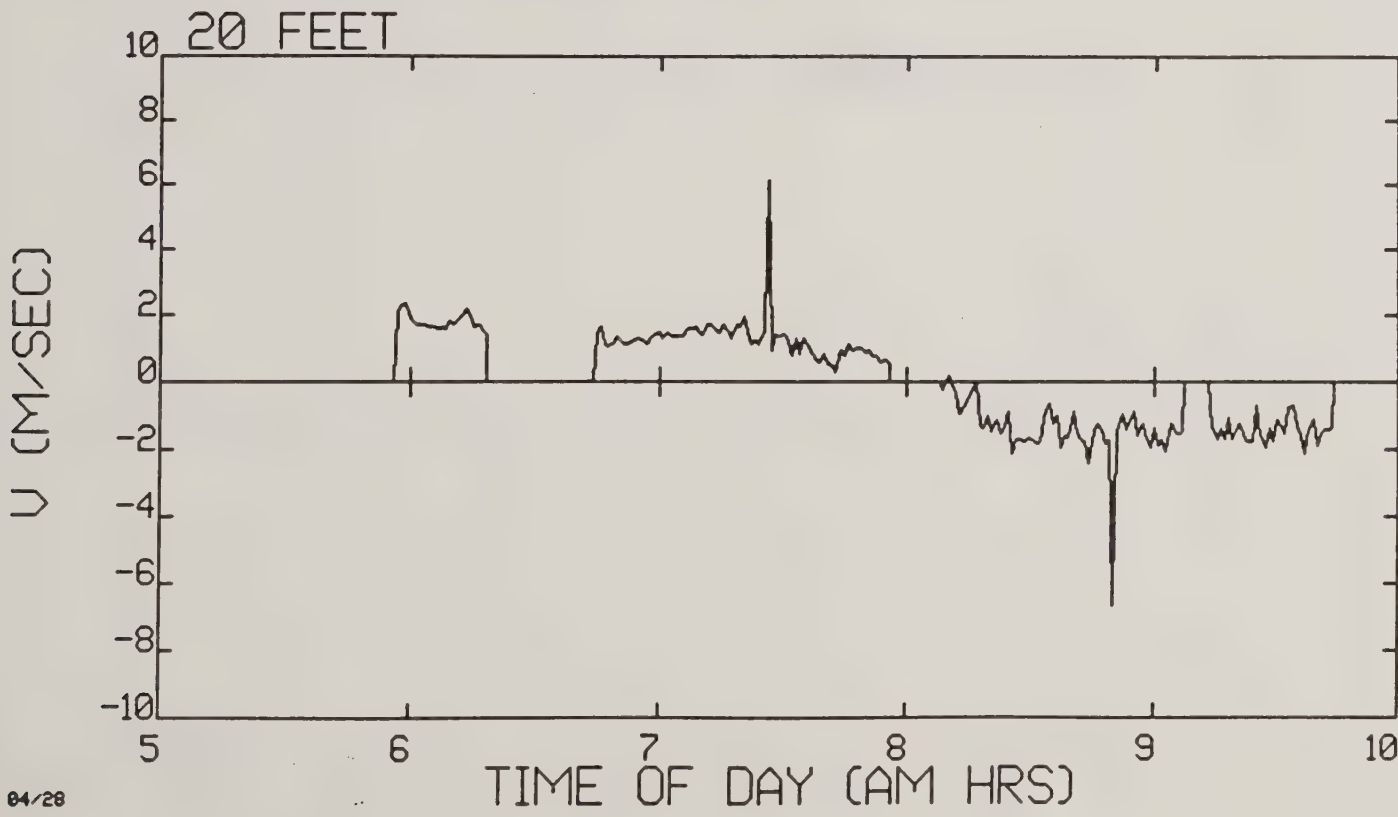
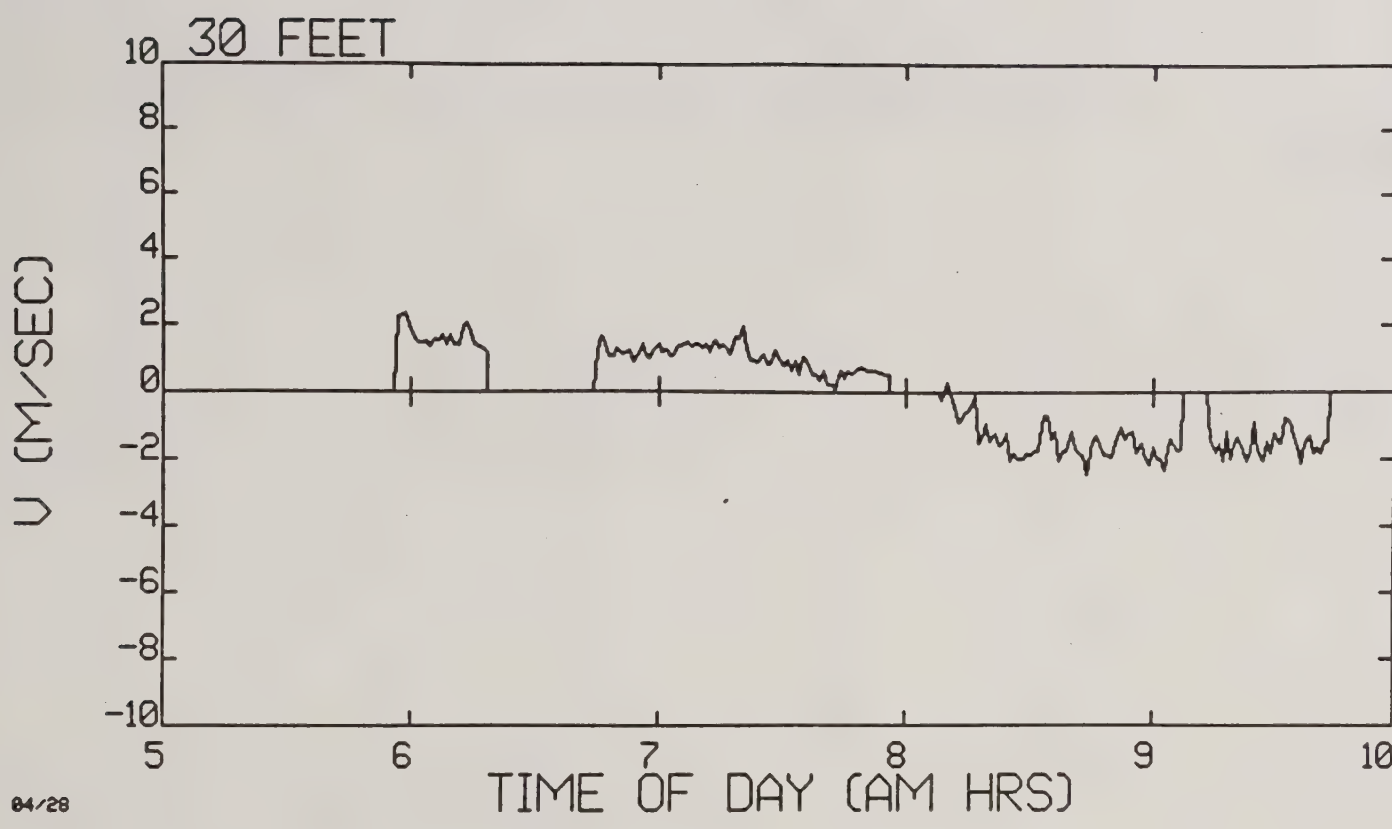


Figure 6-2. One minute averaged lateral V velocity profiles at 30 and 20 ft on tower 1 during test day 04/28. Positive velocities point west; negative velocities point east. Four time intervals are included, along with two A/D dropout points at the 20 ft anemometer.

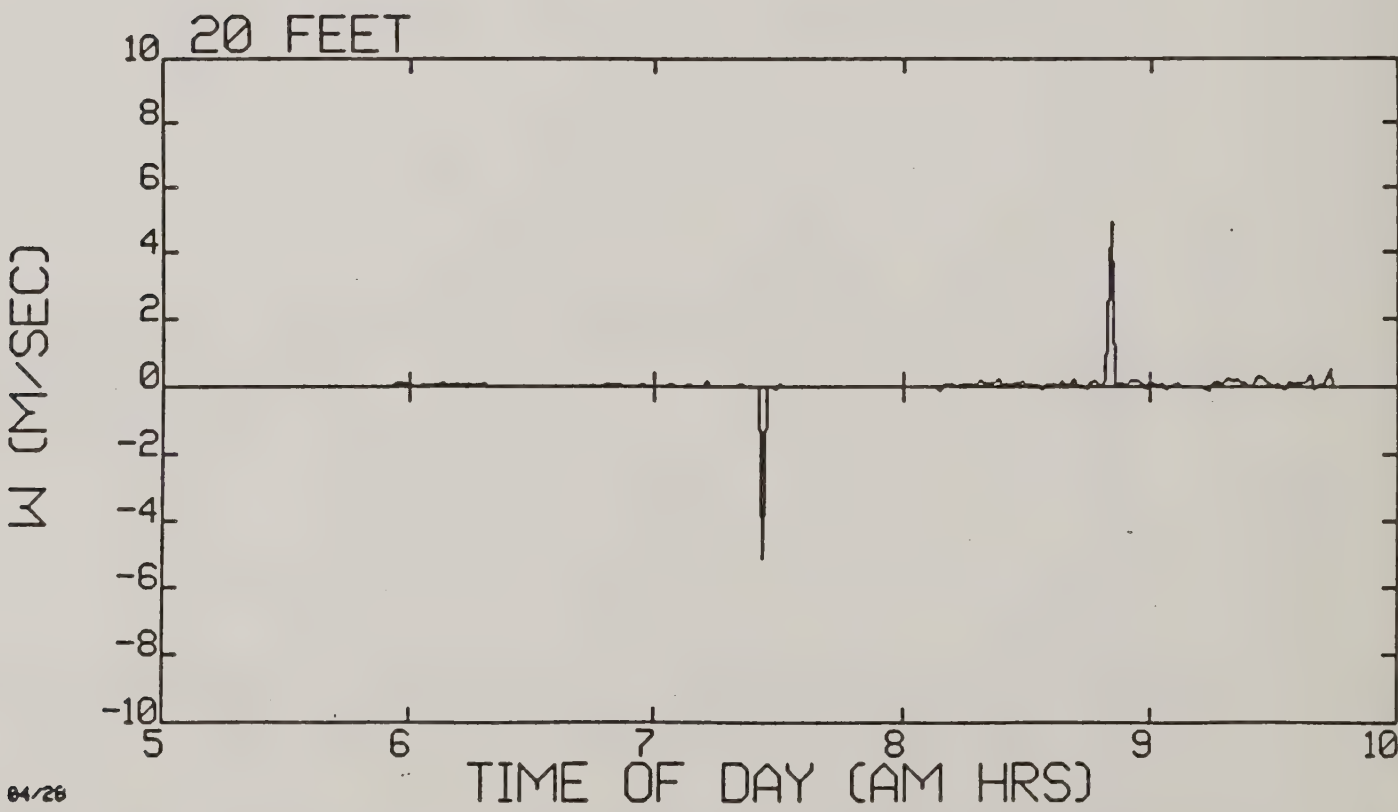
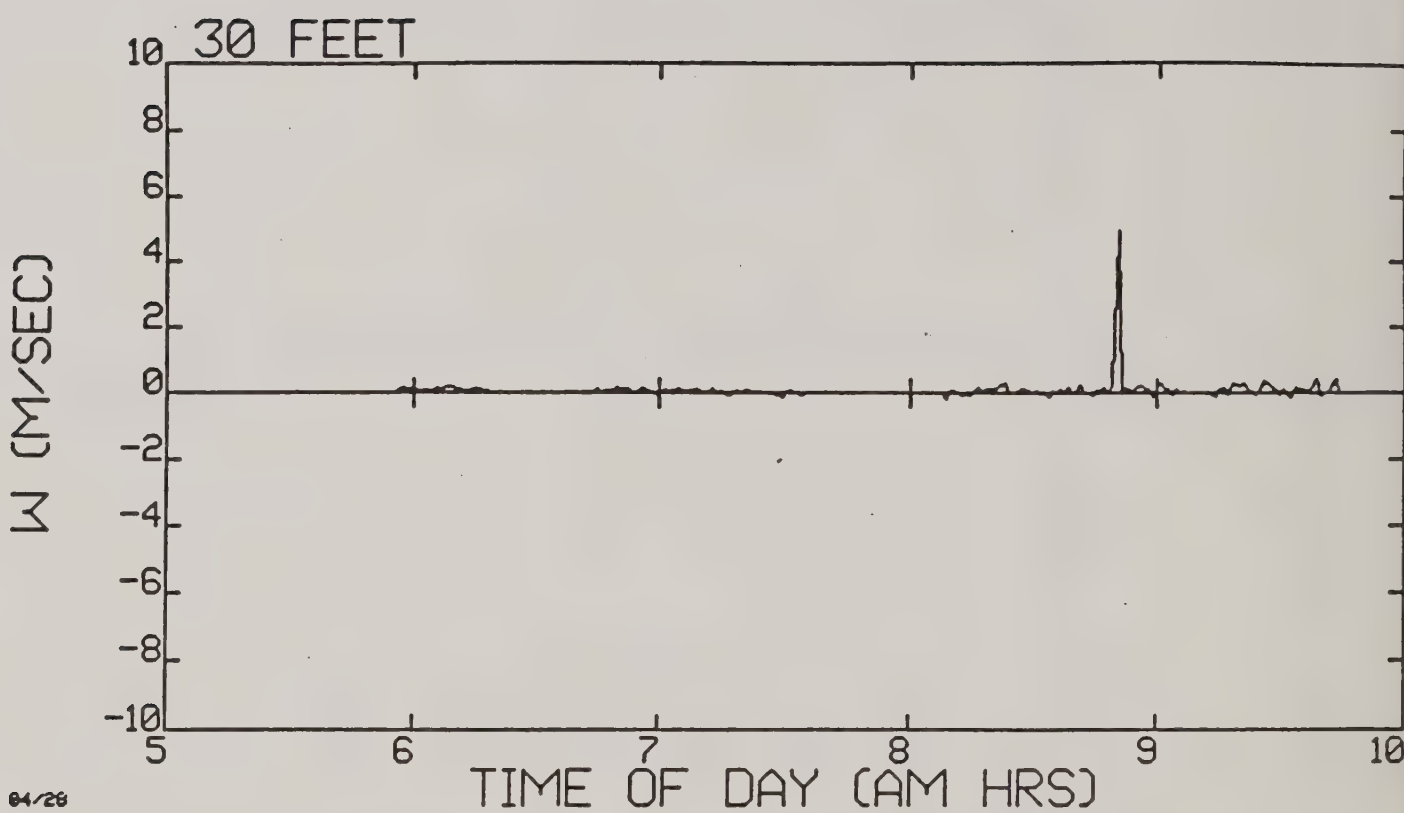


Figure 6-3. One minute averaged vertical W velocity profiles at 30 and 20 ft on tower 1 during test day 04/28. Positive velocities point upward; negative velocities point downward. Four time intervals are included, along with one A/D dropout point at the 30 ft anemometer, and two at the 20 ft anemometer.

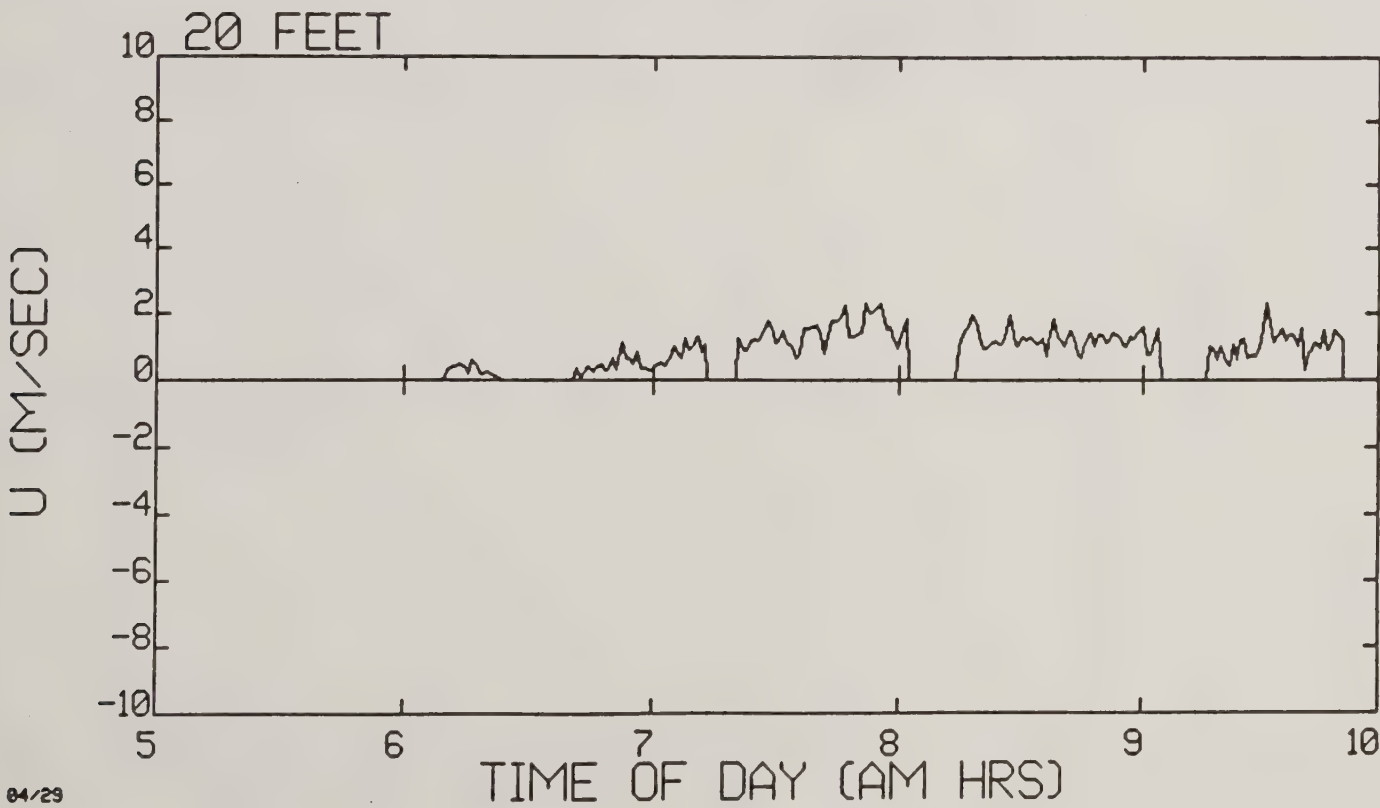
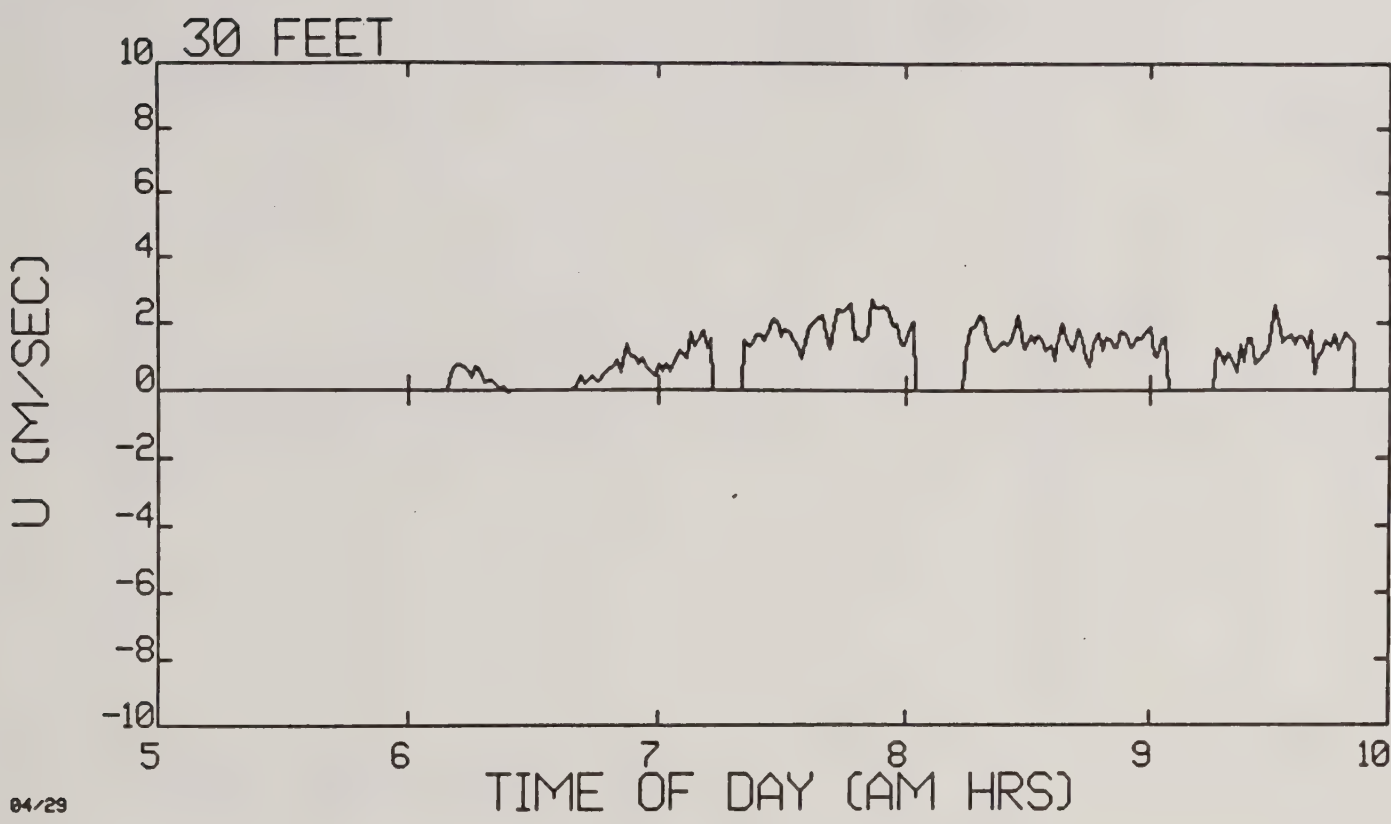


Figure 6-4. One minute averaged axial U velocity profiles at 30 and 20 ft on tower 1 during test day 04/29. Positive velocities point south; negative velocities point north. Five time intervals are included.

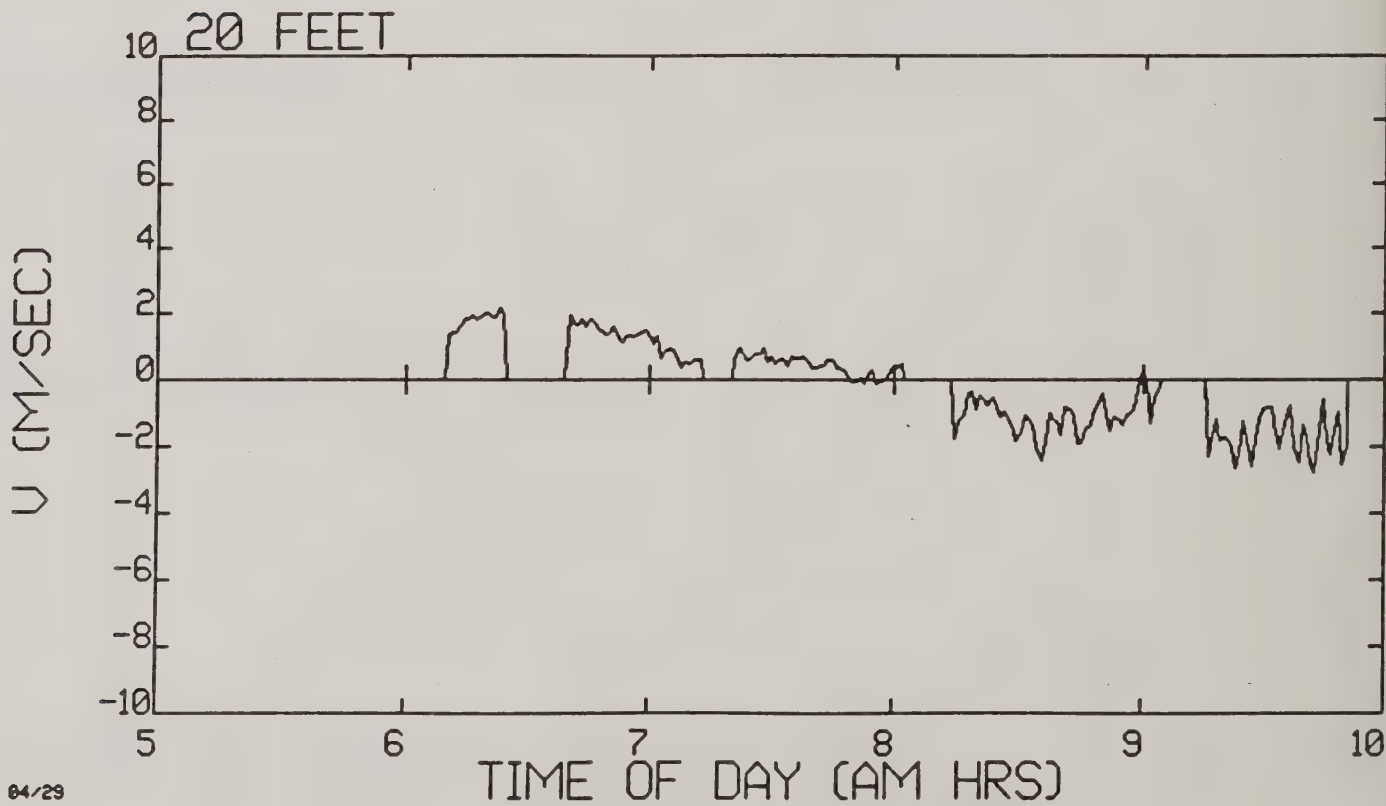
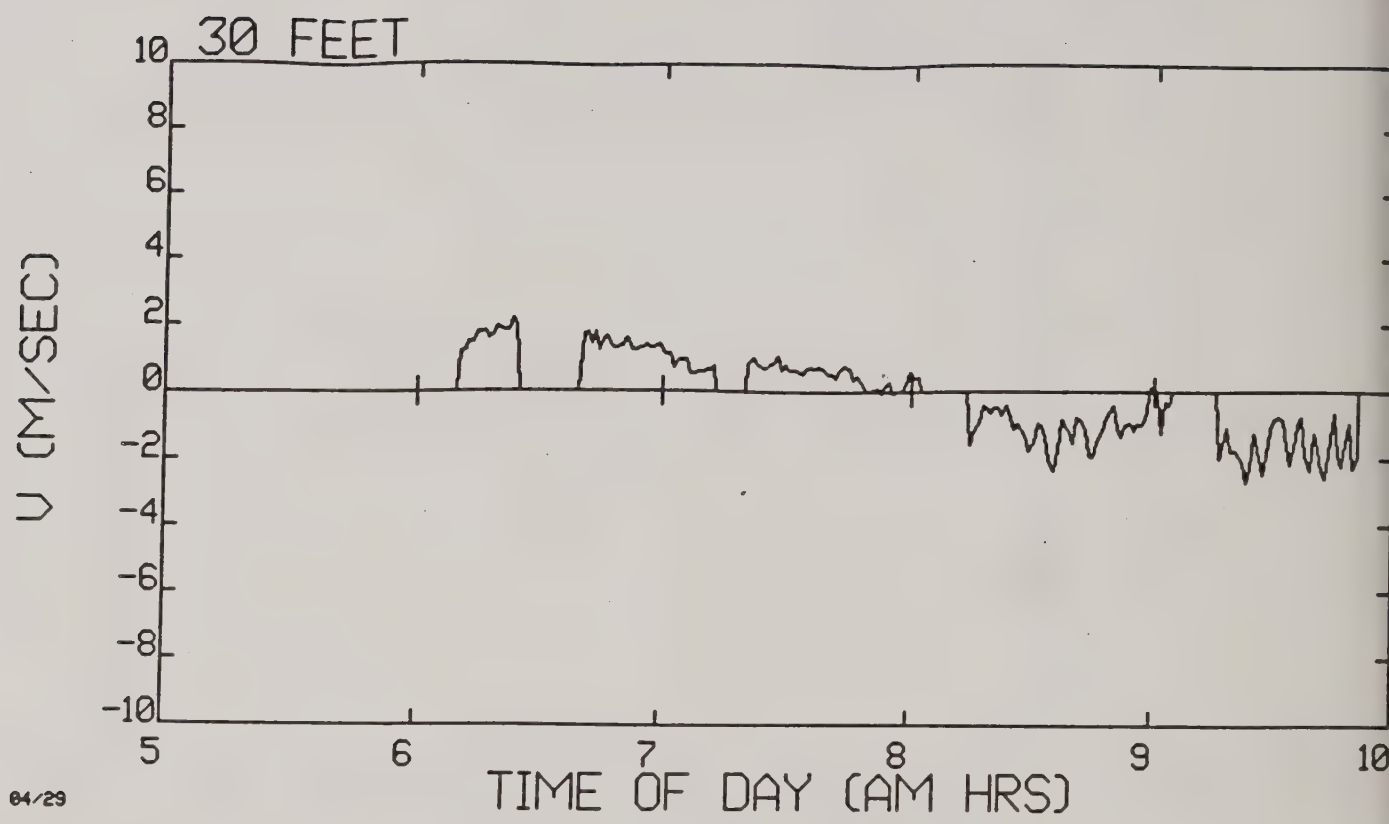


Figure 6-5. One minute averaged lateral V velocity profiles at 30 and 20 ft on tower 1 during test day 04/29. Positive velocities point west; negative velocities point east. Five time intervals are included.

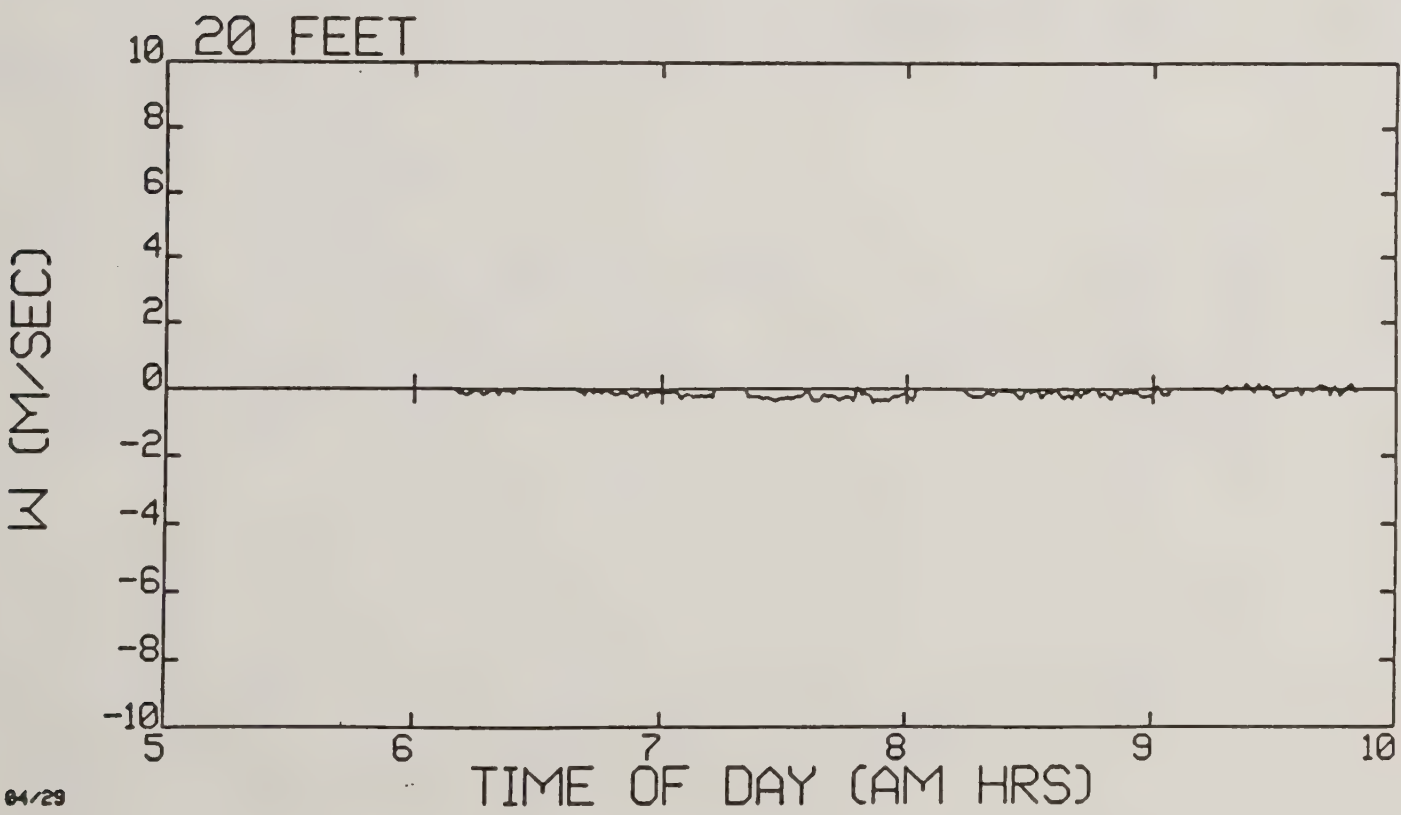
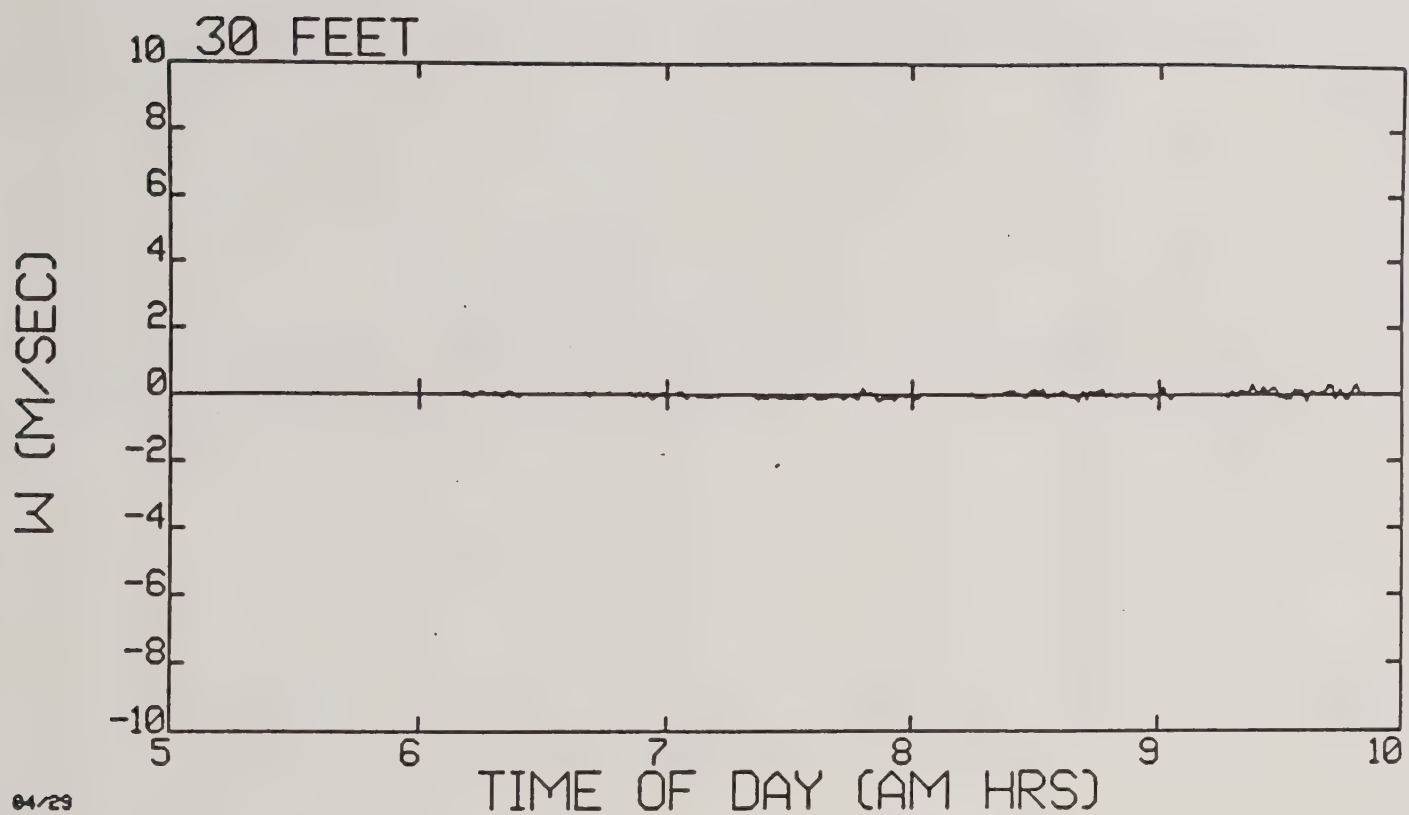


Figure 6-6. One minute averaged vertical W velocity profiles at 30 and 20 ft on tower 1 during test day 04/29. Positive velocities point upward; negative velocities point downward. Five time intervals are included.

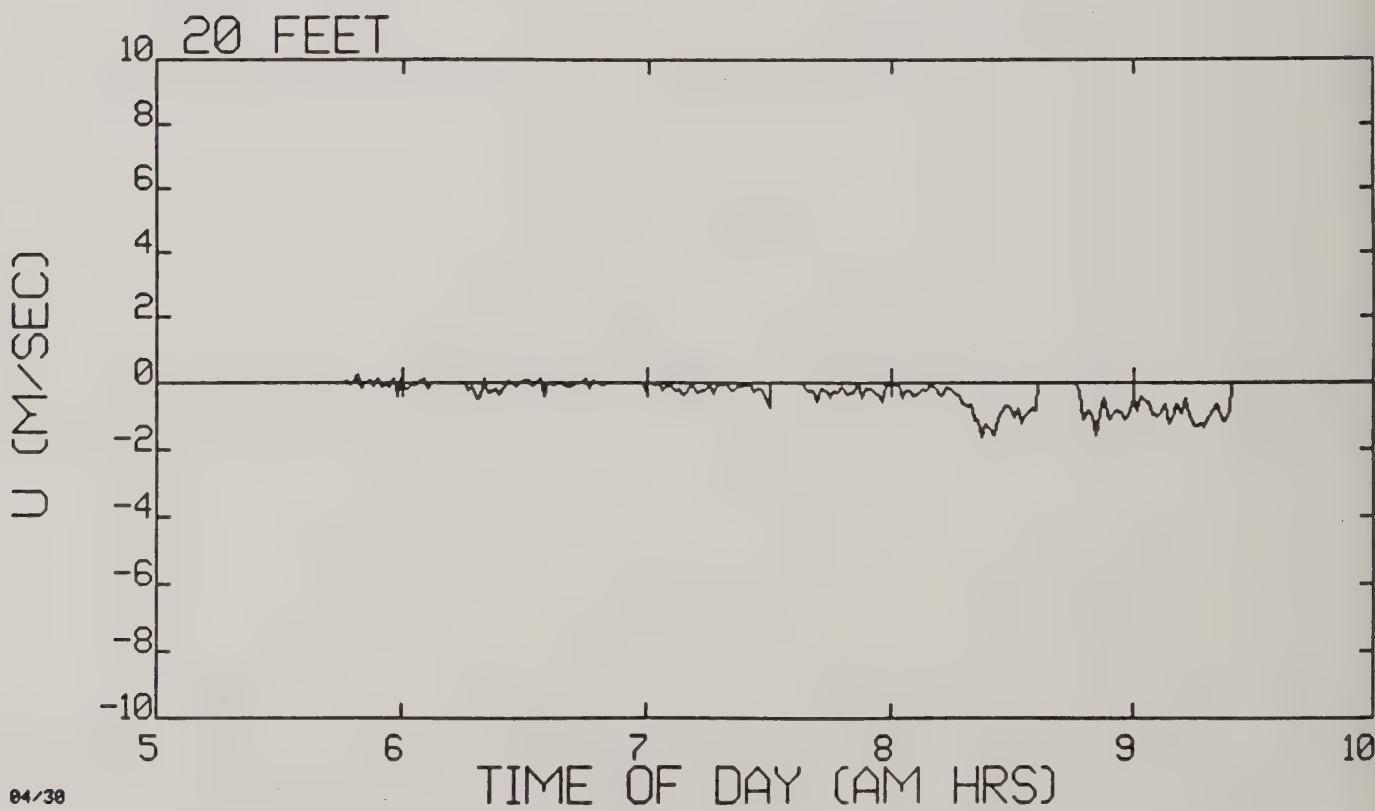
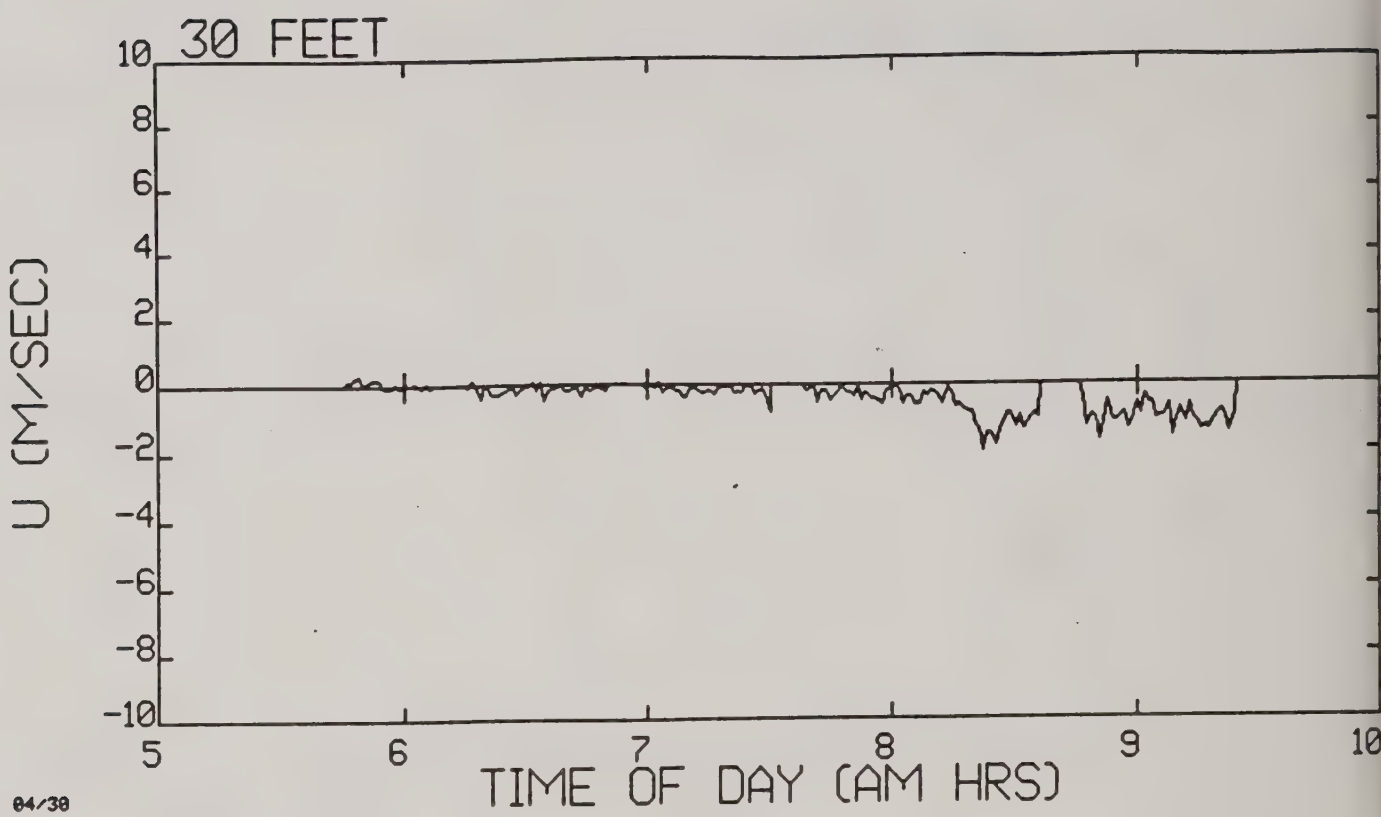


Figure 6-7. One minute averaged axial U velocity profiles at 30 and 20 ft on tower 1 during test day 04/30. Positive velocities point south; negative velocities point north. Five time intervals are included.

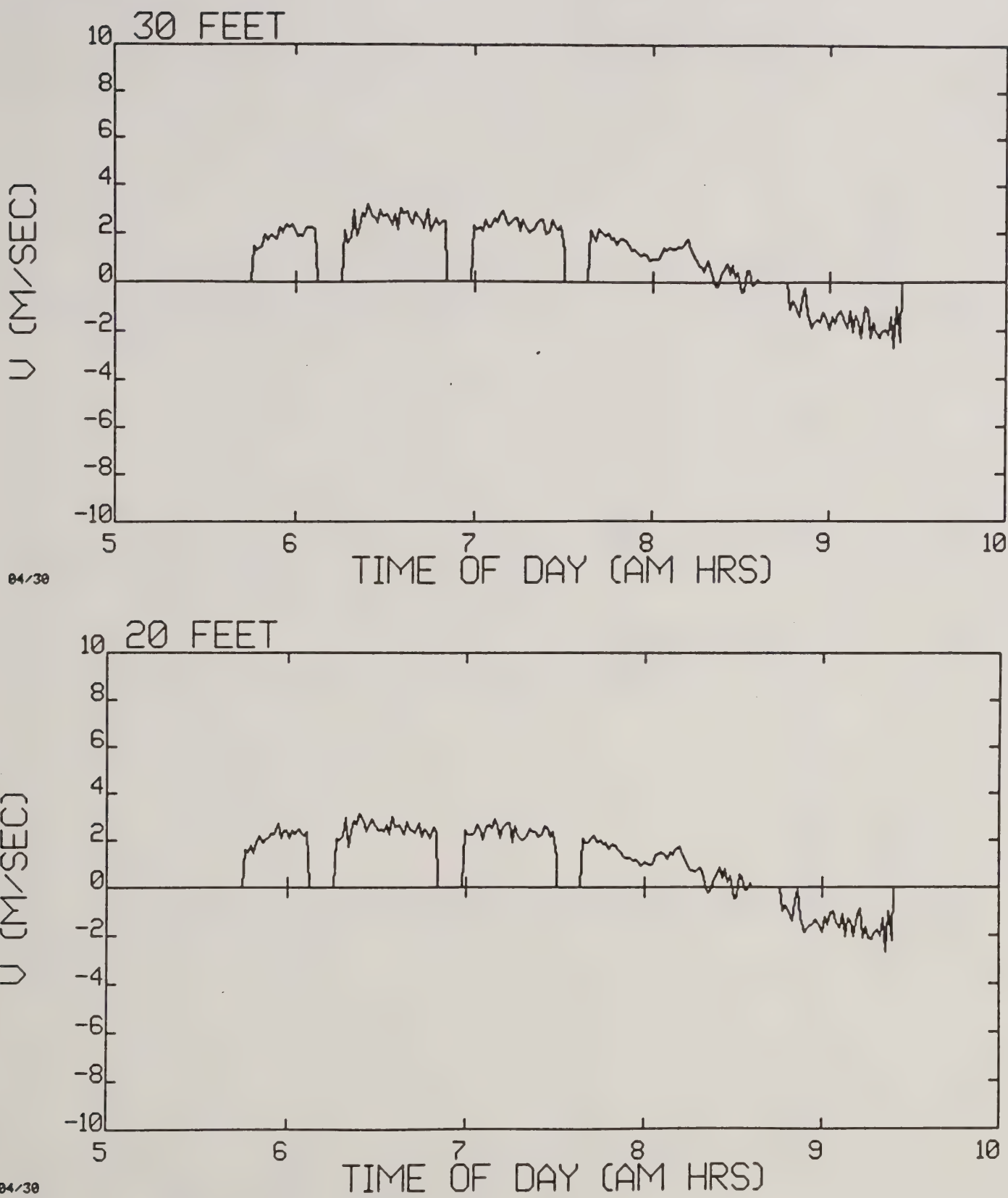


Figure 6-8. One minute averaged lateral V velocity profiles at 30 and 20 ft on tower 1 during test day 04/30. Positive velocities point west; negative velocities point east. Five time intervals are included.

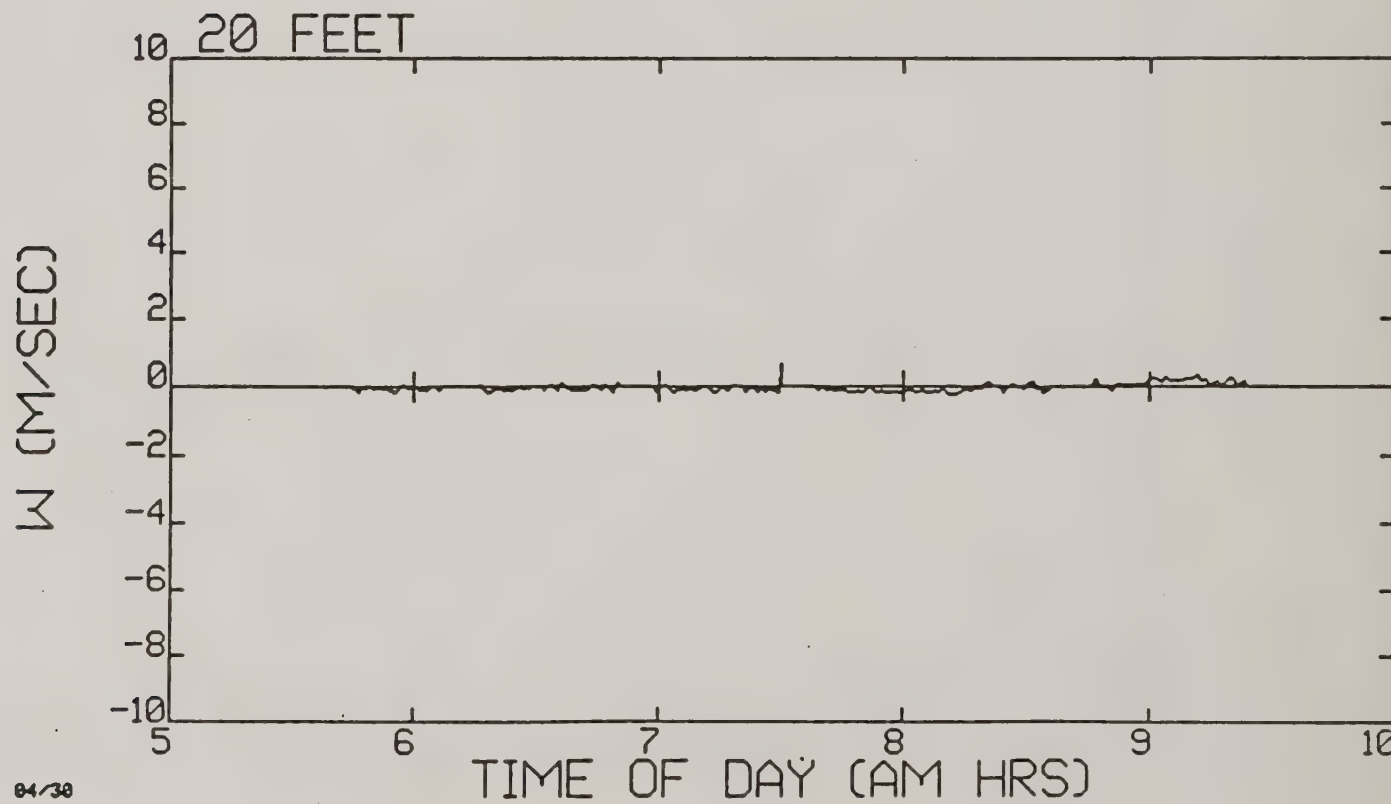
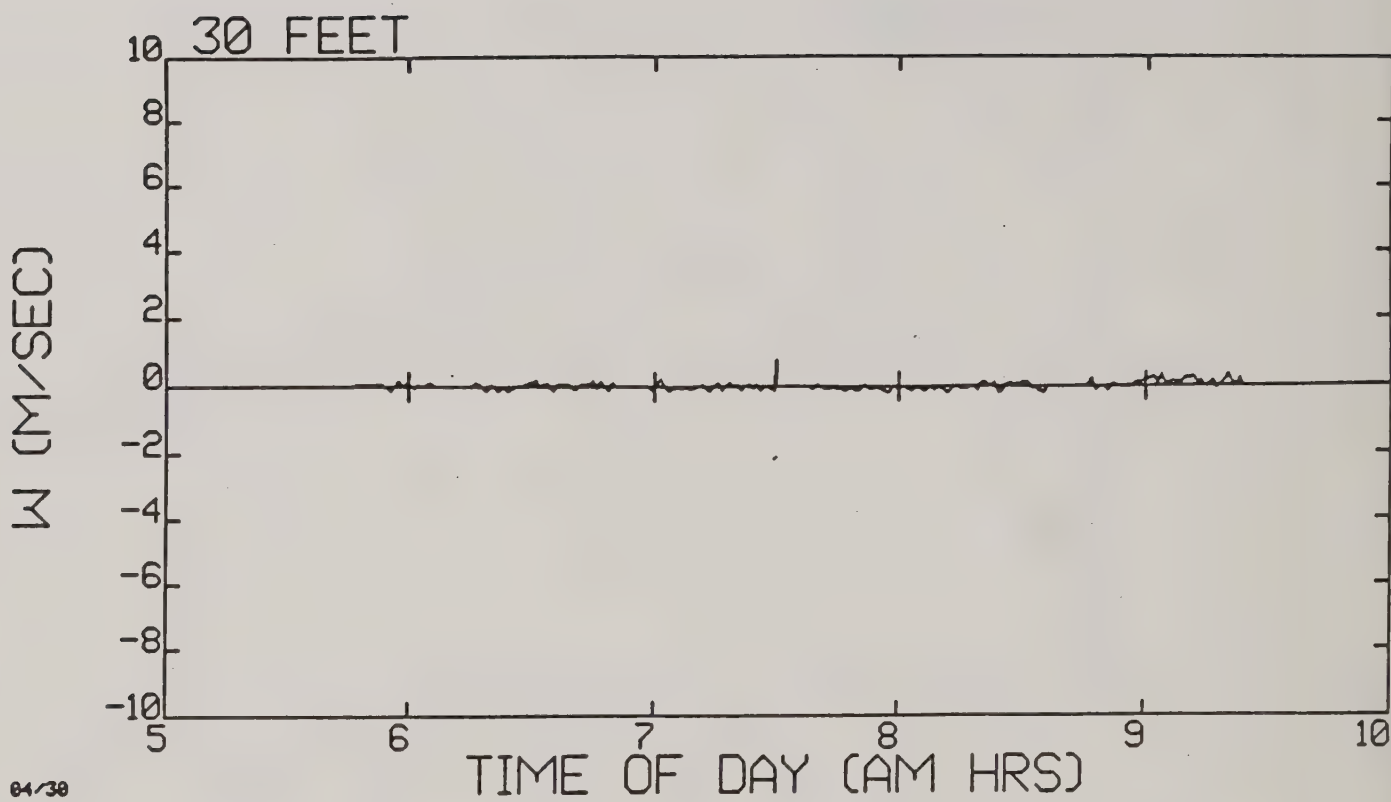


Figure 6-9. One minute averaged vertical W velocity profiles at 30 and 20 ft on tower 1 during test day 04/30. Positive velocities point upward; negative velocities point downward. Five time intervals are included.

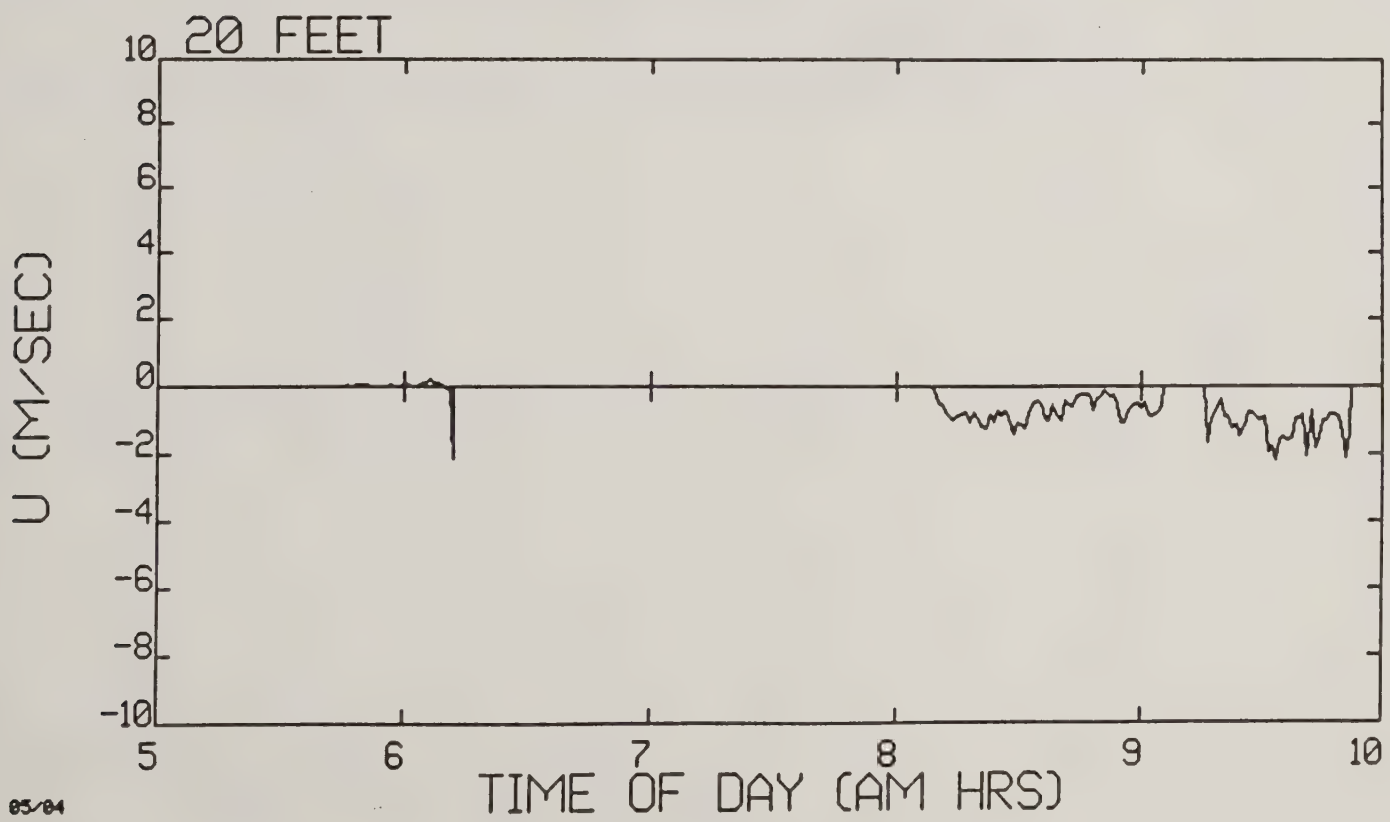
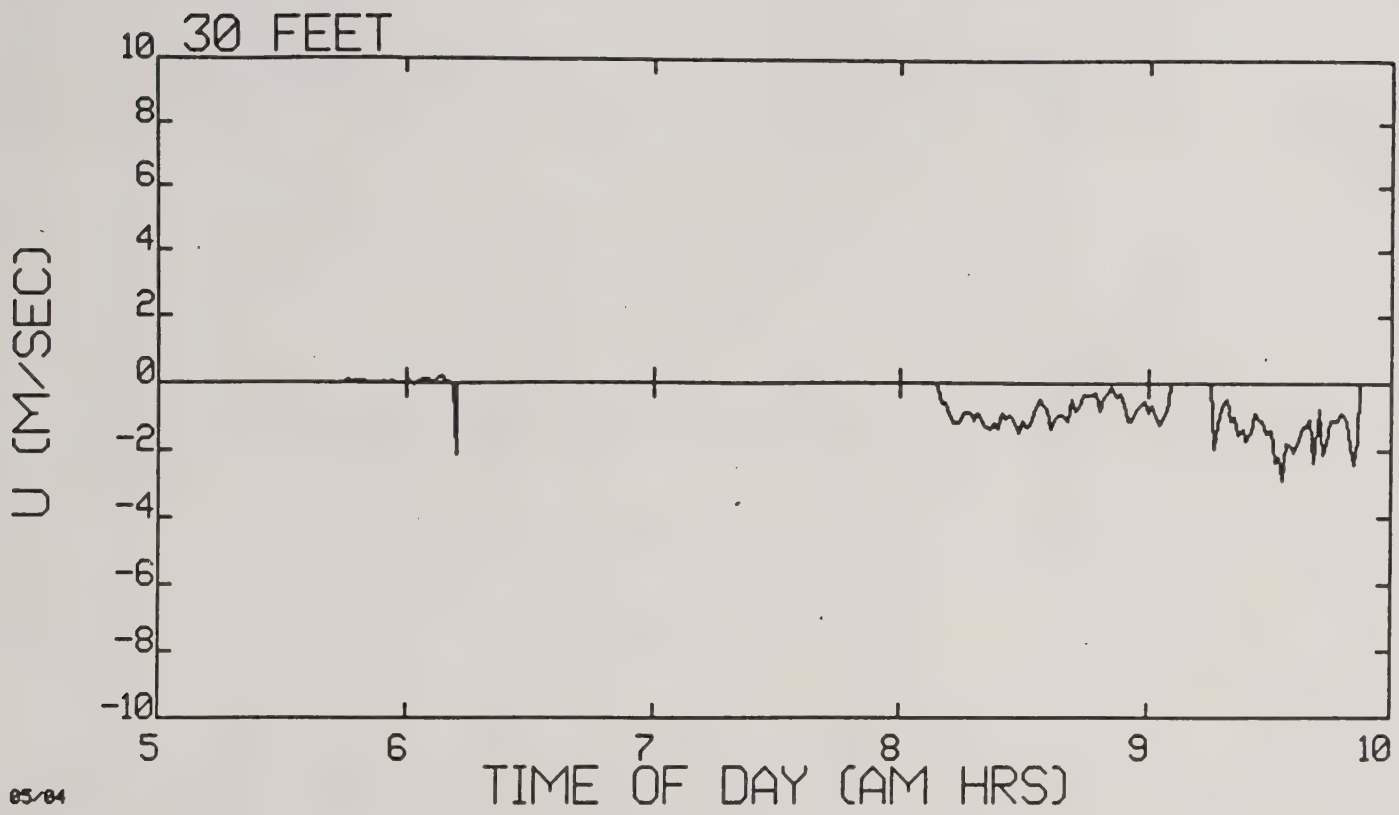


Figure 6-10. One minute averaged axial U velocity profiles at 30 and 20 ft on tower 1 during test day 05/04. Positive velocities point south; negative velocities point north. Three time intervals are included, along with one A/D data dropout point at each anemometer.

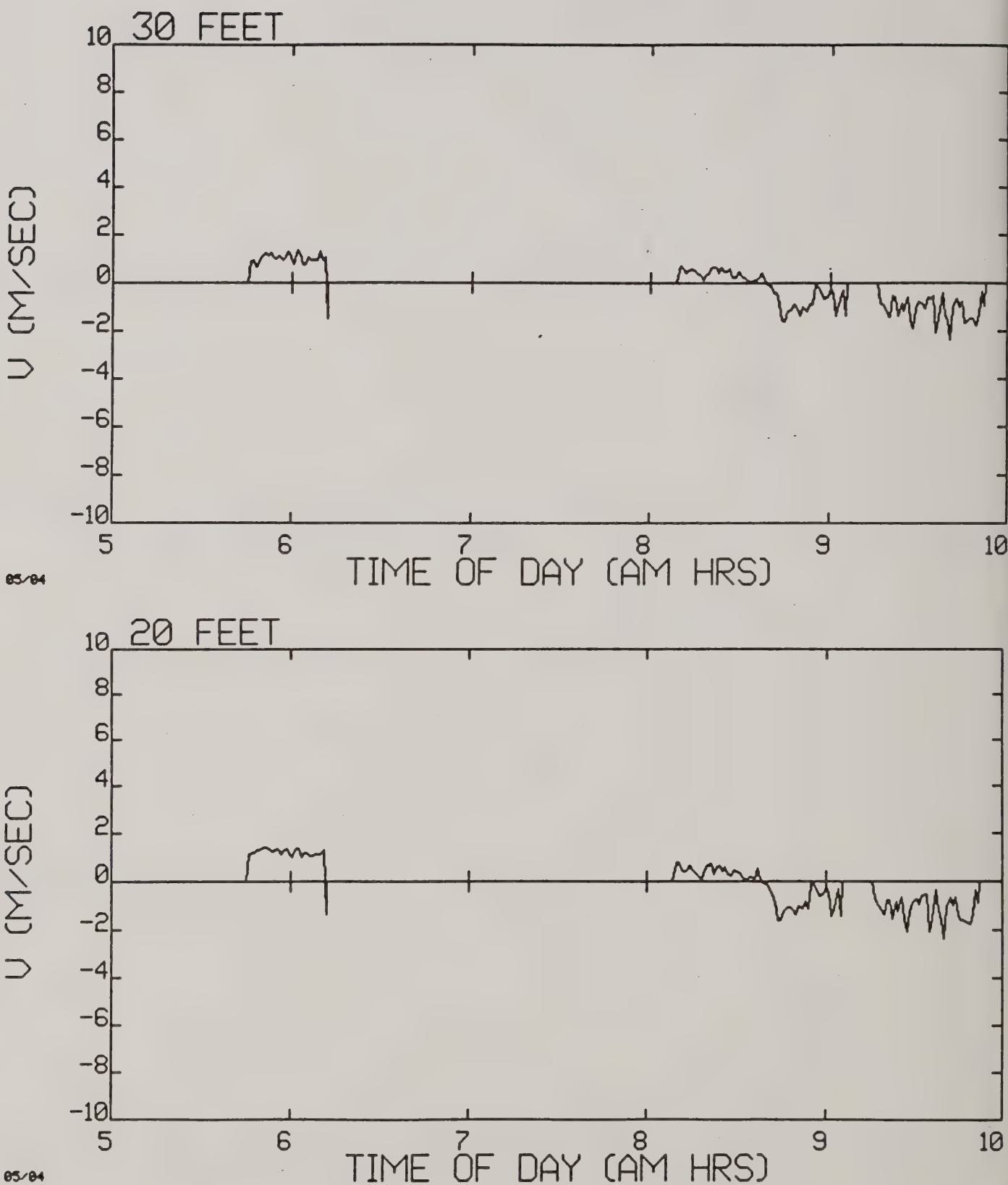


Figure 6-11. One minute averaged lateral V velocity profiles at 30 and 20 ft on tower 1 during test day 05/04. Positive velocities point west; negative velocities point east. Three time intervals are included, along with one A/D data dropout point at each anemometer.

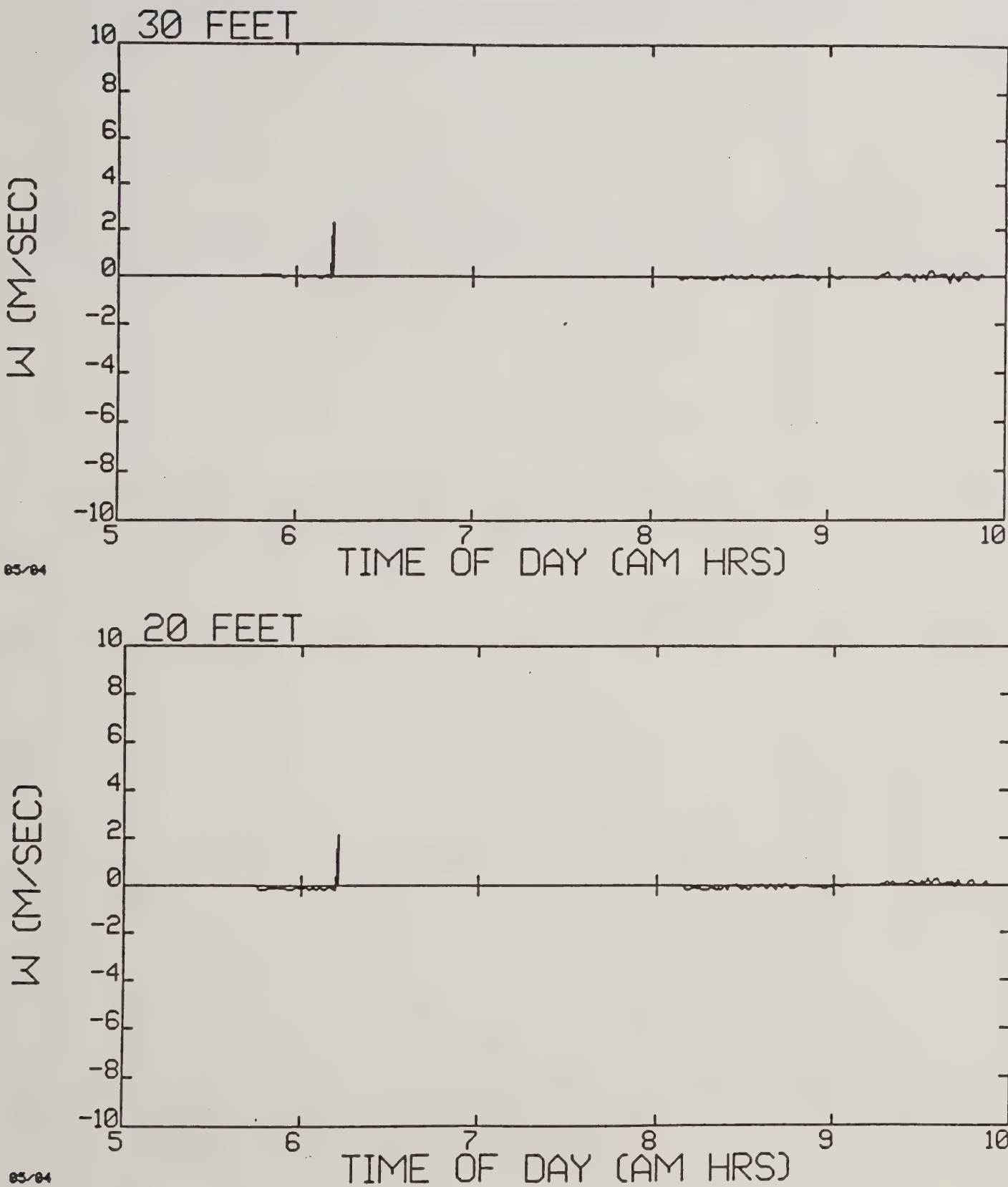


Figure 6-12. One minutes averaged vertical W velocity profiles at 30 and 20 ft on tower 1 during test day 05/04. Positive velocities point upward; negative velocities point downward. Three time intervals are included, along with one A/D data dropout point at each anemometer.

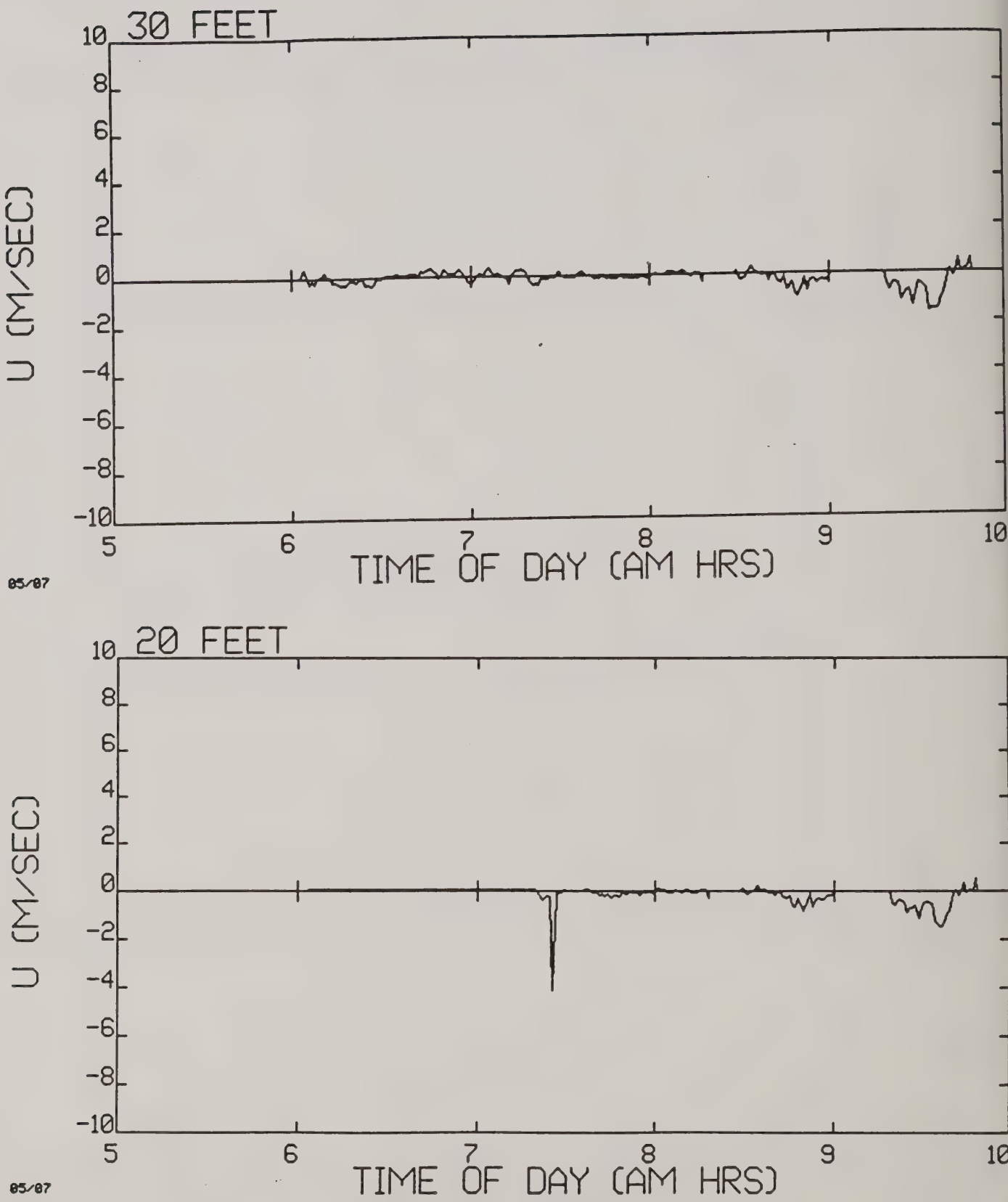


Figure 6-13. One minute averaged axial U velocity profiles at 30 and 20 ft on tower 1 during test day 05/07. Positive velocities point south; negative velocities point north. Three time intervals are included, along with one A/D data dropout point at the 20 ft anemometer. The U profile at 20 ft between 6 - 7 seconds is small but nonzero.

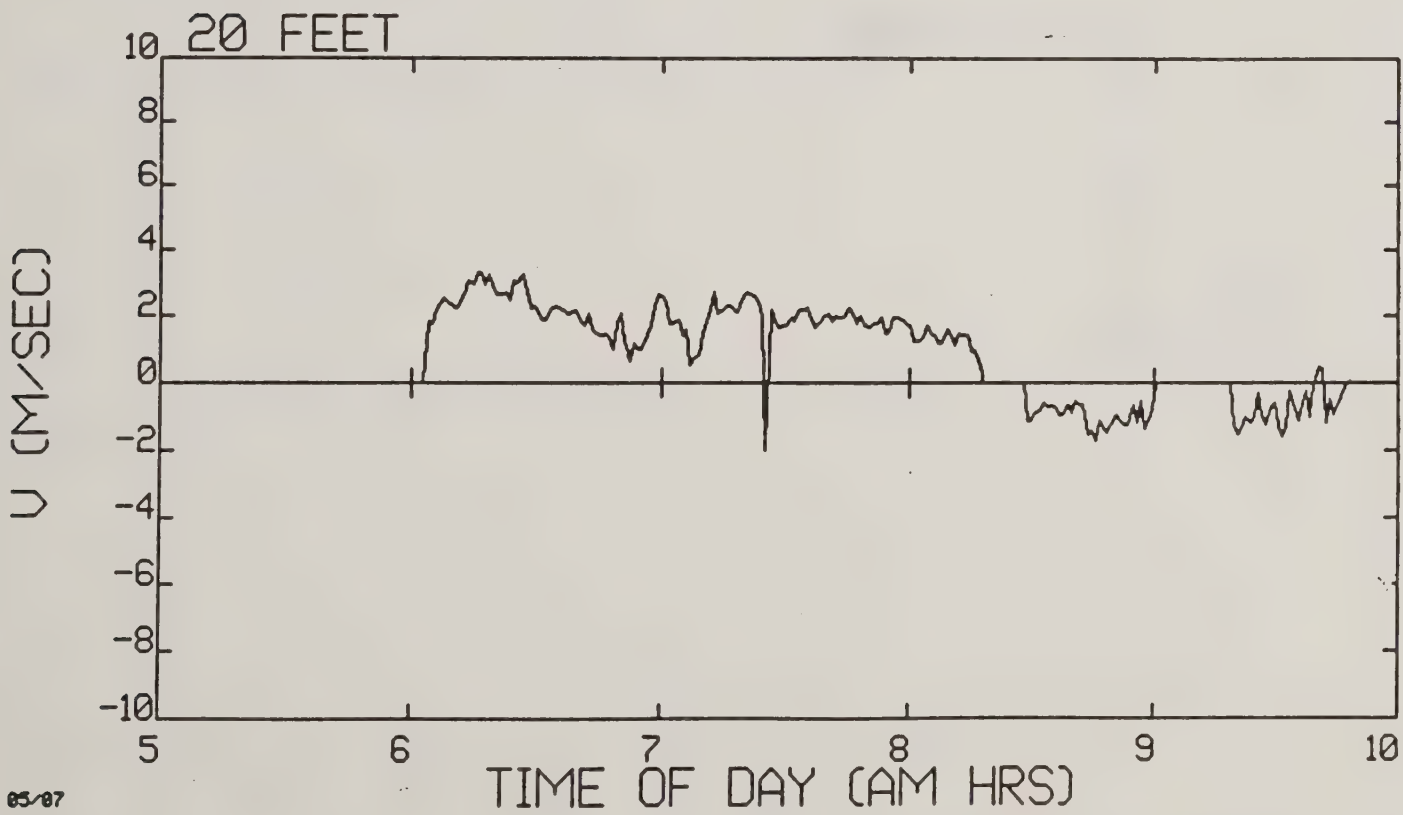
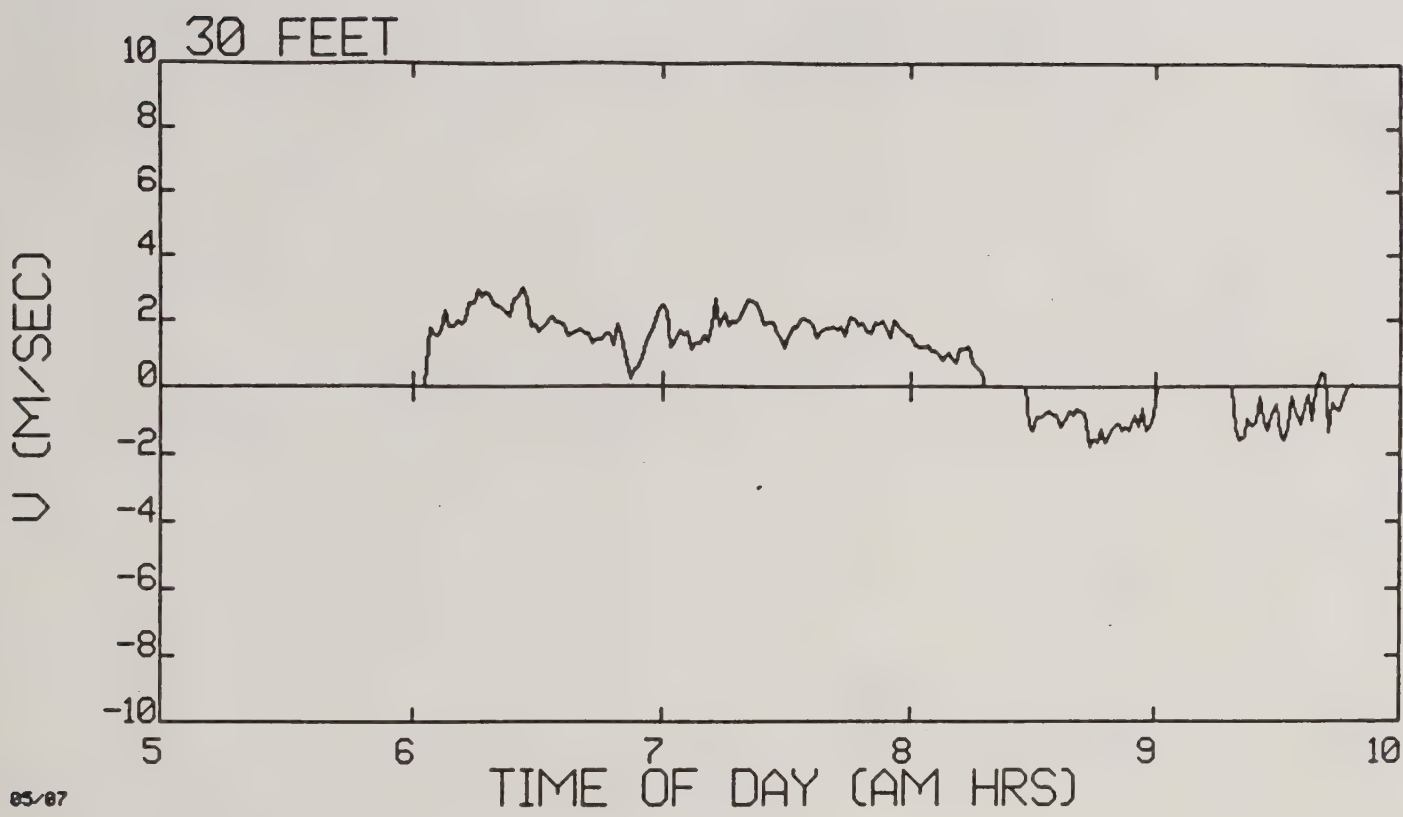


Figure 6-14. One minute averaged lateral V velocity profiles at 30 and 20 ft on tower 1 during test day 05/07. Positive velocities point west; negative velocities point east. Three time intervals are included, along with one A/D data dropout point at the 20 ft anemometer.

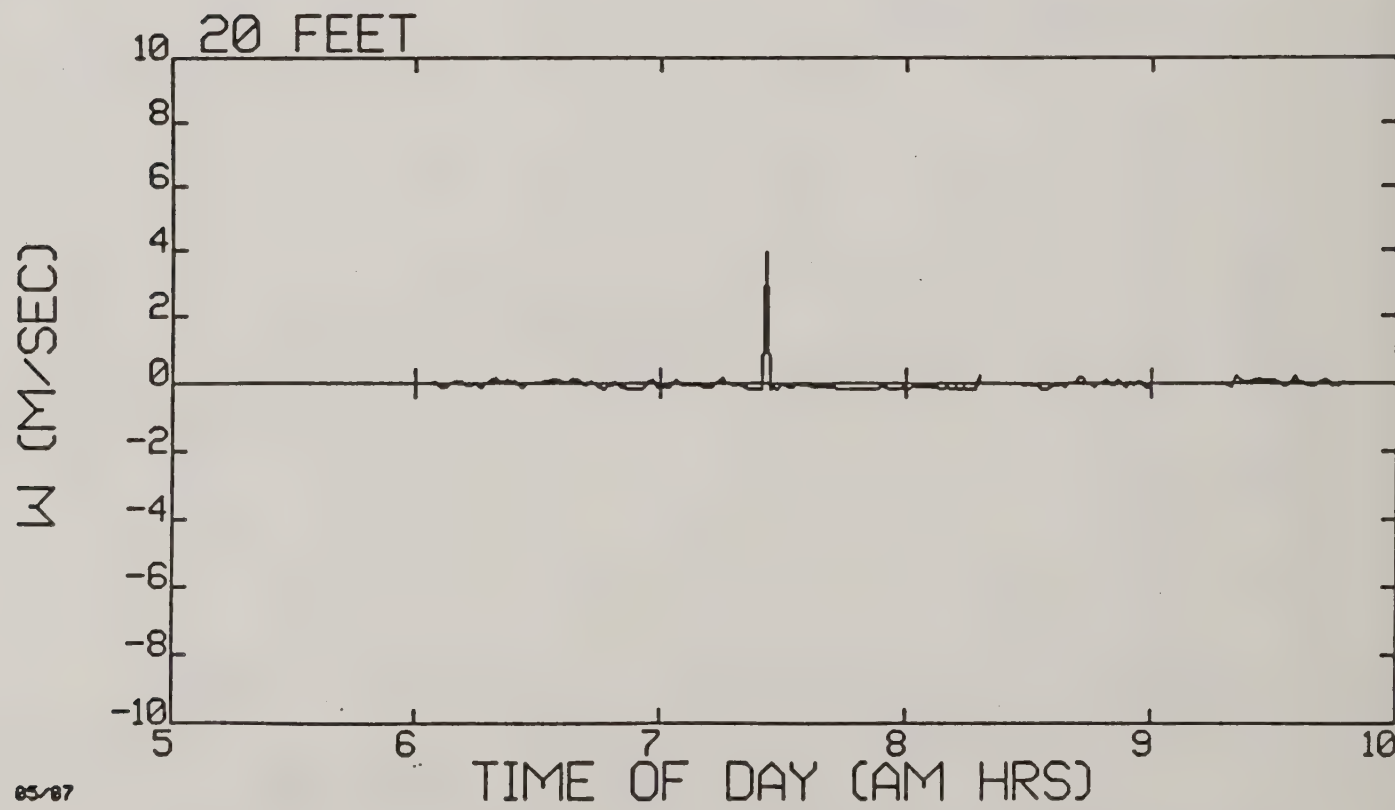
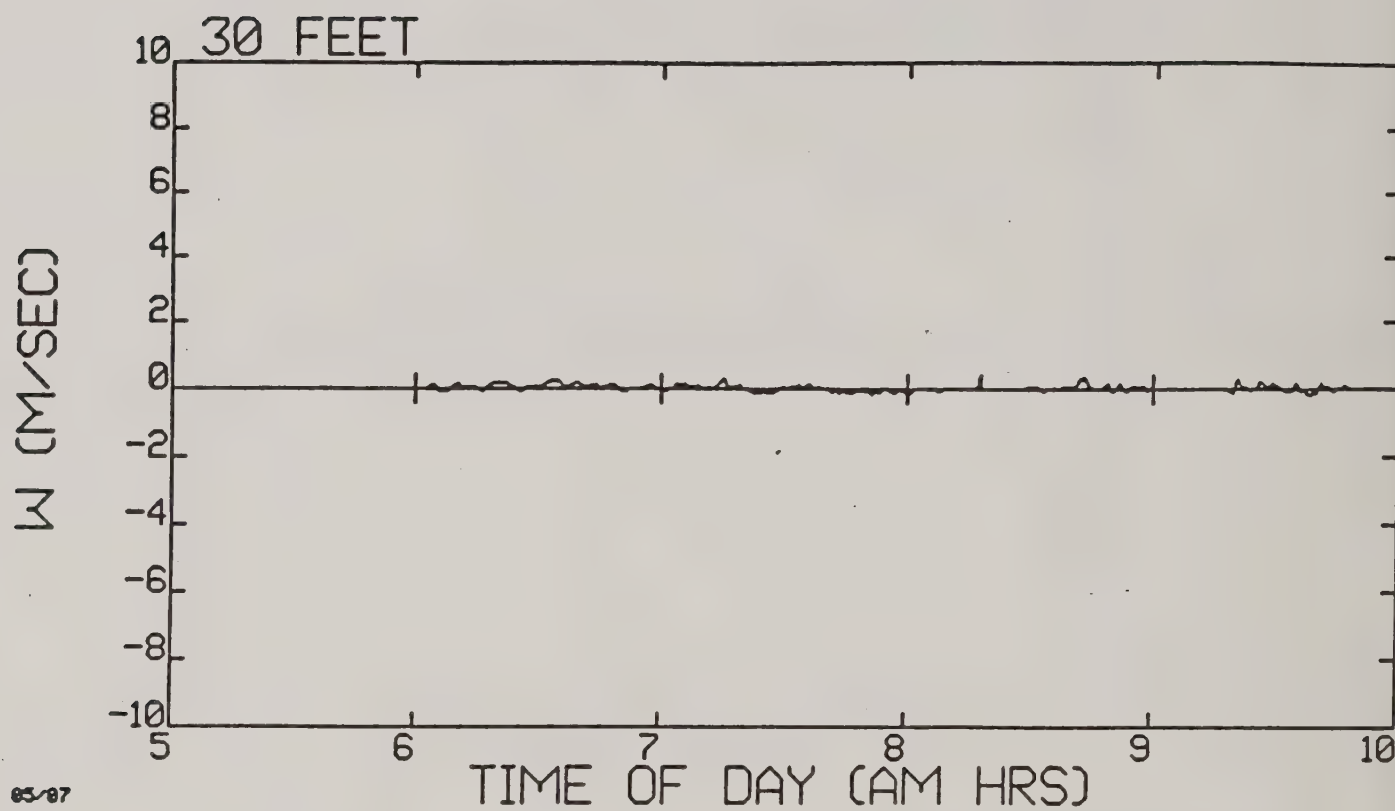


Figure 6-15. One minute averaged vertical W velocity profiles at 30 and 20 ft on tower 1 during test day 05/07. Positive velocities point upward; negative velocities point downward. Three time intervals are included, along with one A/D data dropout point at the 20 ft anemometer.

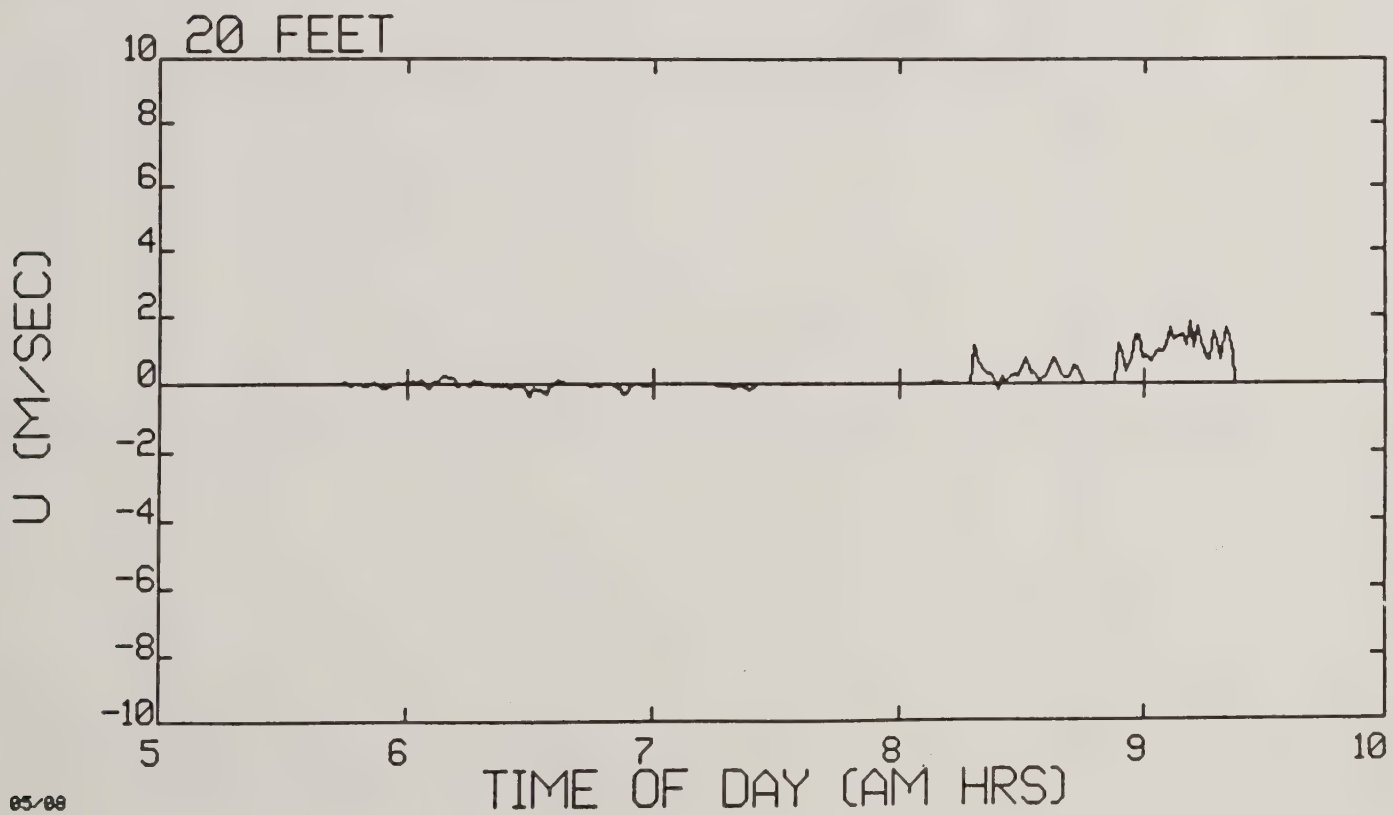
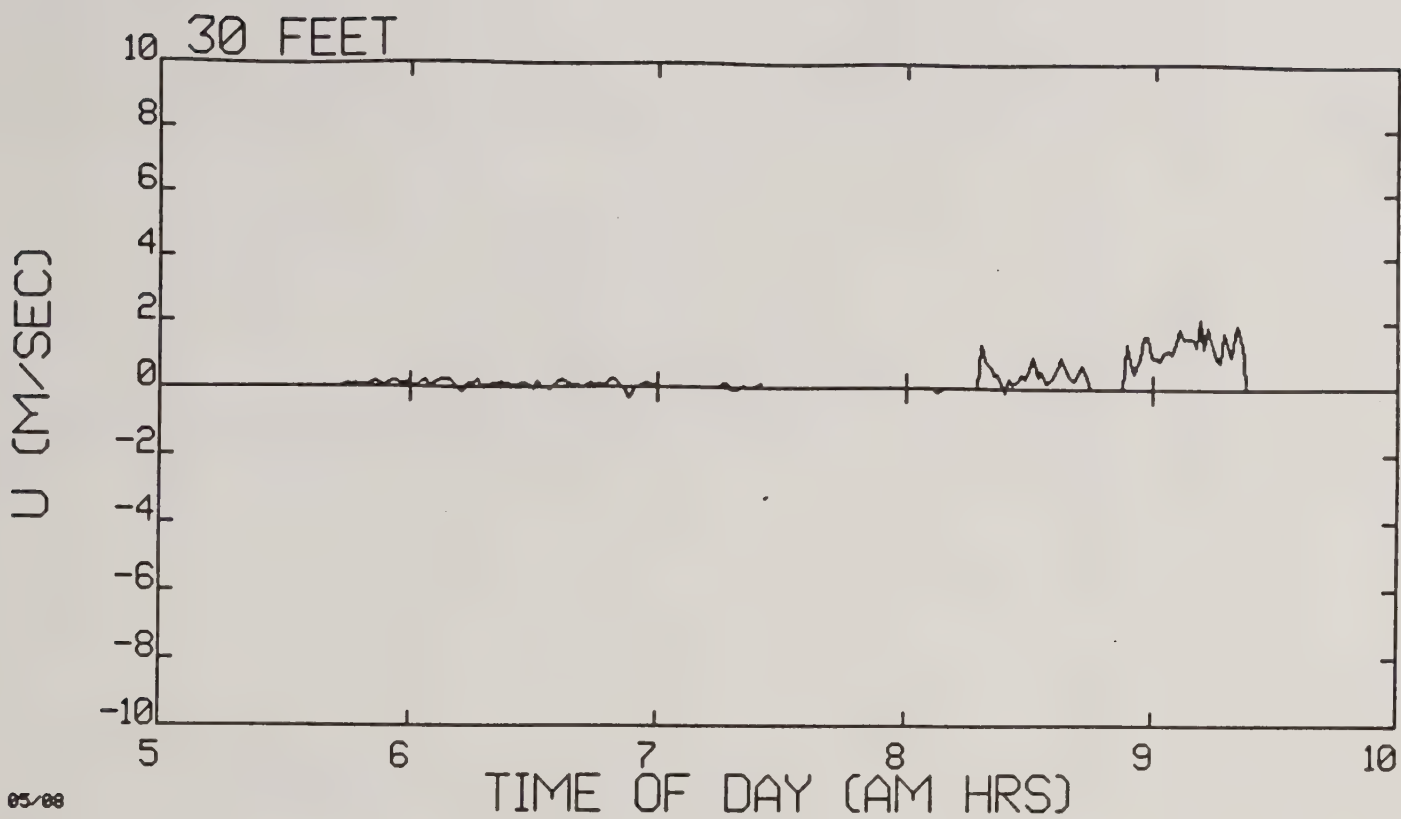


Figure 6-16. One minute averaged axial U velocity profiles at 30 and 20 ft on tower 1 during test day 05/08. Positive velocities point south; negative velocities point north. Five time intervals are included.

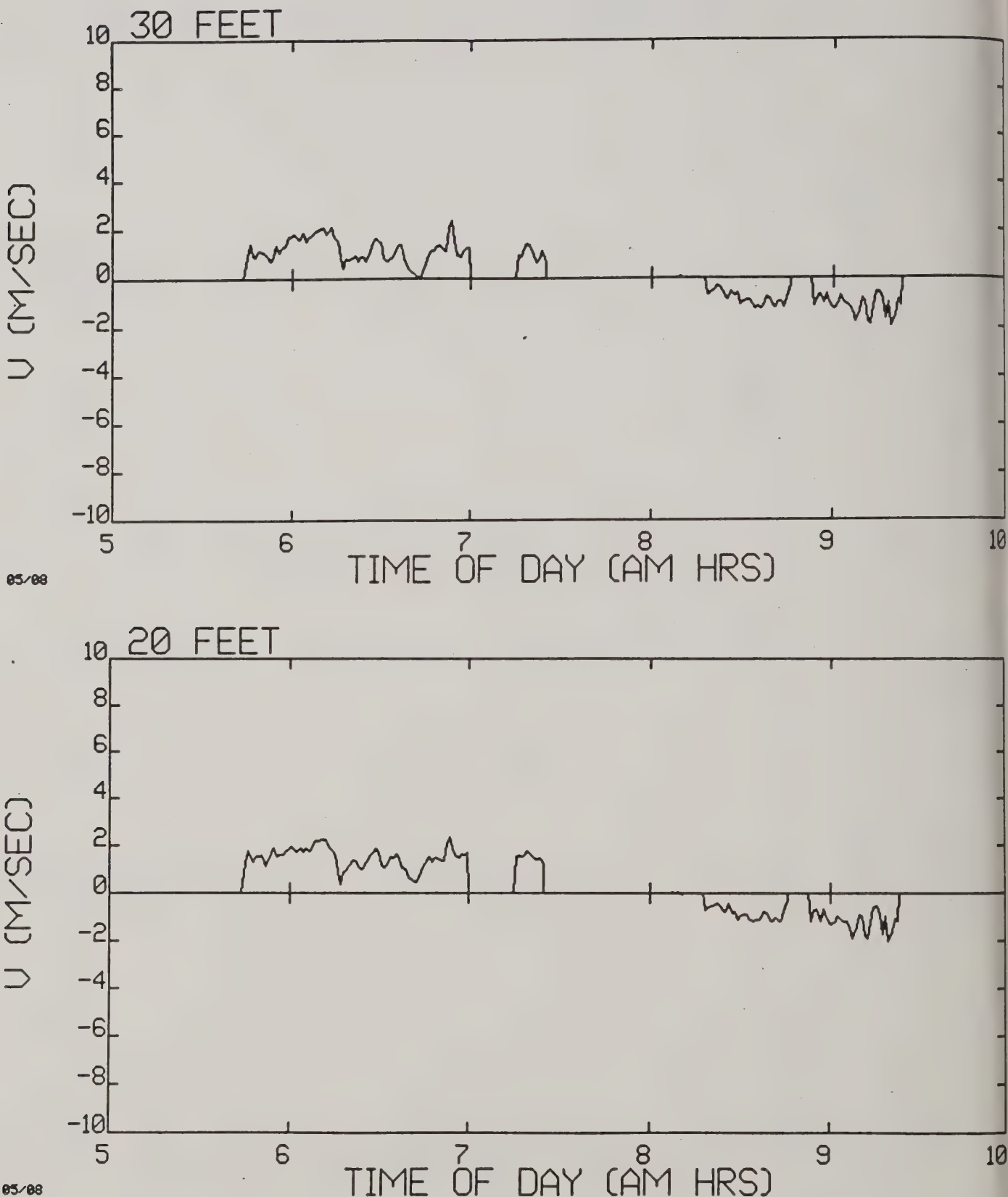


Figure 6-17. One minute averaged lateral V velocity profiles at 30 and 20 ft on tower 1 during test day 05/08. Positive velocities point west; negative velocities point east. Five time intervals are included.

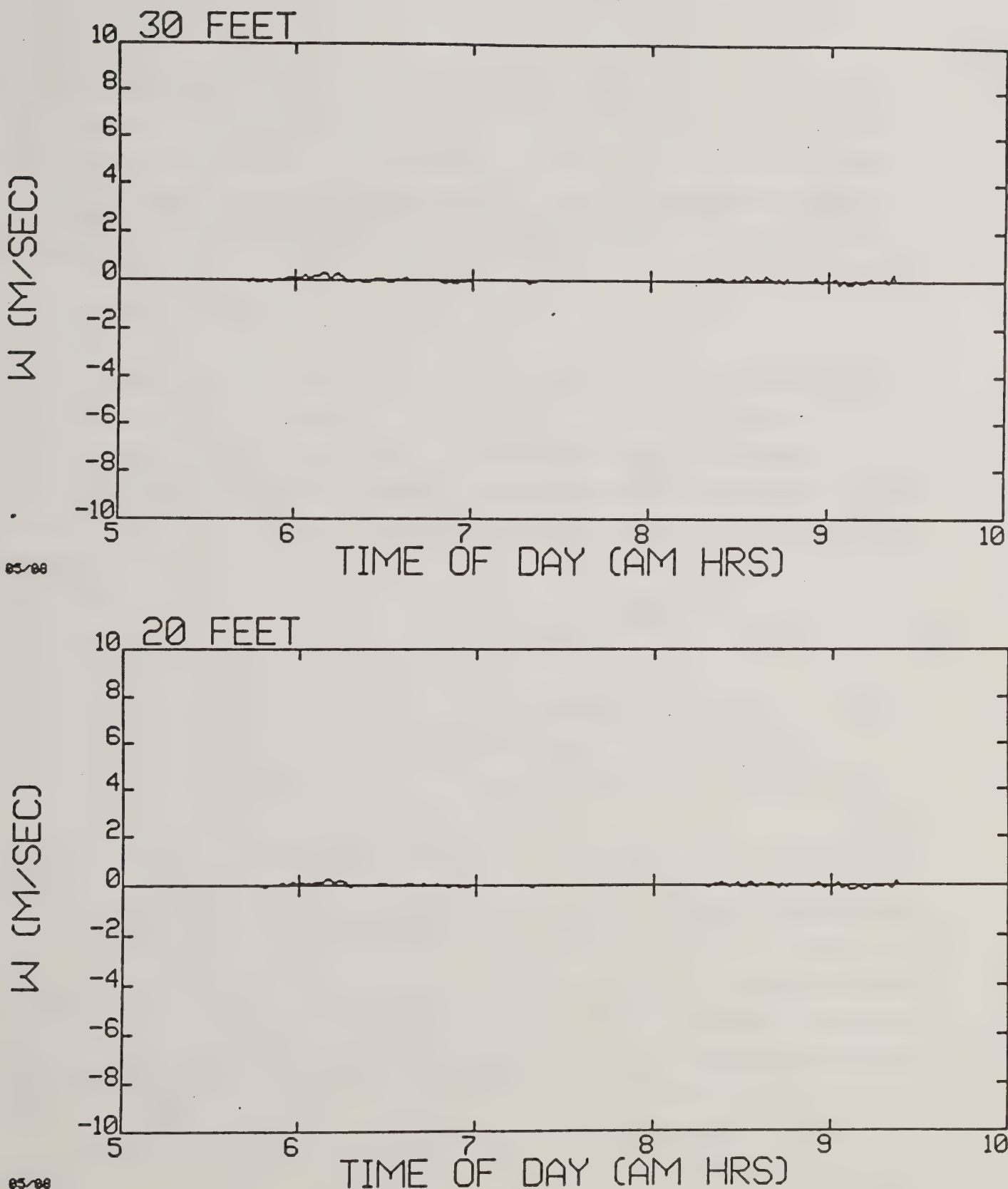


Figure 6-18. One minute averaged vertical W velocity profiles at 30 and 20 ft on tower 1 during test day 05/08. Positive velocities point upward; negative velocities point downward. Five time intervals are included.

7. TOWER GRID DATA REDUCTION

Data reduction followed the technique outlined in the previous test report (Ref. 3), with the added complication of accounting for the slightly tipped ground plane.

7.1 Flow Field Model

The present model assumes that the aircraft wake may be represented by a simple vortex pair (with image vortices below the tipped surface, Figure 7-1), each vortex of which adds a velocity field of the form

$$v = G/2\pi R$$

where v = velocity magnitude
 G = vortex circulation strength, and
 R = radius from vortex center.

The total velocity at any point in the flow field (in particular, at a sensor location) in any run at any time, is then the algebraic sum of the velocity contributions from the four vortices acting on the flow.

The location of the vortex pair is referenced to a coordinate system fixed relative to the tower grid (Figure 7-2). In addition to the vortex circulation strength already introduced, the other unknowns in the problem are

h = the height of the vortex pair relative to the ground plane,
 s = the semispan of the vortex pair (the half distance between their centers), and
 d = the offset distance of the aircraft centerline from the left-most (tower 1) grid centerline.

The procedure employed in Ref. 3 has been extended here to include the fixed terrain slope modification. Error minimization involving an iterative technique with influence coefficients was used to analyze the digitized signals from the 28 vertical anemometers for the duration of all 49 runs.

7.2 Preliminary Results

Figures 7-3 to 7-51 display the preliminary results of this test report. All 49 runs are illustrated by a contour plot of the interpolated vertical velocity data at 20 ft from the initiation of the test (time equals zero) to the completion of data collection, or 120 seconds, whichever came first. These contours are mapped with solid curves denoting positive (upward) velocity contours of 0.5 ft/sec, and dashed curves denoting negative (downward) velocity contours of -0.5 ft/sec. For the runs where the current solution algorithm could easily locate and identify a vortex pair path, an additional smooth curve of the variable d (illustrated in Figure 7-2) is superimposed on the contour plot (see for example Figure 7-8). This curve indicates the direction of travel of the vortex pair through the tower data. Runs that do not contain this curve have not yet been successfully reduced by the current solution algorithm (see for example Figure 7-3). Trajectory analysis is not possible at this time.

Additional sets of figures are included in the cases where the vortex pair path has been identified (see for example Figure 7-8b). These curves summarize the predicted horizontal and vertical positions of the vortex pair, and its predicted circulation strength. The horizontal positions are for the right vortex (the sum of variables d and s illustrated in Figure 7-2) as a solid curve, and the left vortex (the difference of variables d and s in Figure 7-2) as a dashed curve. The vertical positions are a plot of the variable h in Figure 7-2. The circulation G is in the units of ft^2/sec . When the radar gun gave the flight speed of the helicopter, the computed steady state value of the circulation strength is also shown by a heavy solid line.

As in the previous tests, the numerical algorithm does a good job of locating and following the vortex pair as it traverses the tower grid. The algorithm seems to fail whenever one of the vortices moves sufficiently off the end of the tower grid. The common signature of the vortex pair is a region of negative velocity (dashed contours) with positive velocity (solid contours) on either side.

When the velocity data is mostly of one sign (either positive or negative), the present numerical algorithm is not structured to resolve the vortex pair path. The algorithm is also inadequate when the velocity levels are low (below ± 0.5 ft/sec). In this study no attempt was made to improve the numerical algorithm over the algorithm developed in Ref. 3 other than to include the simple terrain effect. One result of the preliminary examination is the cataloguing of several possible code enhancements.

Of the runs that were not reduced by the current algorithm, it is anticipated that all or part of the following runs can be reduced once the numerical algorithm has been modified: runs 1, 4, 8, 11, 13, 14, 15 and 38. This will leave a total of 11 runs (out of 49) or 2 card runs (out of 26) that do not appear to be reduceable. Principally, the vertical velocity profiles become so random that an expected vortex pair path cannot even be hand-drawn through the contour data. This breakup in the velocity profiles could possibly be attributed to intermittent drainage winds. In only a few cases (for example Figure 7-29, run 27) is it clear that the vortex pattern missed the anemometers. In many of the successful runs (for example Figure 7-42, run 40) the careful placement of the helicopter was necessary because the locally prevailing crosswinds quickly moved the vortex pair across the anemometer grid.

That potential success is possible in the unresolved runs may be best illustrated by vertical velocity profiles for a run that was not resolved by the current algorithm. Figure 7-52 presents plots of the vertical velocity along the top row of sensors at four times. Clearly the vortex pair location is evident, although the current algorithm was unable to resolve the vortex pair path for run 4.

Several of the noncard runs were for aircraft flight speeds and wind conditions outside Forest Service normal operating procedures. These tests were conducted to test the limit of the algorithm. Clearly, for the very low, near-hover helicopter speeds, the vortex pair algorithm should be modified to include helicopter downwash effects.

Overall, the data appears to be less smooth than in the previous tests. Since the computer and tower anemometer systems are identical, it is safe to conclude that the environment during the tests was more active than at Foresthill and Chico. The predicted circulation strengths show more fluctuations than in the previous tests. Because of the structure of the numerical algorithm, circulation strength variations tend to reflect solution procedure inaccuracies with identifying vortex location.

It is important to realize that the tower grid is positioned between 0 and 180 ft along the horizontal scale, with the base of tower 1 at the reference vertical height of 0 ft, and its top at 30 ft (see Figure 7-2). All helicopter flights were flown above the 30-ft level so as not to impact the tower grid.

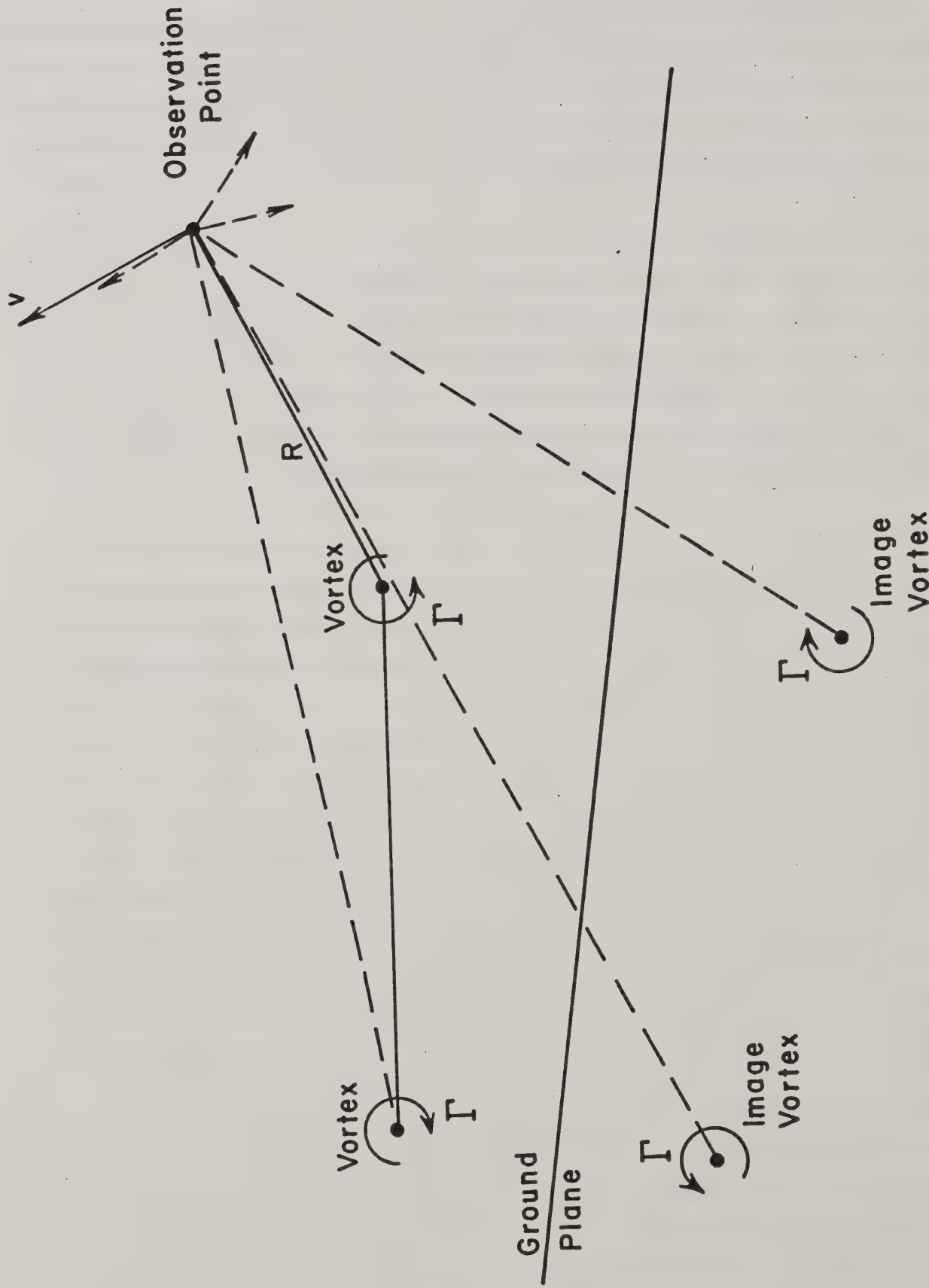


Figure 7-1. The composite velocity vector at an observation point found by summing the contributions of the aircraft vortex and its image system below the tipped ground plane.

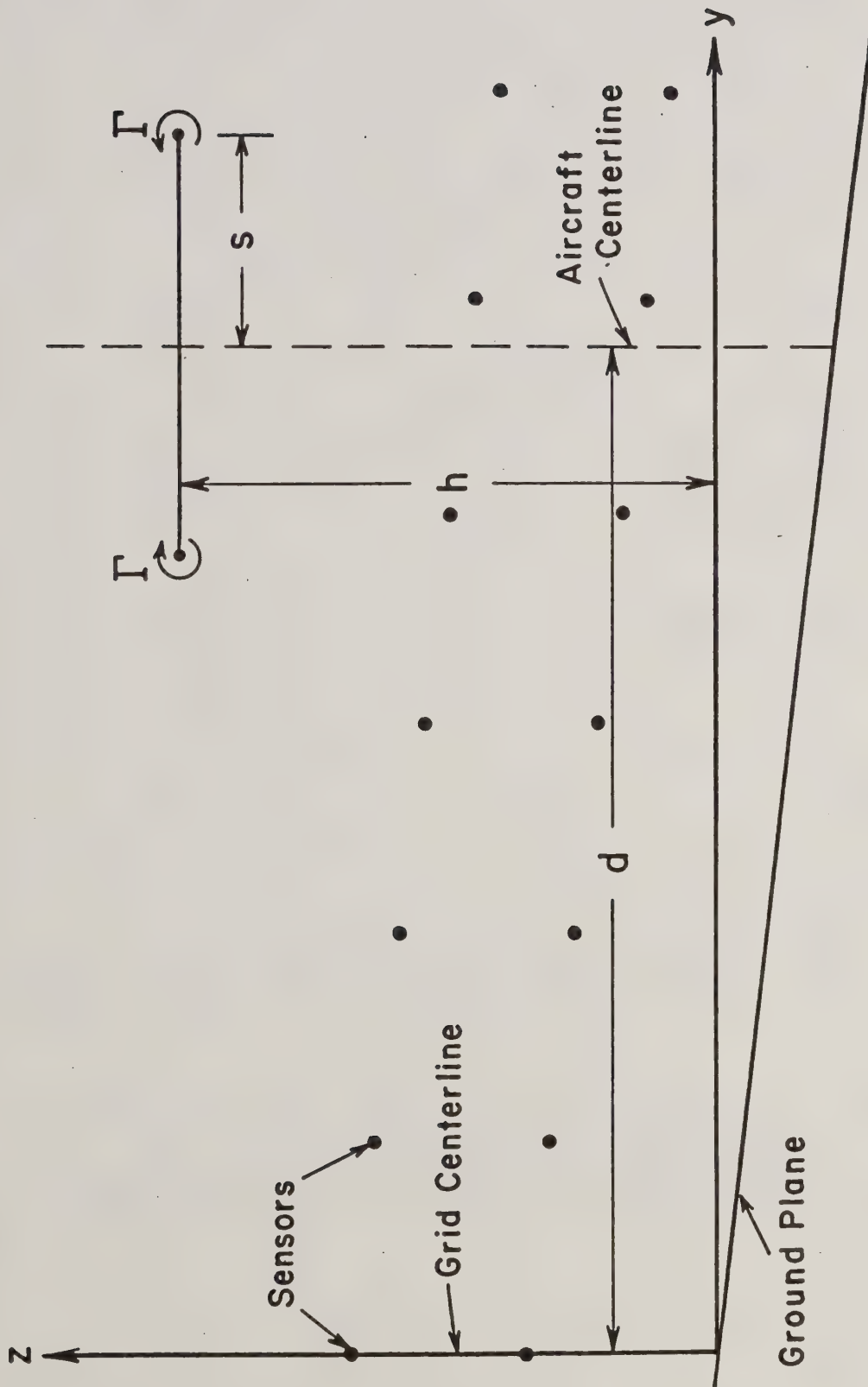


Figure 7-2. The aircraft vortex pair located relative to the sensor grid system. The relevant lengths are the height h of the vortex pair, the semispan distance s between the vortices, and the offset d of the aircraft centerline from the grid centerline.

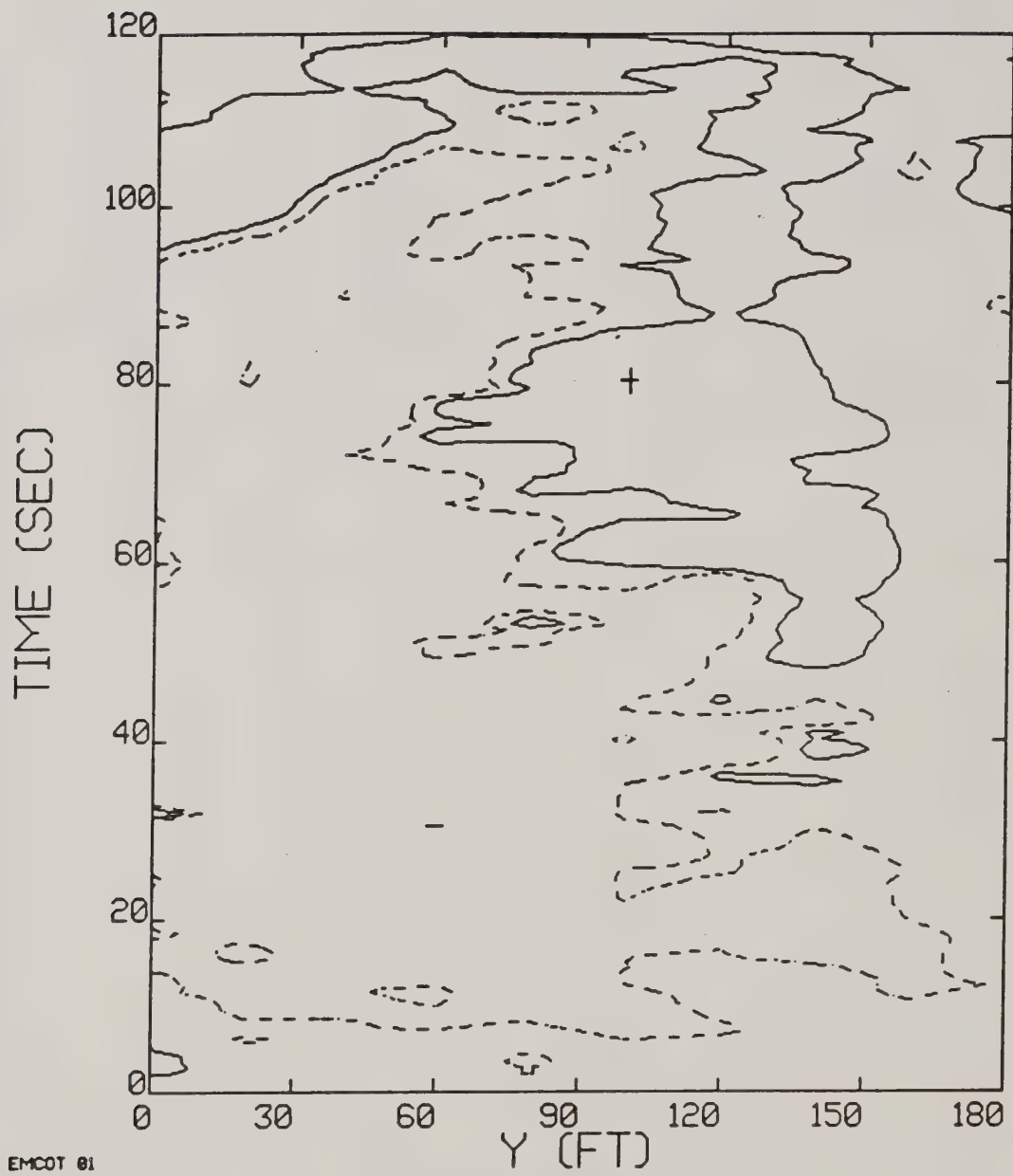


Figure 7-3. Run 1, date 04/27, C-130. Solid contours are (positive) upwash; dashed contours are (negative) downwash. Typically, an aircraft signature will be a region of dashed contours surrounded on either side by a region of solid contours.

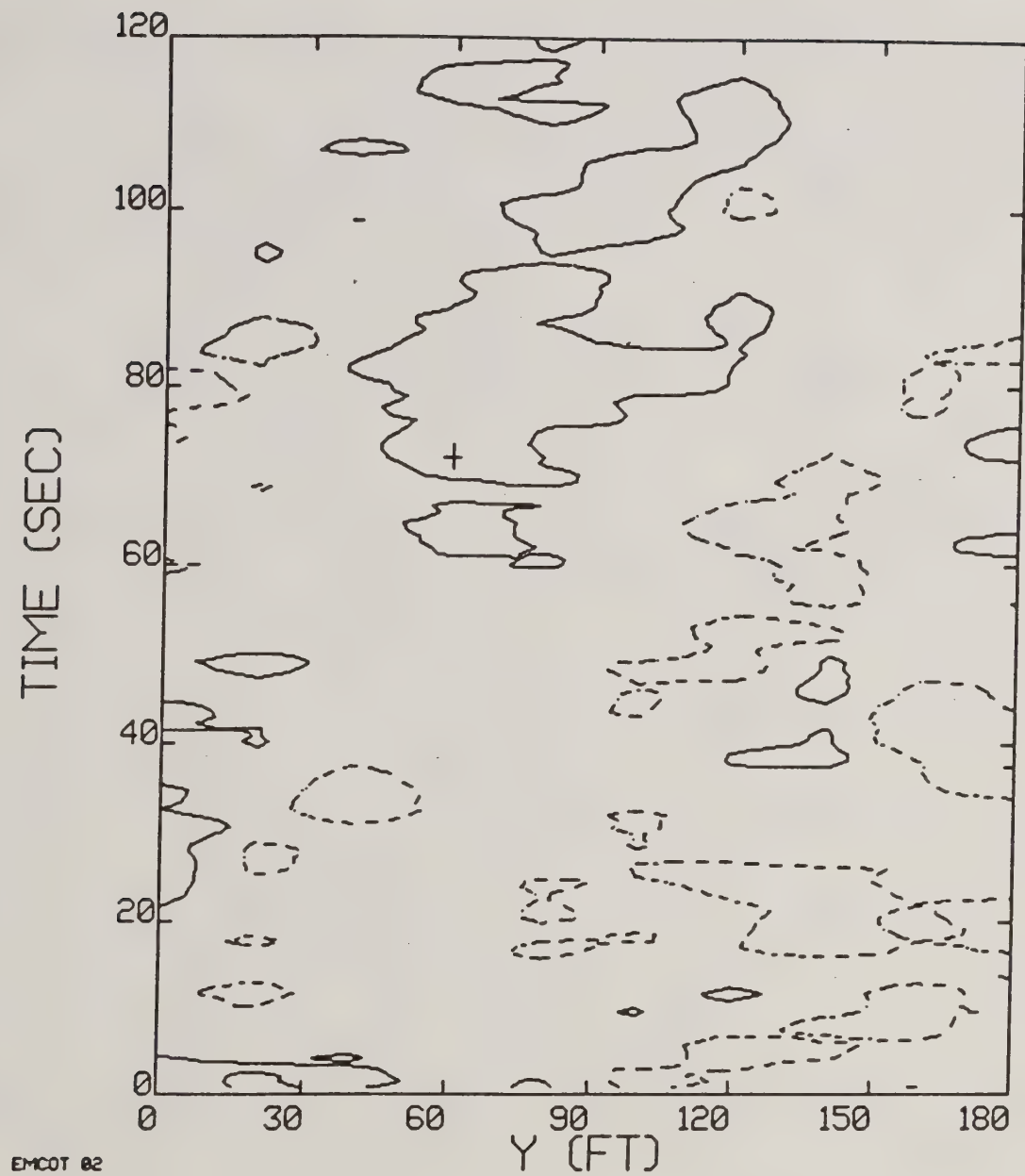


Figure 7-4. Run 2, date 04/27, C-130.

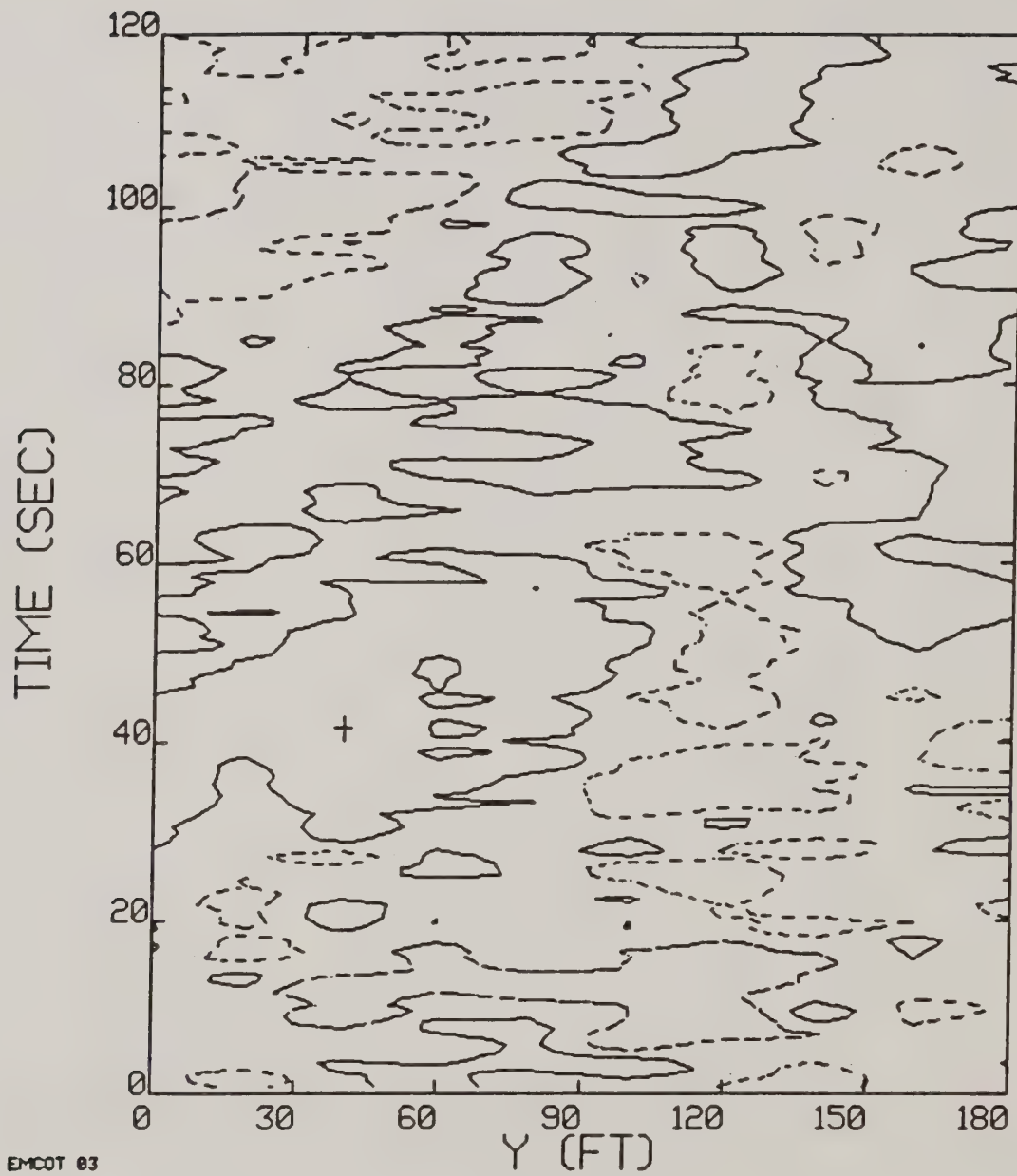


Figure 7-5. Run 3, date 04/27, C-130.

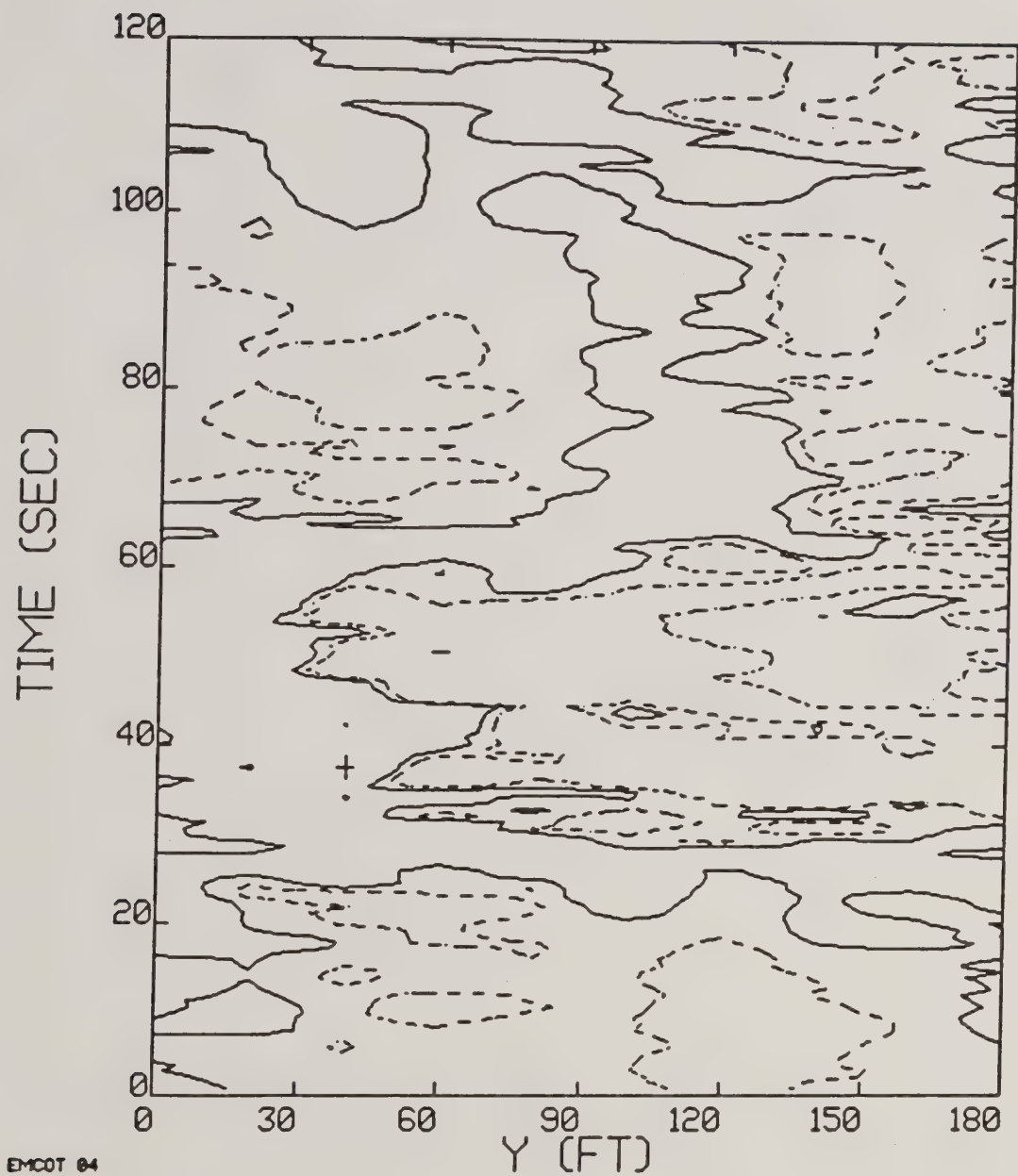


Figure 7-6. Run 4, date 04/27, C-130.

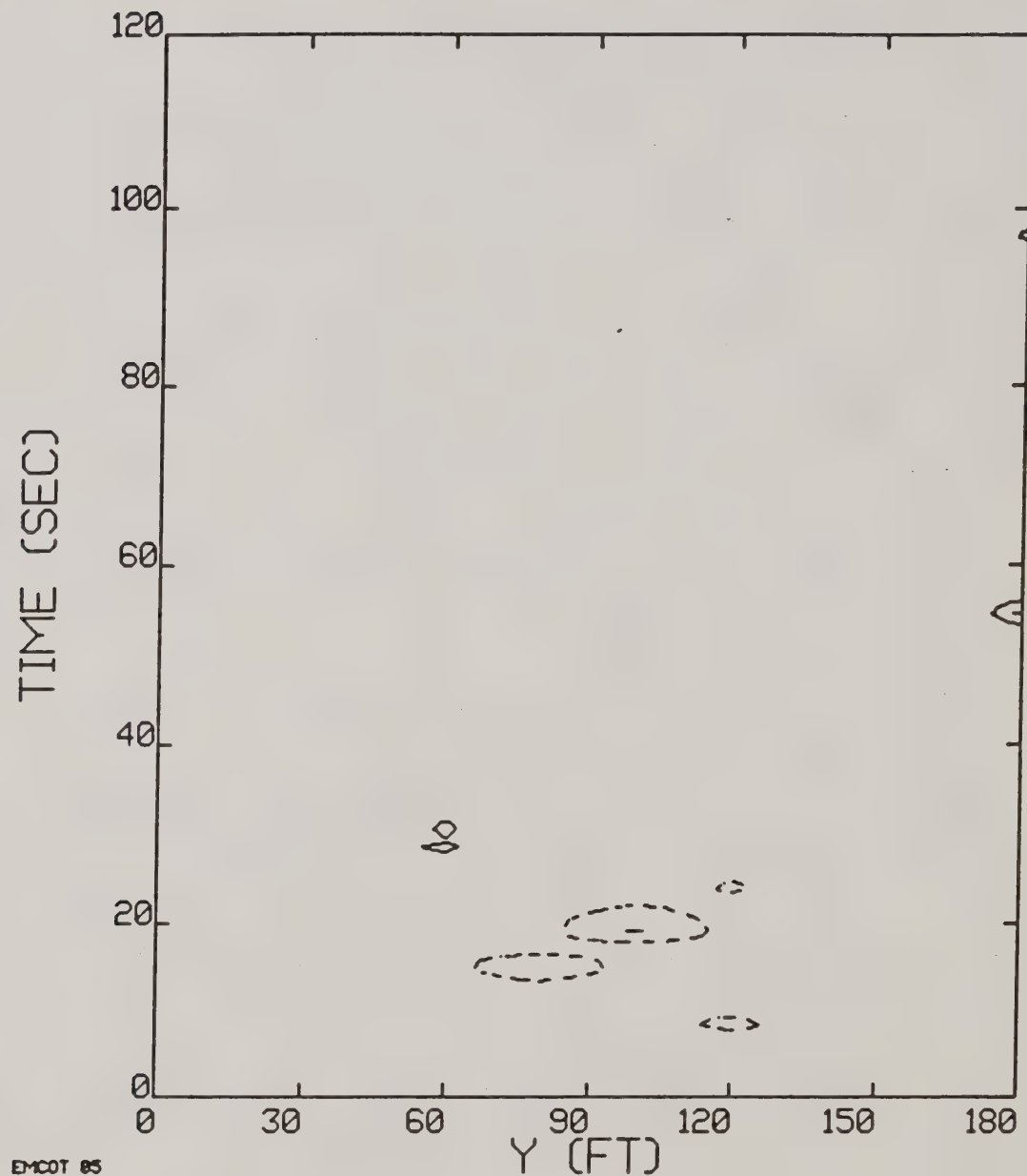


Figure 7-7. Run 5, date 04/28, Bell 206B.

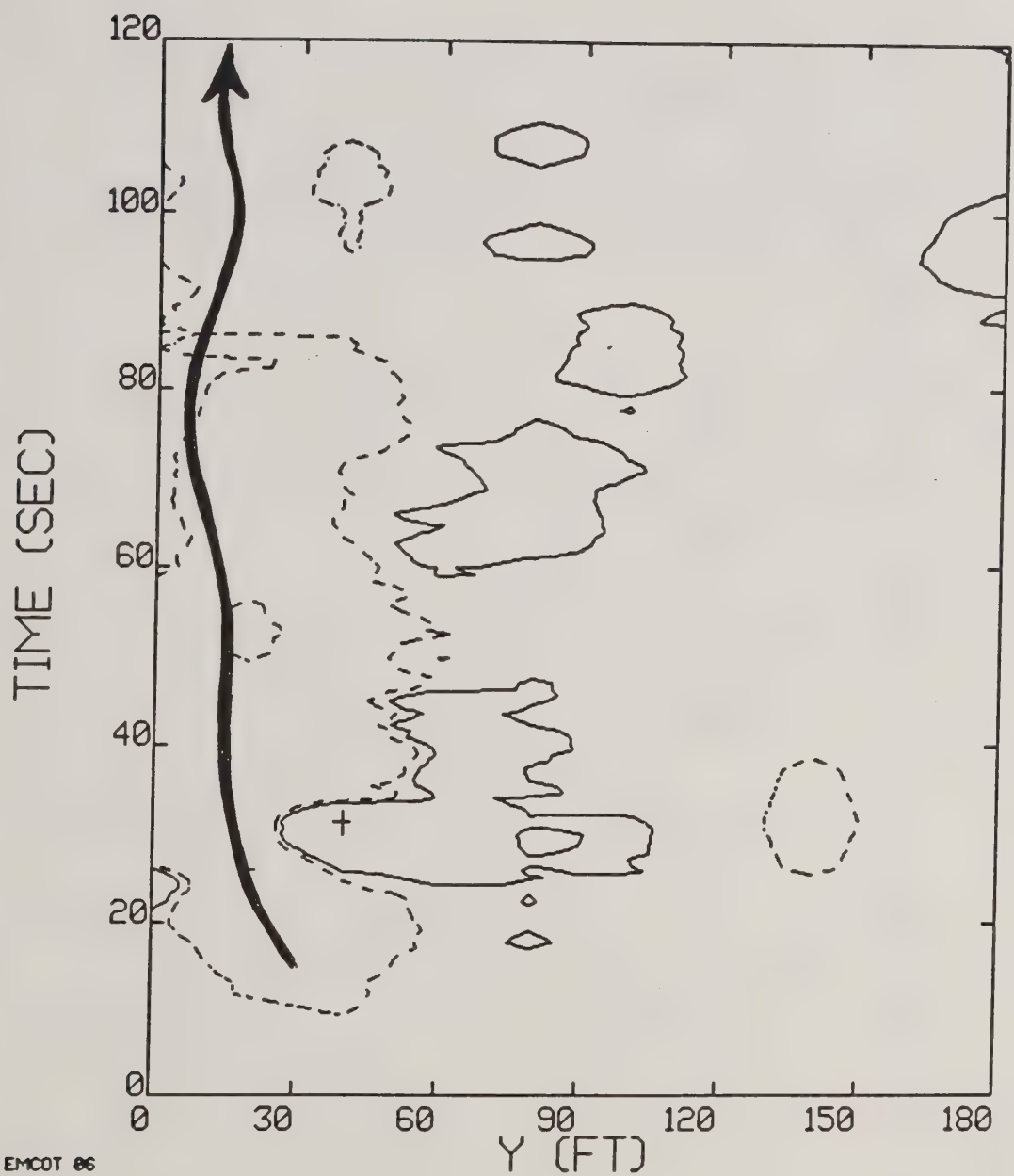


Figure 7-8. Run 6, date 04/28, Bell 206B.

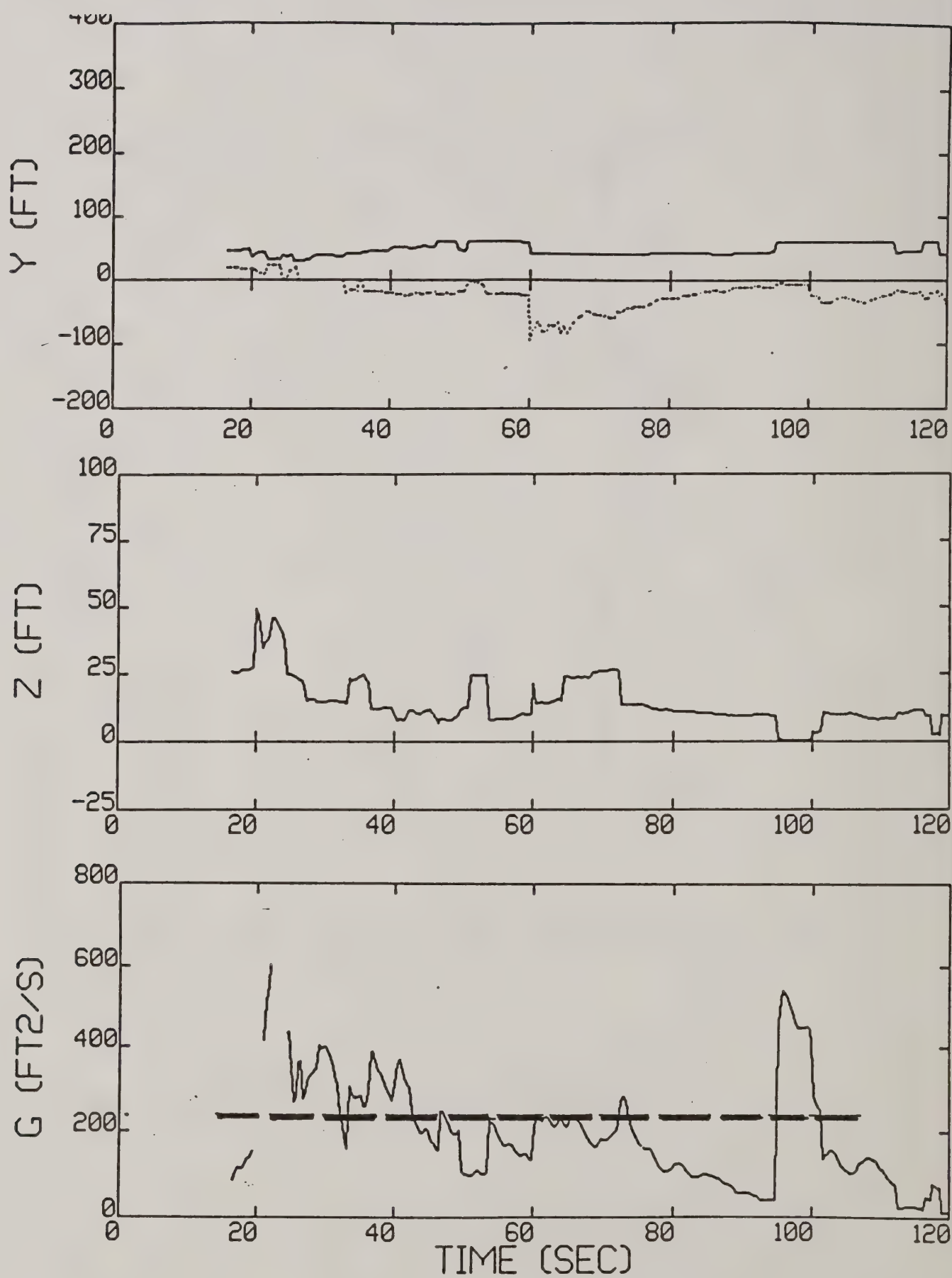


Figure 7-8b. Run 6 reduced data.

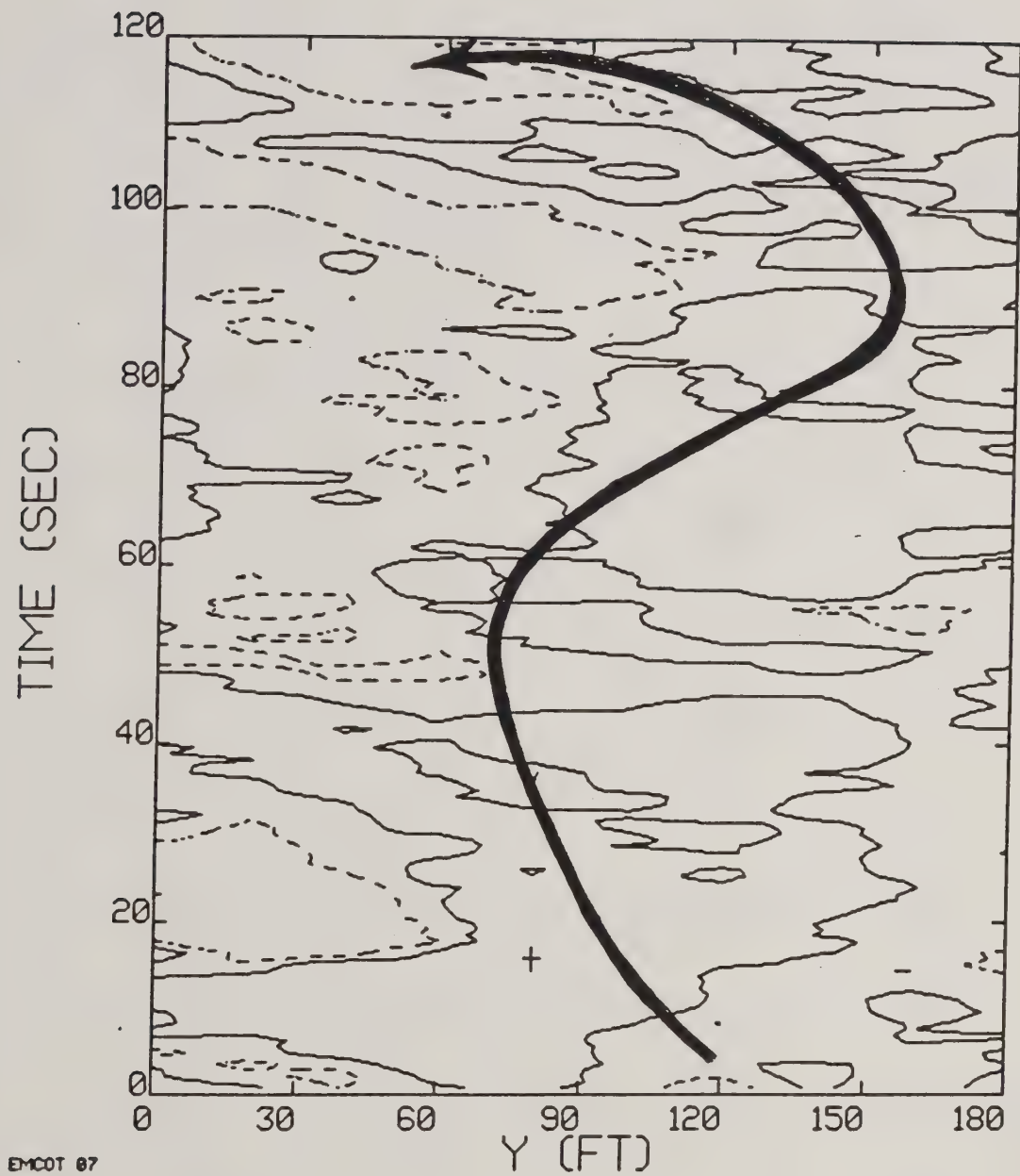


Figure 7-9. Run 7, date 04/28, Bell 206B.

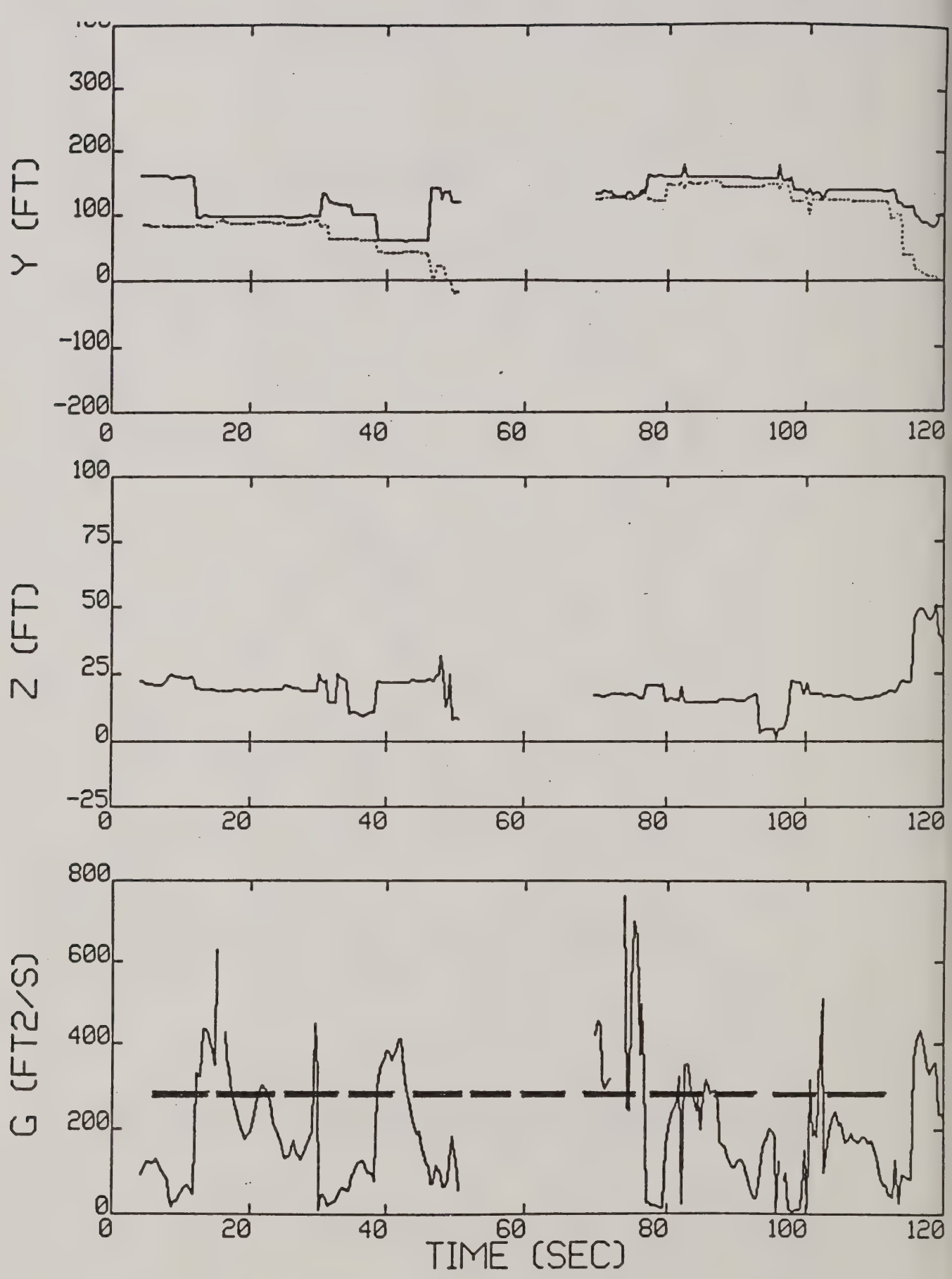


Figure 7-9b. Run 7 reduced data.

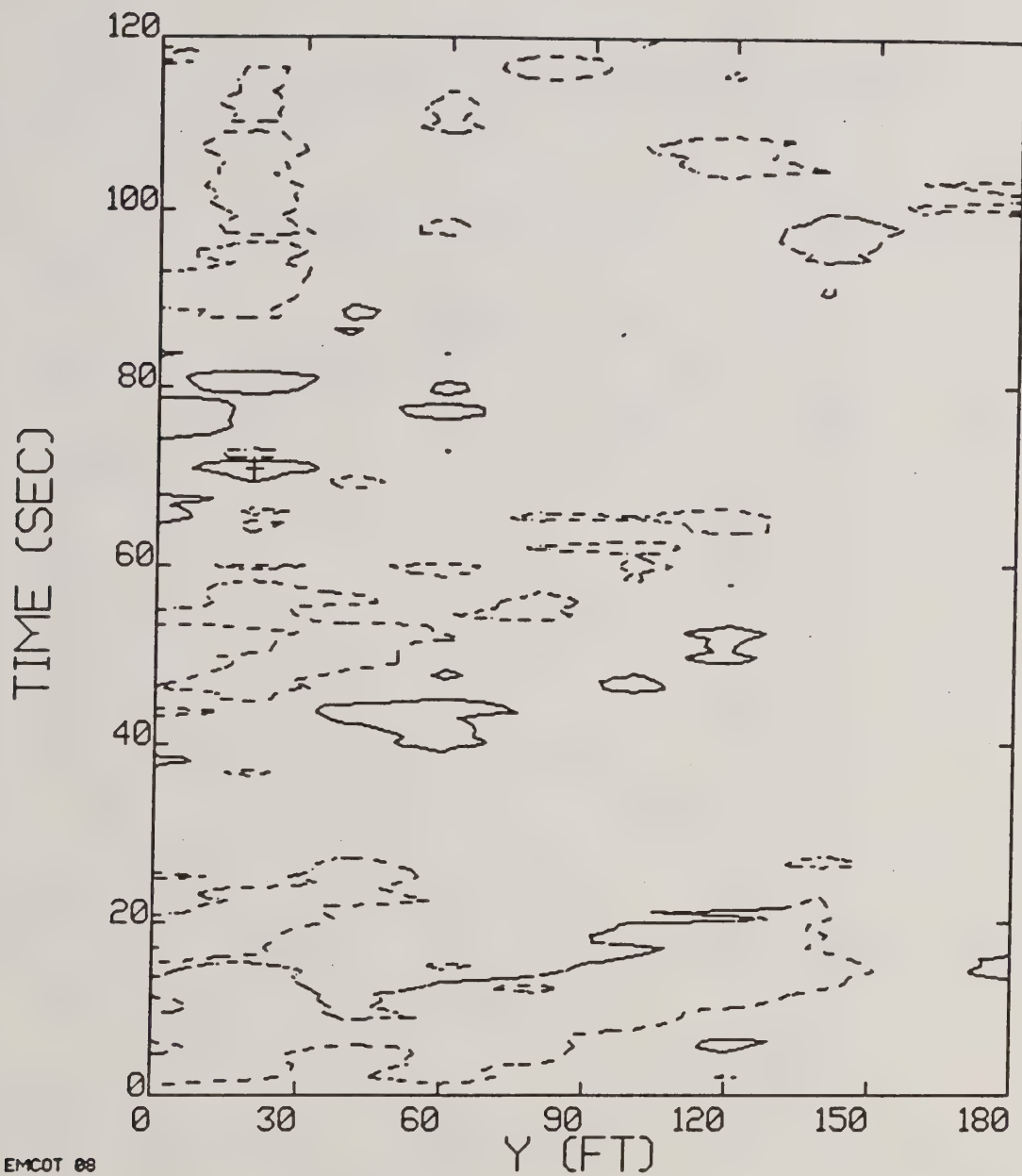


Figure 7-10. Run 8, date 04/29, Bell 206B.

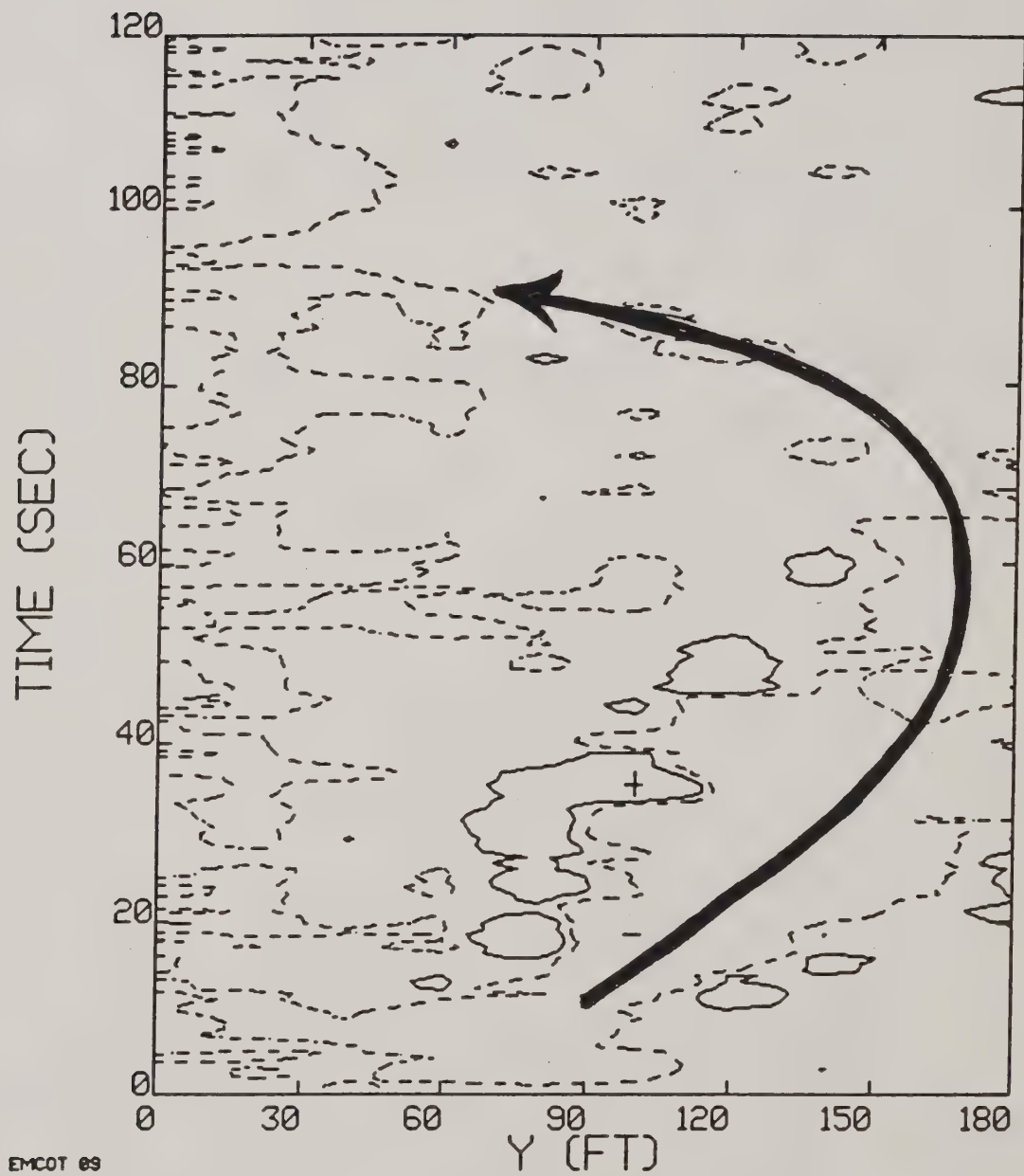


Figure 7-11. Run 9, date 04/29, Bell 206B.

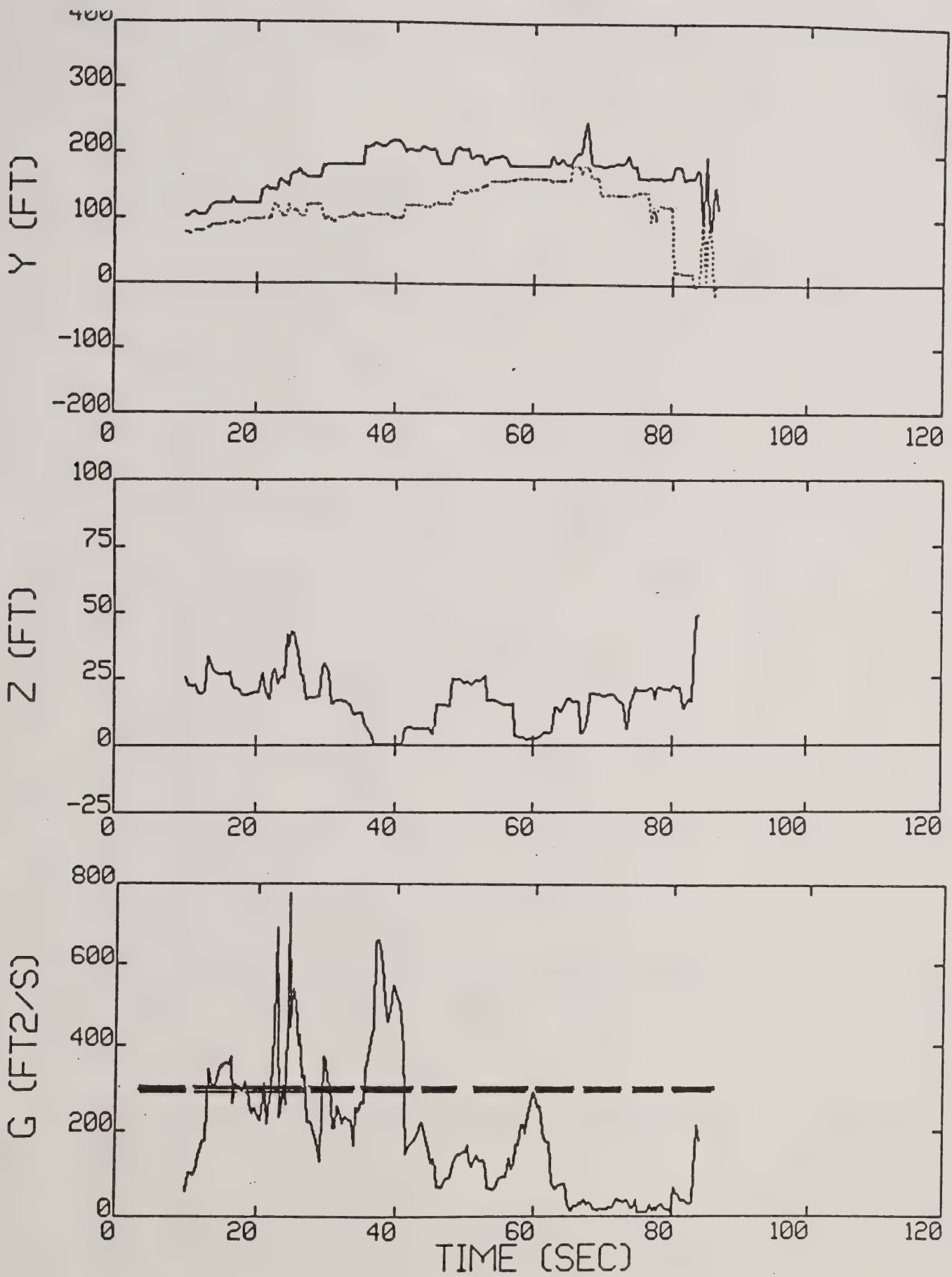


Figure 7-11b. Run 9 reduced data.

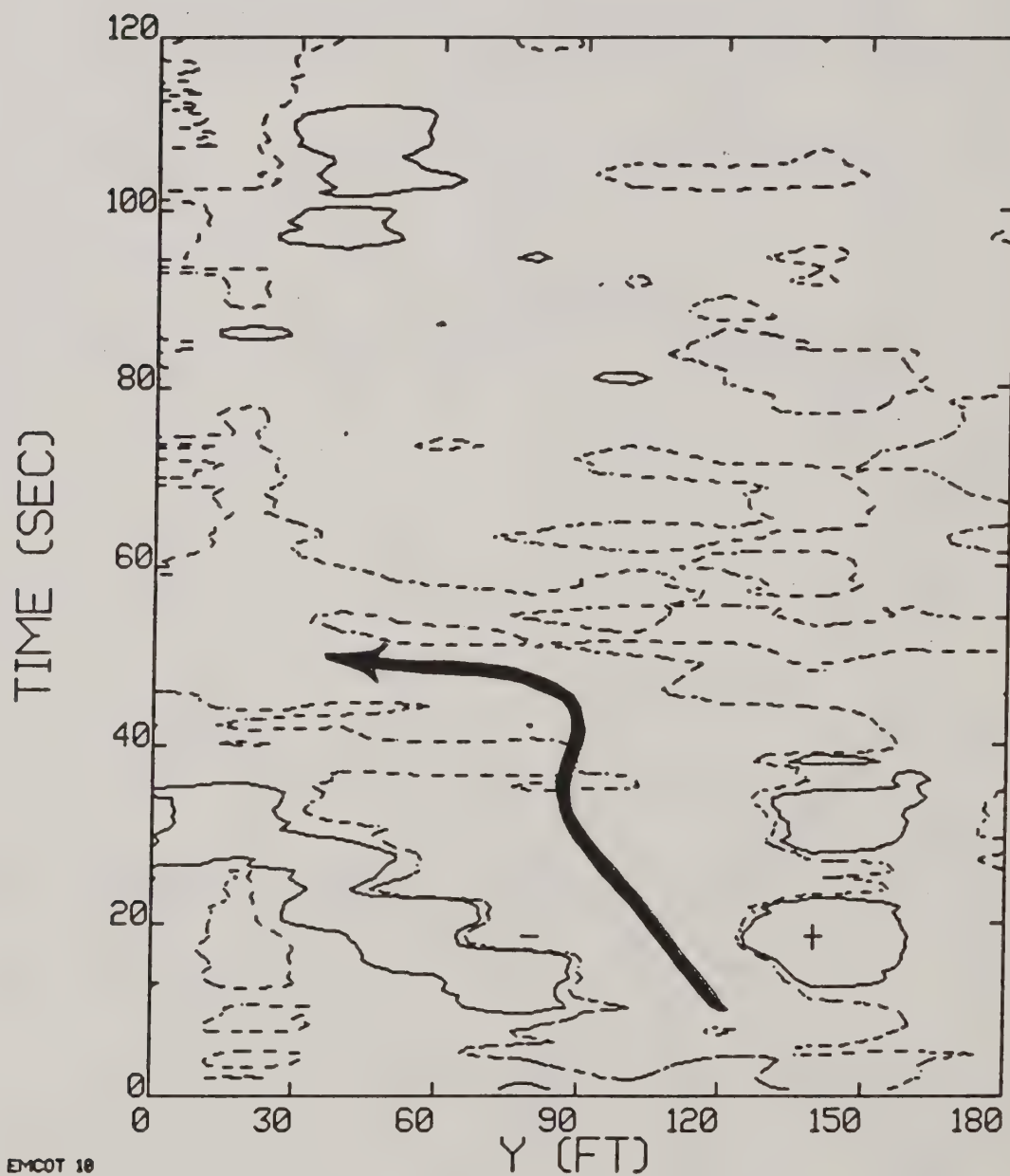


Figure 7-12. Run 10, date 04/29, Bell 206B.

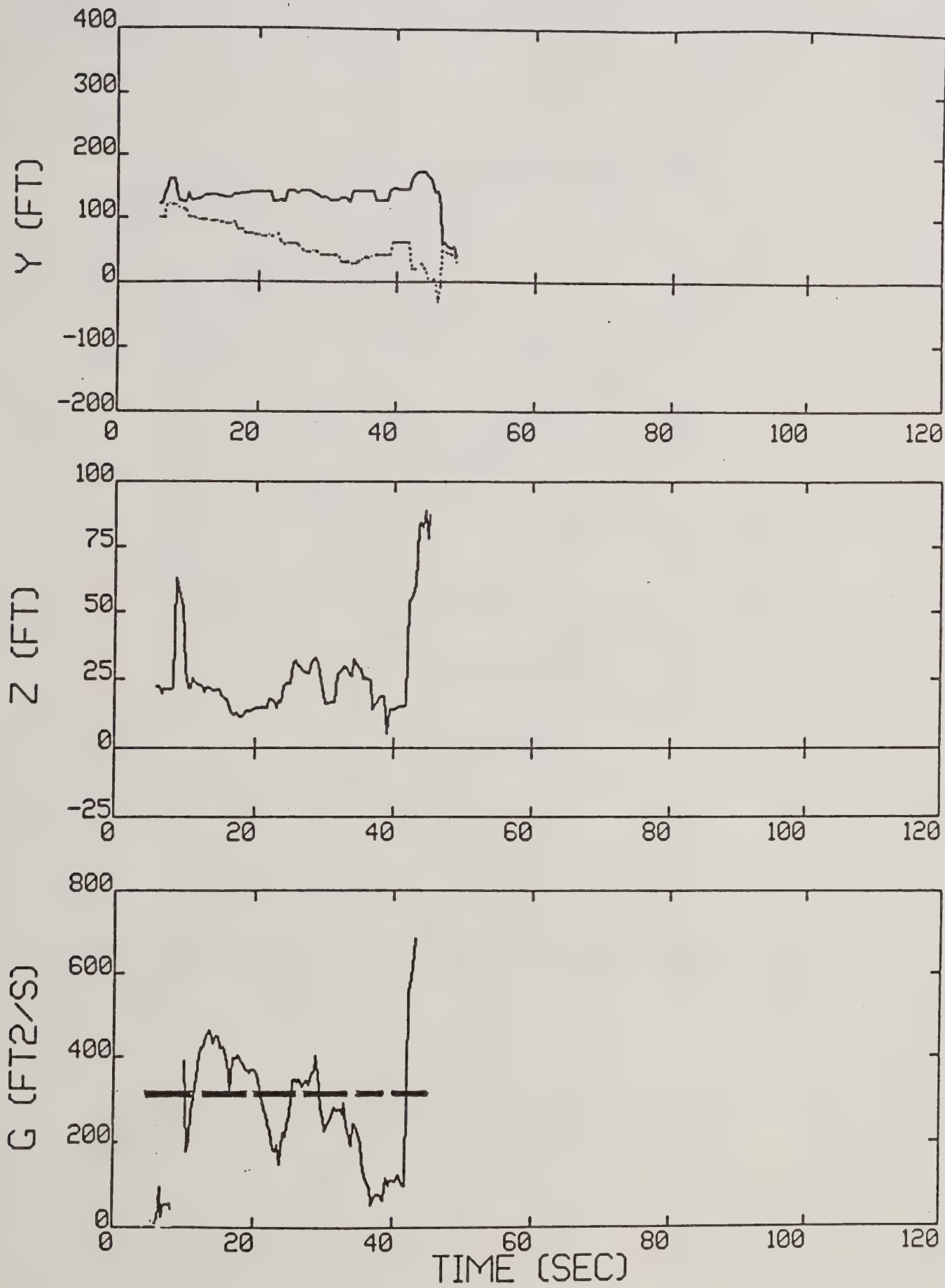


Figure 7-12b. Run 10 reduced data.

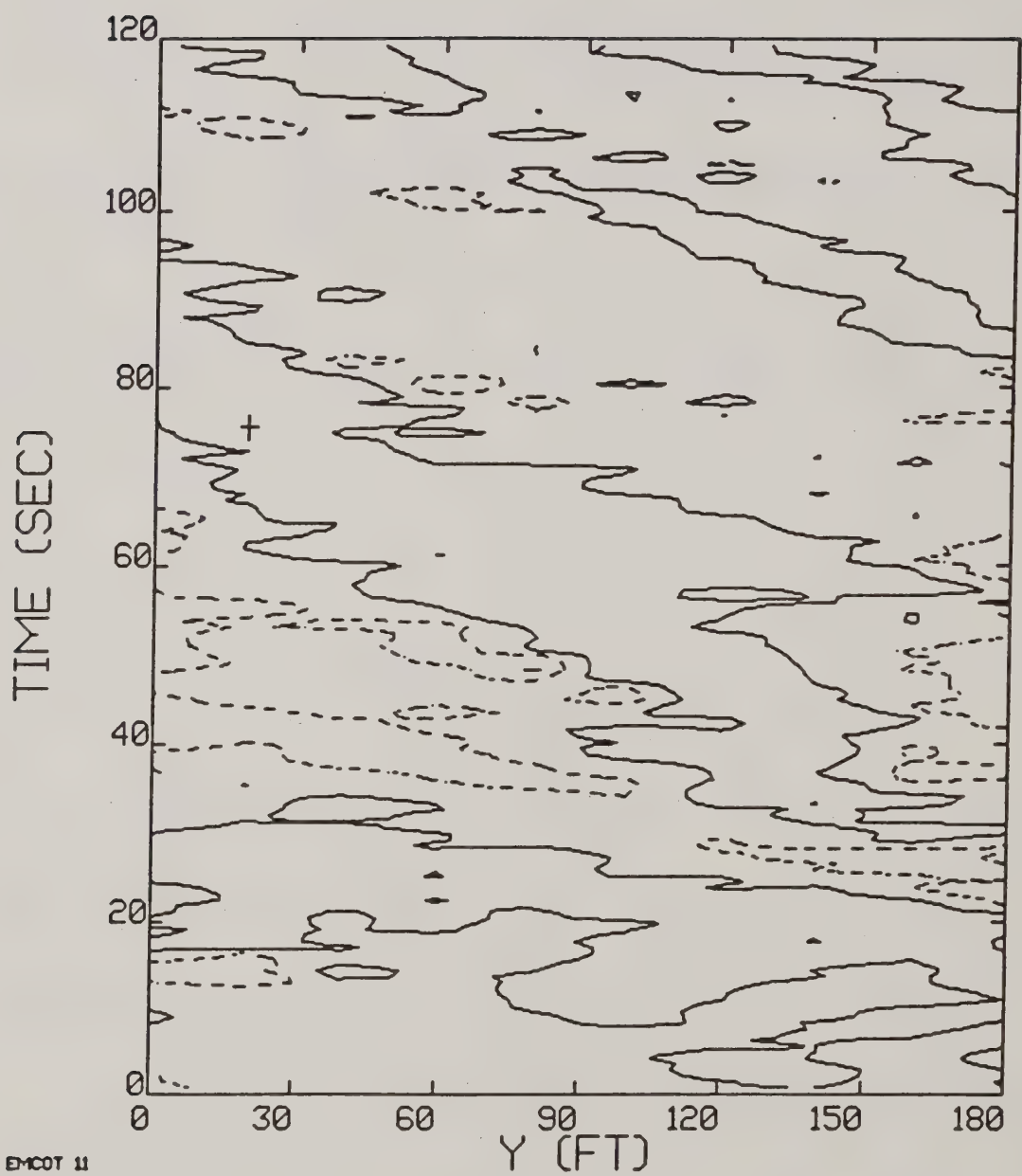


Figure 7-13. Run 11, date 04/29, Bell 206B.

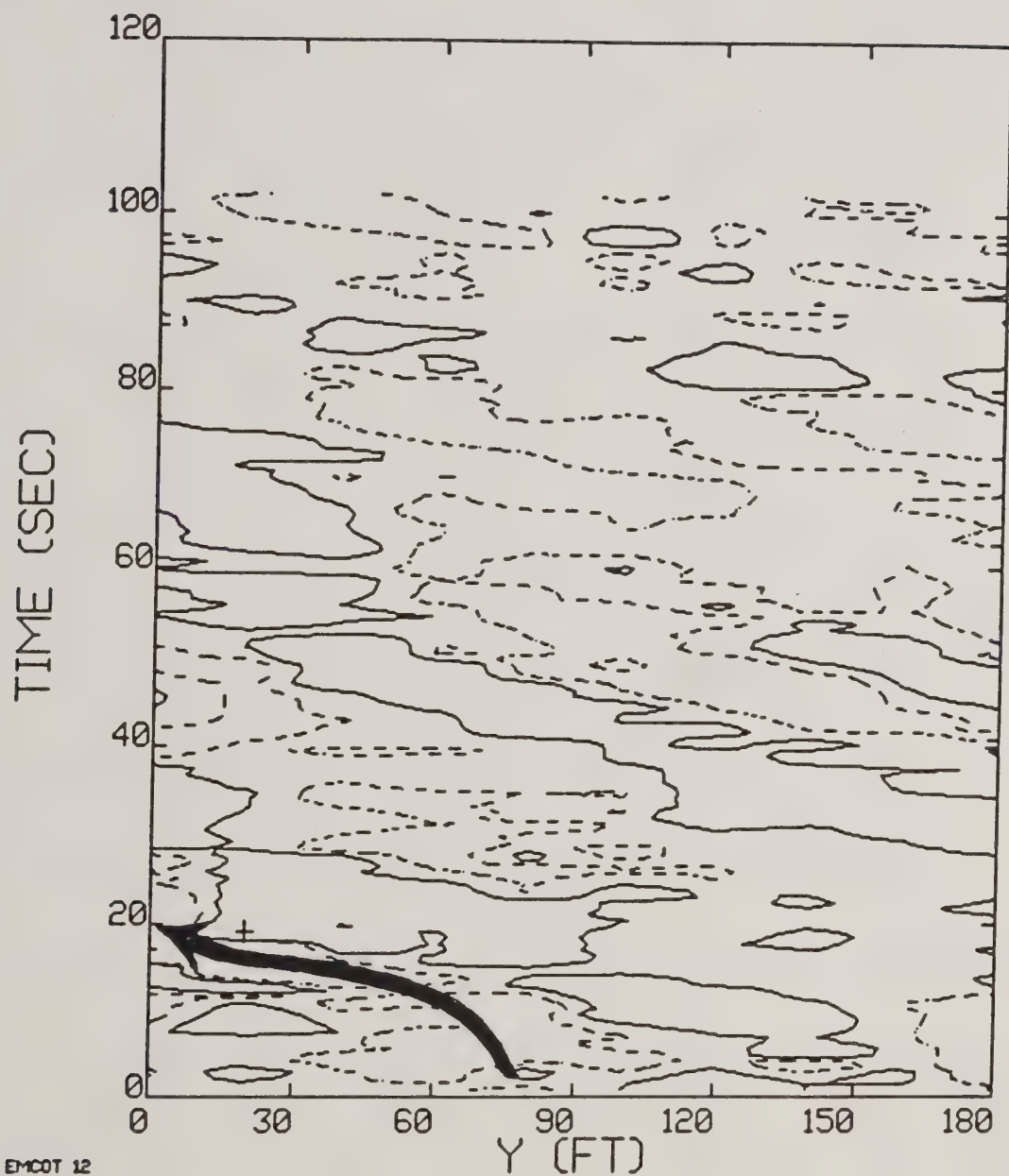


Figure 7-14. Run 12, date 04/29, Bell 206B.

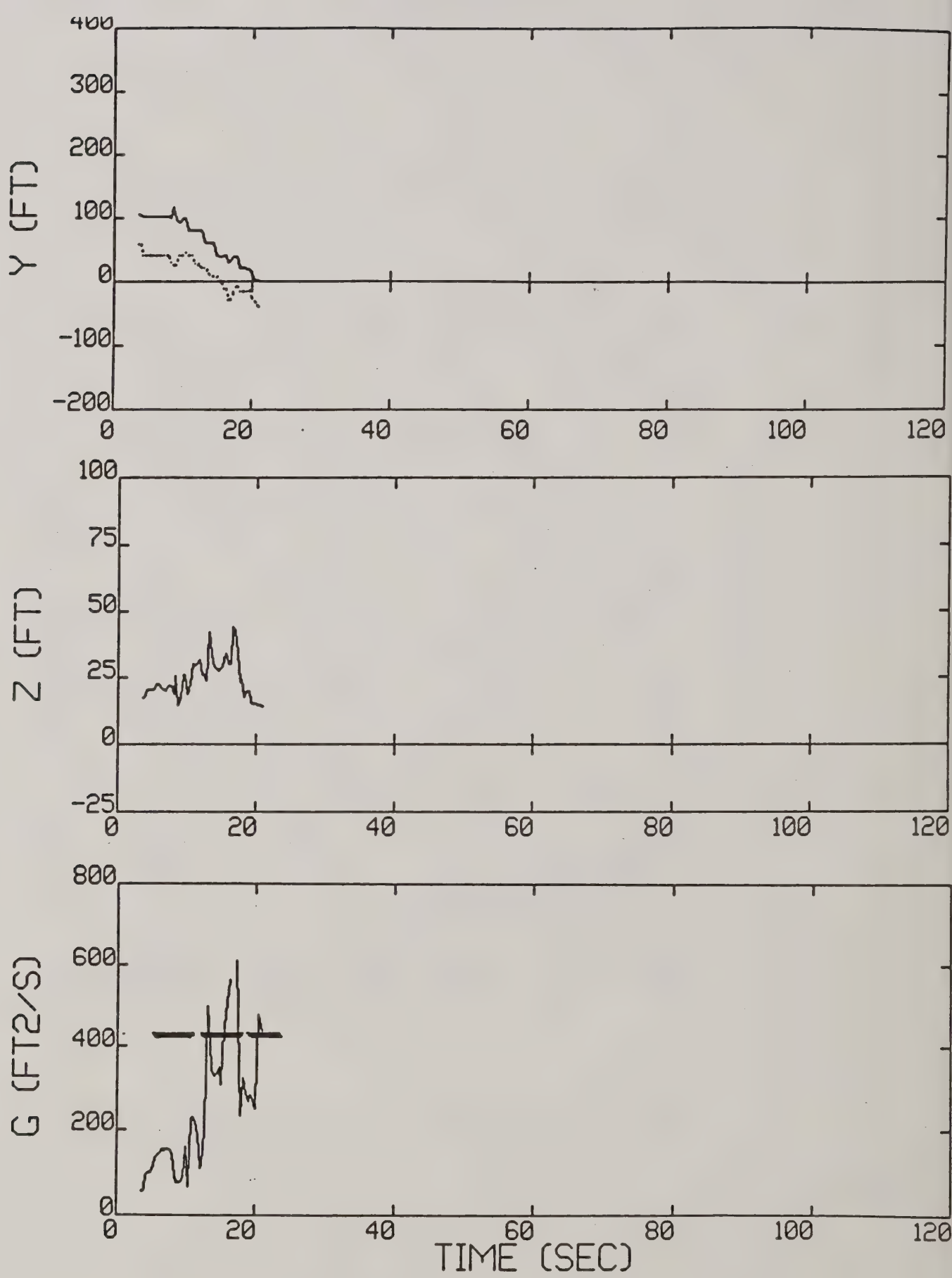


Figure 7-14b. Run 12 reduced data.

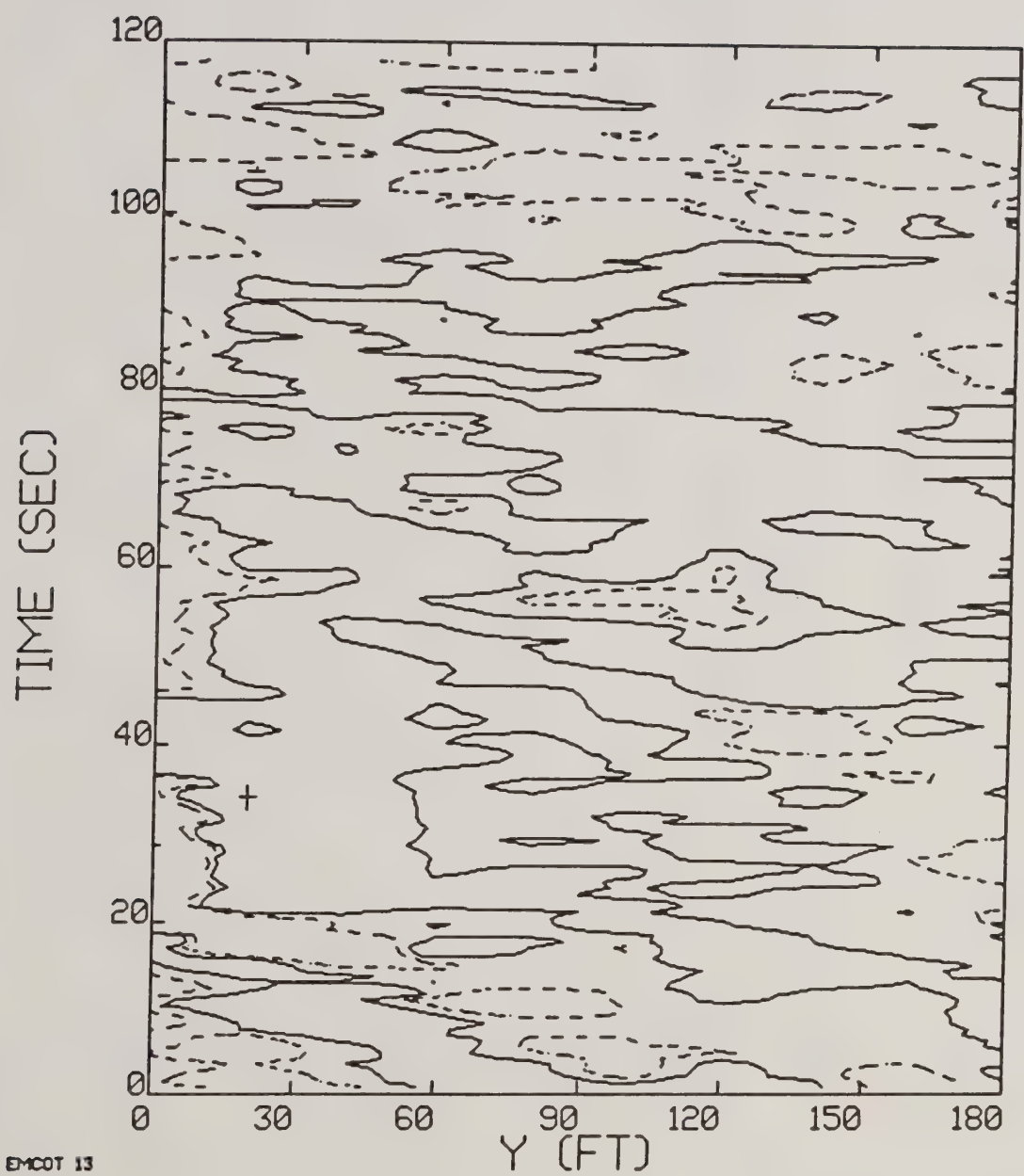


Figure 7-15. Run 13, date 04/29, Bell 206B.

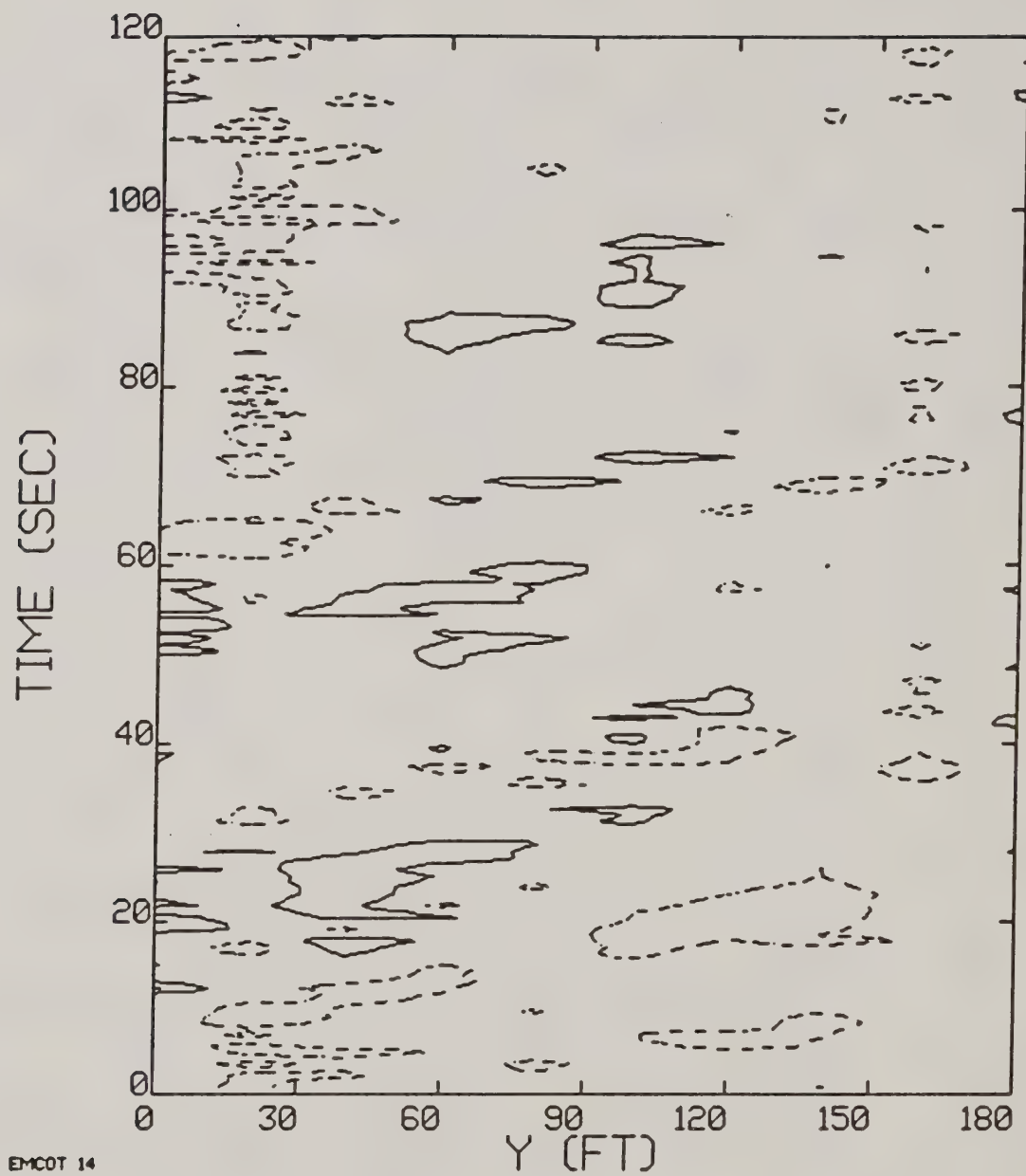


Figure 7-16. Run 14, date 04/30, Bell 206B.

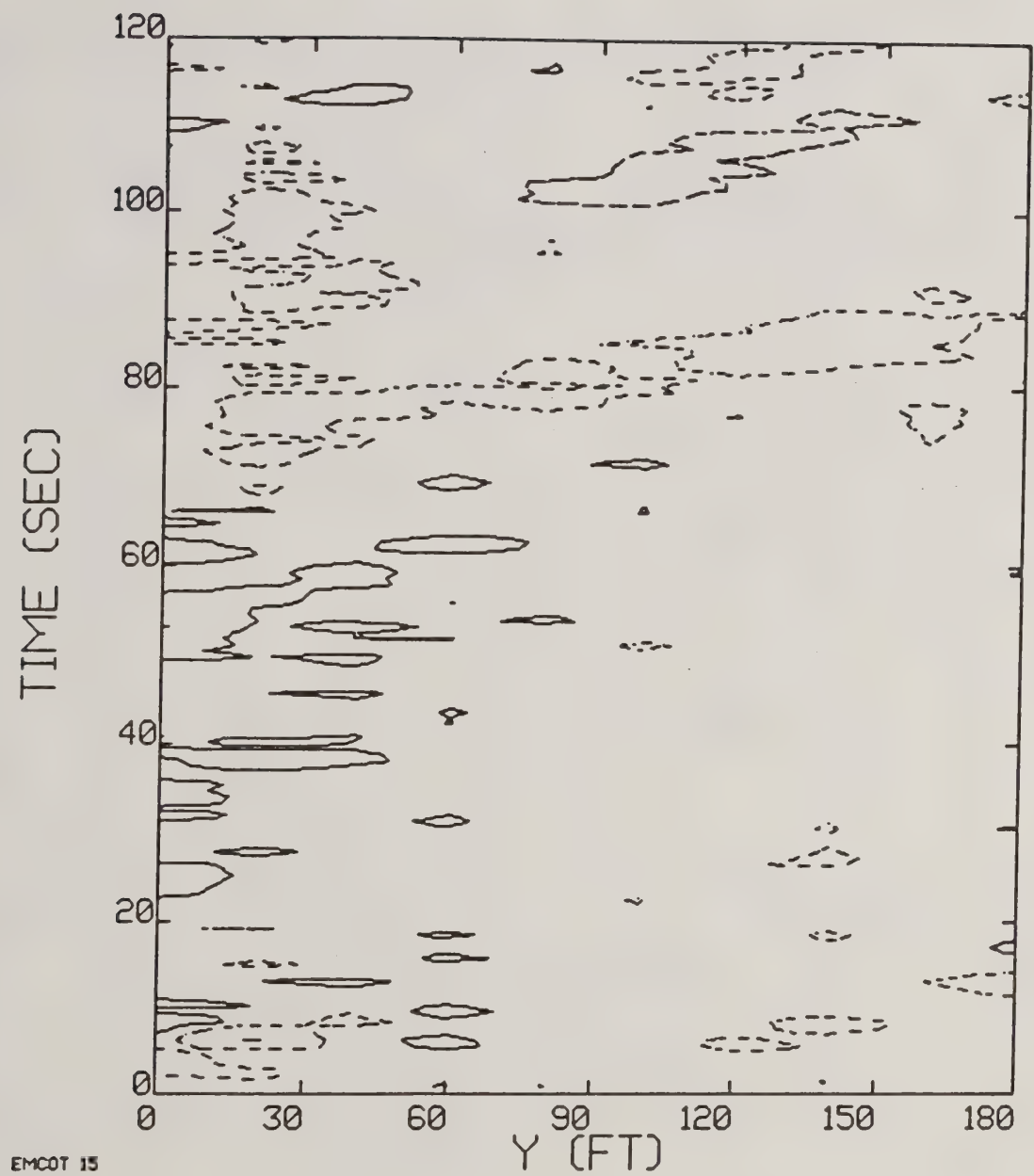


Figure 7-17. Run 15, date 04/30, Bell 206B.

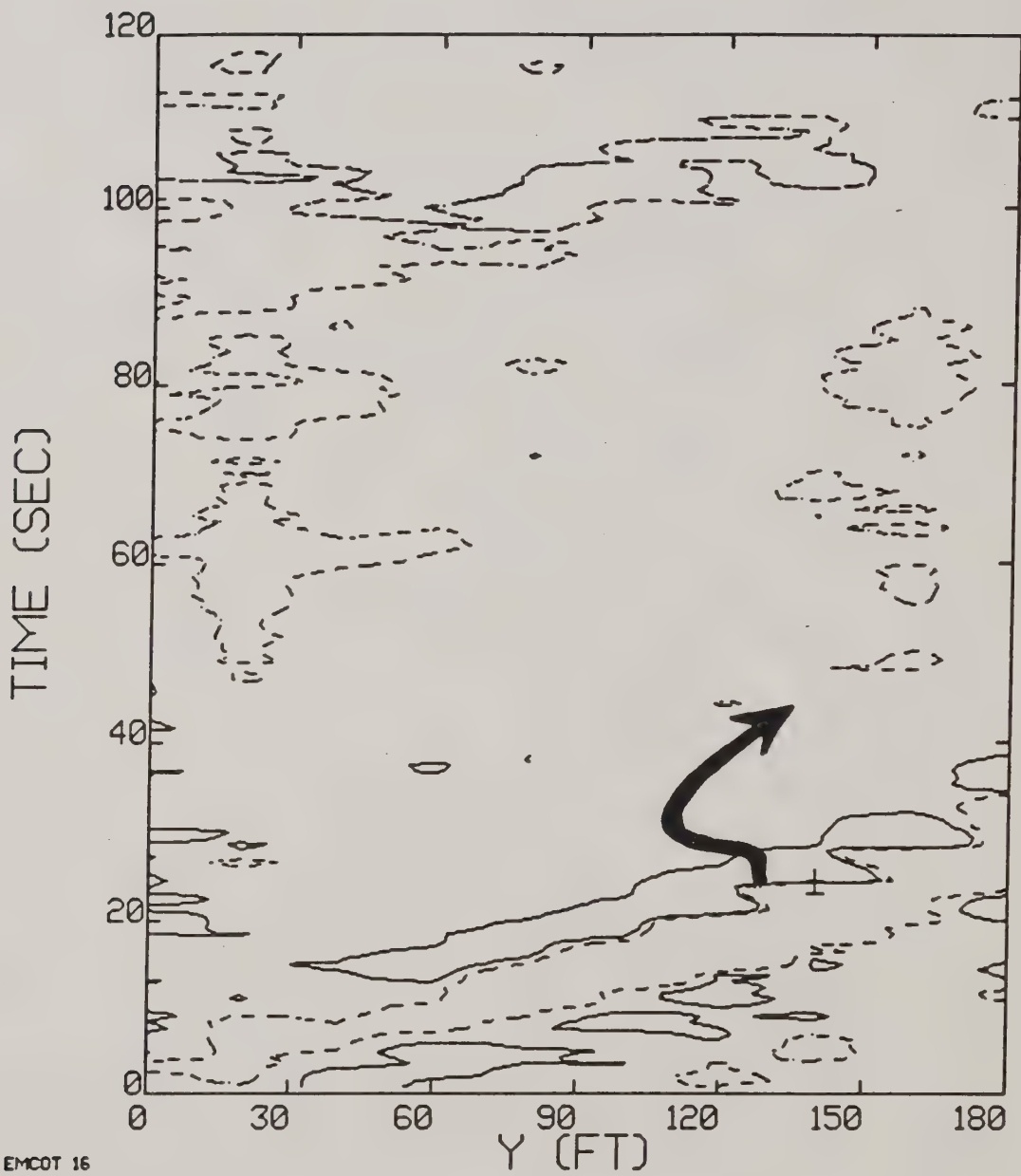


Figure 7-18. Run 16, date 04/30, Bell 206B.

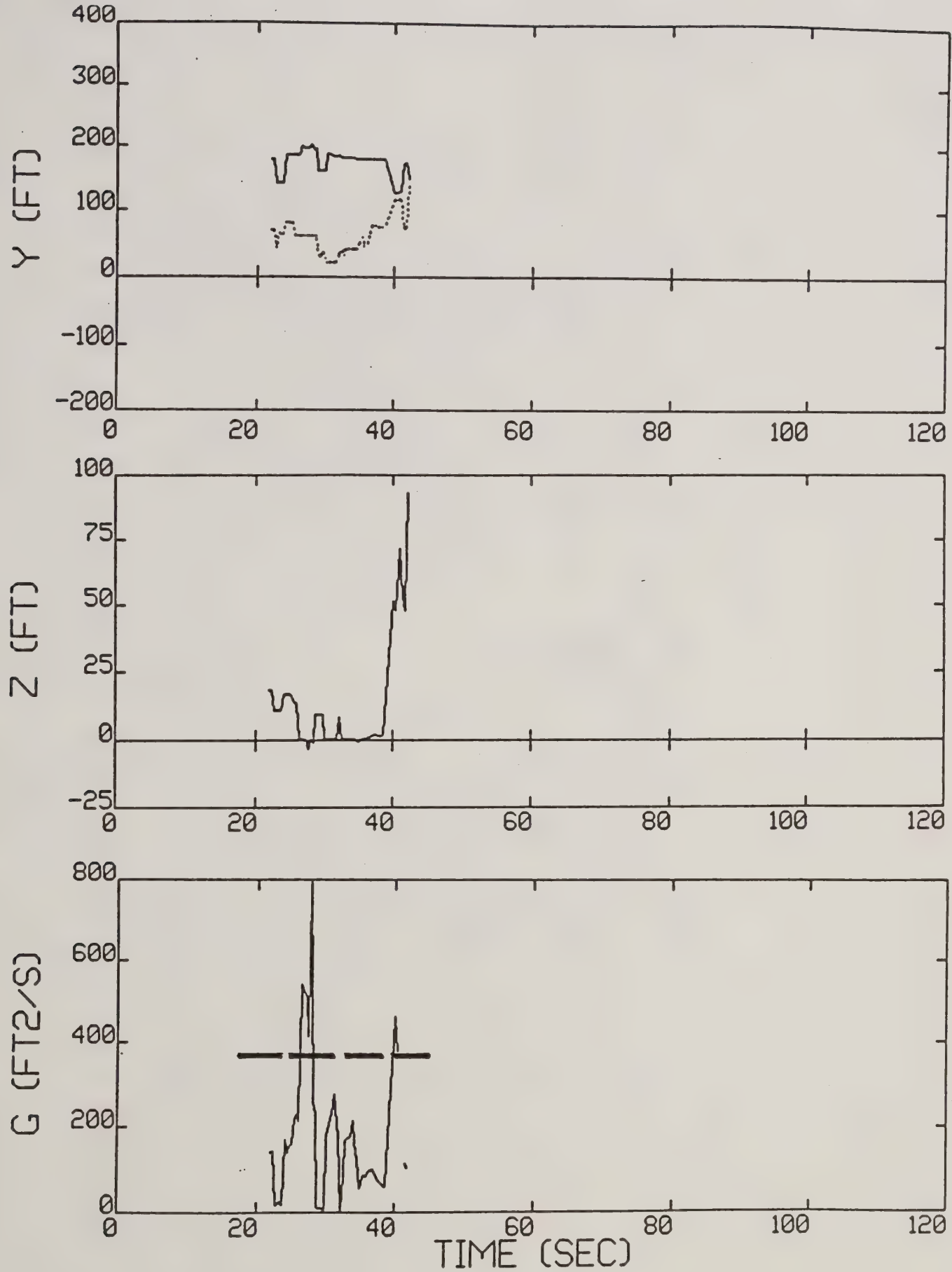


Figure 7-18b. Run 16 reduced data.

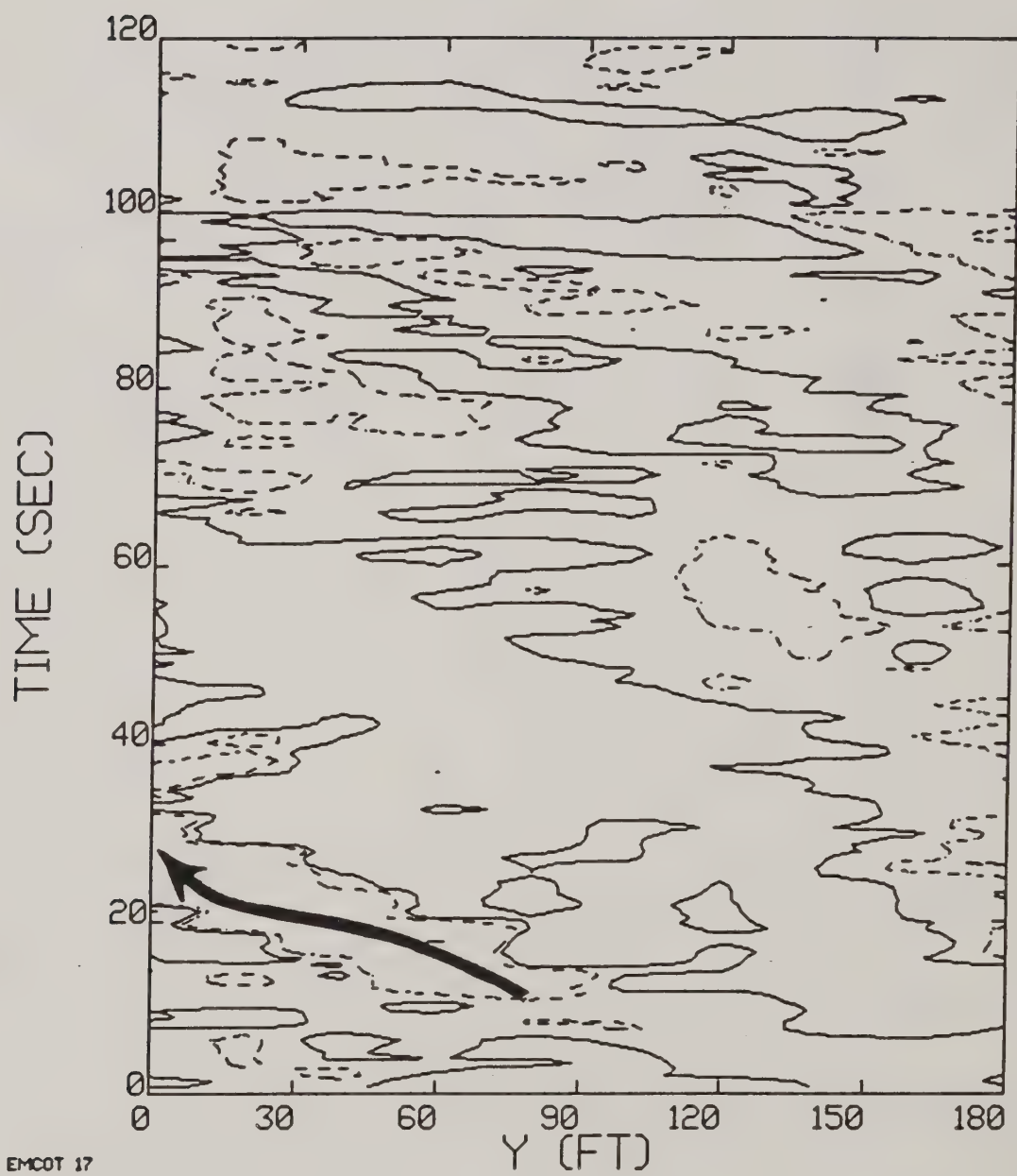


Figure 7-19. Run 17, date 04/30, Bell 206B.

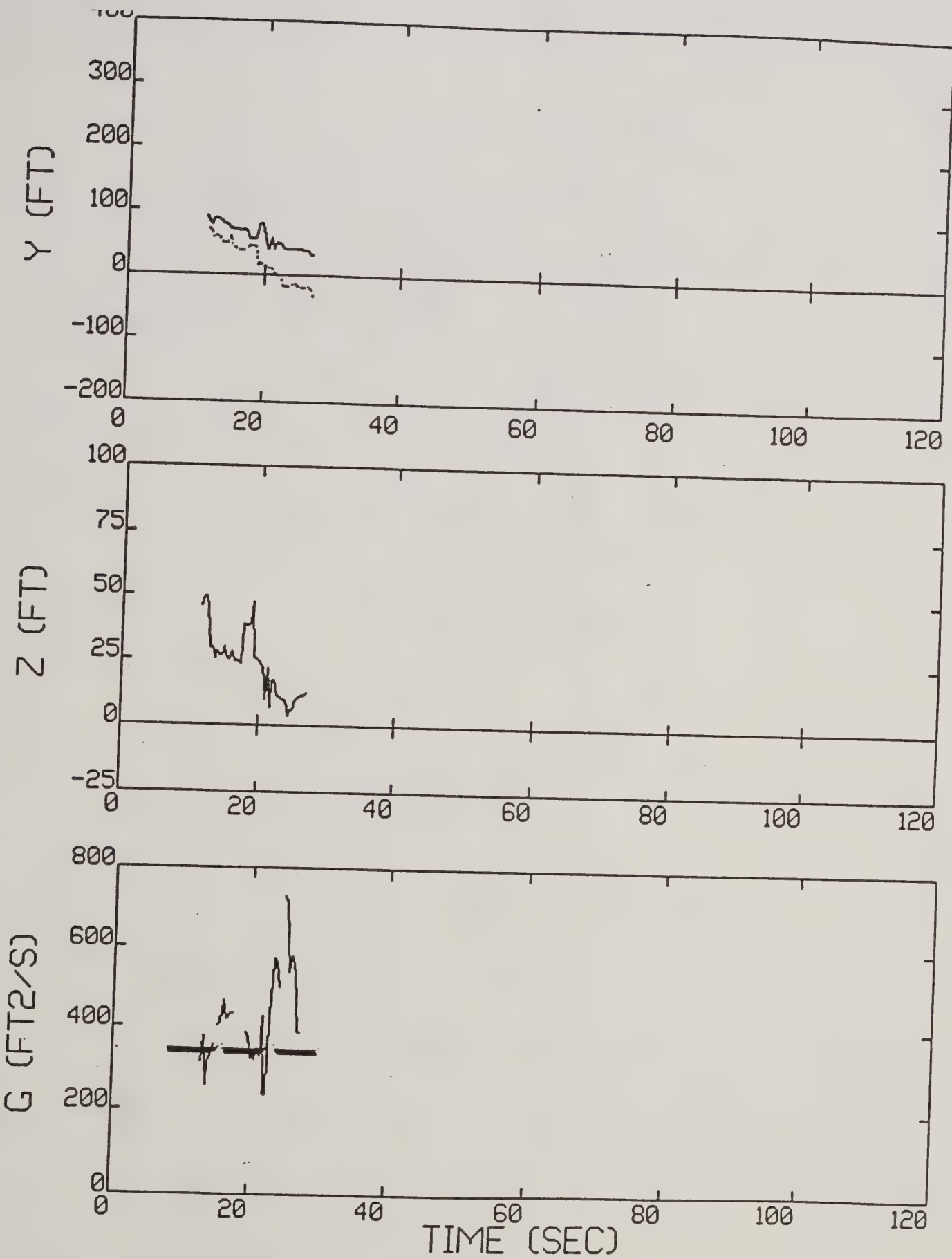


Figure 7-19b. Run 17 reduced data.

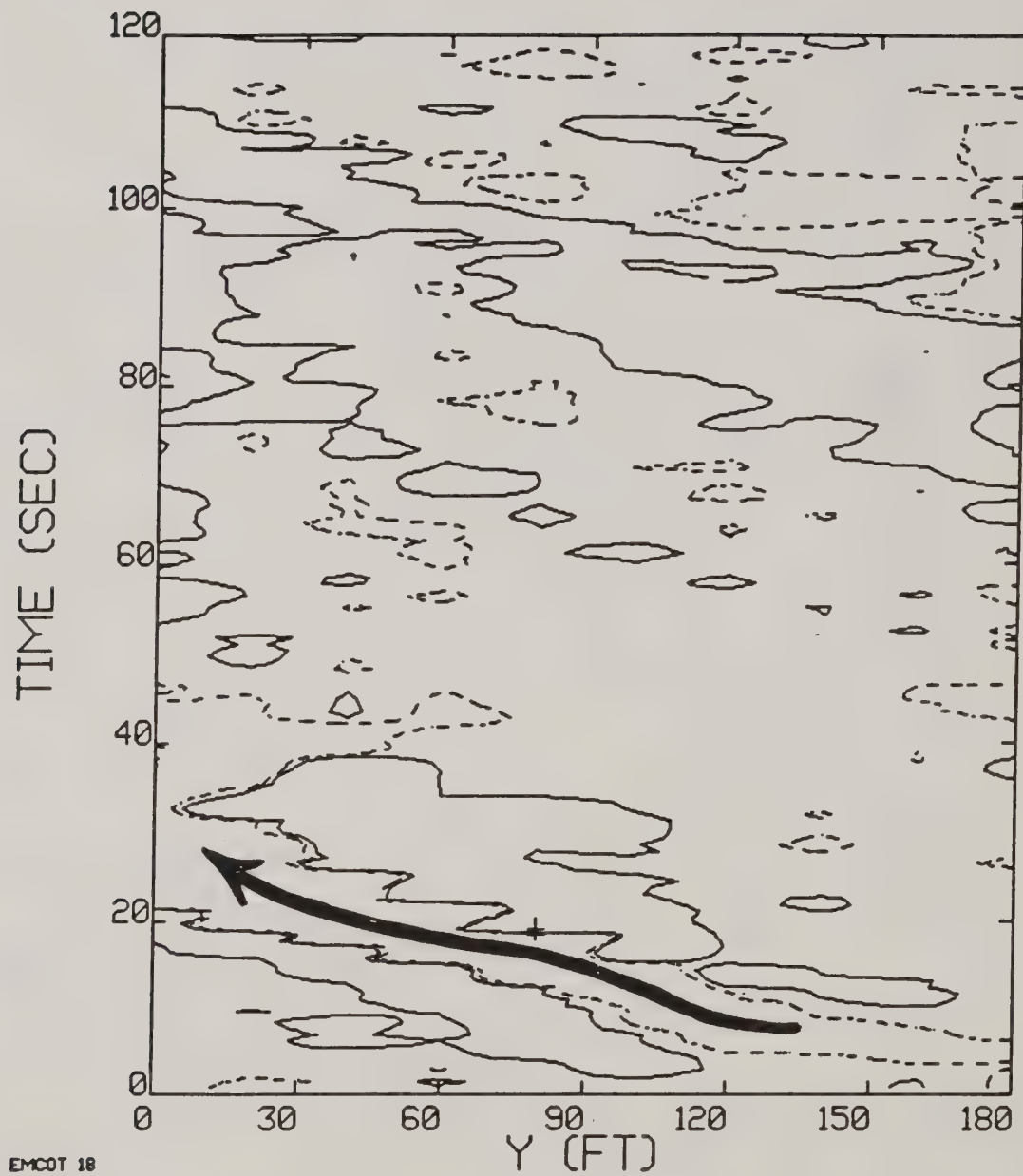


Figure 7-20. Run 18, date 05/30, Bell 206B.

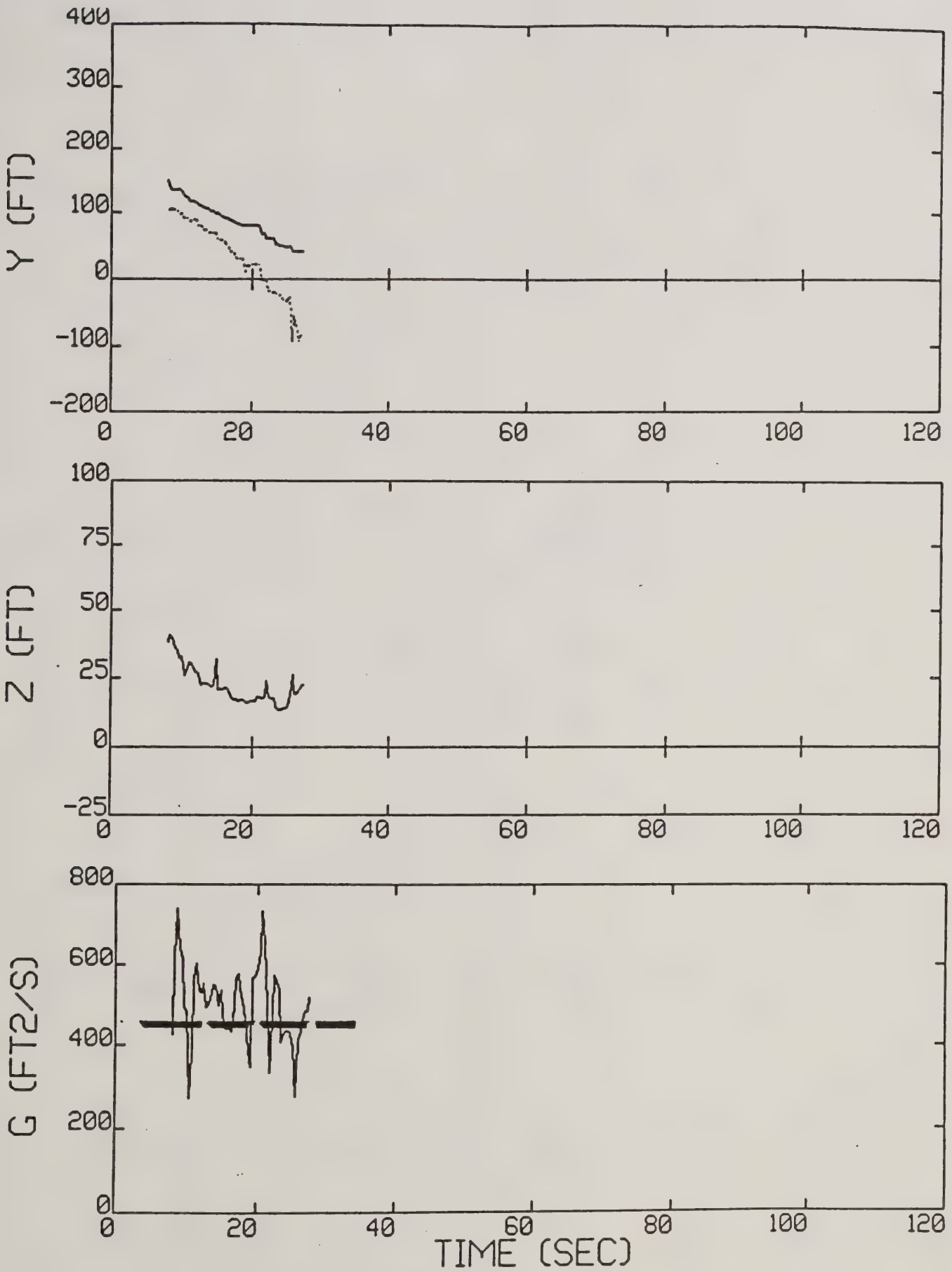


Figure 7-20b. Run 18 reduced data.

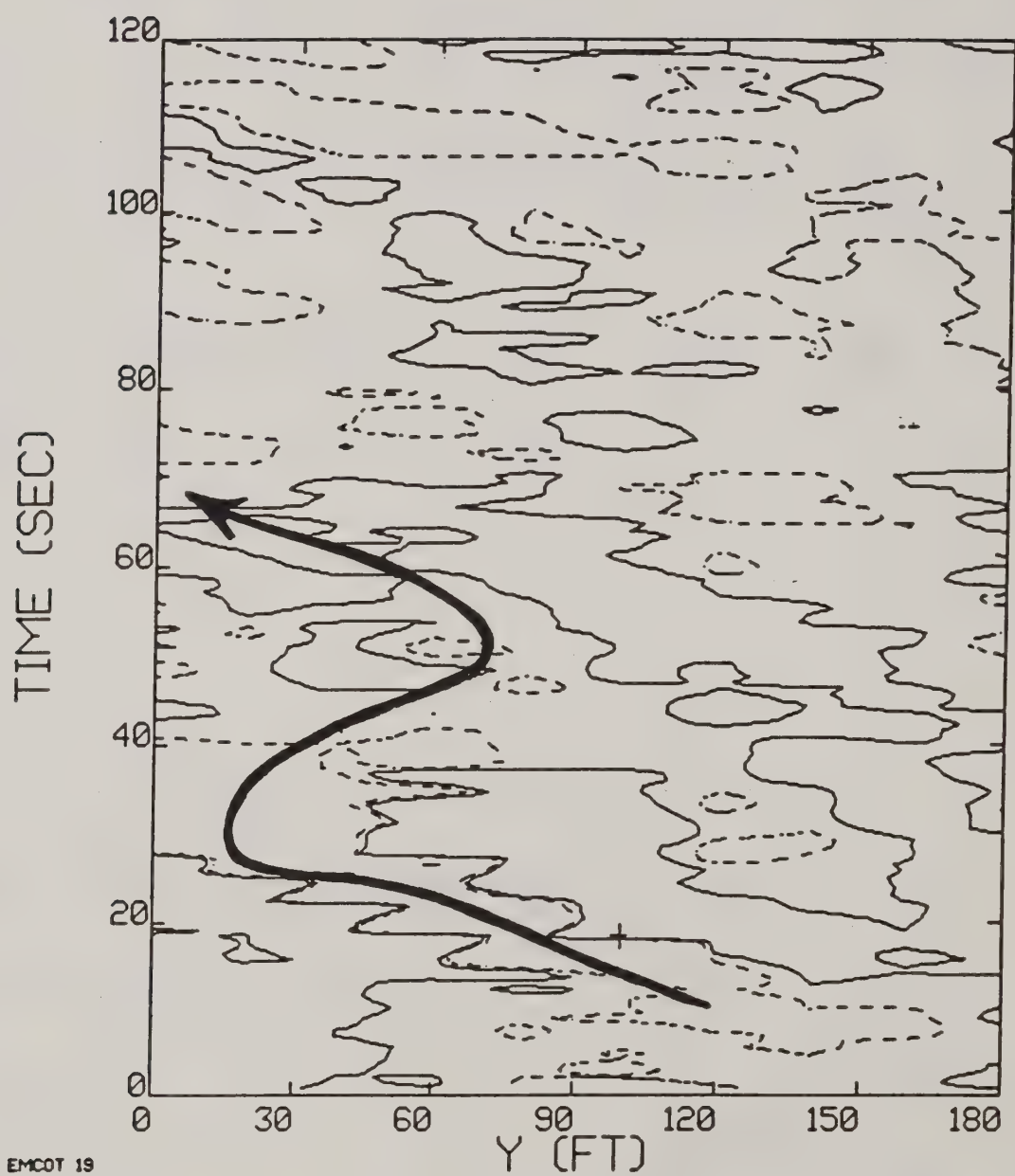


Figure 7-21. Run 19, date 04/30, Bell 206b.

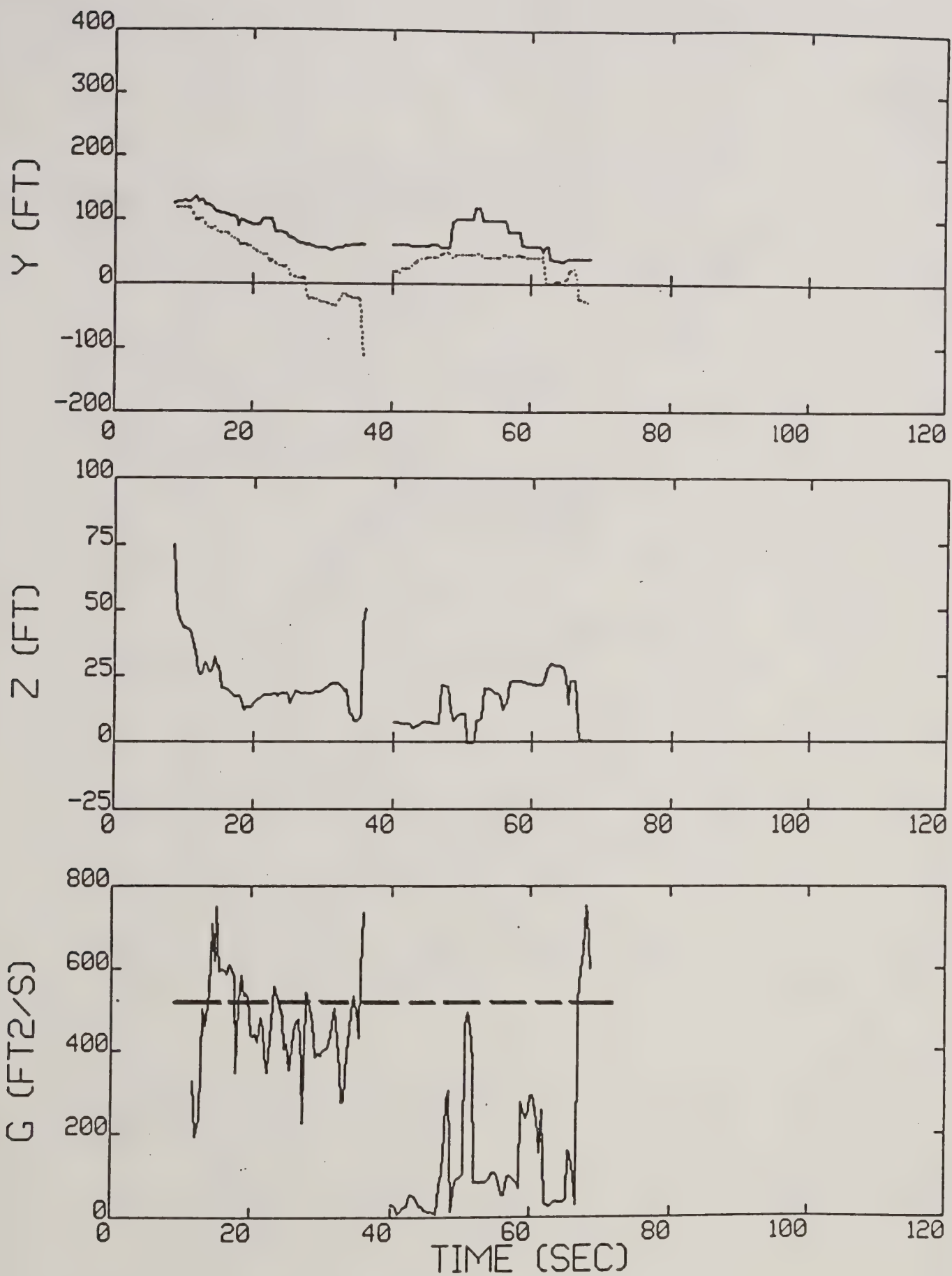


Figure 7-21b. Run 19 reduced data.

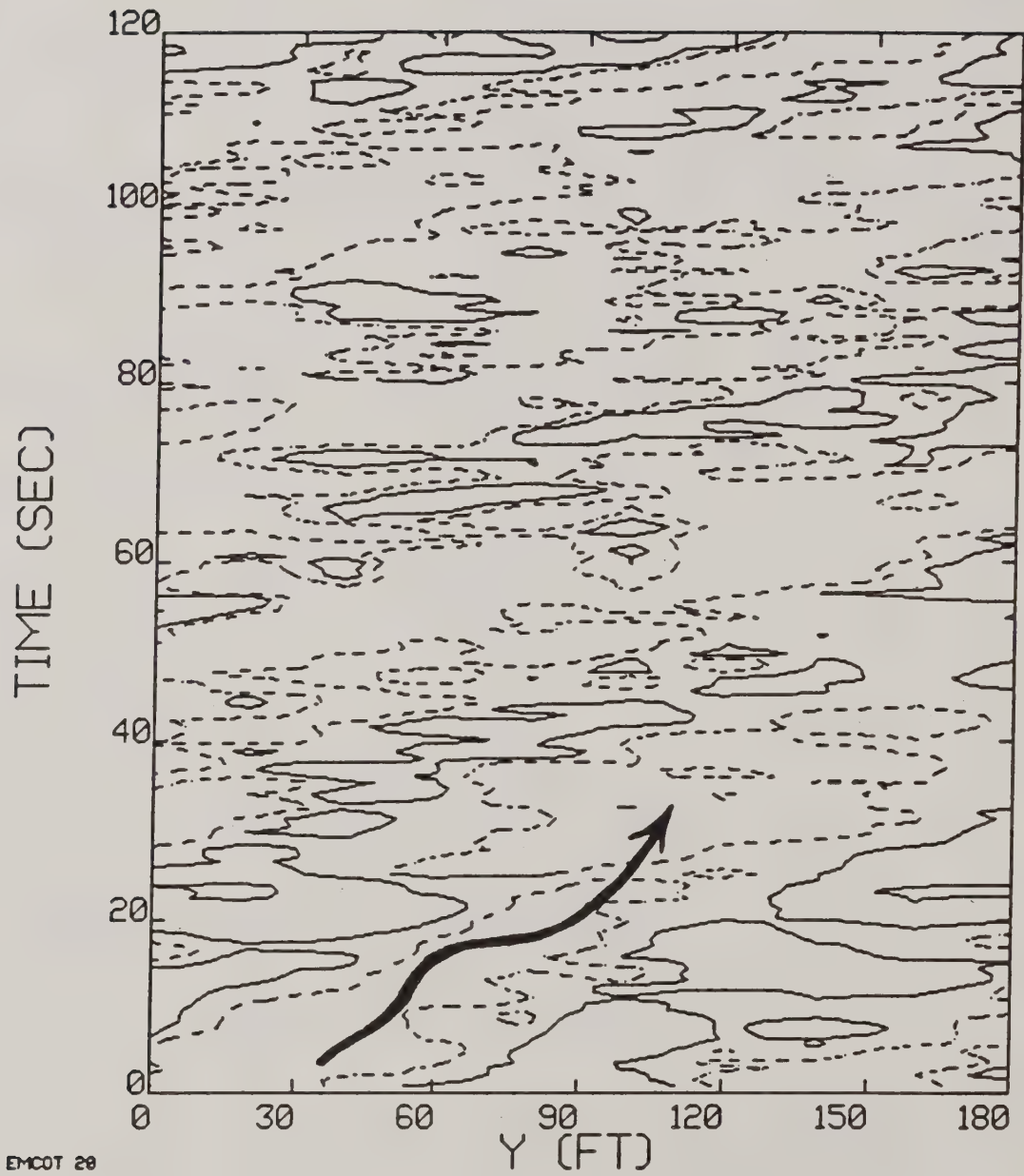


Figure 7-22. Run 20, date 05/01, Bell 206B.

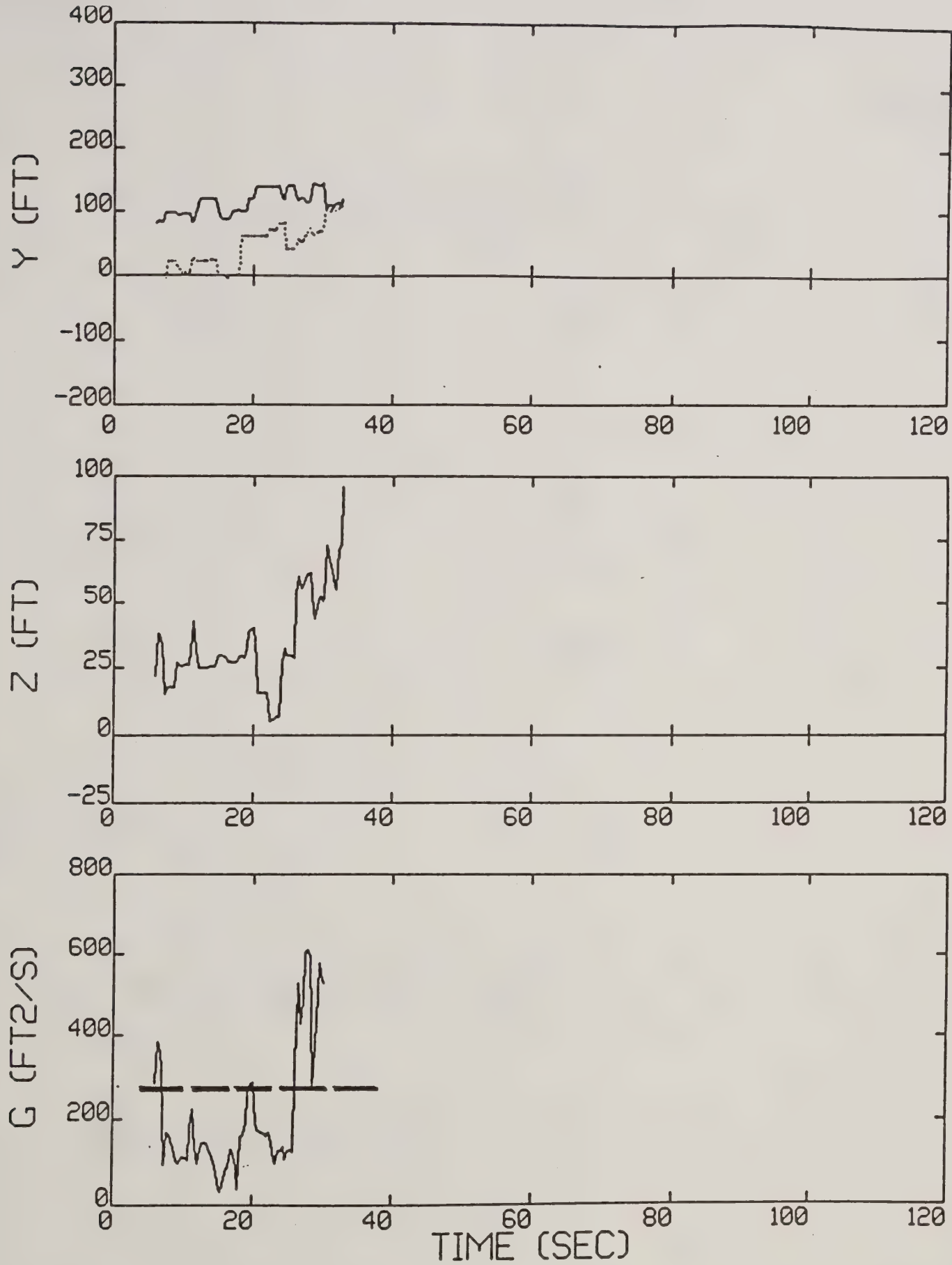


Figure 7-22b. Run 20 reduced data.

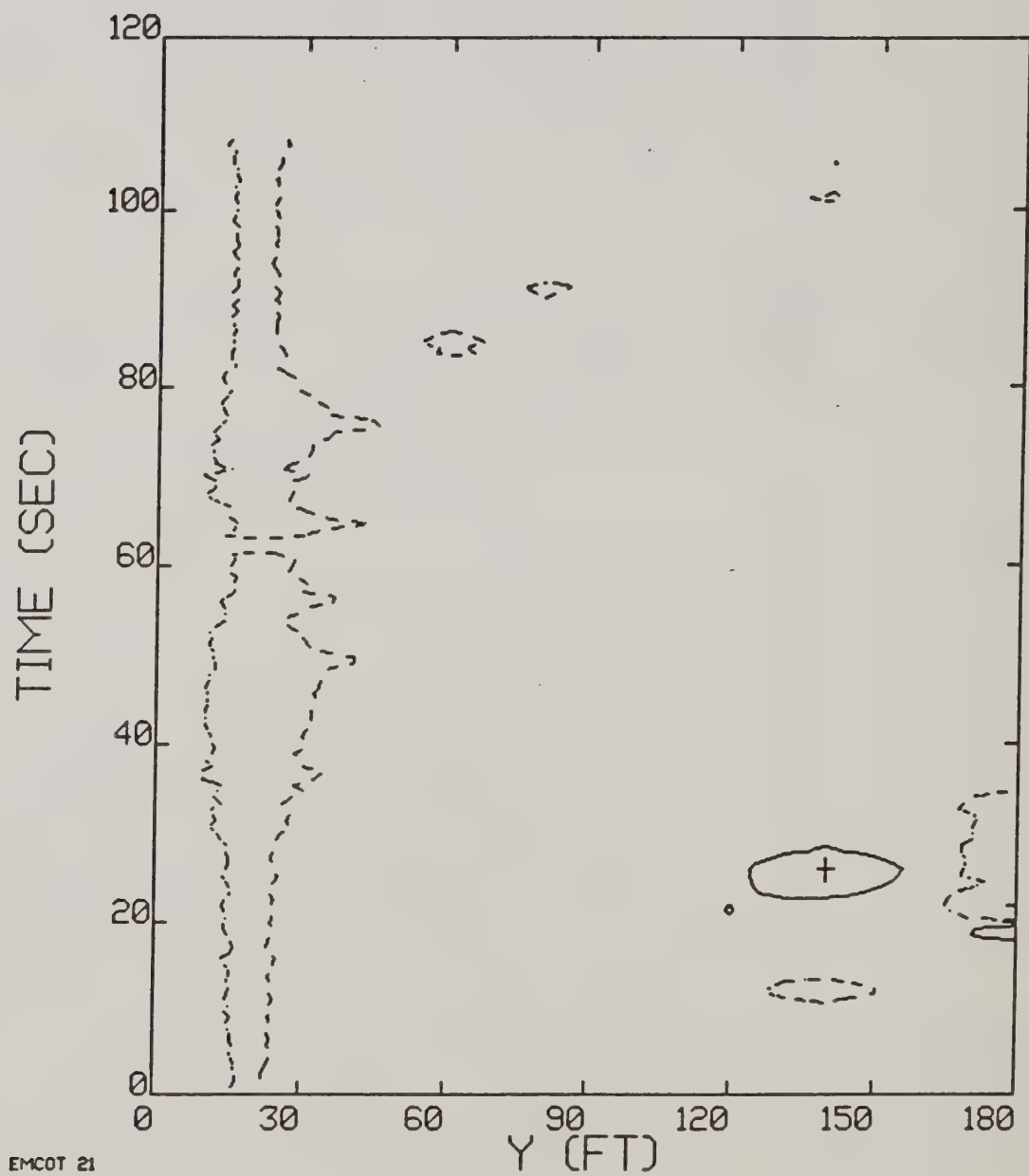


Figure 7-23. Run 21, date 05/04, Bell 206B.

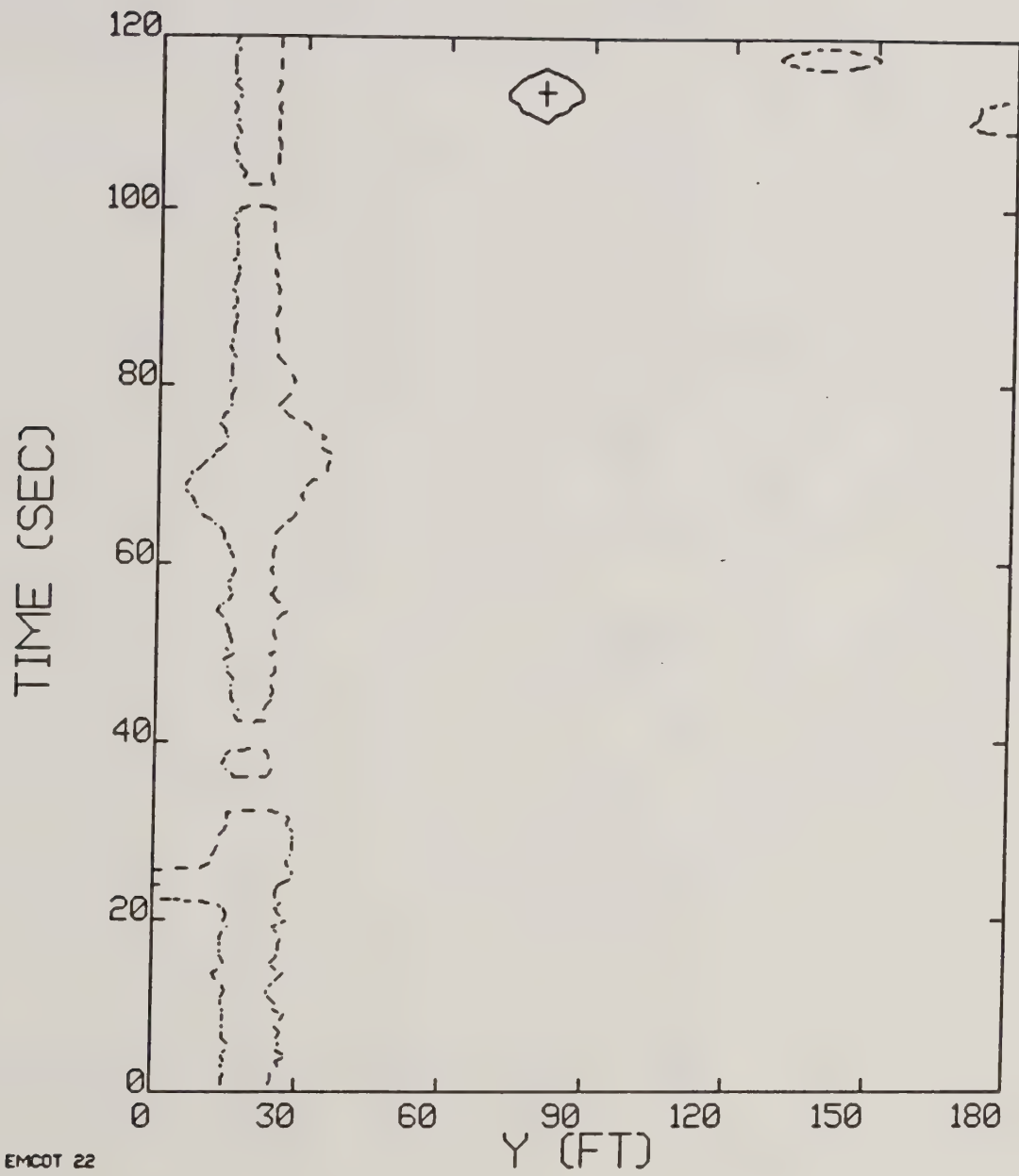


Figure 7-24. Run 22, date 05/04, Bell 206B.

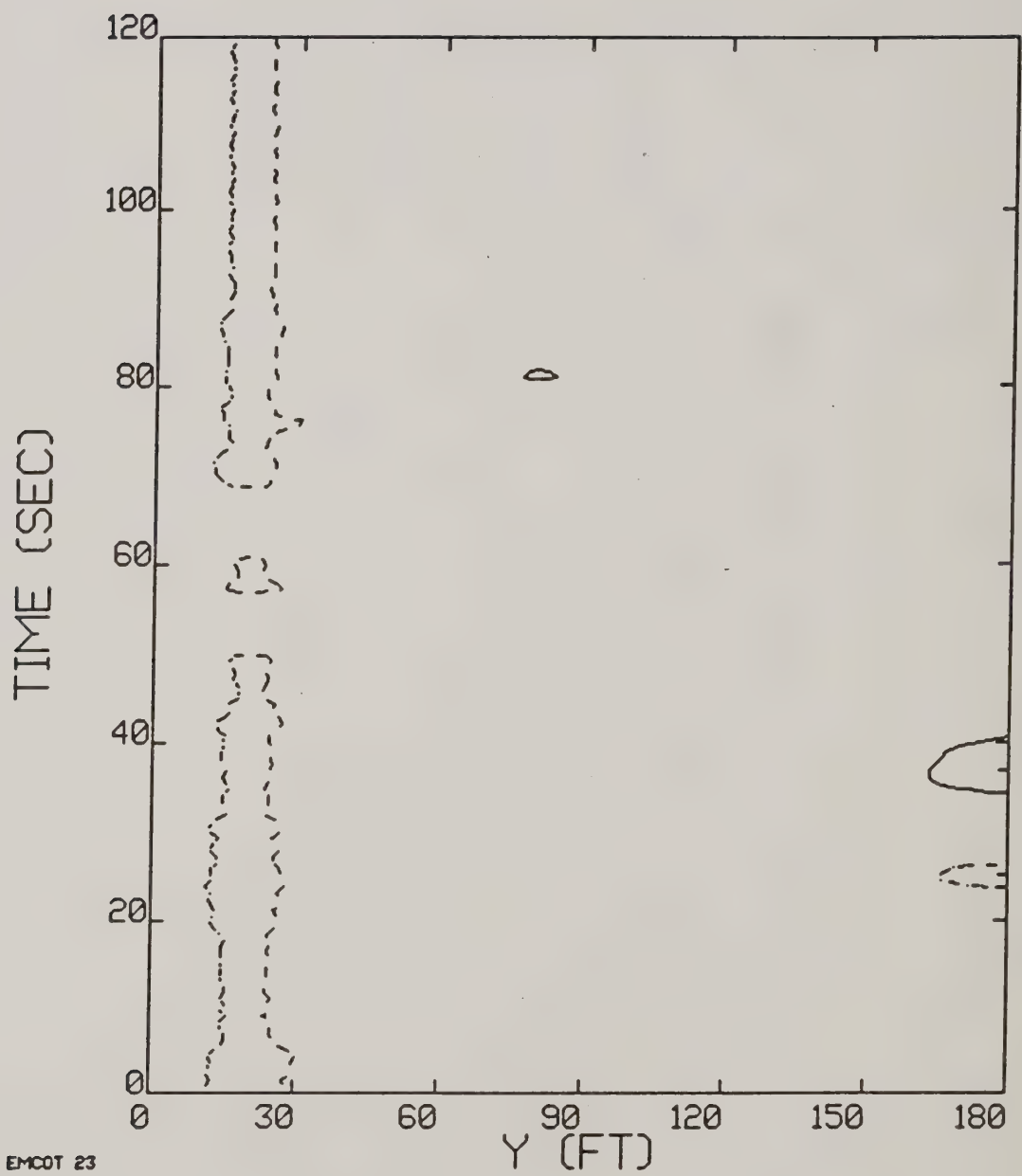


Figure 7-25. Run 23, date 05/04, Bell 206B.

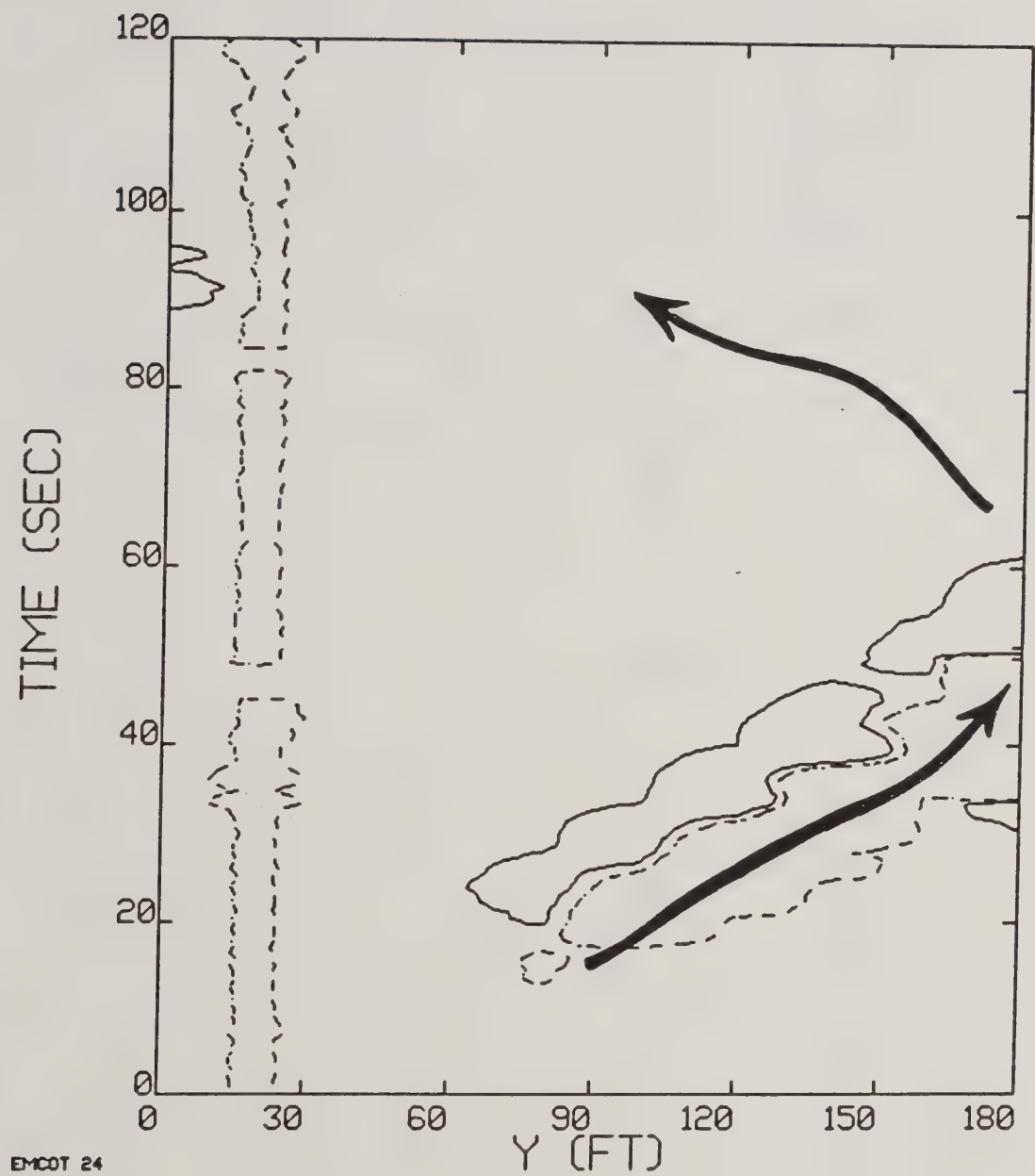


Figure 7-26. Run 24, date 05/04, Bell 206B.

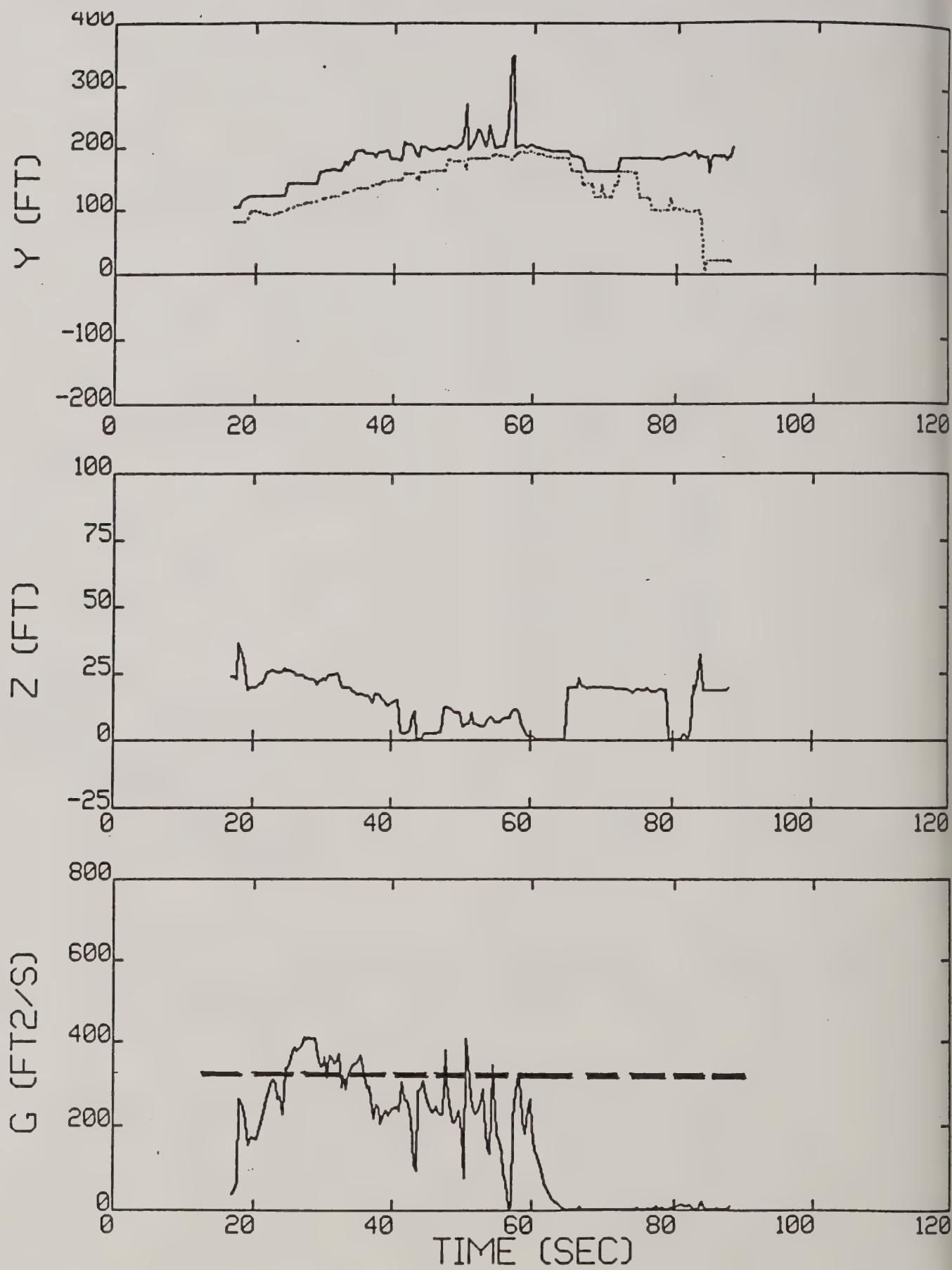


Figure 7-26b. Run 24 reduced data.

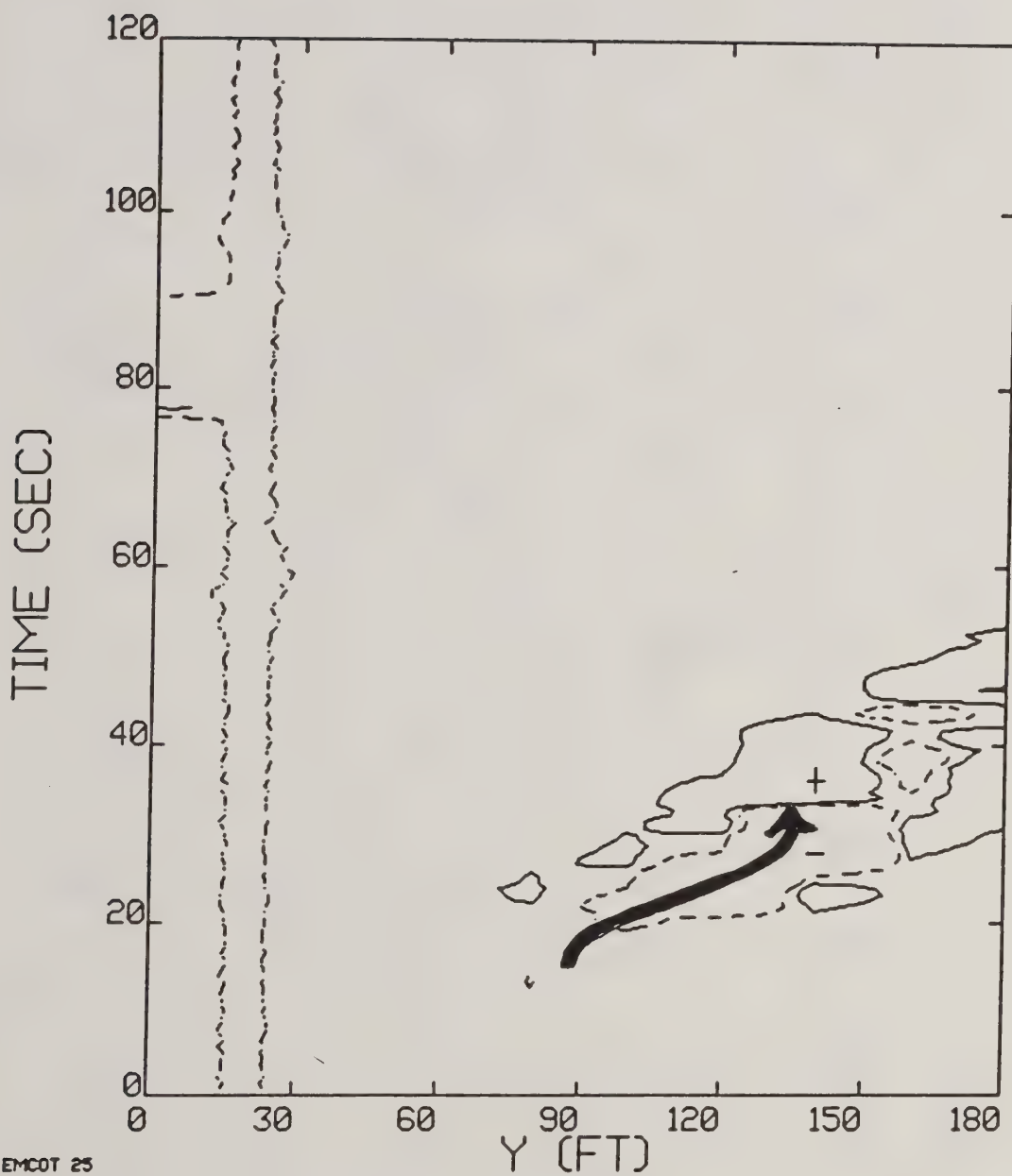


Figure 7-27. Run 25, date 05/04, Bell 206B.

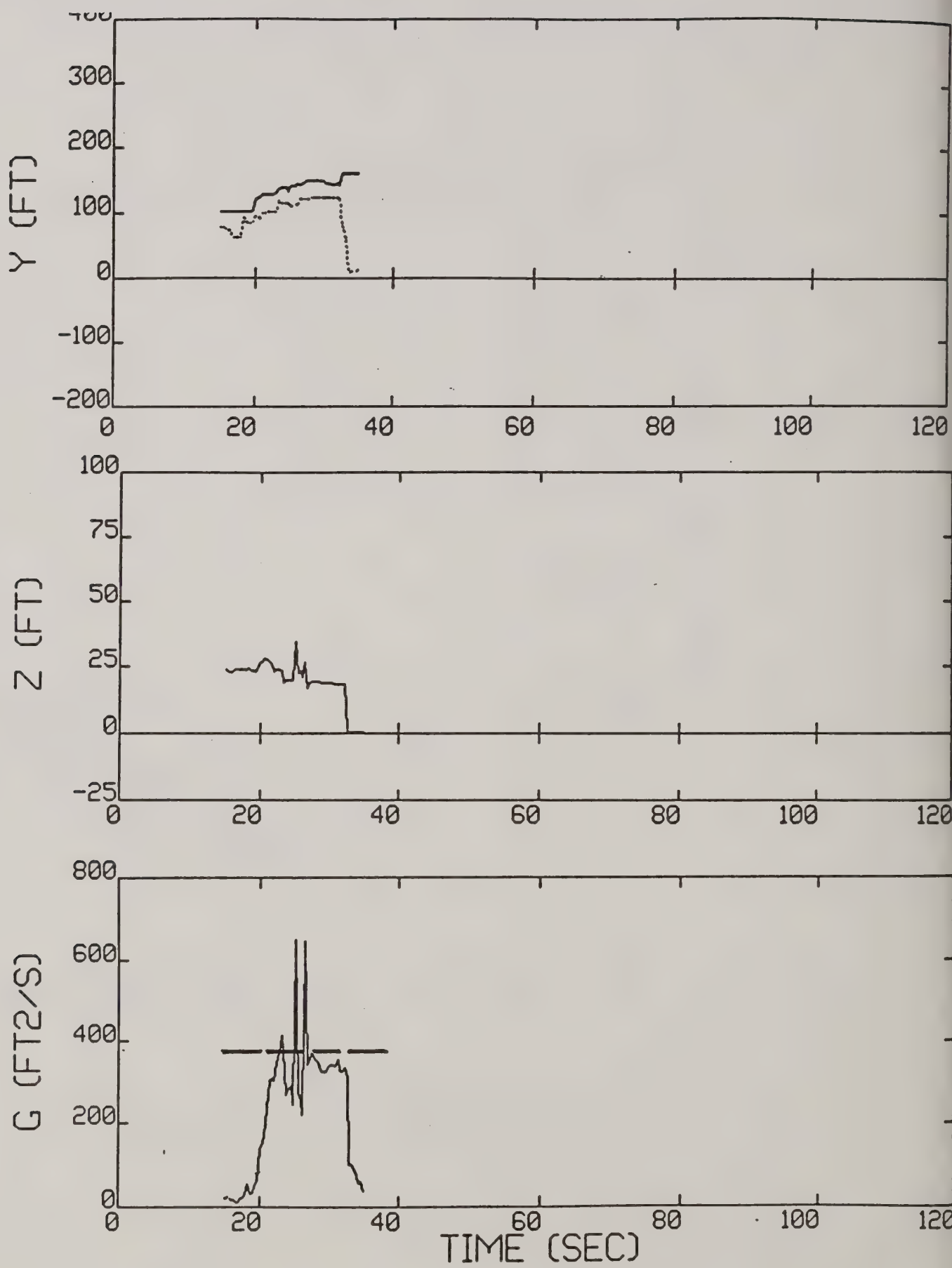


Figure 7-27b. Run 25 reduced data.

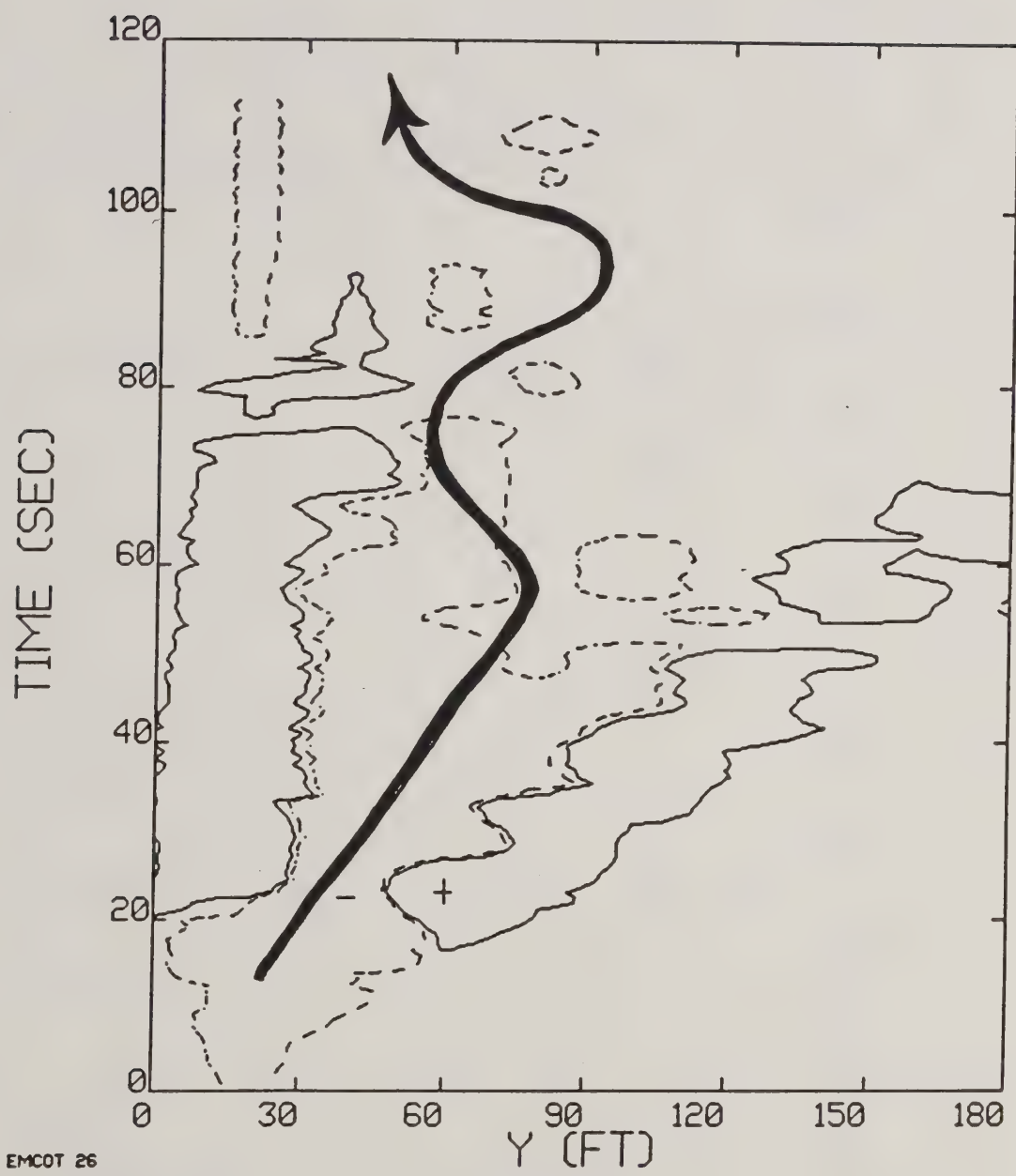


Figure 7-28. Run 26, date 05/04, Bell 206B.

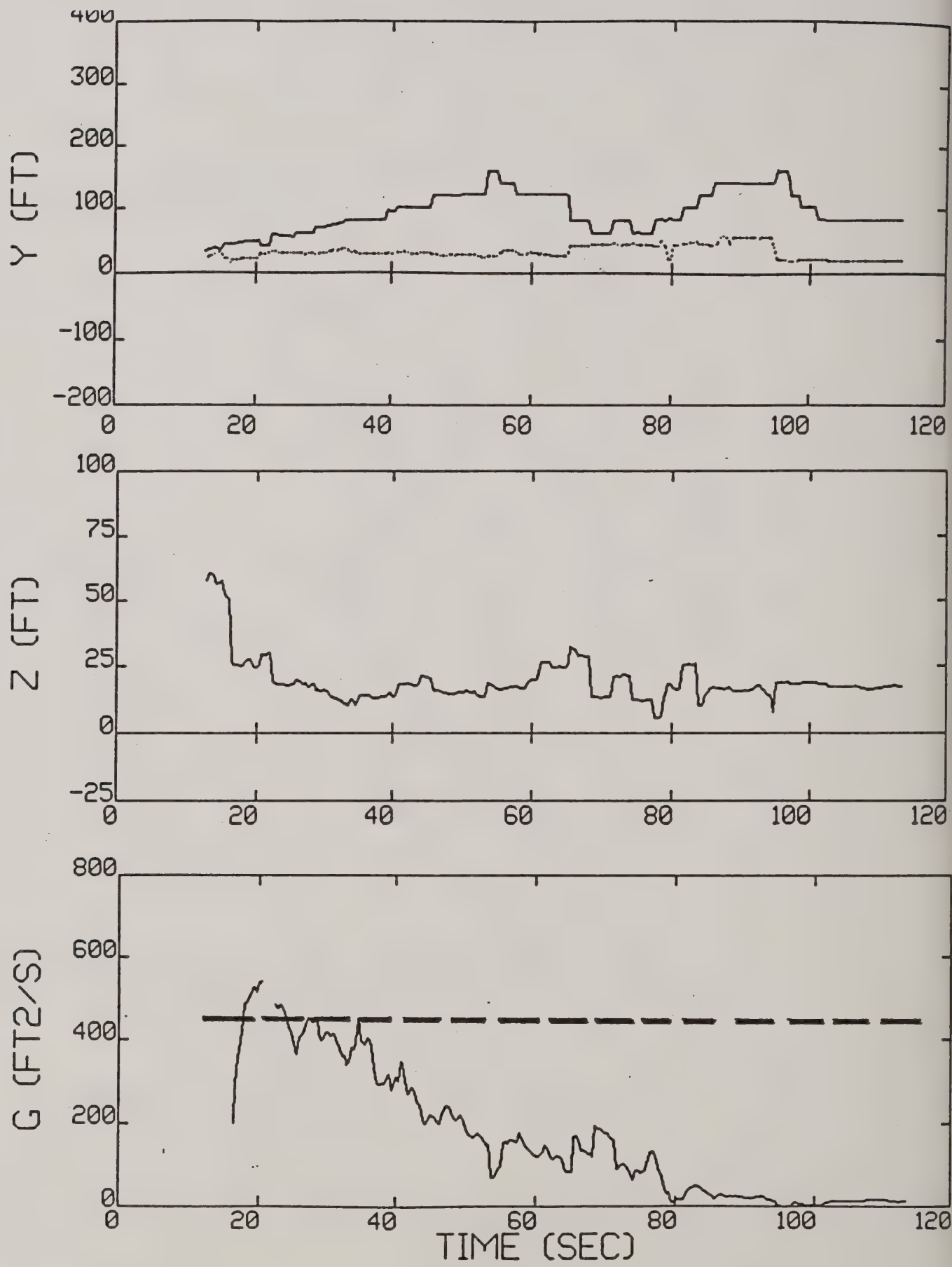


Figure 7-28b. Run 26 reduced data.

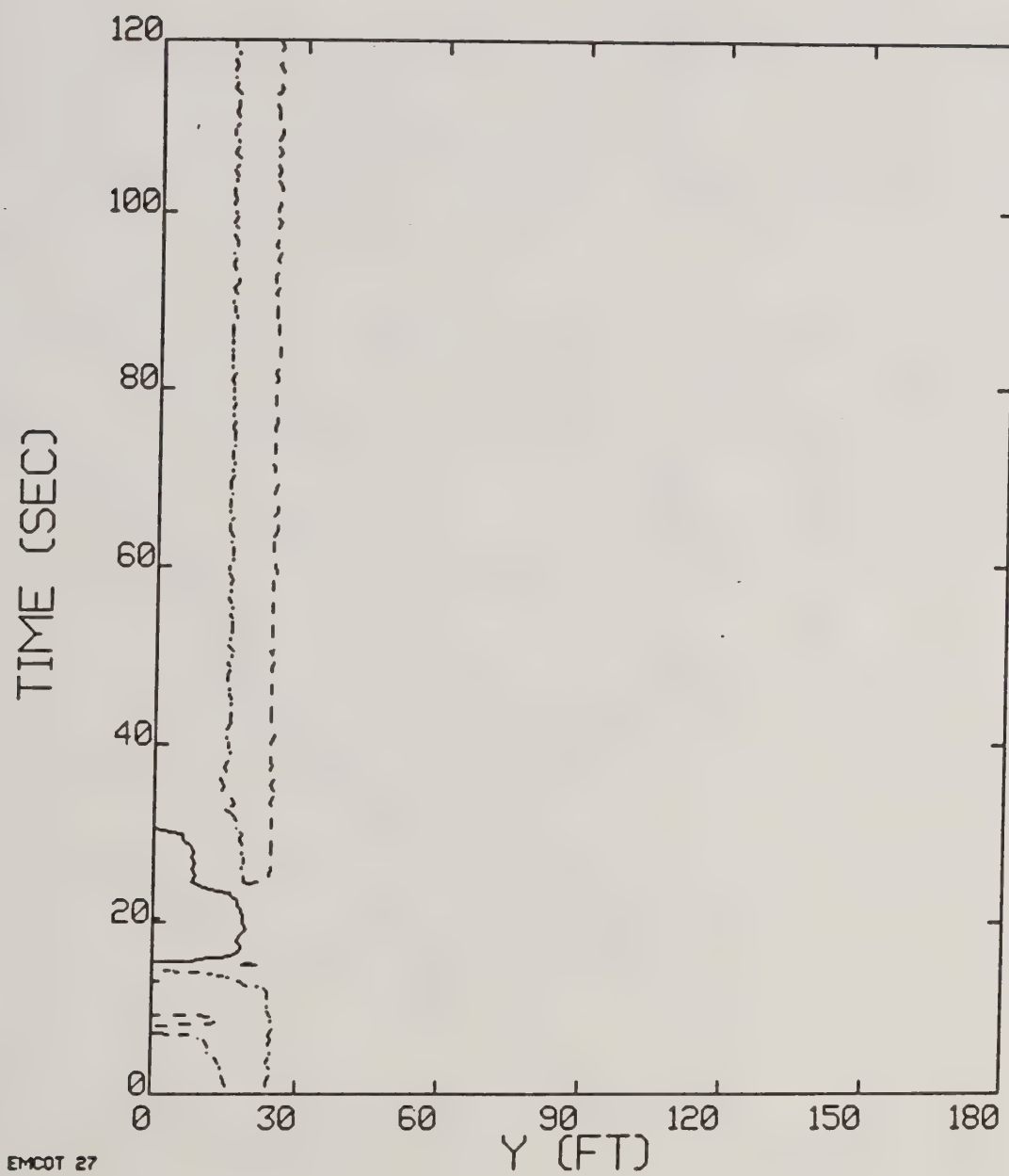


Figure 7-29. Run 27, date 05/04, Bell 206B.

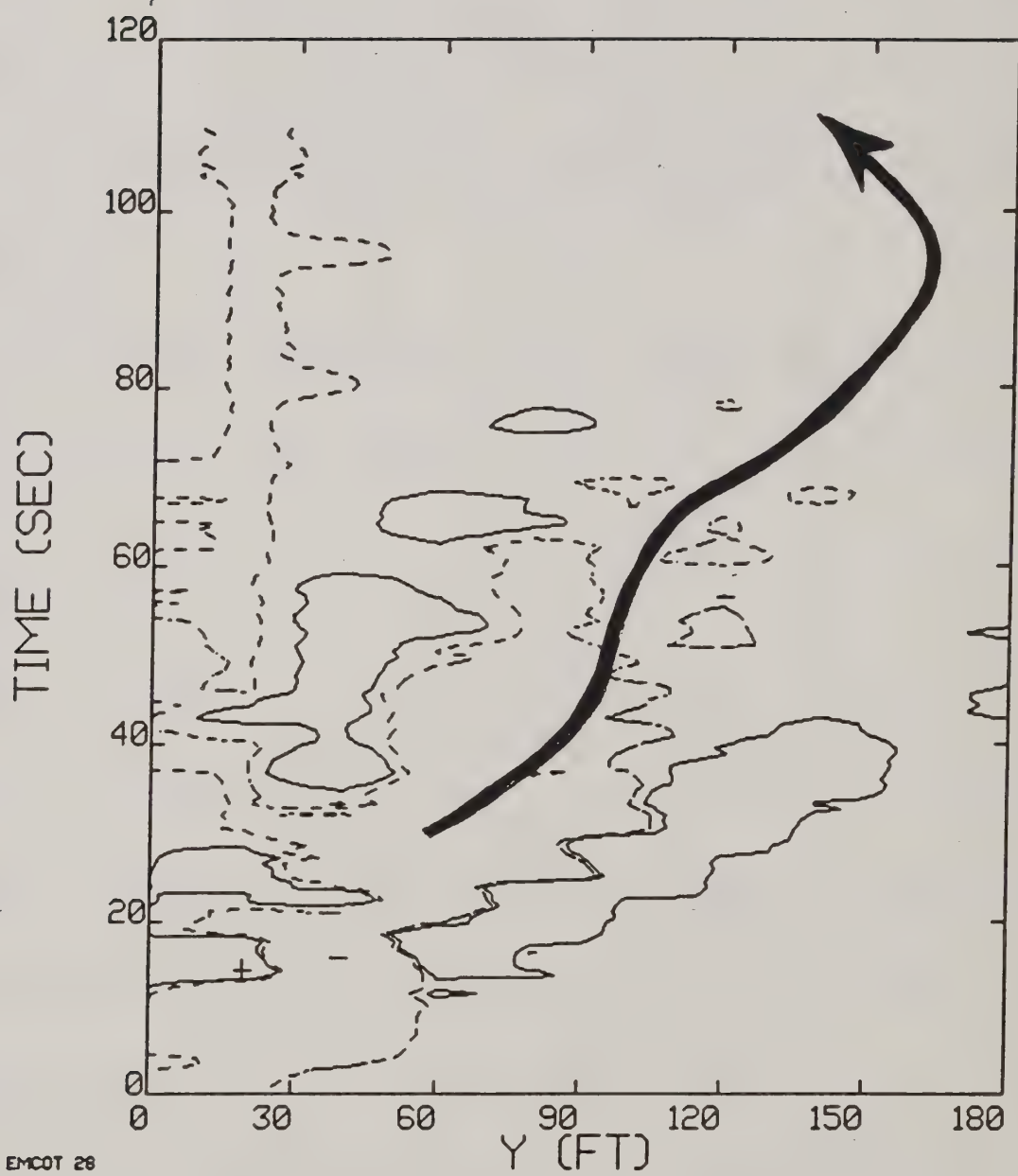


Figure 7-30. Run 28, date 05/04, Bell 206B.

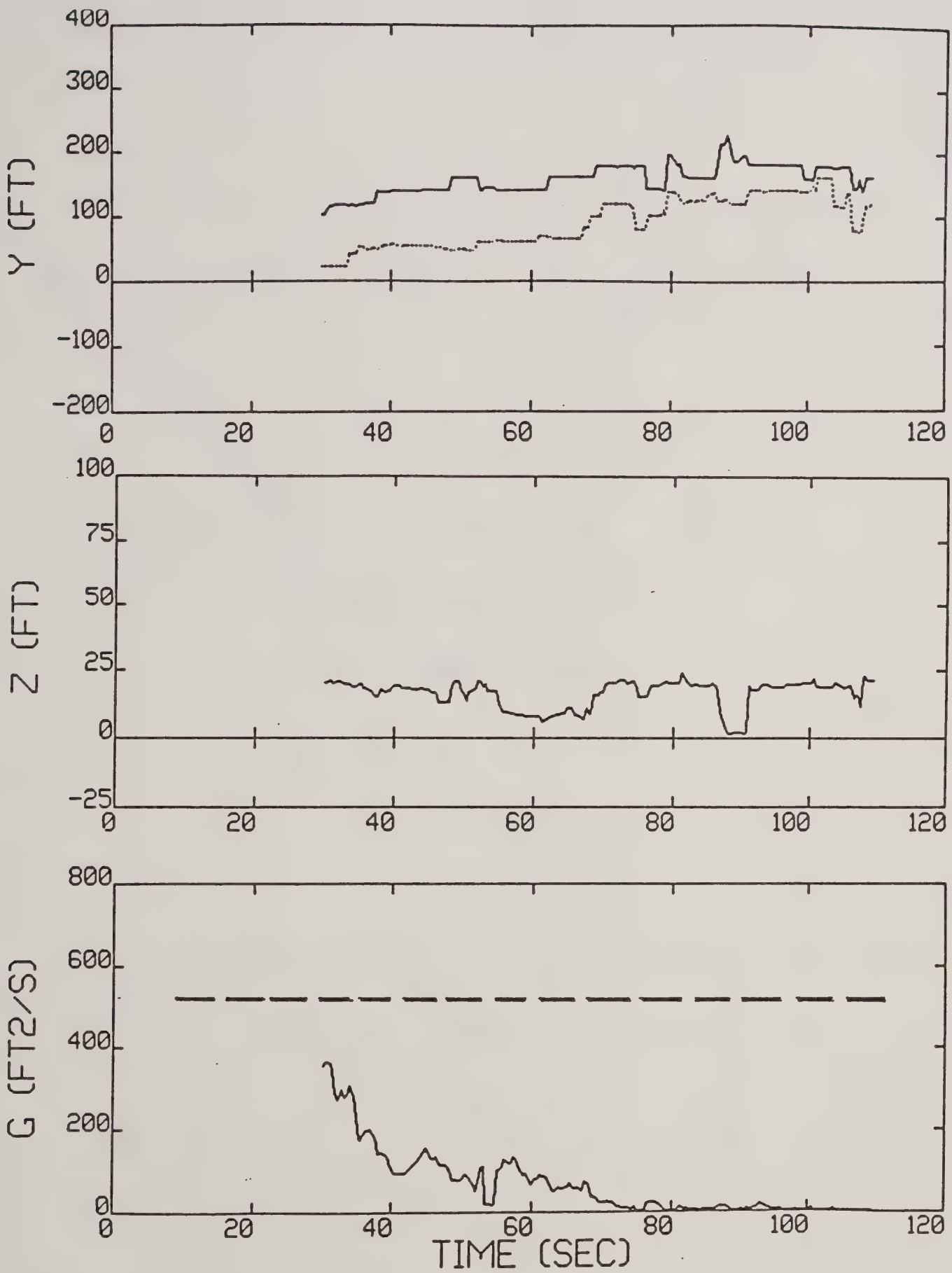


Figure 7-30b. Run 28 reduced data.

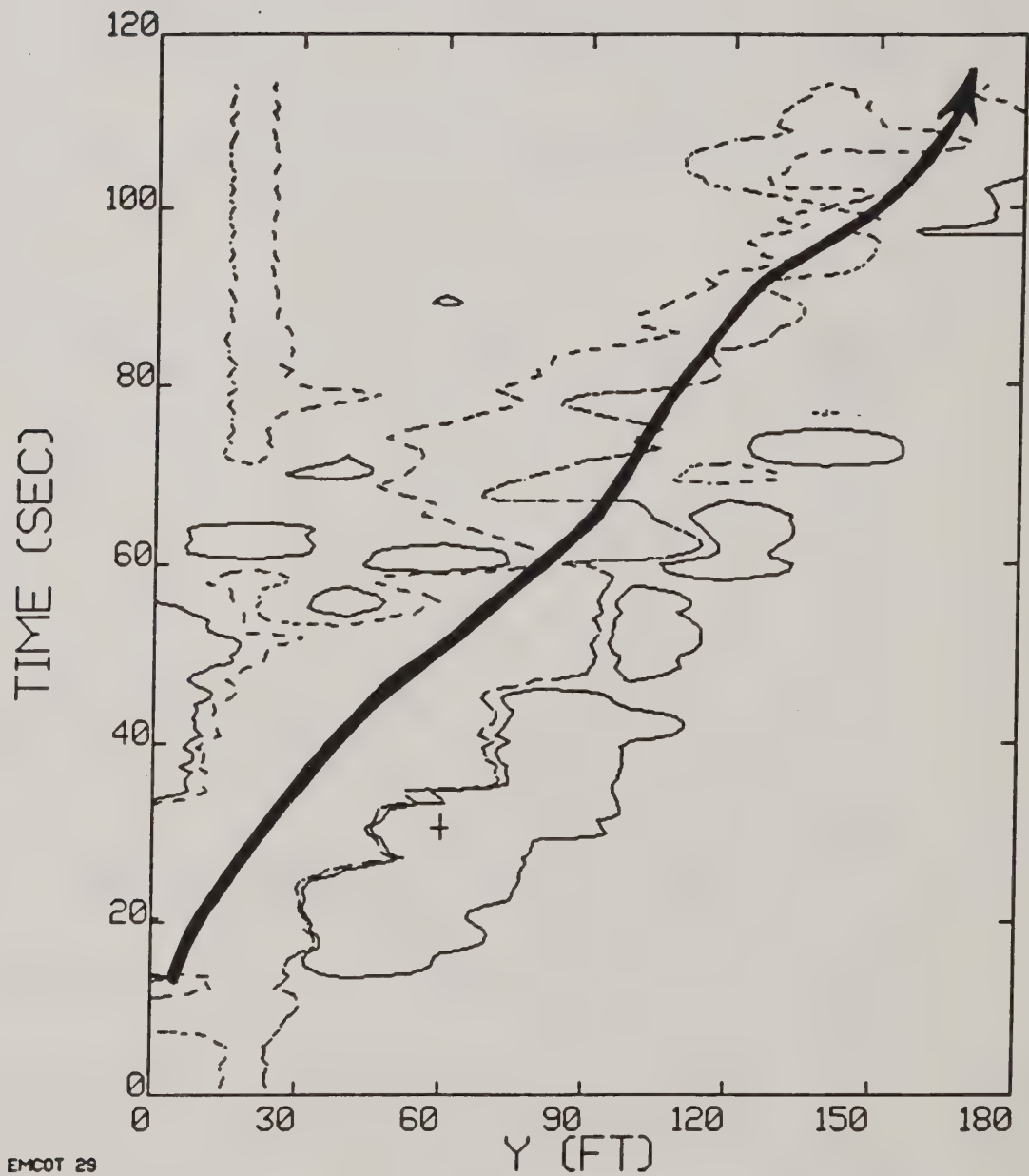


Figure 7-31. Run 29, date 05/04, Bell 206B.

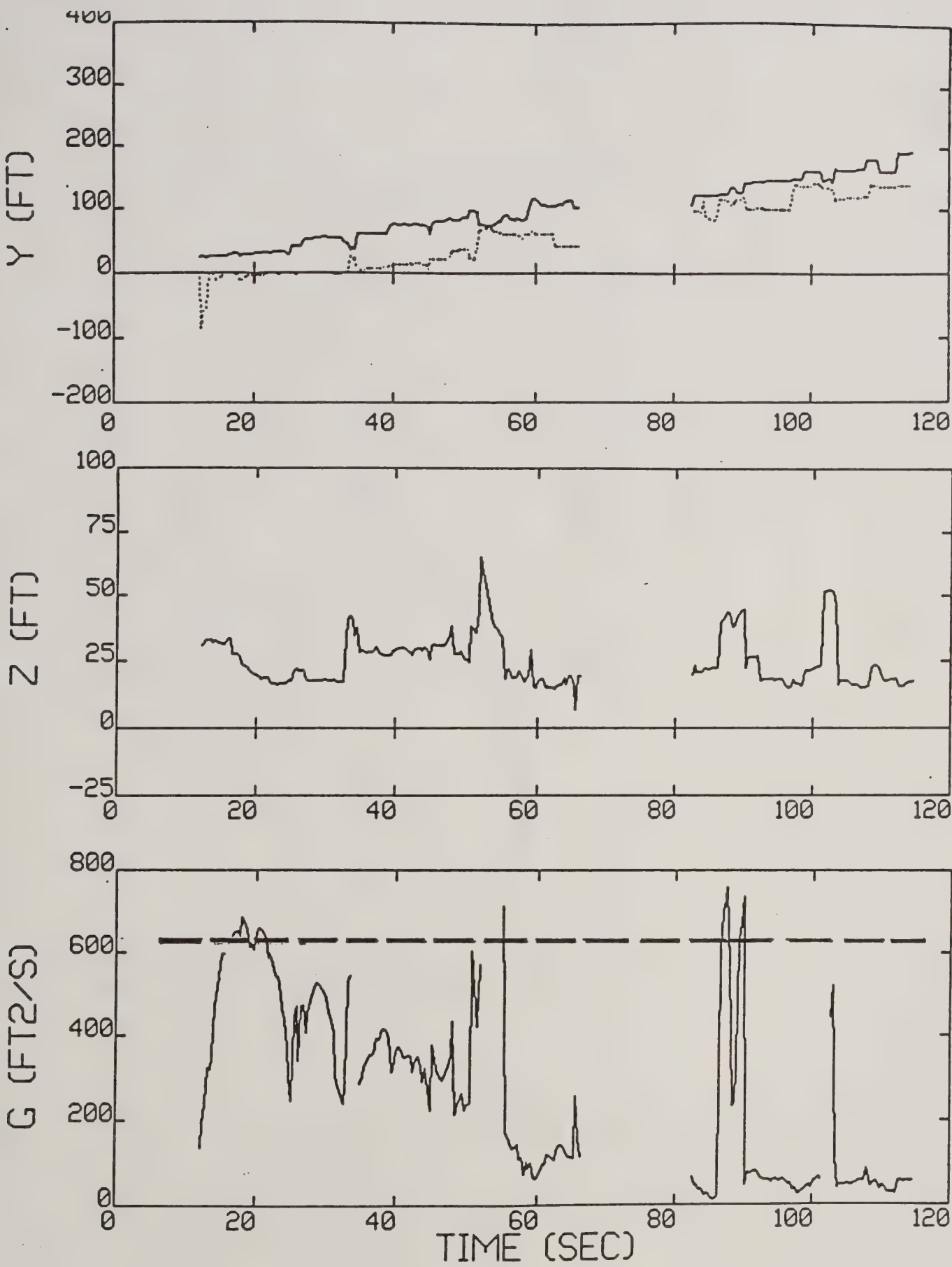


Figure 7-31b. Run 29 reduced data.

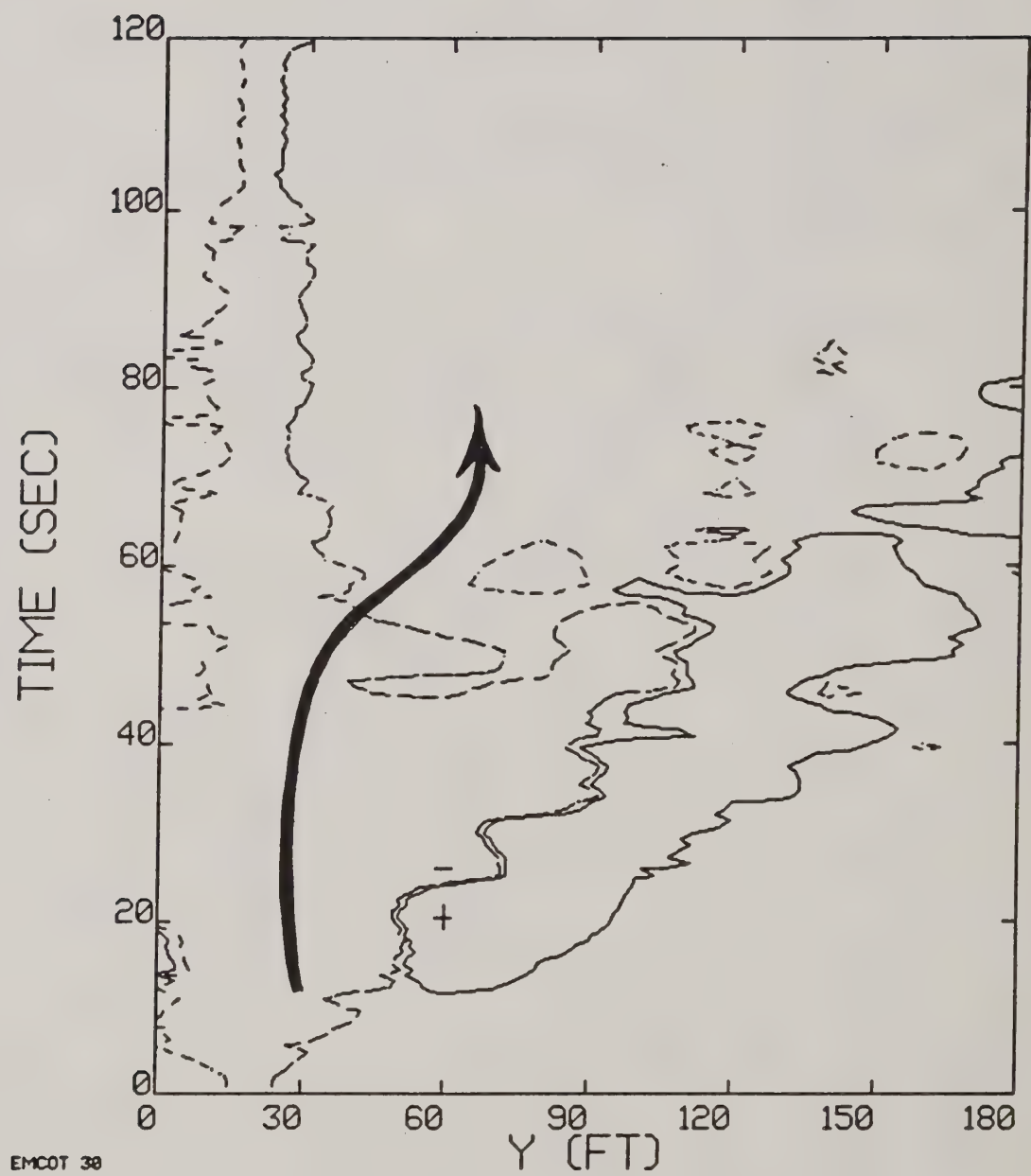


Figure 7-32. Run 30, date 05/04, Bell 206B.

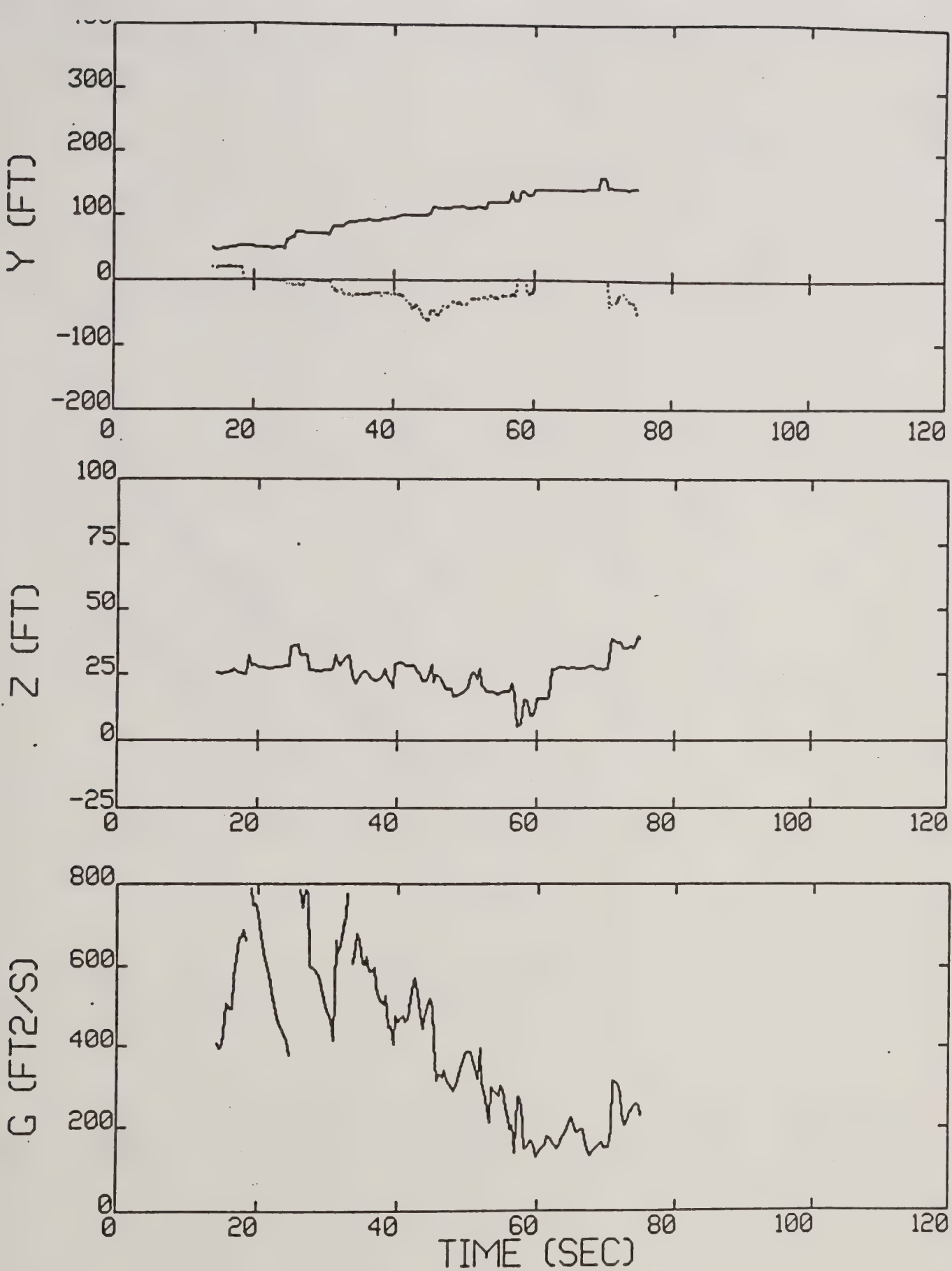


Figure 7-32b. Run 30 reduced data.

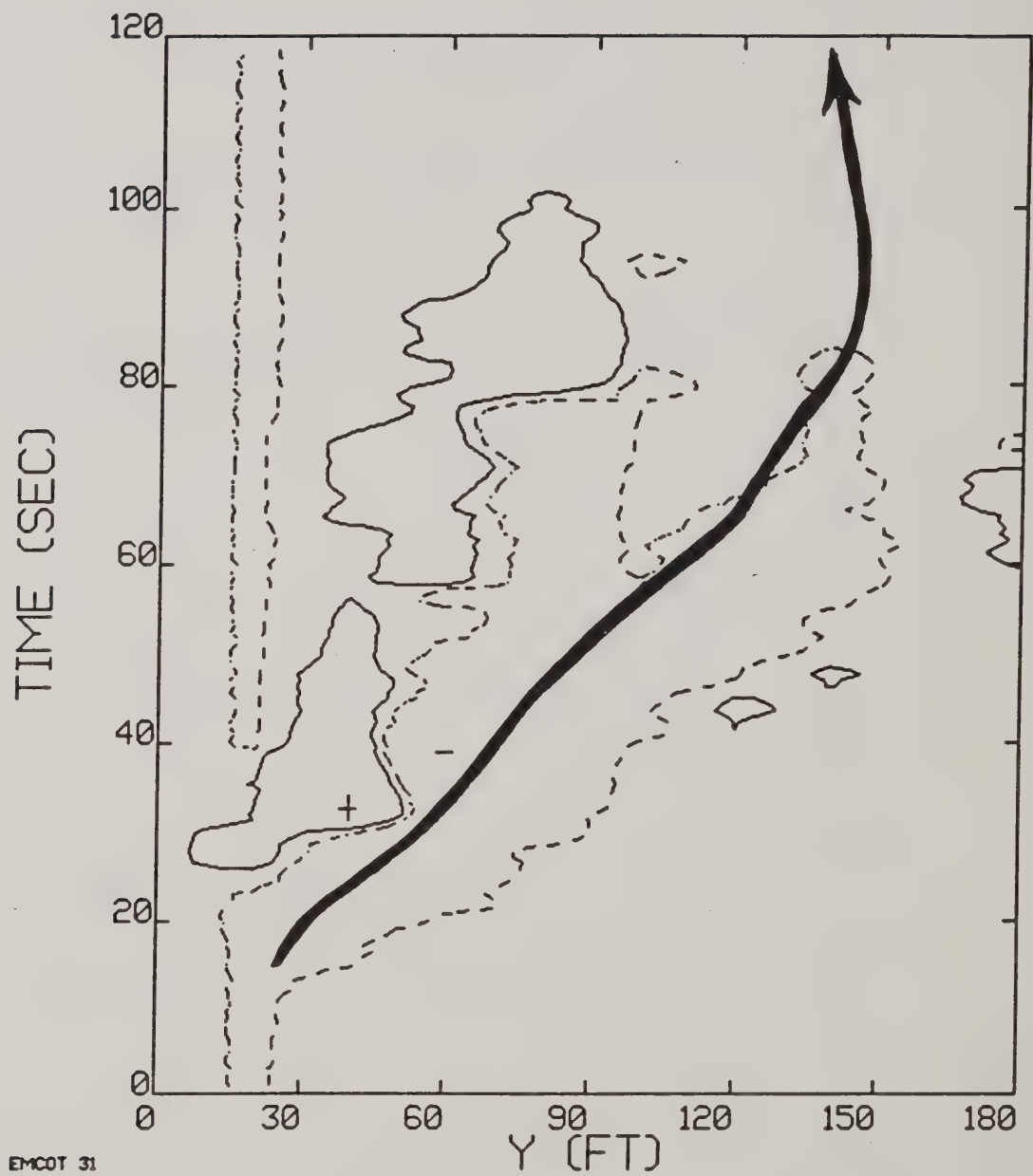


Figure 7-33. Run 31, date 05/04, Bell 206B.

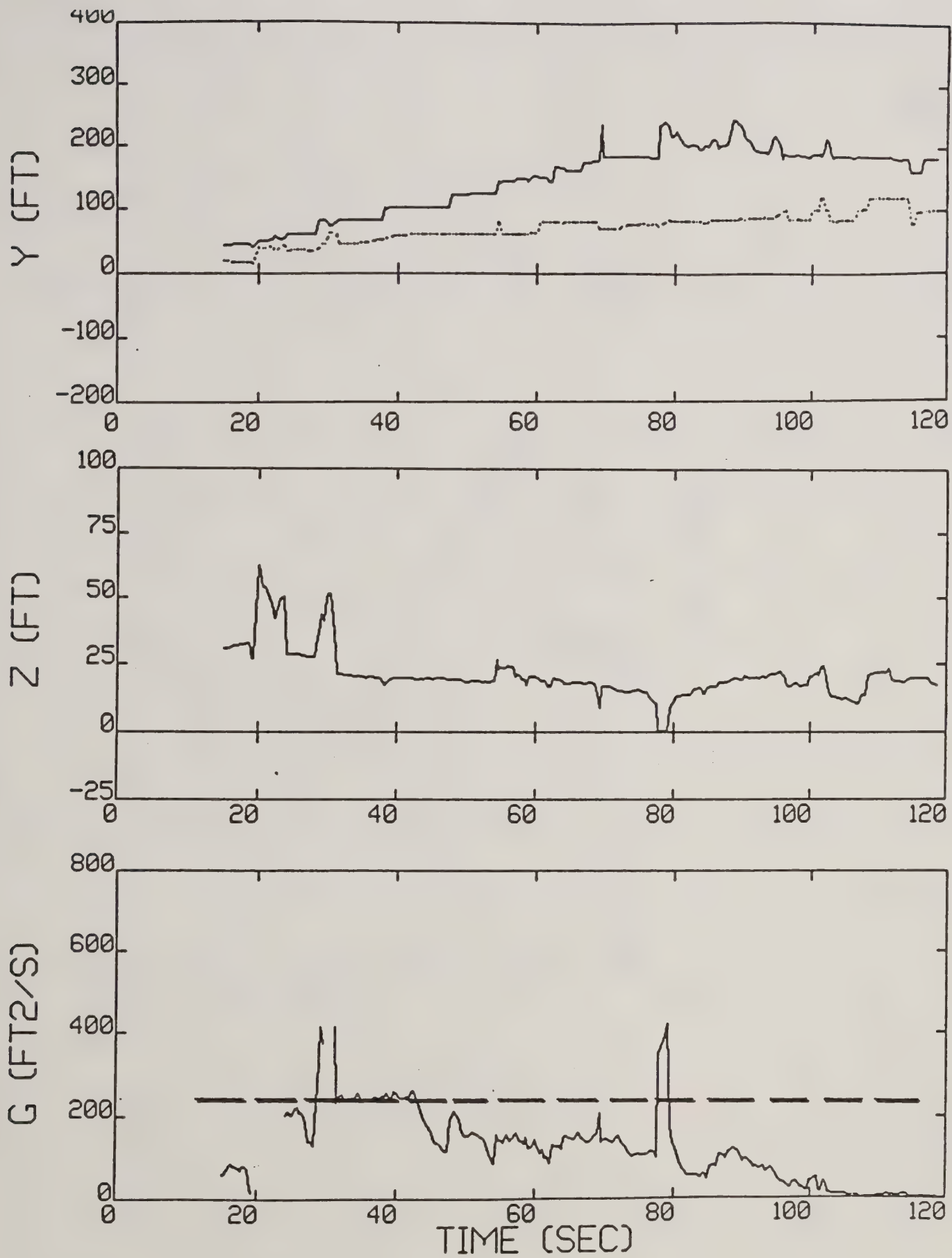


Figure 7-33b. Run 31 reduced data.

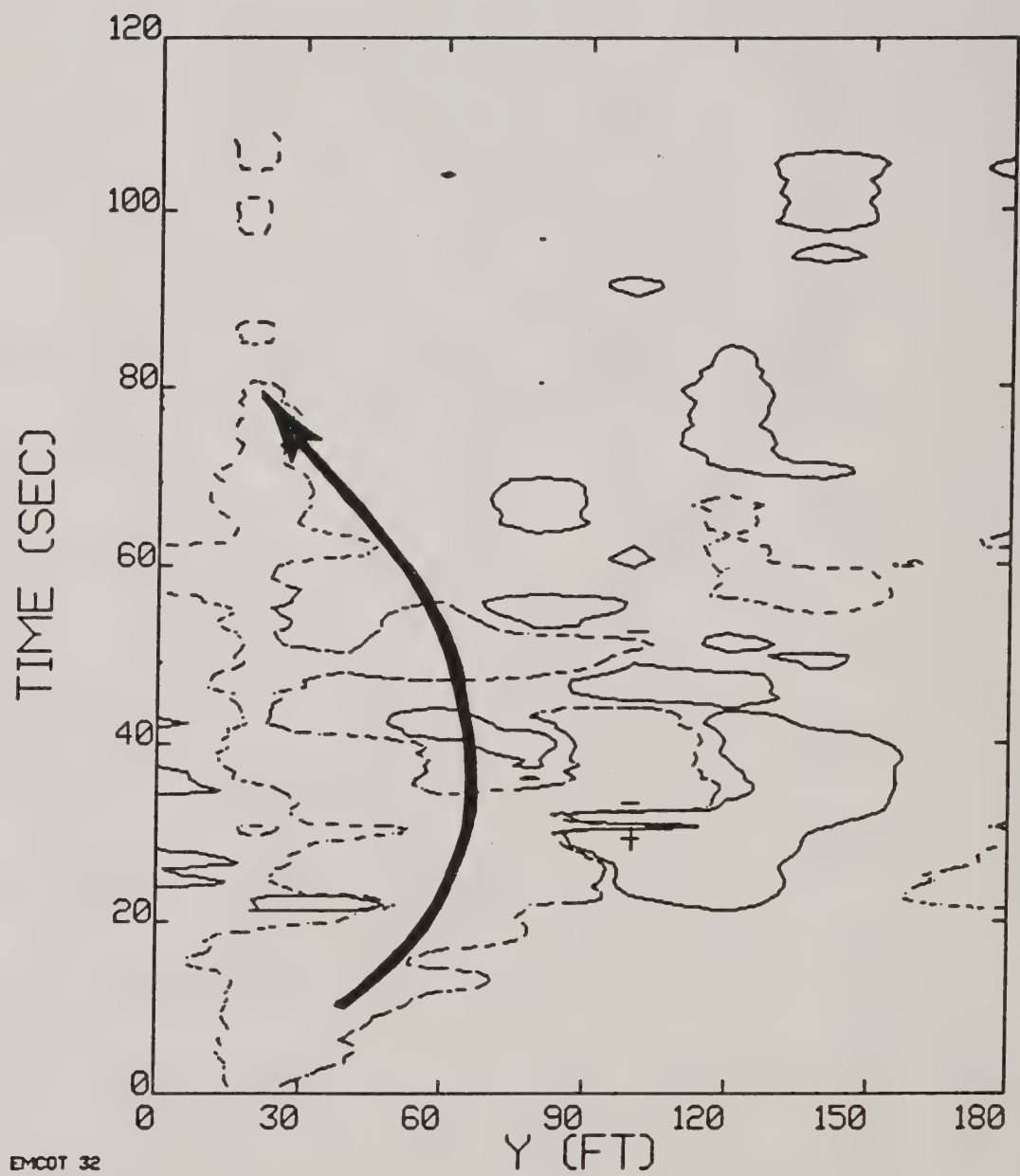


Figure 7-34. Run 32, date 05/04, Bell 206B.

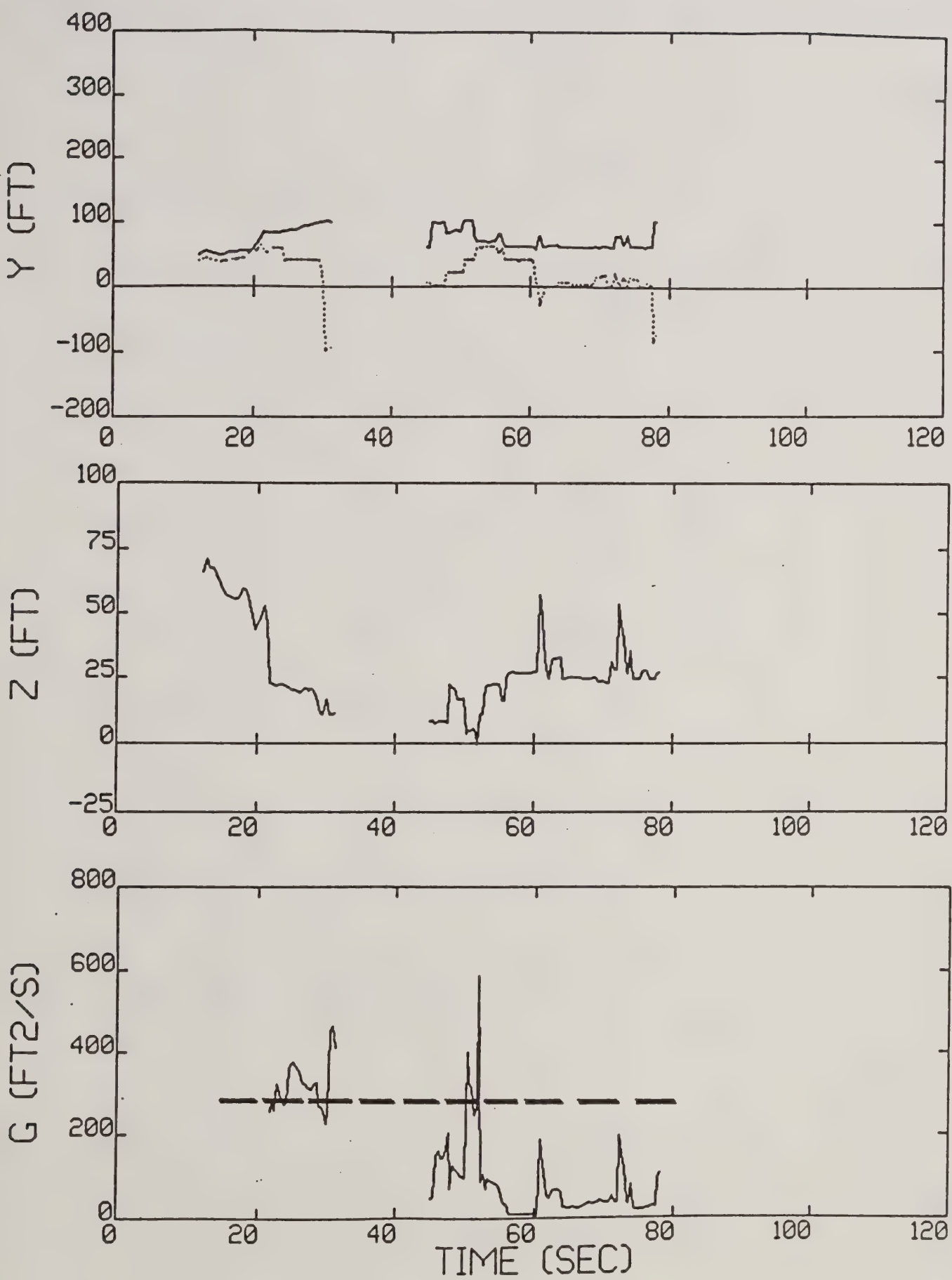


Figure 7-34b. Run 32 reduced data.

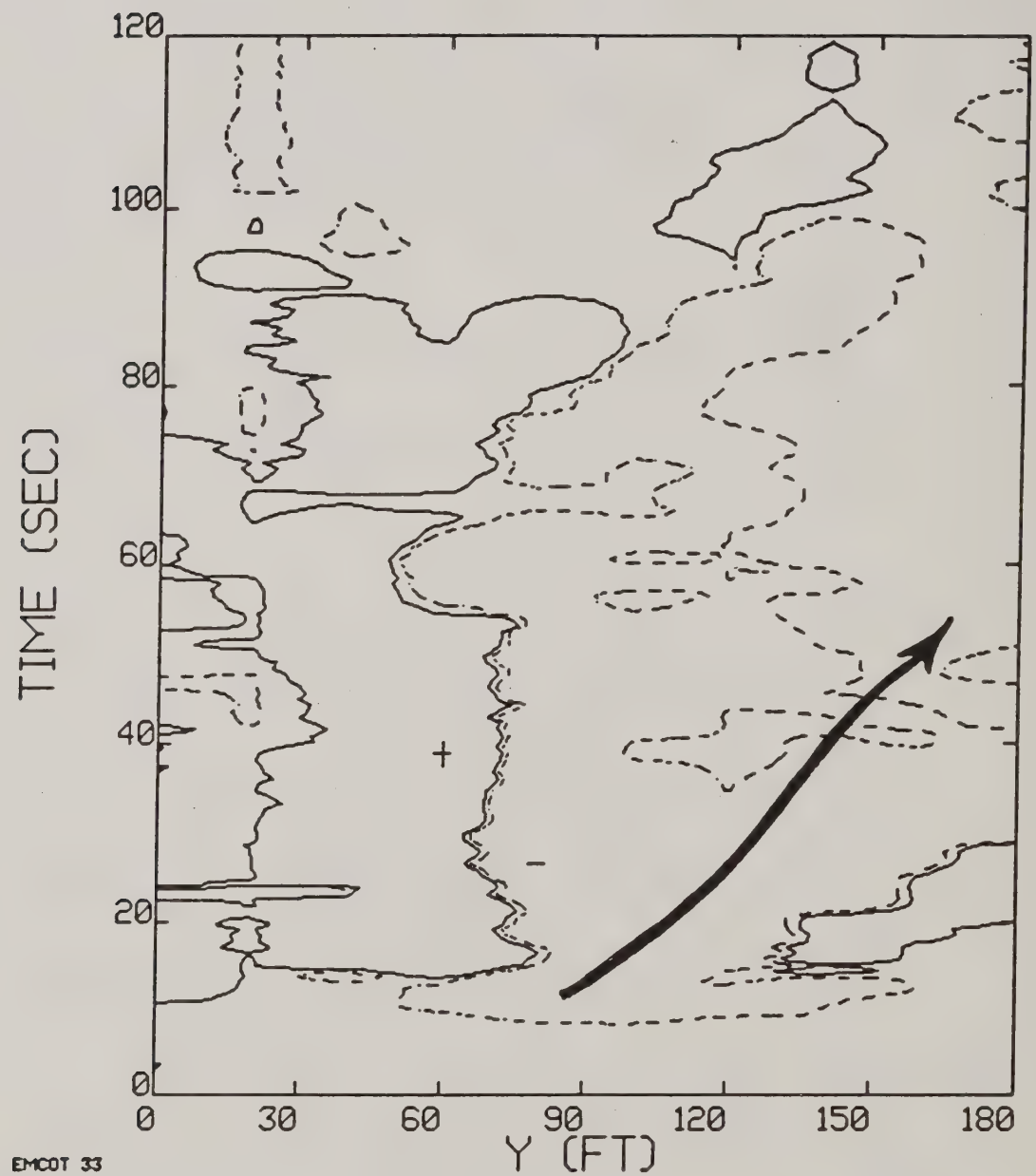


Figure 7-35. Run 33, date 05/04, Bell 206B.

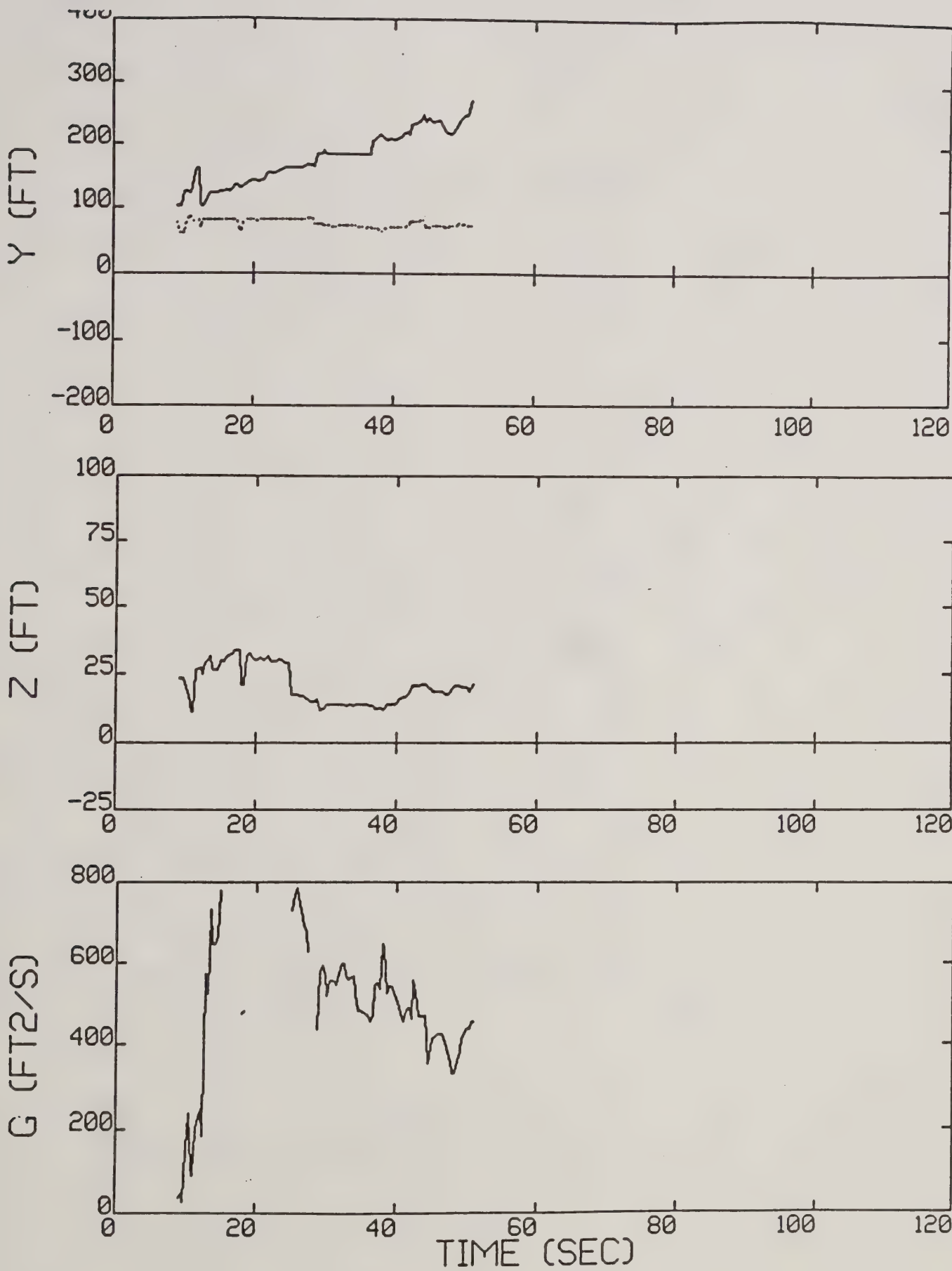


Figure 7-35b. Run 33 reduced data.

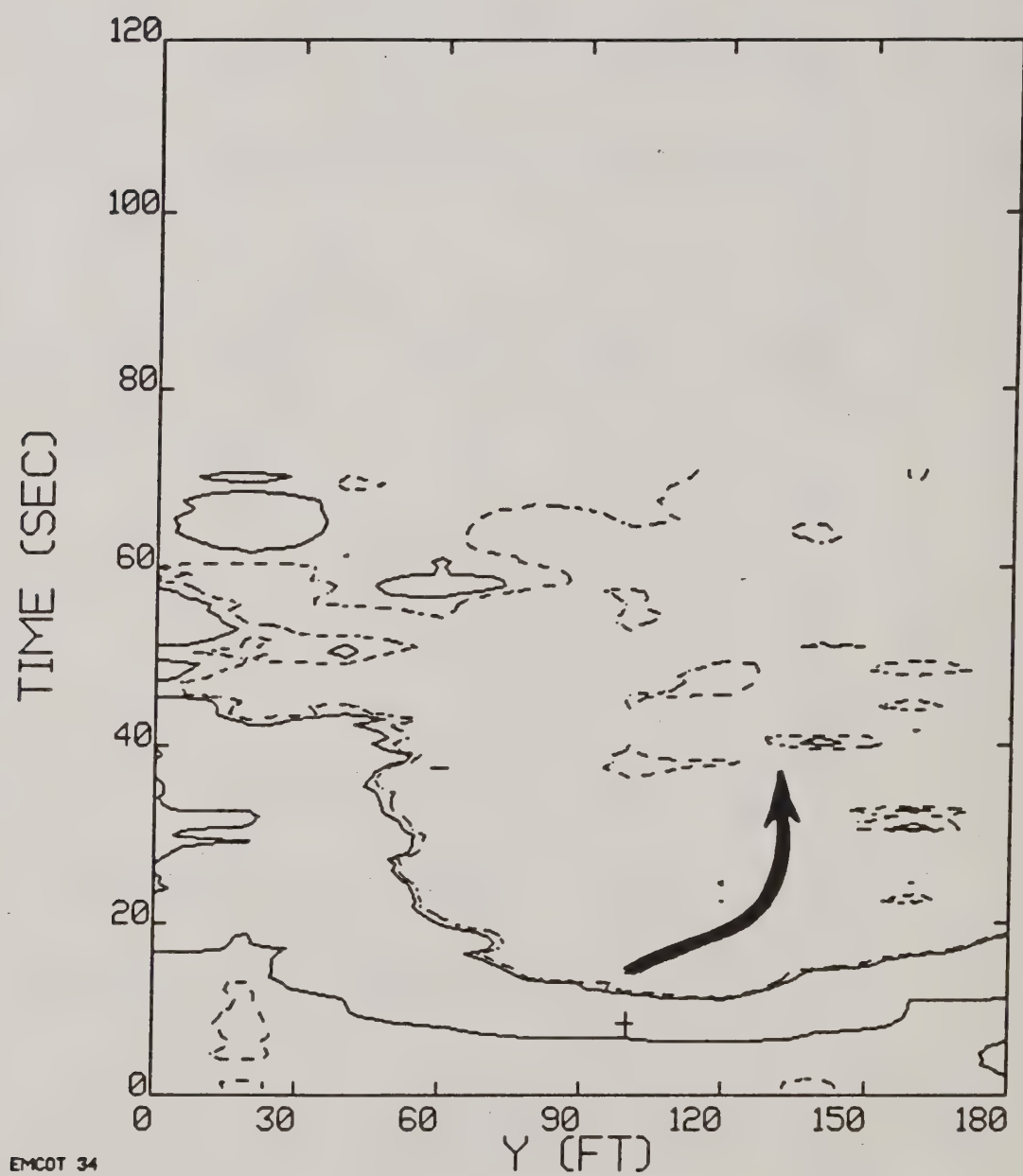


Figure 7-36. Run 34, date 05/04, Bell 206B.

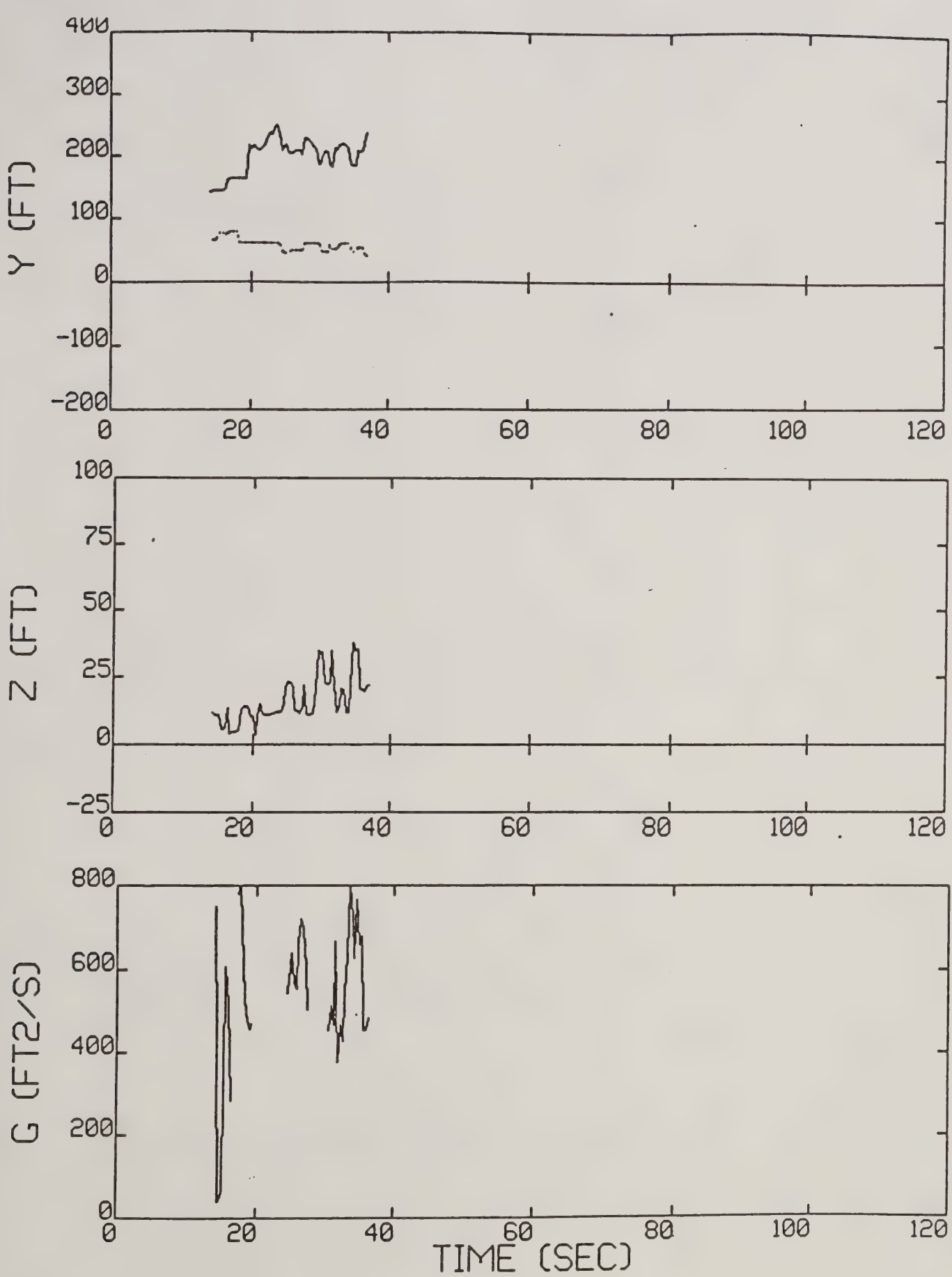


Figure 7-36b. Run 34 reduced data.

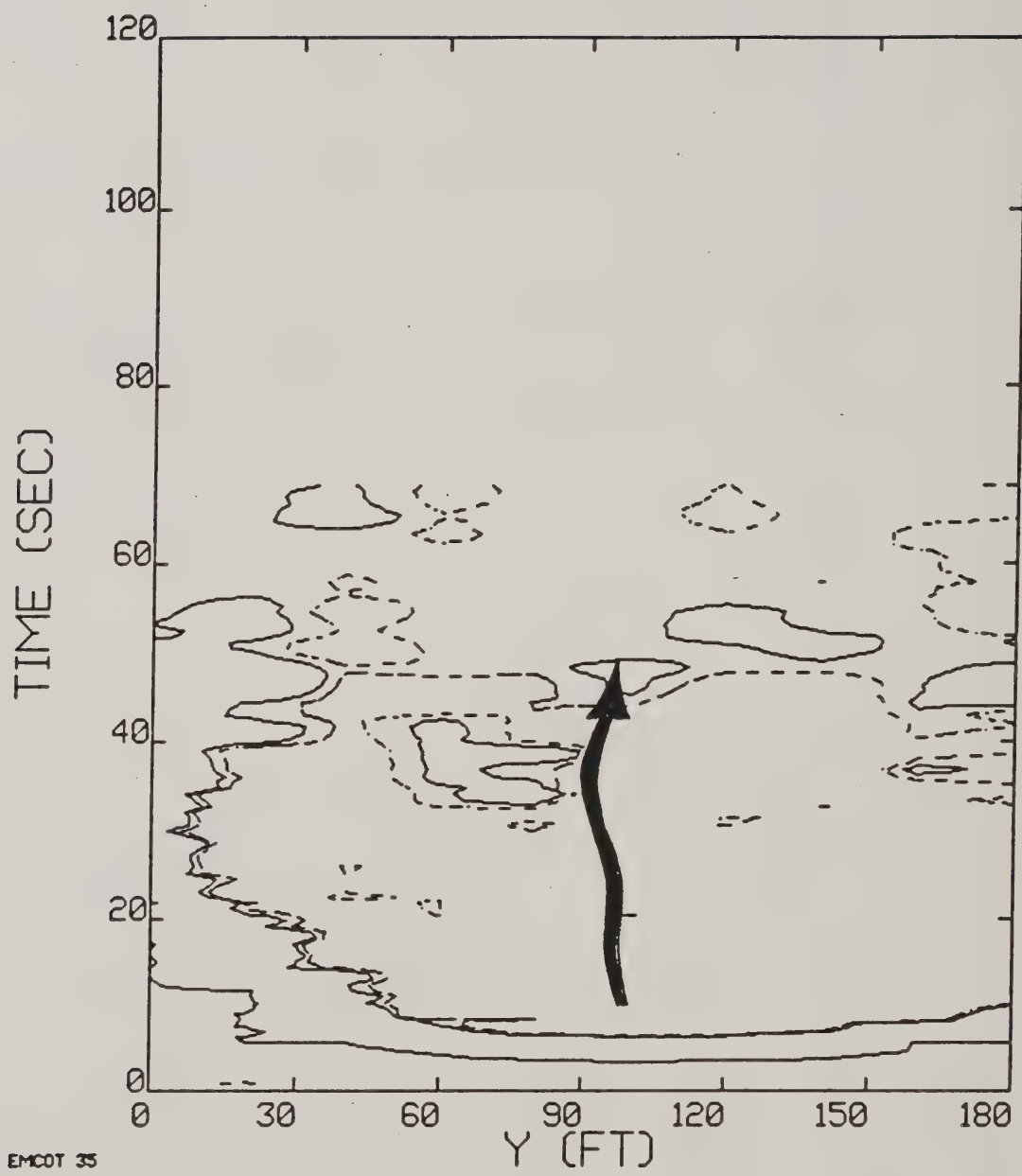


Figure 7-37. Run 35, date 05/04, Bell 206B.

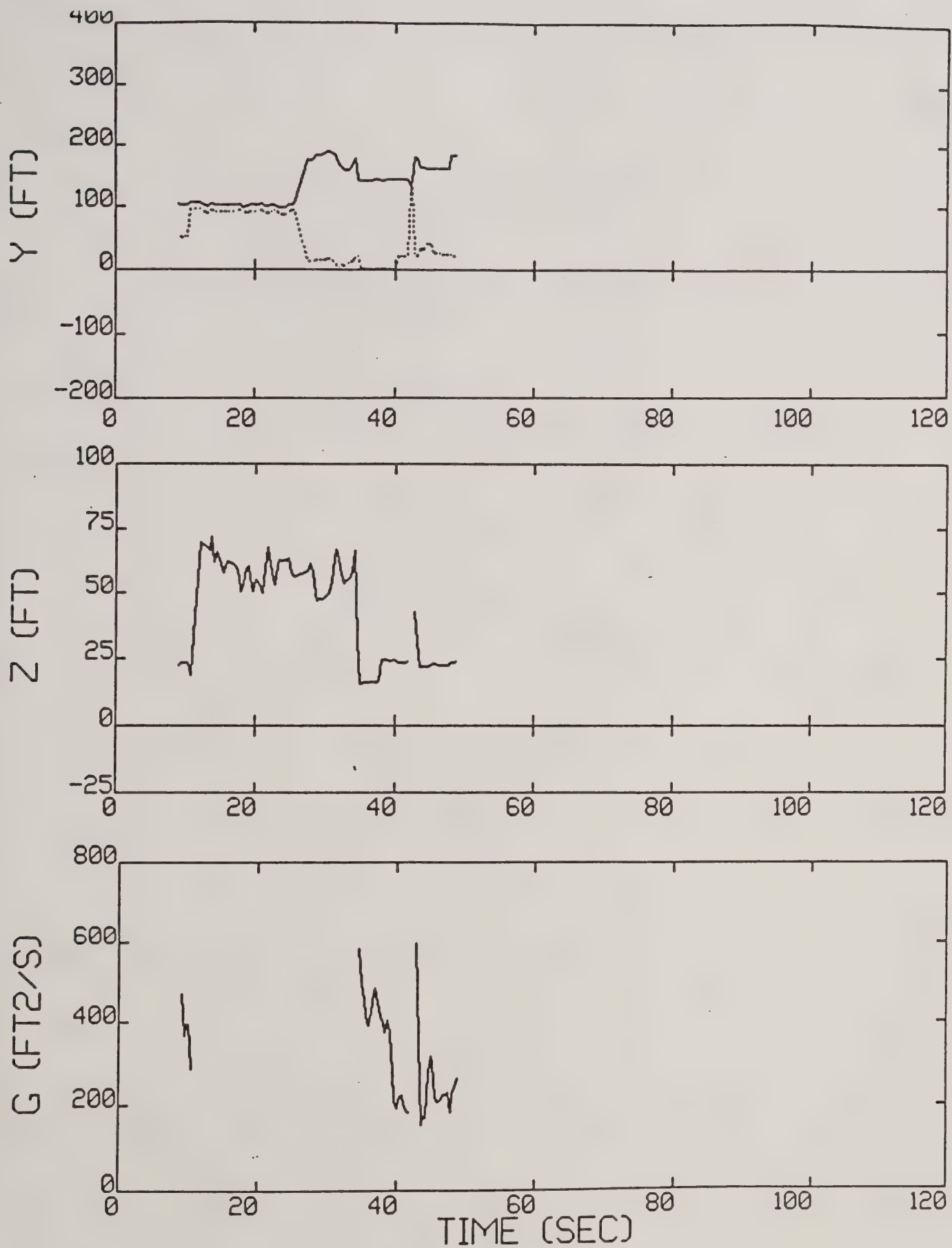


Figure 7-37b. Run 35 reduced data.

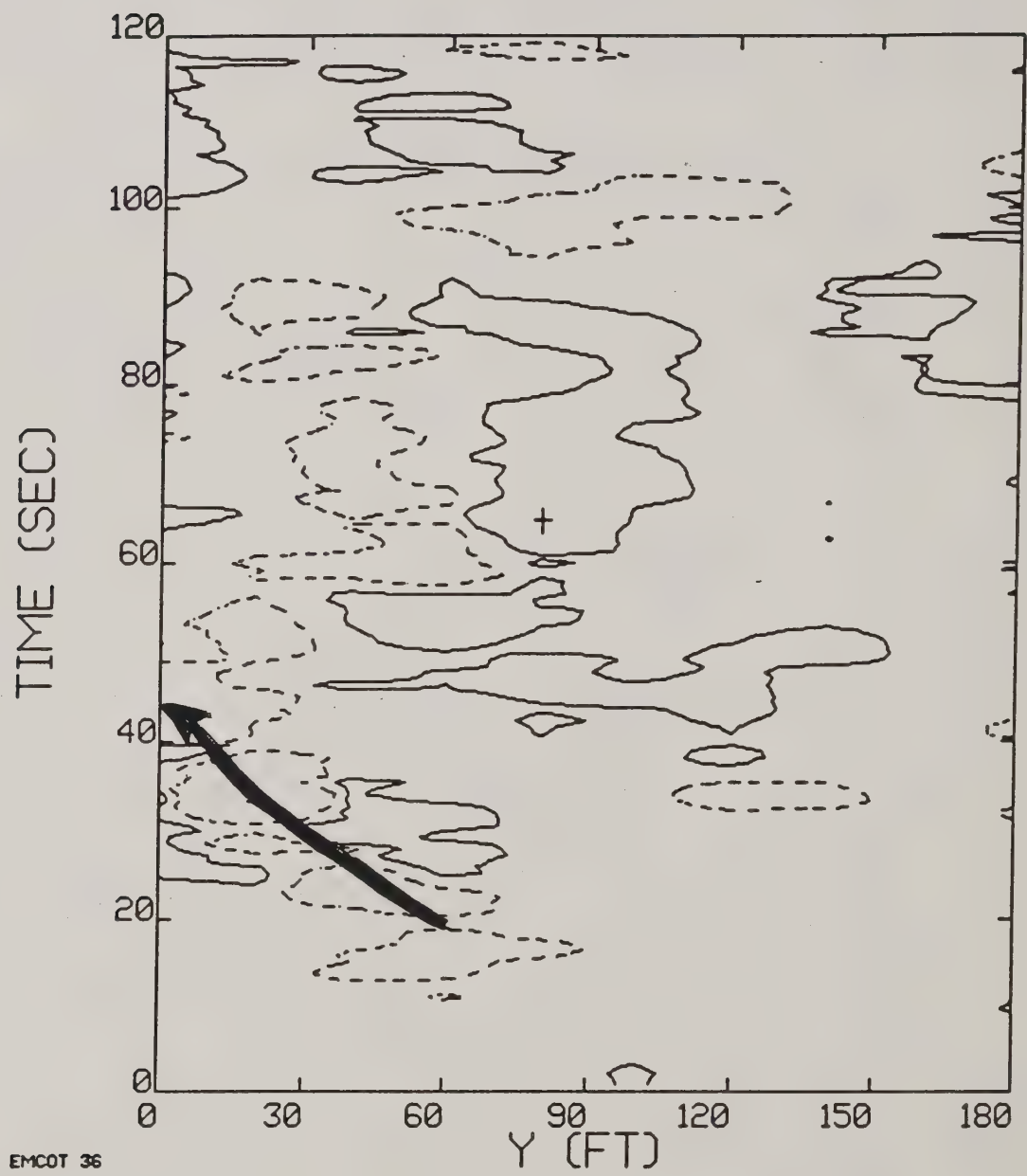


Figure 7-38. Run 36, date 05/04, Bell 206B.

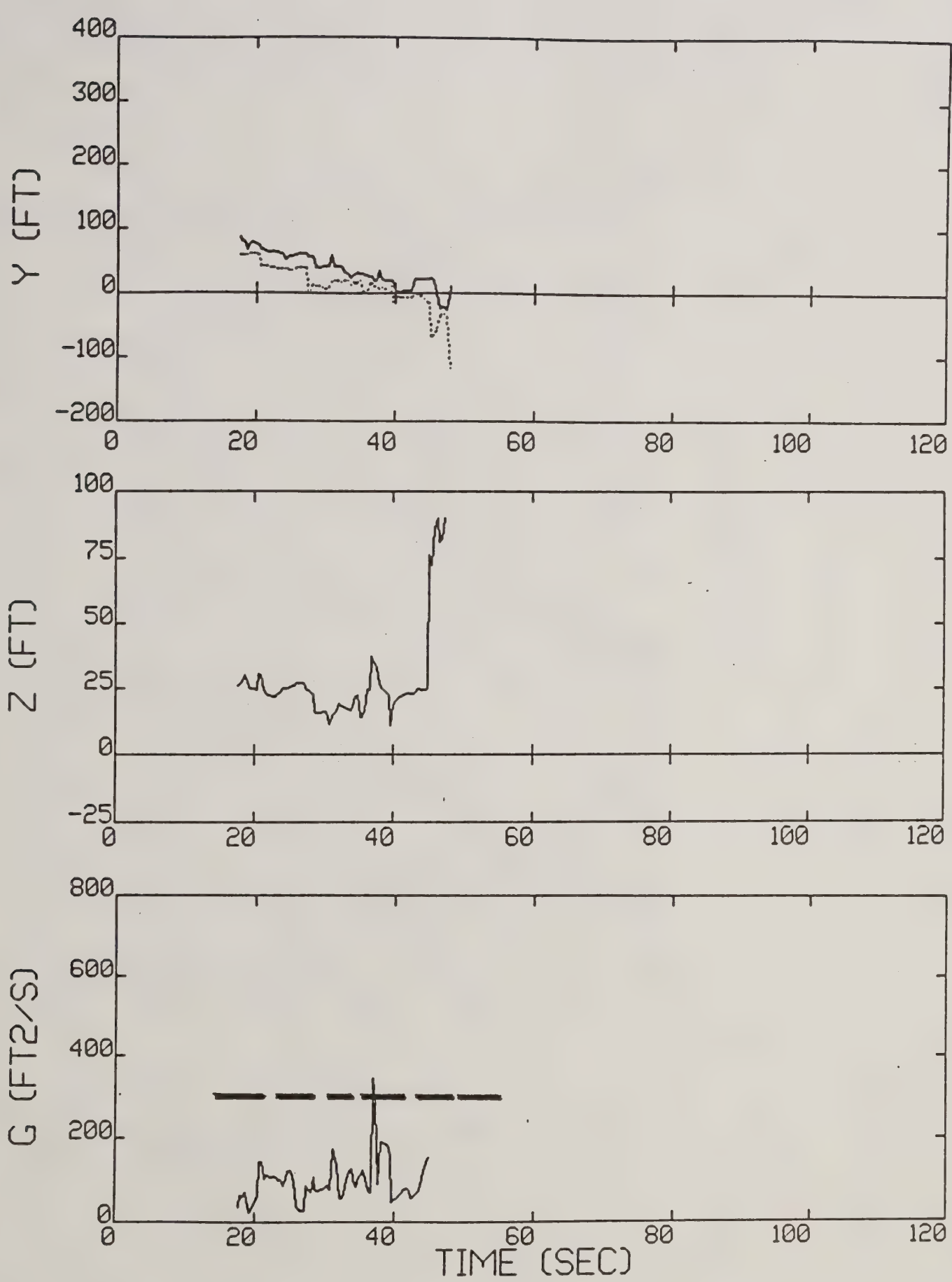


Figure 7-38b. Run 36 reduced data.

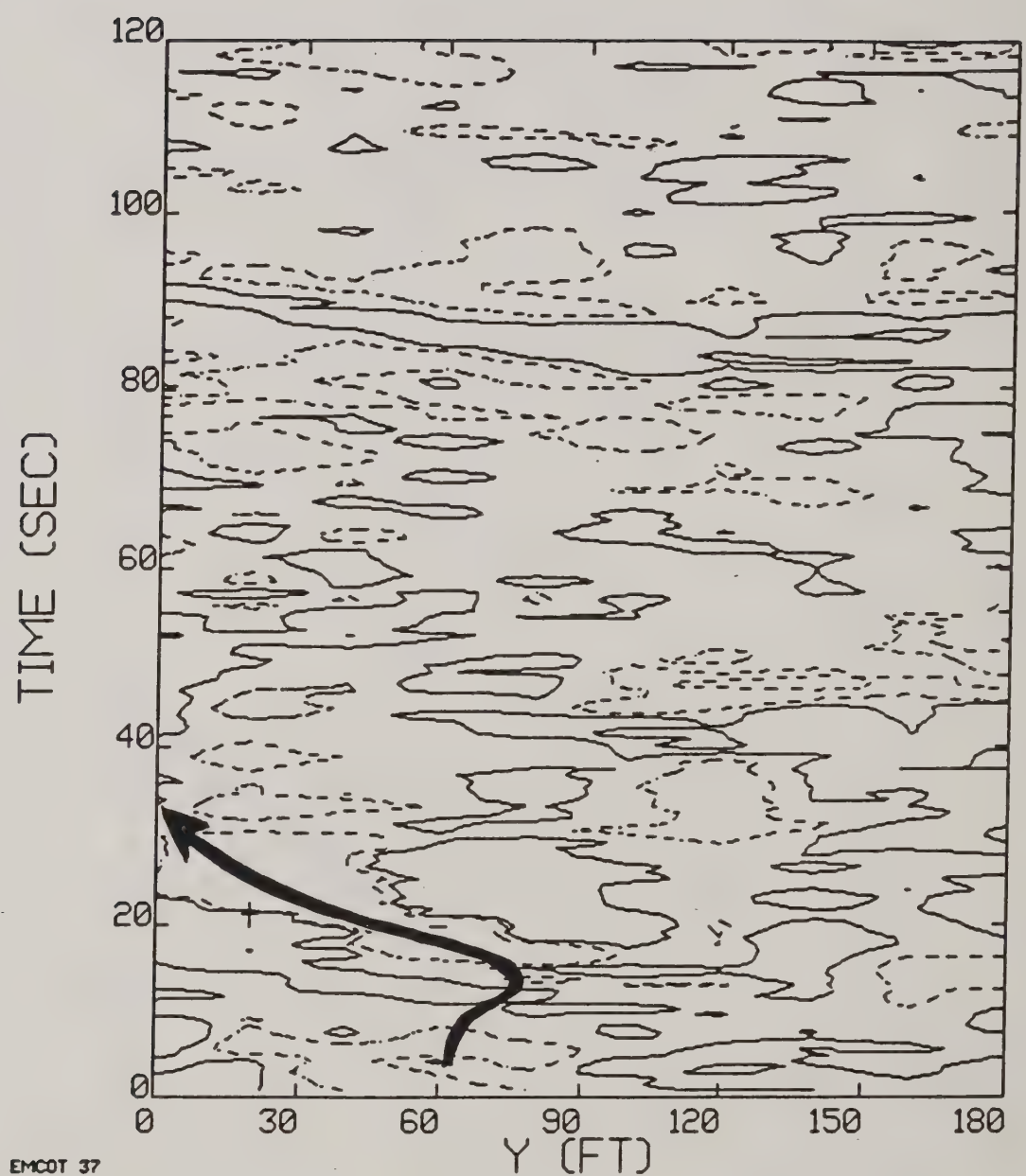


Figure 7-39. Run 37, date 05/04, Bell 206B.

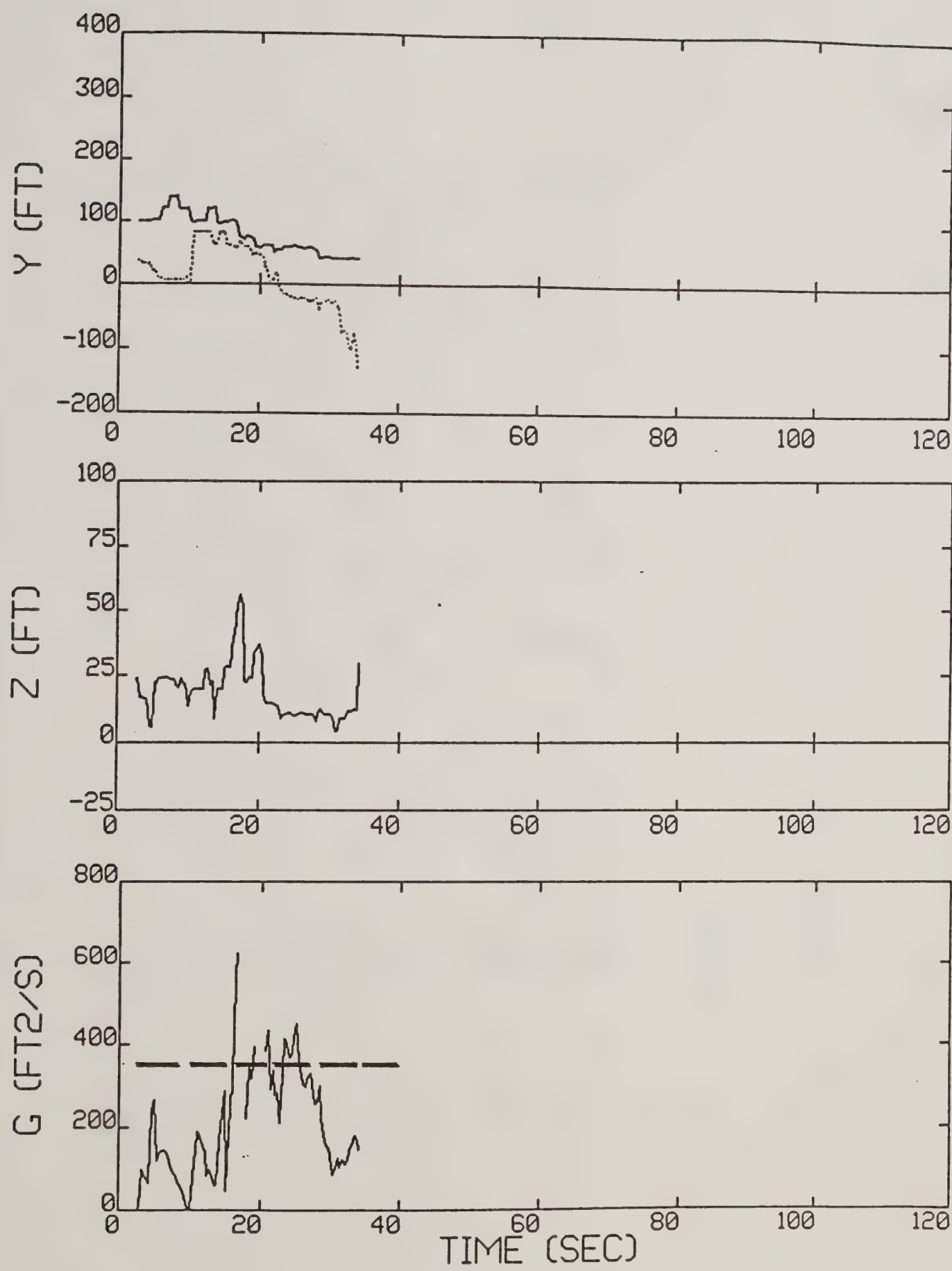


Figure 7-39b. Run 37 reduced data.

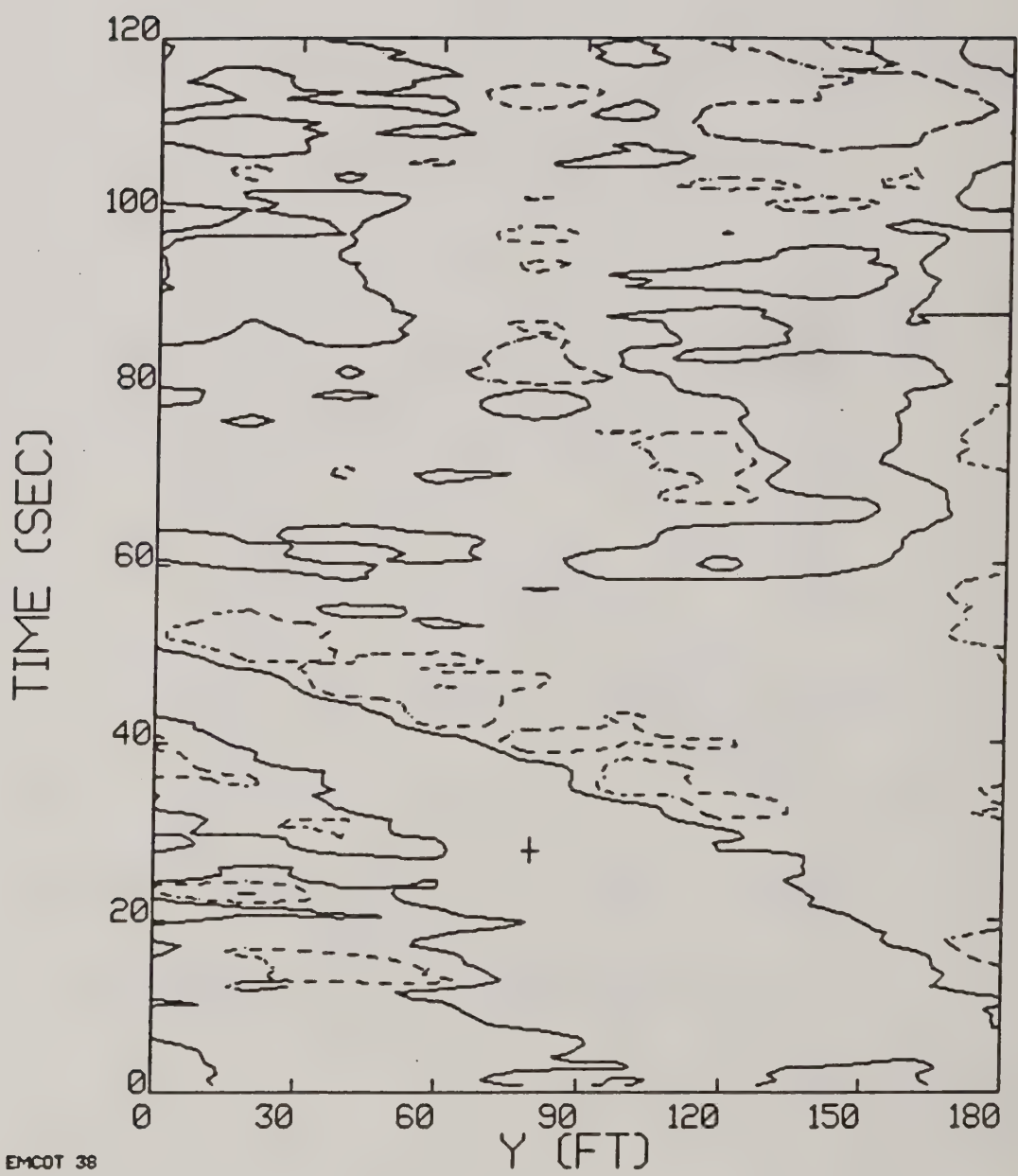


Figure 7-40. Run 38, date 05/04, Bell 206B.

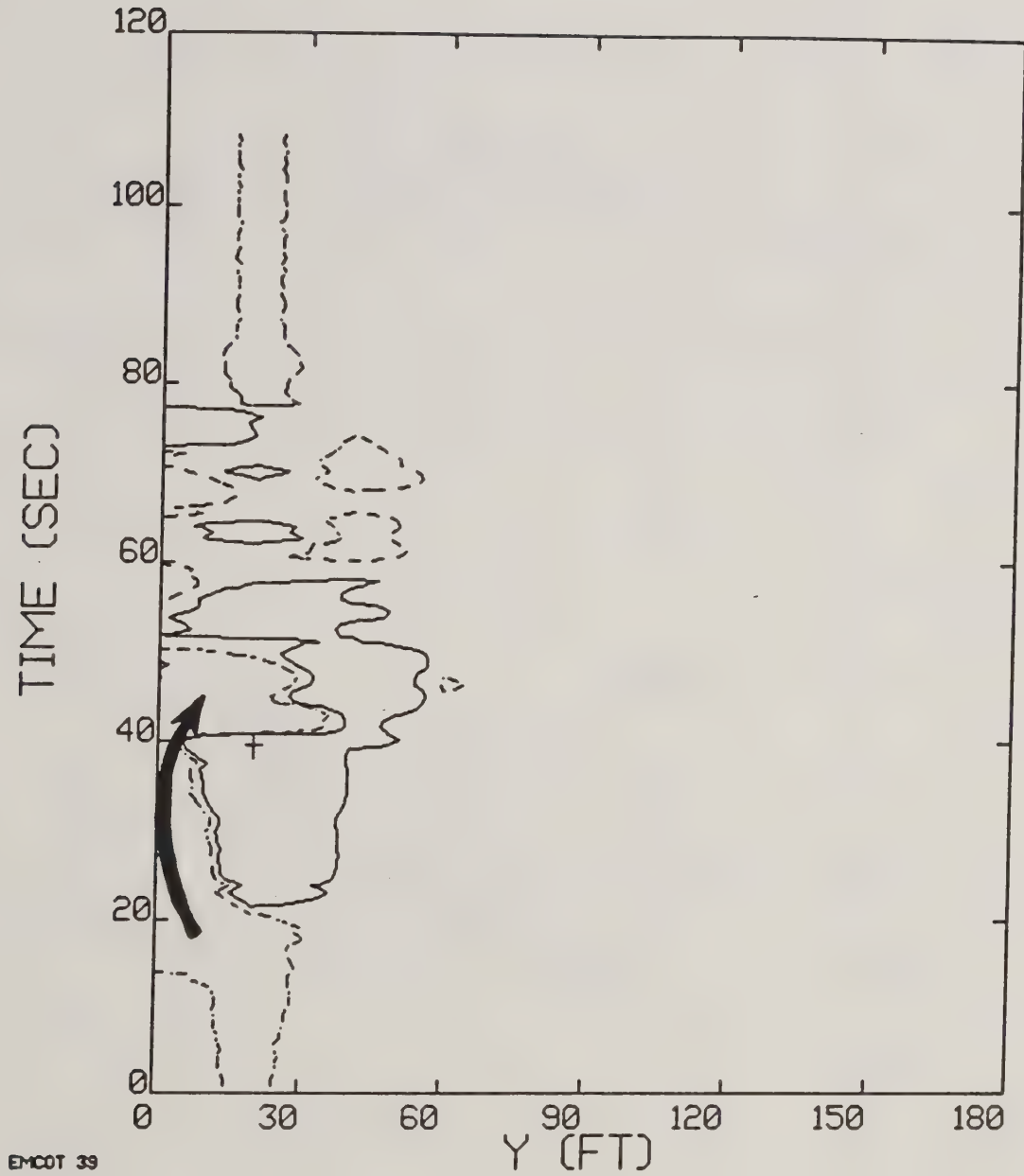


Figure 7-41. Run 39, date 05/07, Bell 206B.

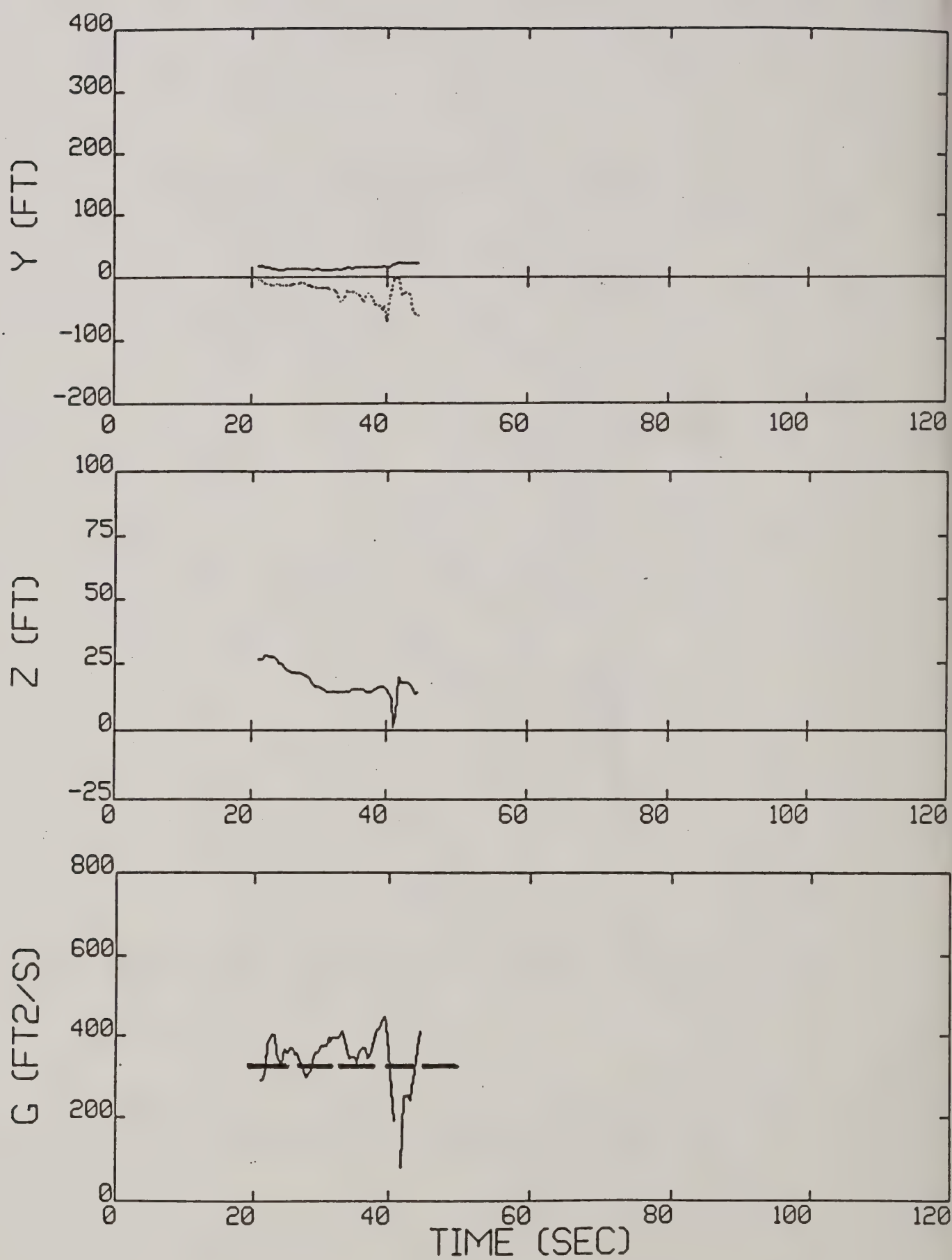


Figure 7-41b. Run 39 reduced data.

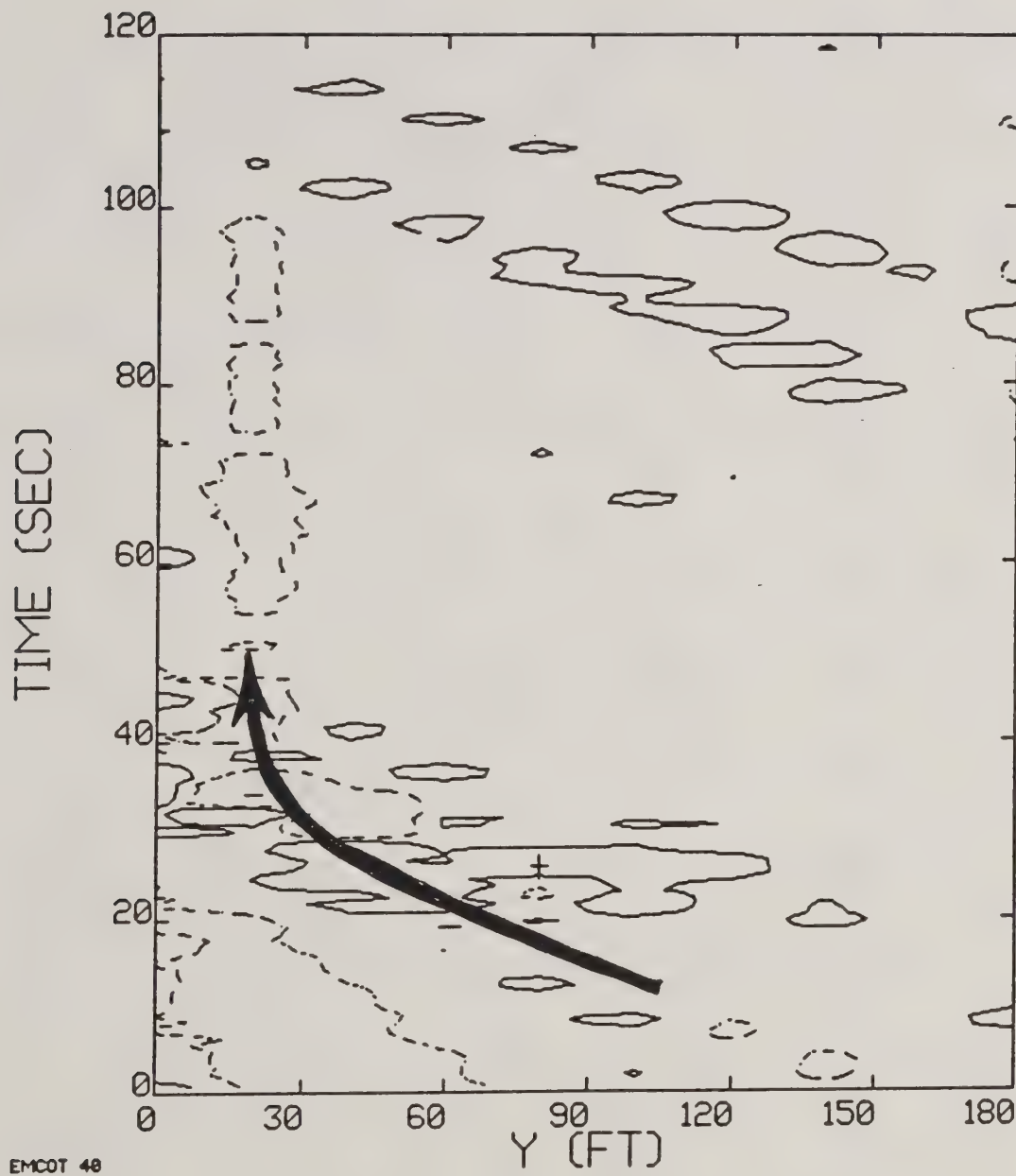


Figure 7-42. Run 40, date 05/05, Bell 206B.

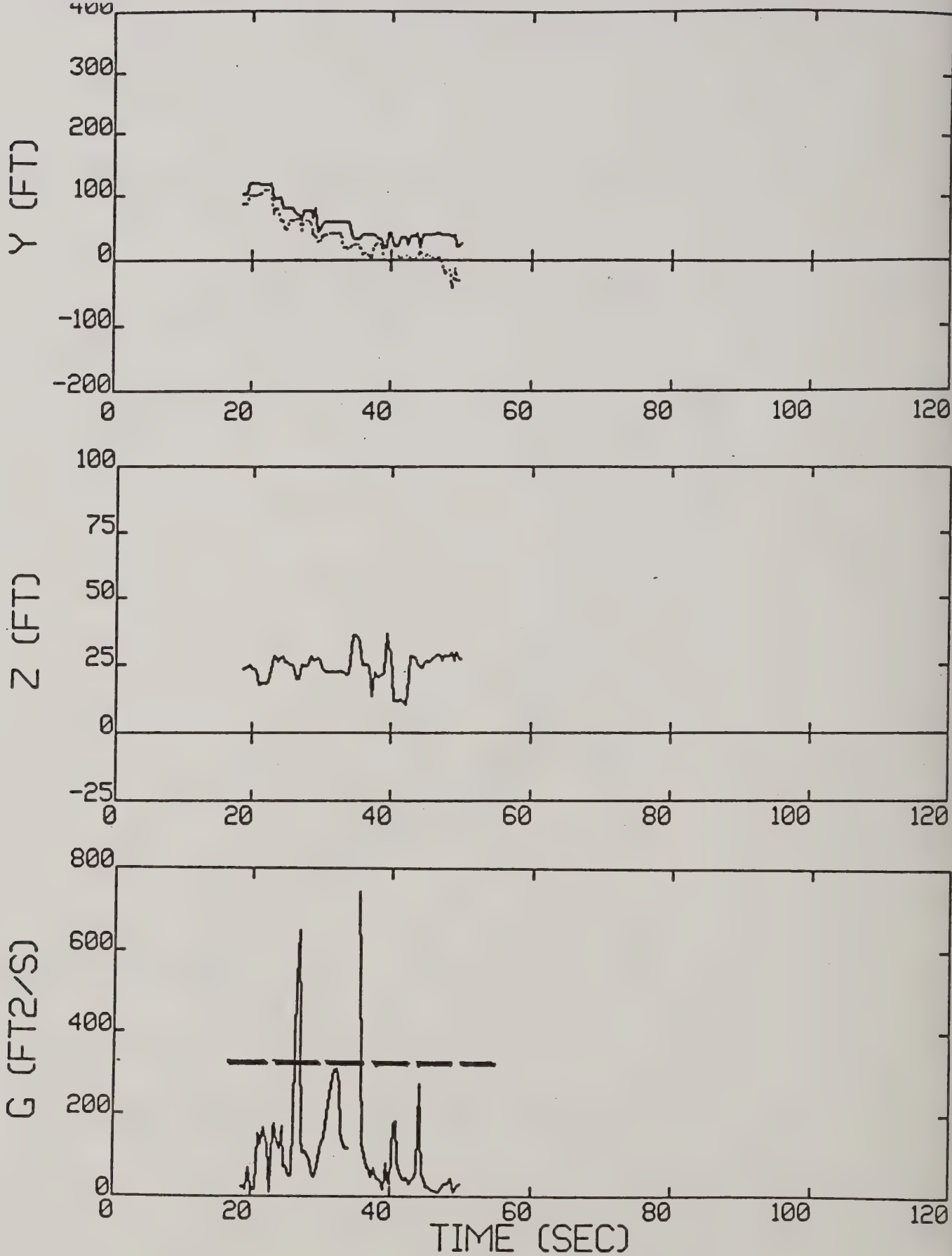


Figure 7-42b. Run 40 reduced data.

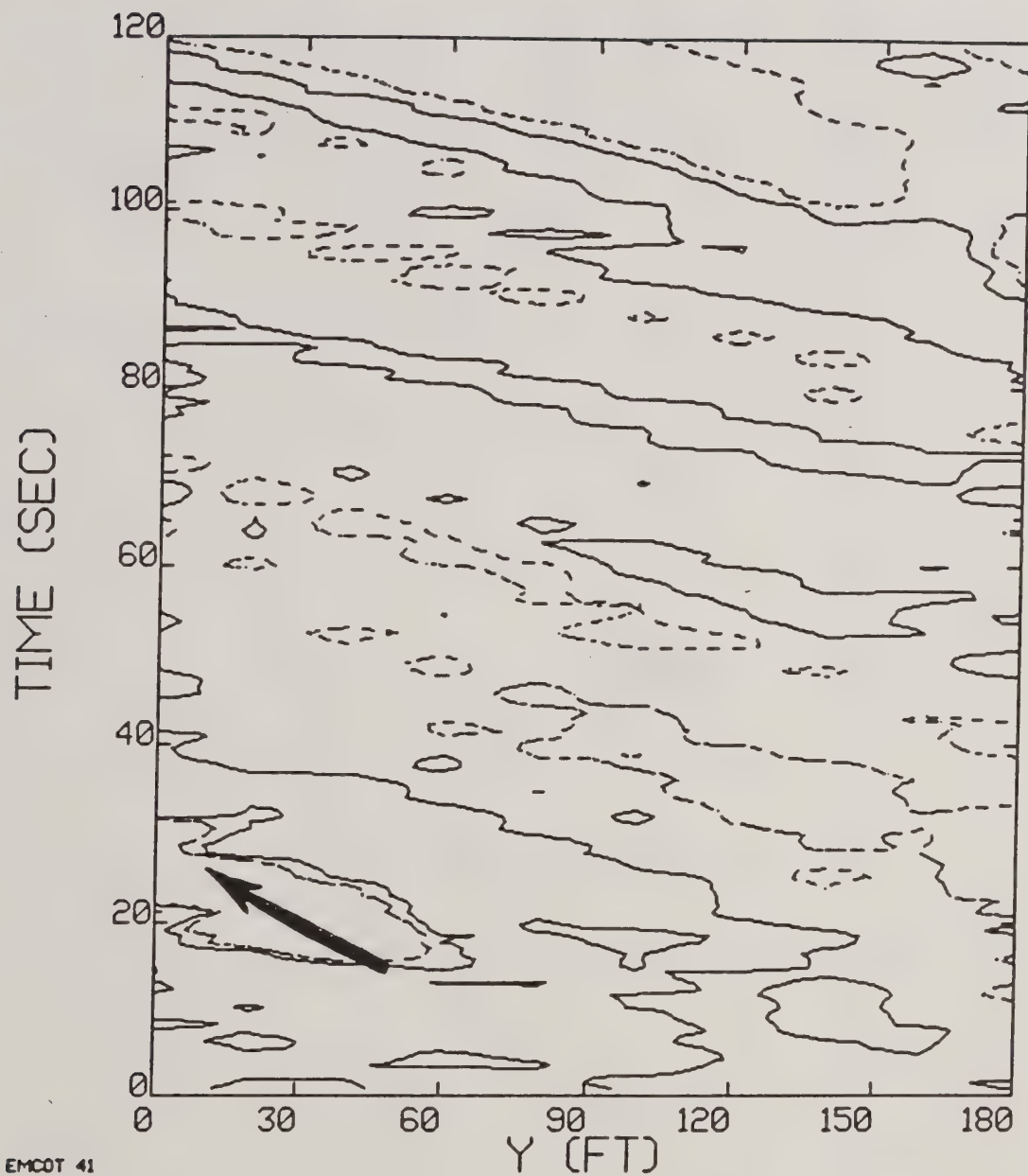


Figure 7-43. Run 41, date 05/07, Bell 206B.

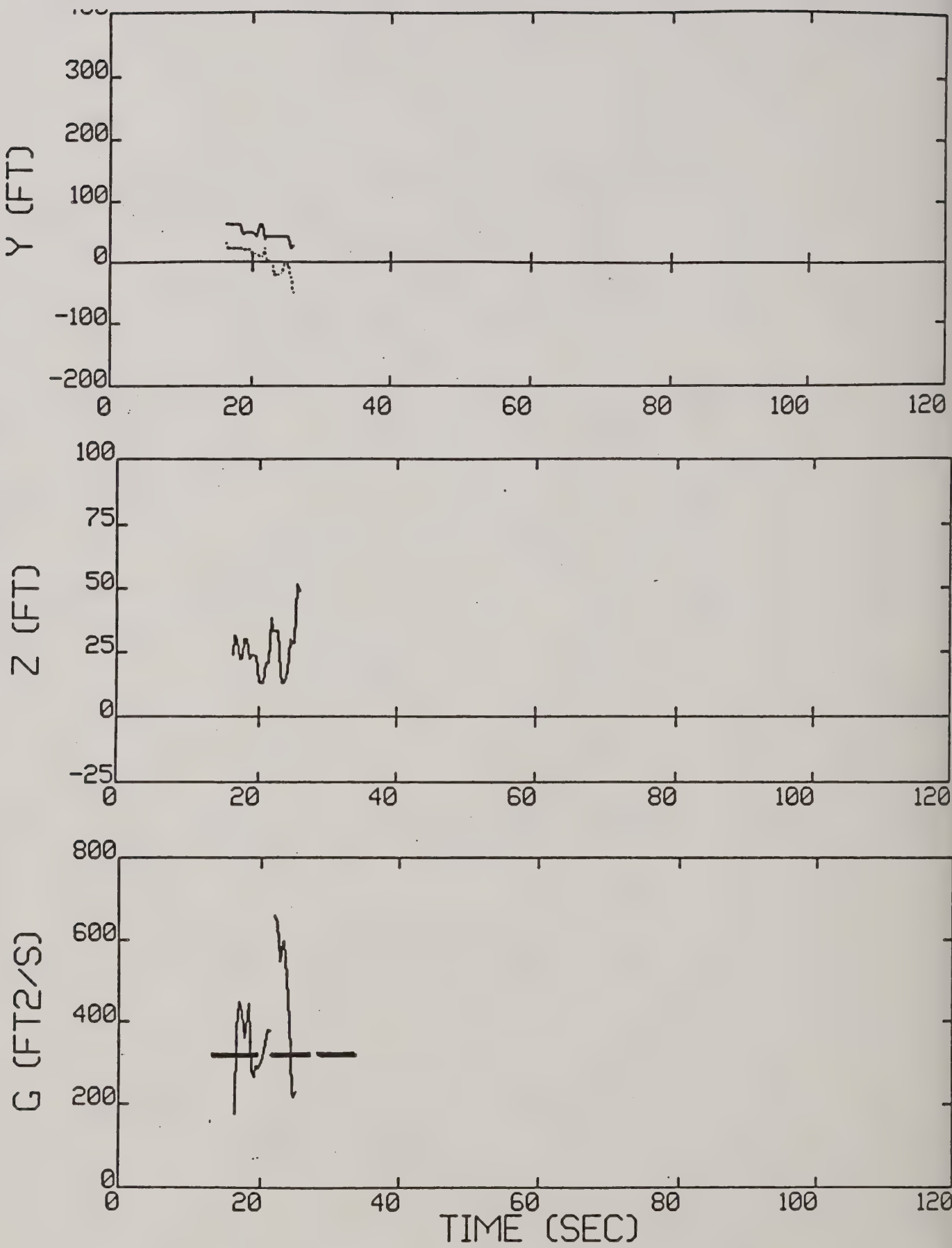


Figure 7-43b. Run 41 reduced data.

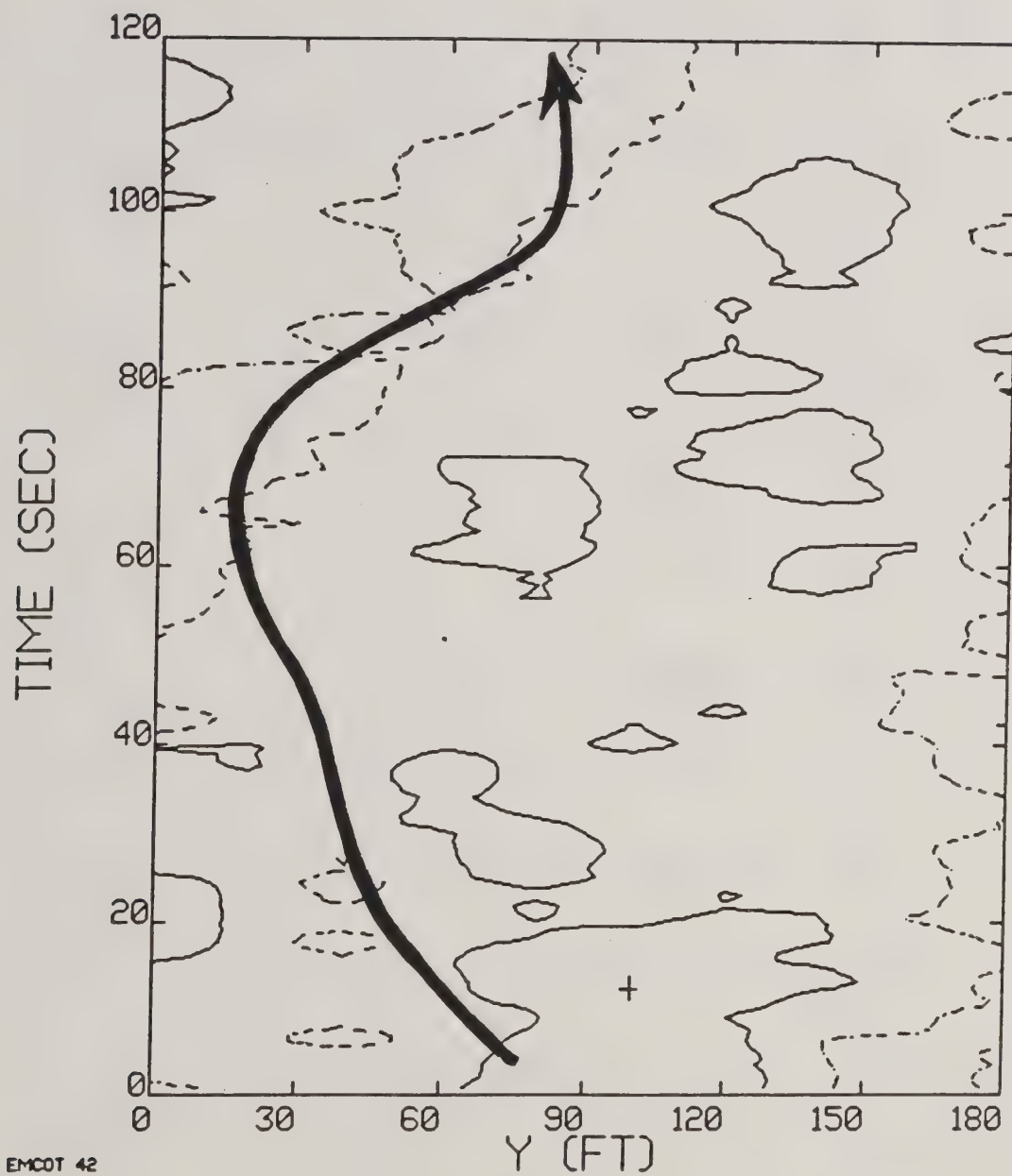


Figure 7-44. Run 42, date 05/07, Bell 206B.

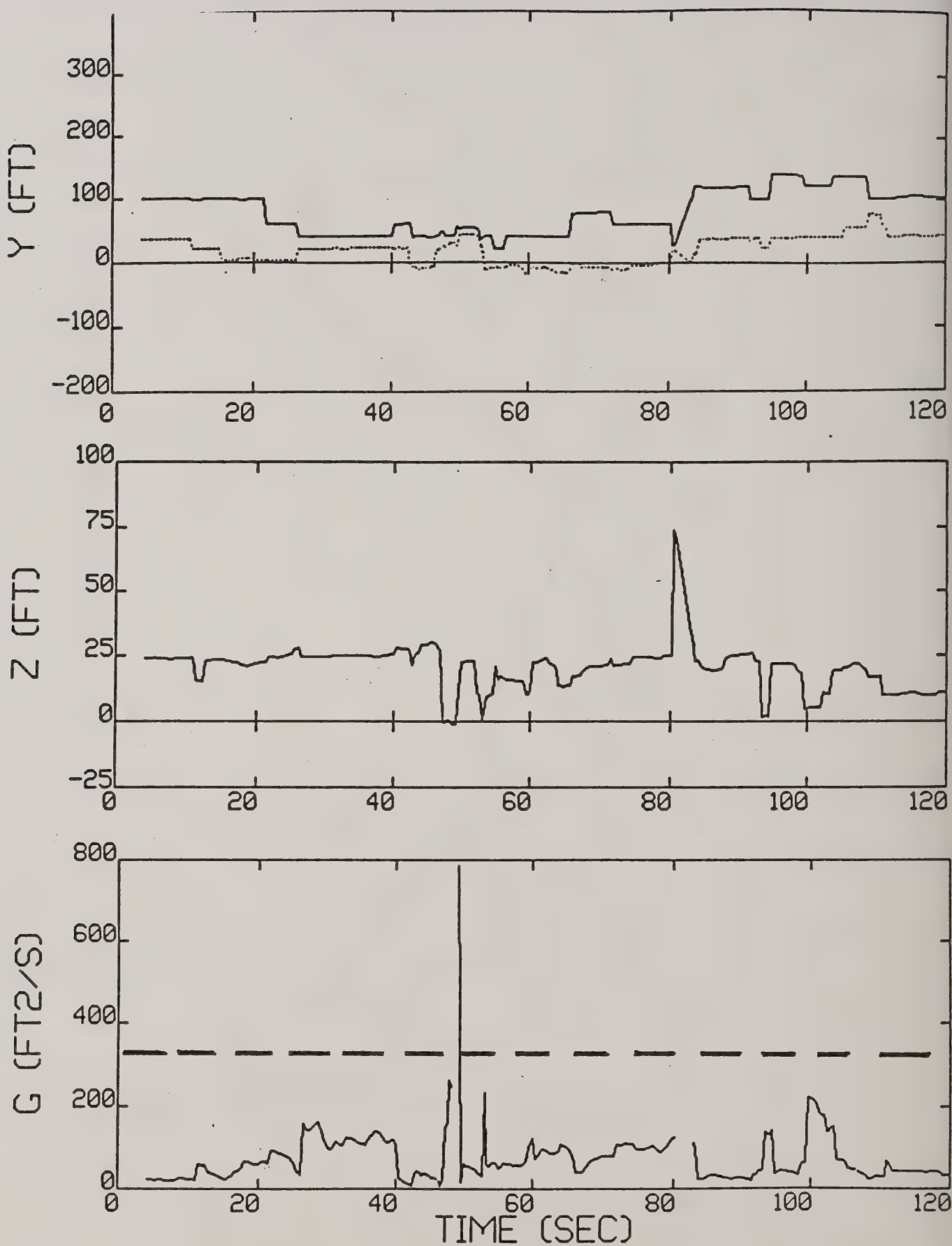


Figure 7-44b. Run 42 reduced data.

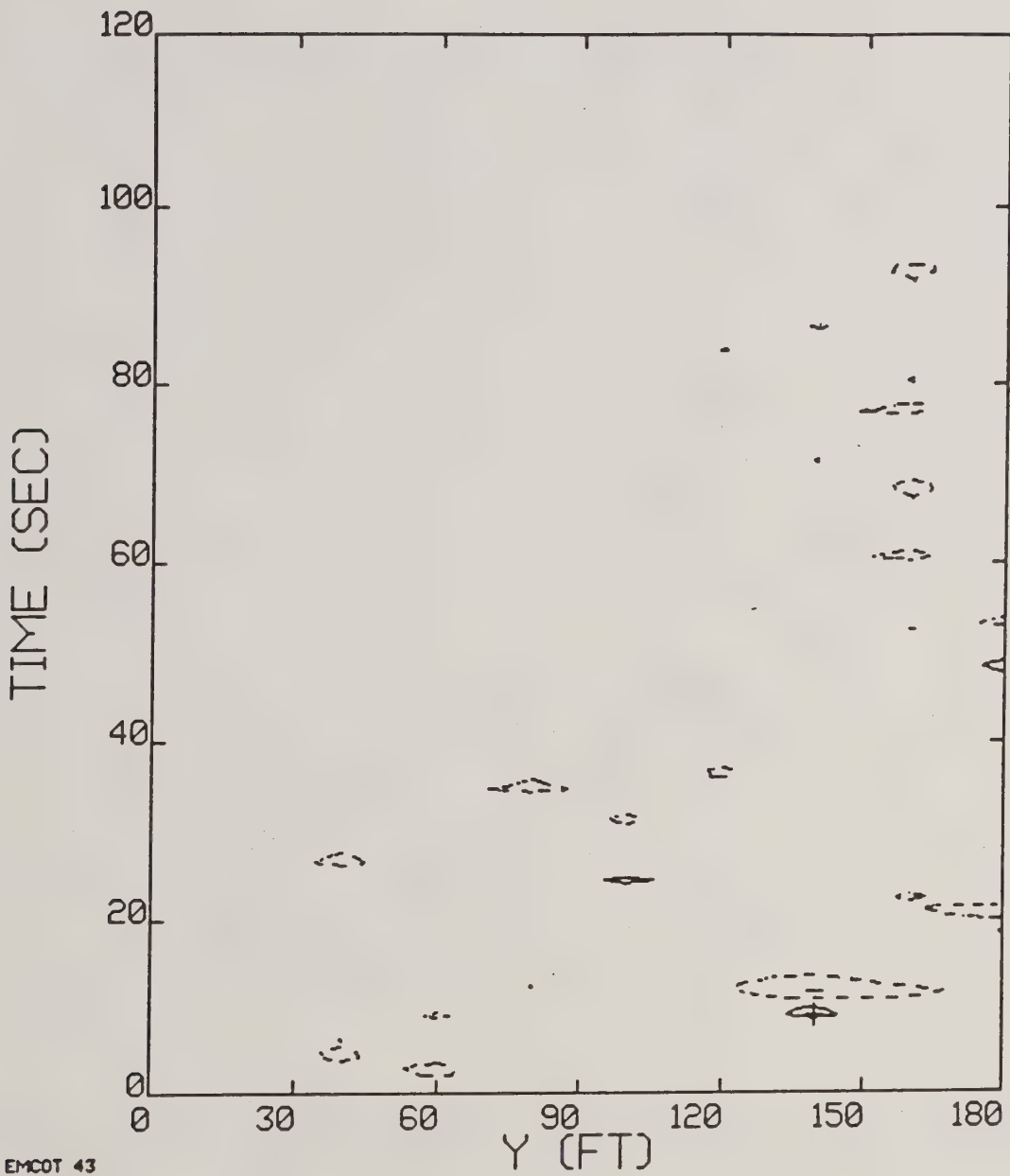


Figure 7-45. Run 43, date 05/08, Bell 206B.

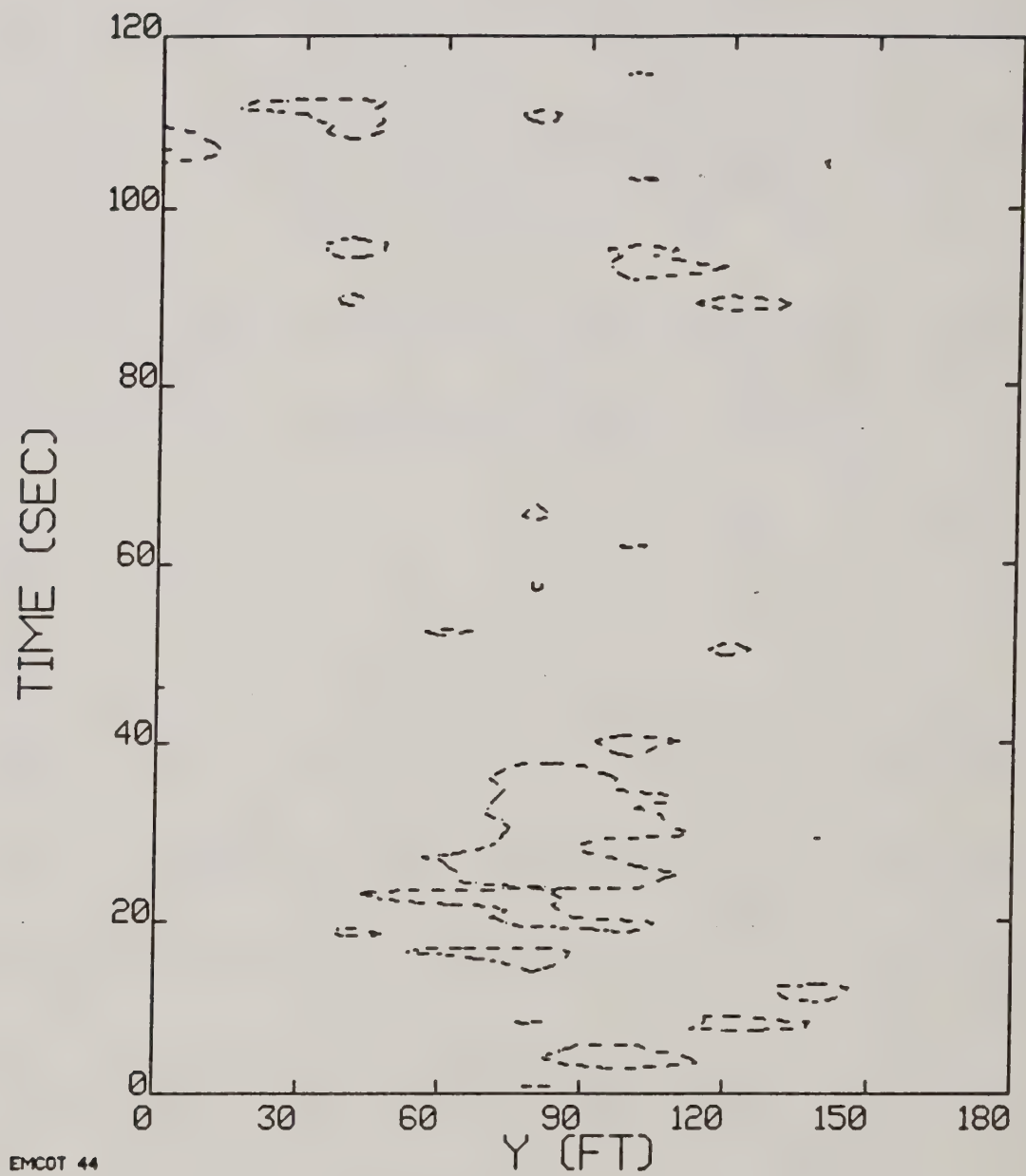


Figure 7-46. Run 44, date 05/05, Bell 206B.

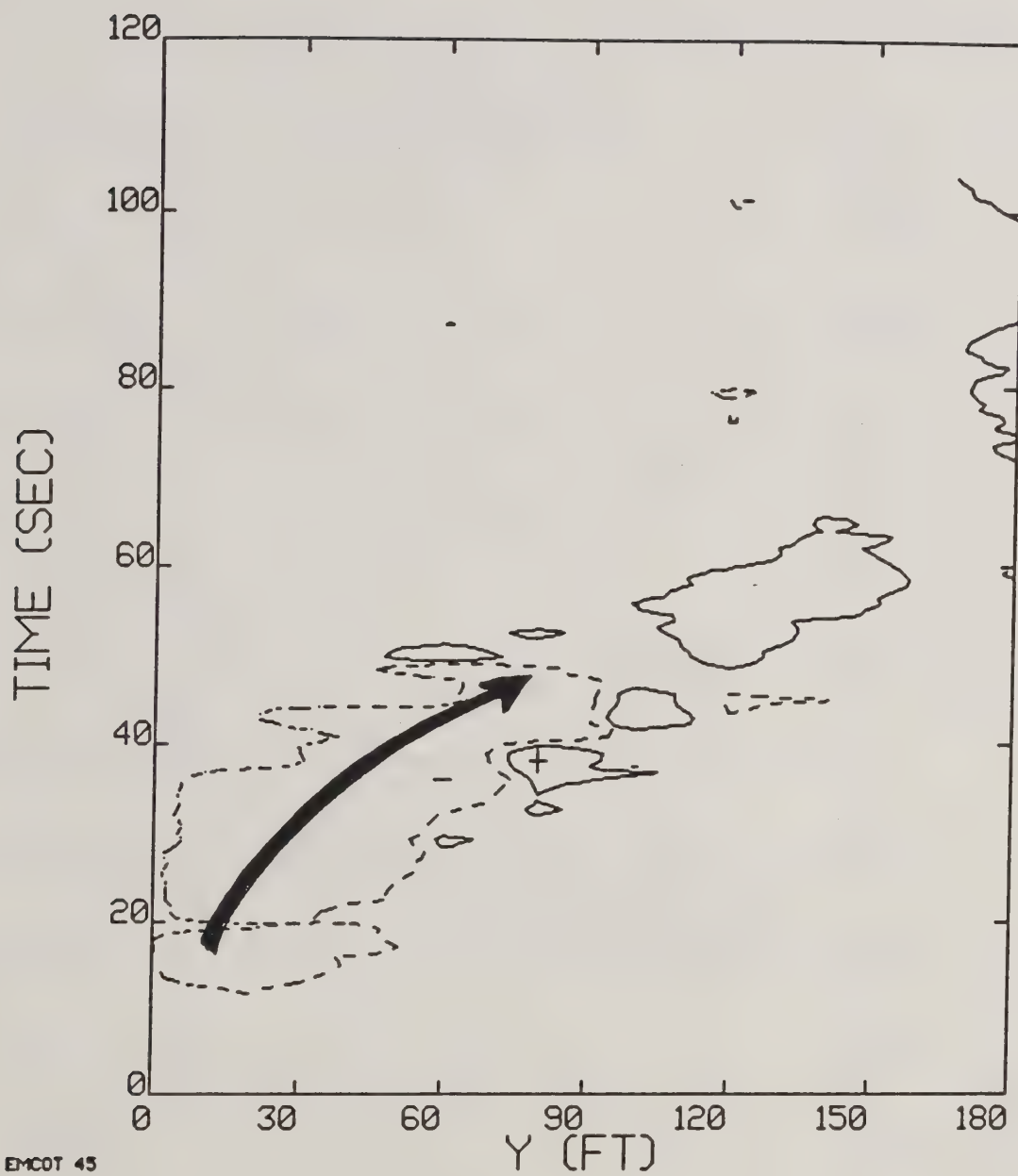


Figure 7-47. Run 45, date 05/05, Bell 206B.

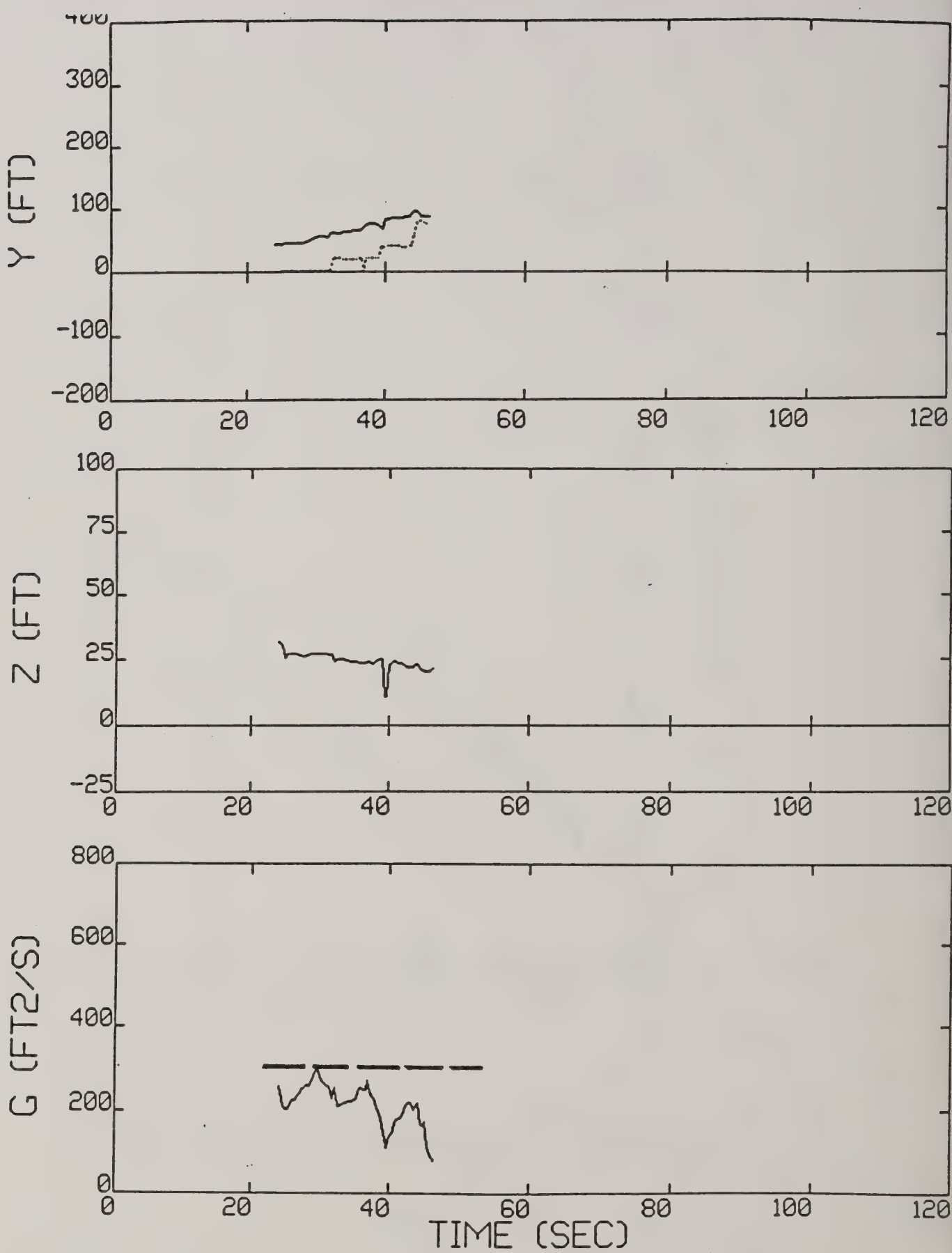


Figure 7-47b. Run 45 reduced data.

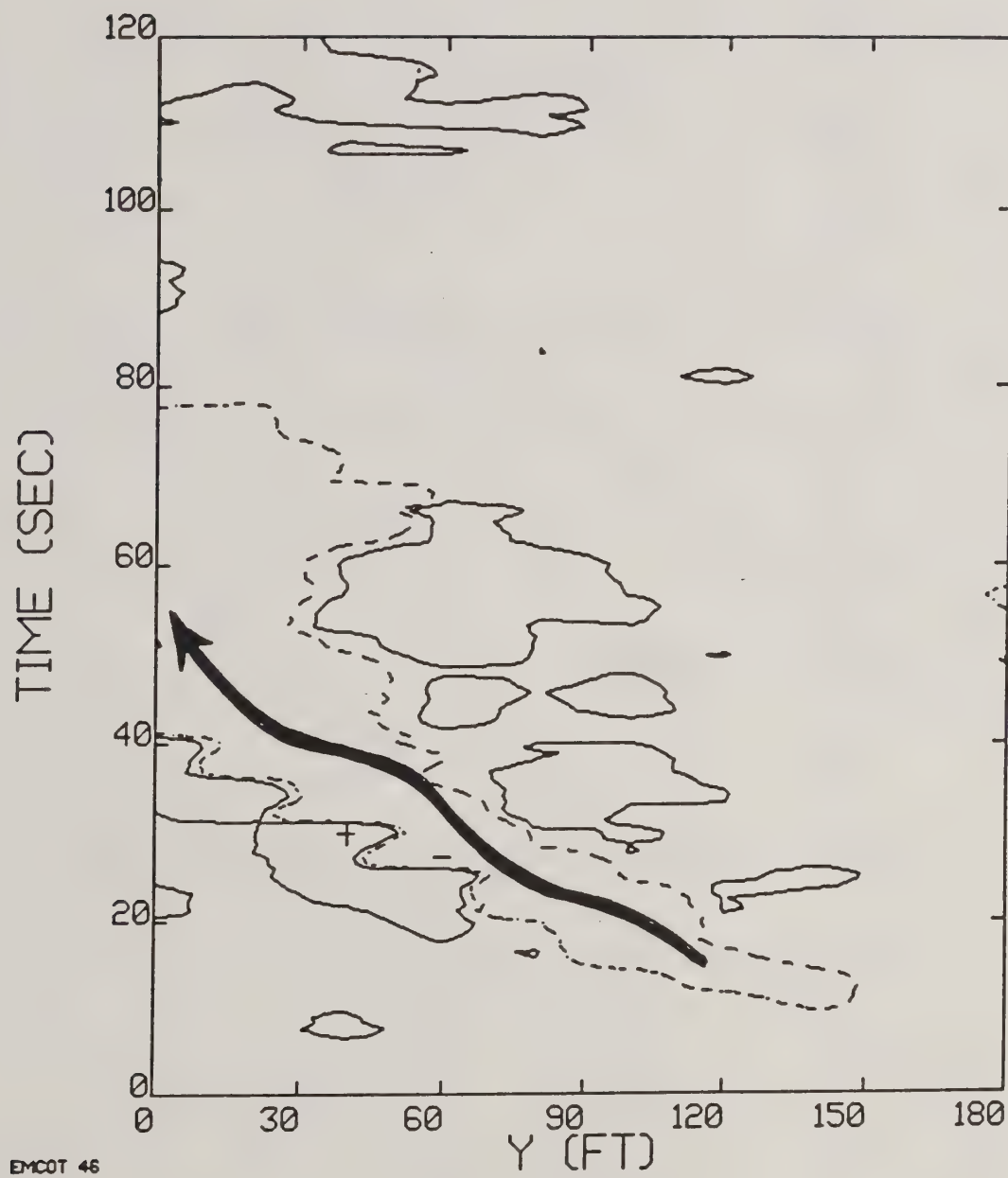


Figure 7-48. Run 46, date 05/08, Bell 206B.

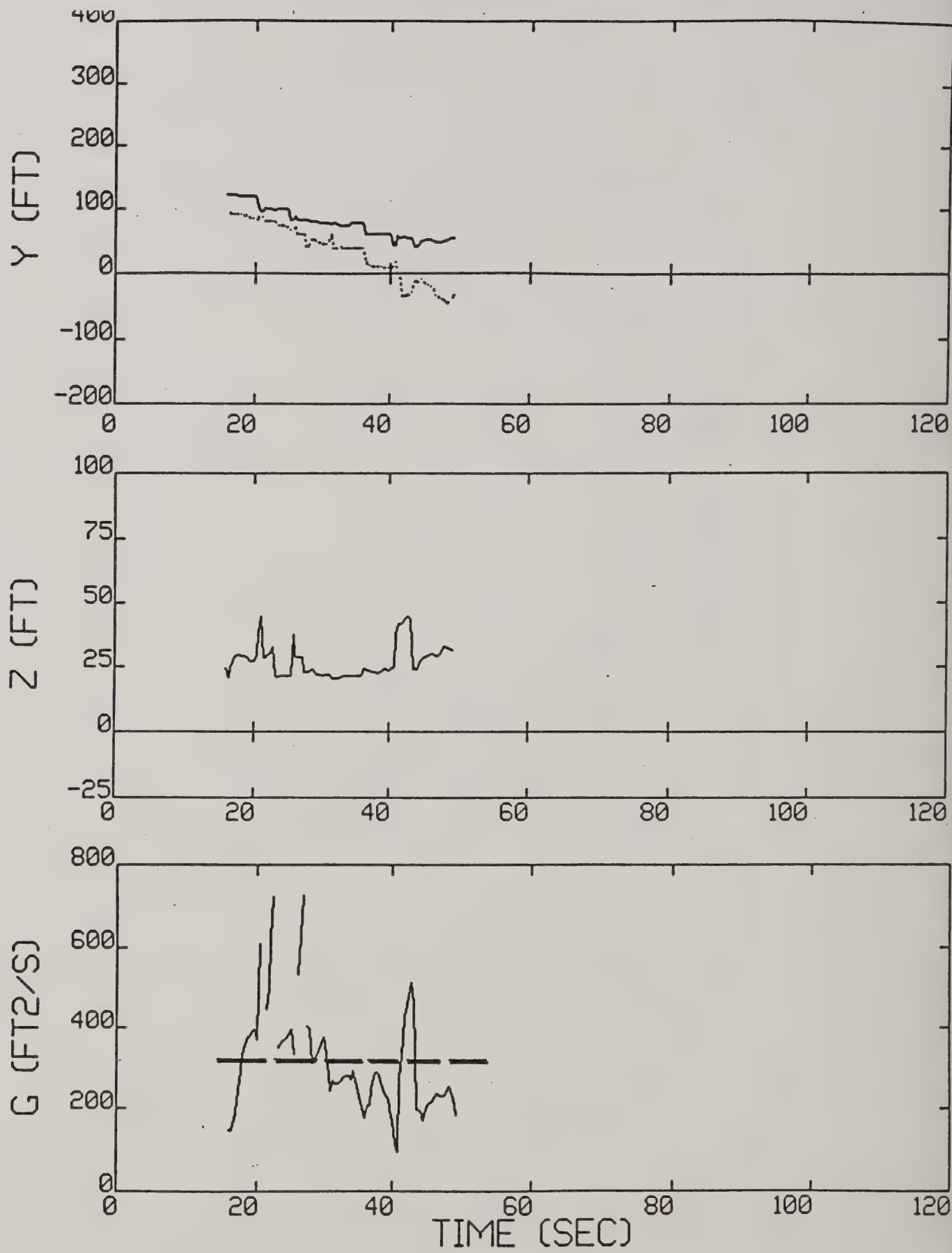


Figure 7-48b. Run 46 reduced data.

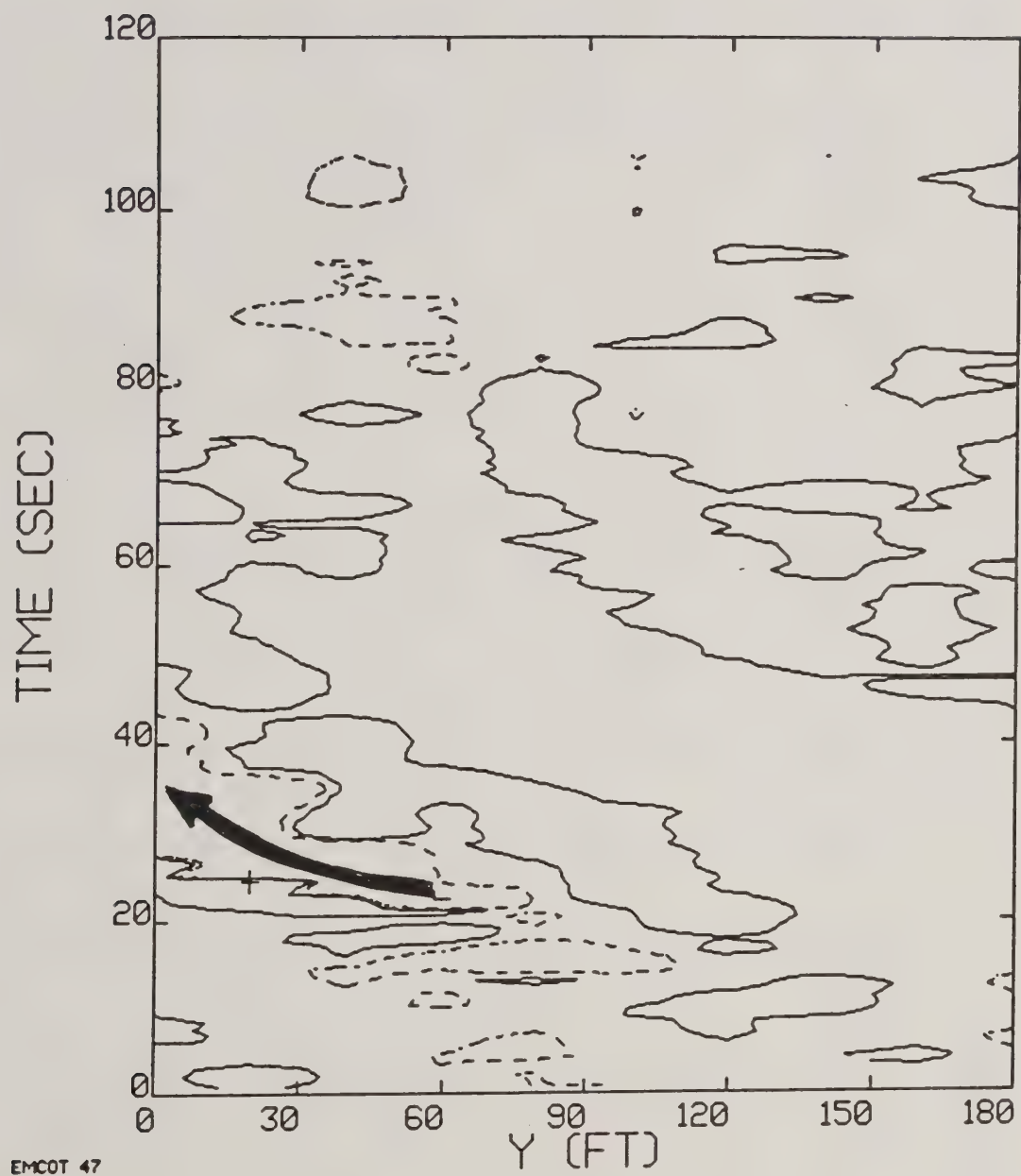


Figure 7-49. Run 47, date 05/08, bell 206B.

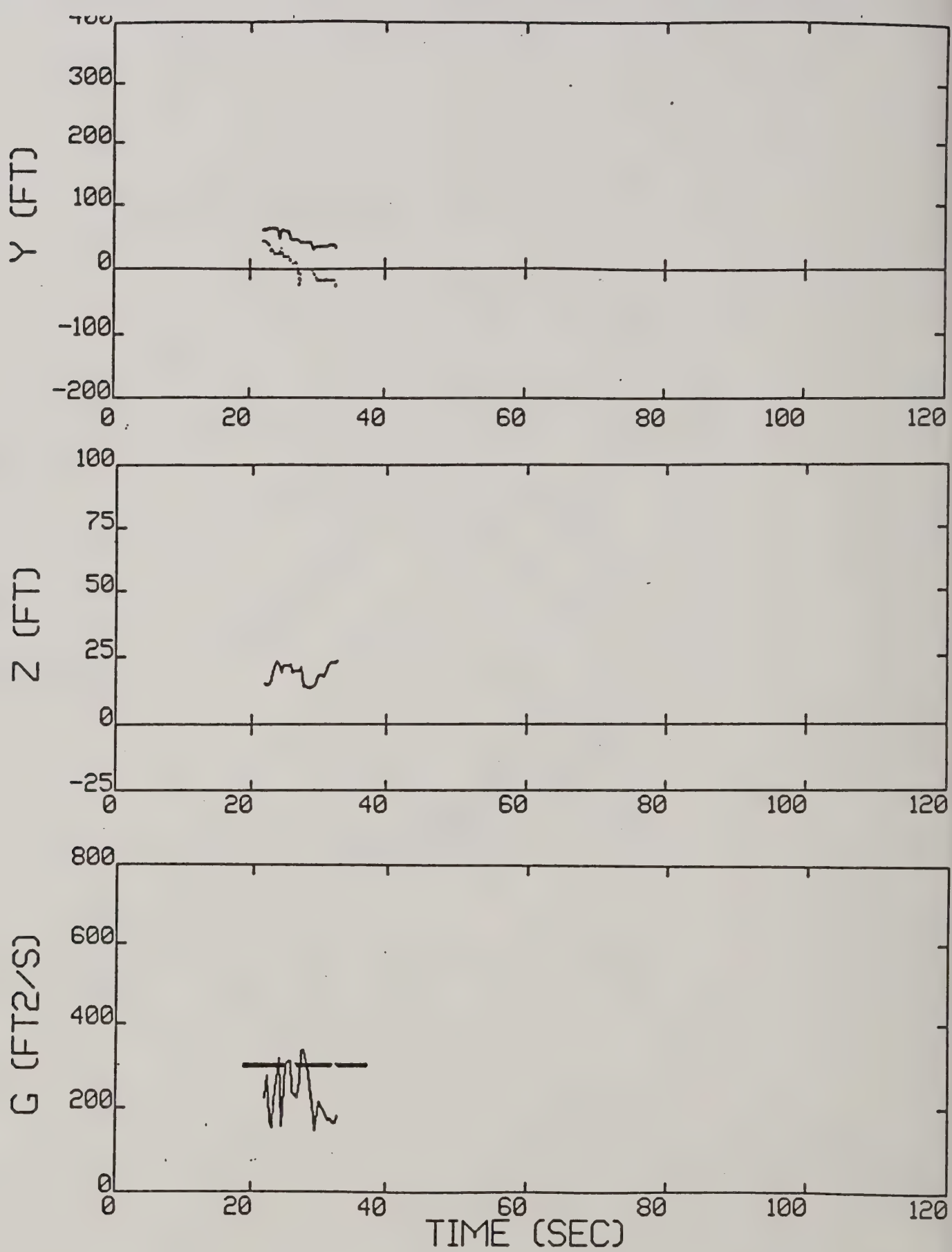


Figure 7-49b. Run 47 reduced data.

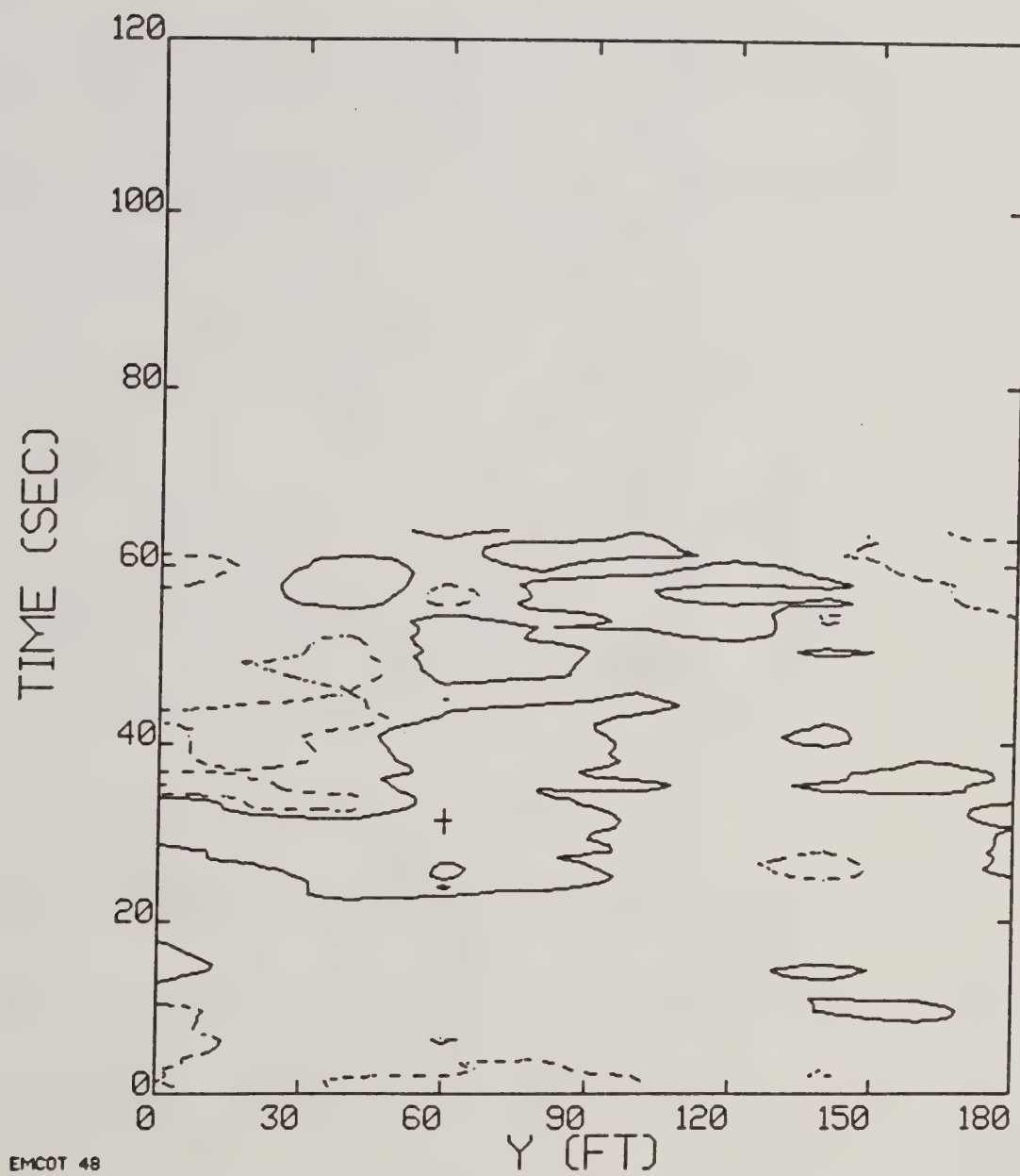


Figure 7-50. Run 48, date 05/08, Bell 206B.

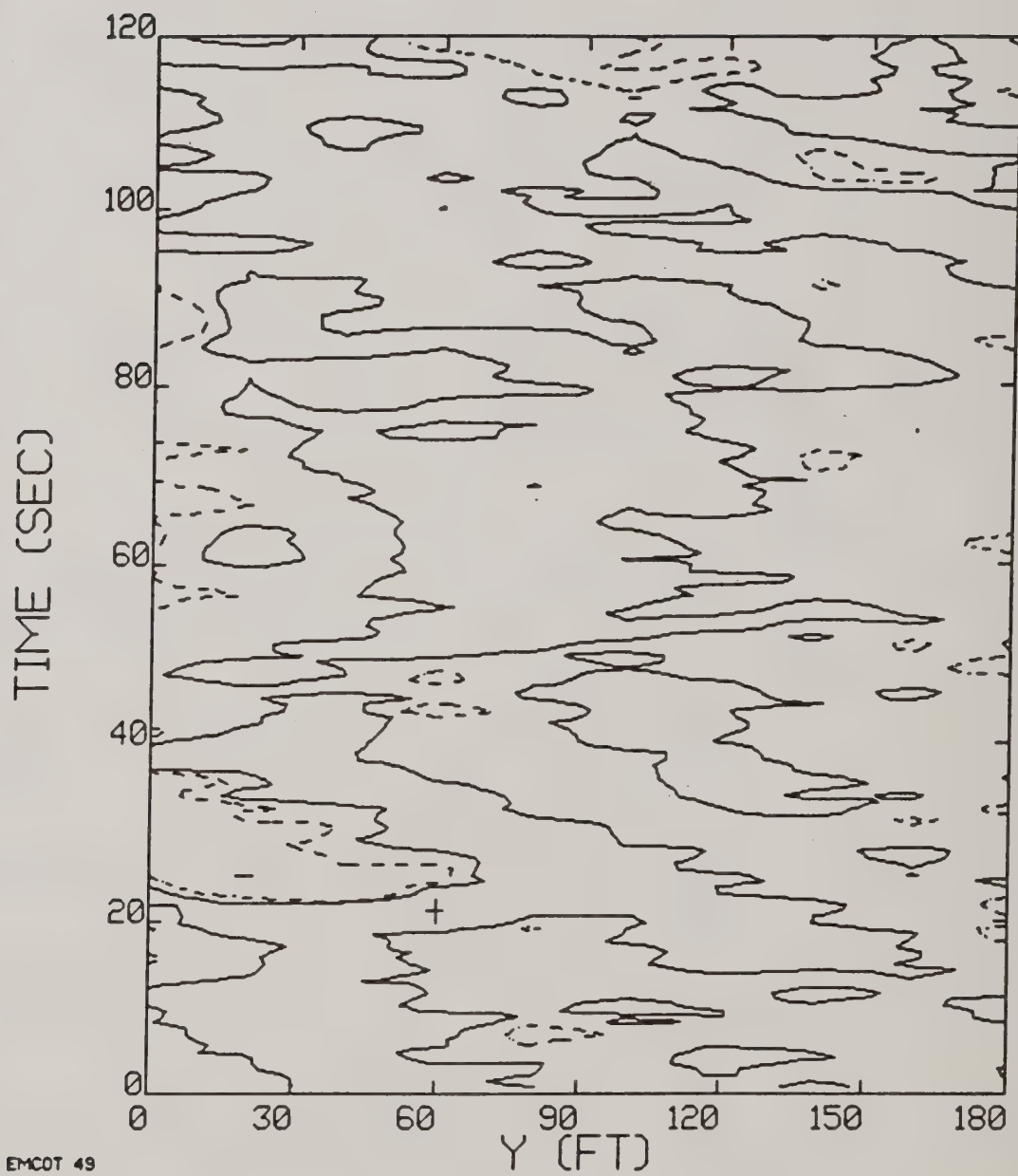


Figure 7-51. Run 49, date 05/08, Bell 206B.

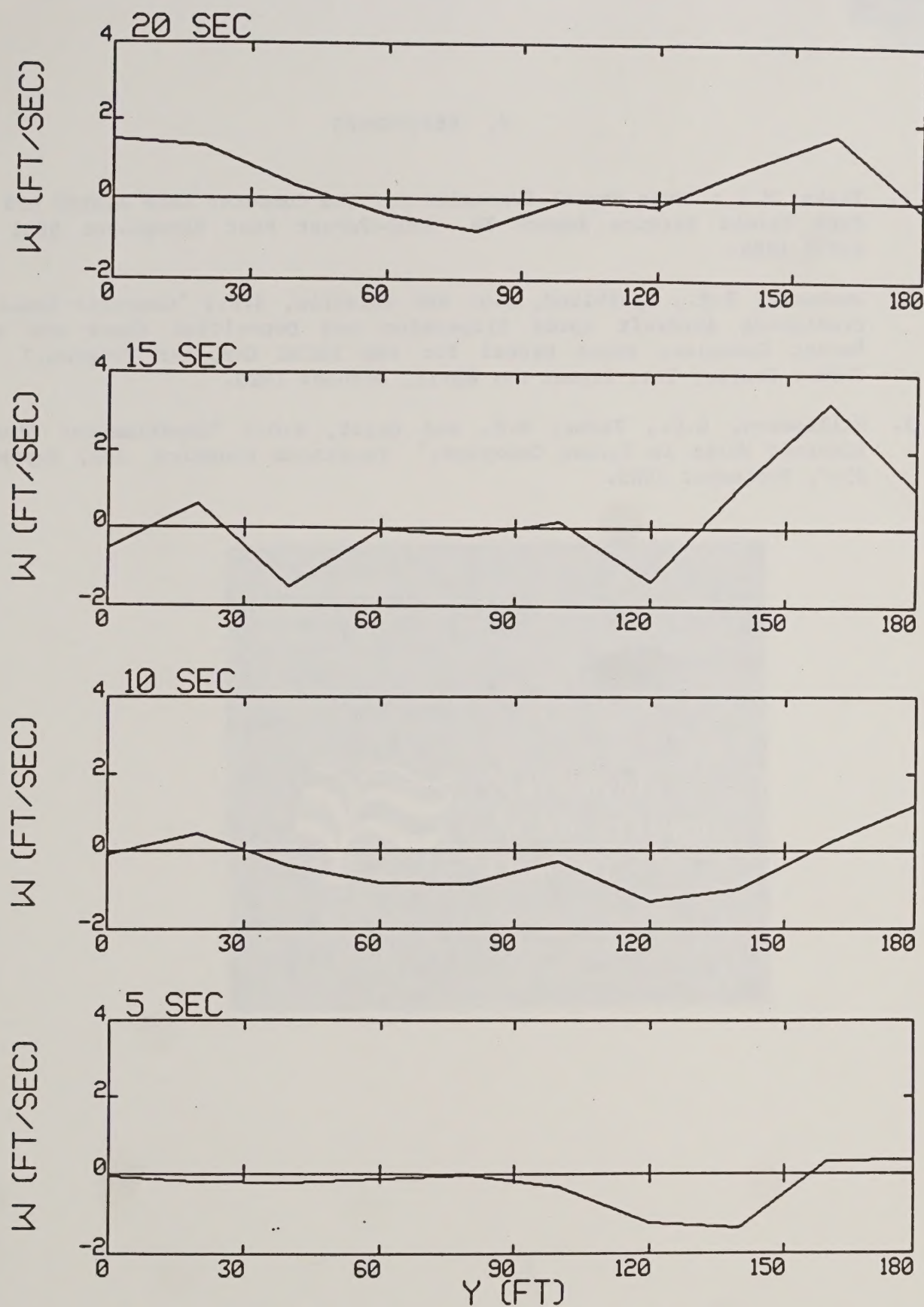


Figure 7-52. Vertical velocity profiles across the top row of grid anemometers at four times during the C-130 run 4. The aircraft appears to be located between 60 and 120 ft in the horizontal direction.

8. REFERENCES

1. Teske, M.E.: "User Manual Extension for the Computer Code AGDISP Mod 4.0," USDA Forest Service Report No. 3400-Forest Pest Management 8634 2809, April 1986.
2. Dumbauld, R.K., Bjorklund, J.R. and Saterlie, S.F.: "Computer Models for Predicting Aircraft Spray Dispersion and Deposition above and within Forest Canopies: Users Manual for the FSCBG Computer Program," H.E. Cramer Company Inc. Report No. 80-11, October 1980.
3. Williamson, G.G., Teske, M.E. and Geyer, R.G.: "Experimental Study of Aircraft Wakes in Forest Canopies," Continuum Dynamics, Inc. Report No. 85-7, September 1985.



1023055634

United States
Department of
Agriculture



NATIONAL
AGRICULTURAL
LIBRARY

Advancing Access to
Global Information for
Agriculture

NATIONAL AGRICULTURAL LIBRARY



1023055634